Microbial Degradation of Acetaldehyde in Freshwater, Estuarine and Marine Environments

Phillip Robert Kenneth Pichon

A thesis submitted for the degree of Doctor of Philosophy
in Microbiology

School of Life Sciences
University of Essex

October 2020

This thesis is dedicated to the memory of my mum,

Elizabeth "Taylor" Pichon

Acknowledgements

To my Dad and Roisin, your support and encouragement have helped me through the toughest parts of my project. My love and thanks to you both. Finally, I wish to thank my partner, Beth. I could not have finished my PhD without your love and support. My decision to eat that sloe berry in Flatford was probably the best decision I have ever made. I look forward to the next journey with you (and Dylan).

Abstract

The oxygenated volatile organic compound, acetaldehyde, plays a fundamental role in atmospheric chemistry by altering the atmosphere's oxidative status or "self-cleaning capacity". Acetaldehyde flux from freshwater, estuarine, and marine environments is thought to be under significant microbial control, yet the identity and diversity of microbial acetaldehyde degraders, and the mechanisms of acetaldehyde degradation, are largely unknown. In this thesis, the key acetaldehyde-degrading microorganisms in the Colne Estuary, the River Colne and the River Gipping were identified using metagenetic sequencing and quantitative PCR. Bacteria were primarily responsible for acetaldehyde degradation, with members of the genera *Pseudomonas* and *Arcobacter* identified as key acetaldehyde degraders. Seventeen bacterial isolates were cultivated from the Colne Estuary and degraded acetaldehyde at a concentration of 2.27 mM, with *Halobacillus* strains A4 and A5, *Rhodococcus* strain A14, and *Bacillus* strain A17 identified as important acetaldehyde degraders. Fourteen previously identified bacteria, belonging to the Actinobacteria, Bacteroidetes, Firmicutes, Proteobacteria, and Verrucomicrobia, also degraded acetaldehyde, suggesting that the microbial acetaldehyde sink is highly diverse. Using genomics and proteomics, the pathway of acetaldehyde metabolism used by *Rhodococcus* strain A14 was proposed. Acetaldehyde is oxidised to acetate by aldehyde dehydrogenase enzymes, with acetate converted to acetyl-CoA via acetyl-CoA synthetase. These reactions are thought to be conserved amongst acetaldehyde-degrading bacteria. Under favourable growth conditions, acetaldehyde is dissimilated to CO_2 for energy production via the oxidative decarboxylation steps of the tricarboxylic acid cycle. Acetaldehyde-derived carbon is assimilated into biomass by upregulating the glyoxylate shunt and gluconeogenesis pathway, ensuring carbon is conserved for growth. Using ^{14}C-radiolabelling, rates of microbial dissimilation were shown to be significantly higher than assimilation rates in the freshwater rivers, estuaries, and coastal seas of south-west

England, with summer rates significantly higher than winter. These findings suggest that microorganisms exert considerable control over acetaldehyde emissions and represent an important component of the global acetaldehyde cycle.

Contents

List of Tables

Supplementary tables

List of Figures

Supplementary figures

Abbreviations

^{14}C	Carbon-14
AAI	Average amino acid identity
ACS	Acetyl-CoA synthetase
ALD	Alcohol dehydrogenase
ALDH	Aldehyde dehydrogenase
ALDH2	Mitochondrial class 2 aldehyde dehydrogenase
AMP	Adenosine monophosphate
ANCOVA	Analysis of covariance
ANI	Average nucleotide identity
ANOVA	Analysis of variance
atmMOB	Atmospheric methane-oxidising bacteria
ATP	Adenosine triphosphate
BLAST	Basic Local Alignment Search Tool
bp	Base pair
BVOC	Biogenic volatile organic compound
CAM-Chem	Community Atmosphere Model with Chemistry
CCN	Cloud condensation nuclei
CCR	Carbon catabolite repression
CDOM	Chromophoric dissolved organic matter
CH_4	Methane
$C_2H_3O_2$	Acetate
C_2H_4O	Acetaldehyde
C_2H_6O	Ethanol
C_5H_8	Isoprene
CO	Carbon monoxide
CO_2	Carbon dioxide
CoA	Coenzyme A
CPM	Counts per minute
CTM	Chemical transport model
CYT	Cytochrome P450 isoenzyme
DDBJ	DNA Data Bank of Japan
DmdA	Dimethylsulfoniopropionate demethylase
DmdB	3-methylmercaptopropionyl-CoA ligase
DmdC	3-methylmercaptopropionyl-CoA dehydrogenase
DmdD	Methylthioacryloyl-CoA hydratase

DMS	Dimethylsulfide
DMSO	Dimethylsulfoxide
DMSP	Dimethylsulfoniopropionate
DNA	Deoxyribonucleic acid
DPM	Disintegrations per minute
dsDNA	Double-stranded DNA
ENA	European Nucleotide Archive
FISH	Fluorescence in-situ hybridisation
FDR	False discovery rate
GBDP	Genome BLAST distance phylogeny
GC-FID	Gas chromatography with flame-ionisation detection
GDP	Guanosine diphosphate
GEOS-Chem	Goddard Earth Observing System-Chemistry
GLIMMER	Gene Locator and Interpolated Markov ModelER
Glu	Glutamate
GTP	Guanosine-5'-triphosphate
H^+	Proton
HCHO	Formaldehyde
HO_2	Hydroperoxyl
HO_x	Hydrogen oxide radicals
Hv	Photodegradation (photolysis)
ITS2	Internal transcribed spacer 2 region
IUPAC	International Union of Pure and Applied Chemistry
LC-MS/MS	Liquid chromatography-tandem mass spectrometry
LTQ	Linear trap quadrupole
MACR	Methacrolein
MAR-FISH	Microautoradiography-fluorescence in-situ hybridisation
MEGA	Molecular Evolutionary Genetics Analysis
MEGAN	Model of Emissions of Gases and Aerosols from Nature
MiGA	Microbial Genomes Atlas
MLST	Multilocus sequence typing
MMPA	Methylmercaptopropionate
mRNA	Messenger RNA
MTA	Methylthioacryloyl
MUM	Maximal unique matches
MUSCLE	MUltiple Sequence Comparison by Log-Expectation
MVK	Methyl vinyl ketone

MVOC	Microbial volatile organic compound
NAD^+	Nicotinamide adenine dinucleotide (oxidised)
NADH	Nicotinamide adenine dinucleotide (reduced)
$NADP^+$	Nicotinamide adenine dinucleotide phosphate (oxidised)
NADPH	Nicotinamide adenine dinucleotide phosphate (reduced)
NanoSIMS	Nanoscale secondary ion mass spectrometry
NCBI	National Center for Biotechnology Information
NMHC	Non-methane hydrocarbon
NMVOC	Non-methane volatile organic compound
NO	Nitric oxide
NO_2	Nitrogen dioxide
NO_x	Nitrogen oxide
NOAA	No-acetaldehyde control
O_3	Ozone
OD	Optical density
OGDC E3	α-ketoglutarate dehydrogenase complex E3 subunit
·OH	Hydroxyl radical
OTU	Operational taxonomic unit
OVOC	Oxygenated volatile organic compound
PAGE	Polyacrylamide gel electrophoresis
PAN	Peroxyacetyl nitrate
PCA	Principal component analysis
PCR	Polymerase chain reaction
PDC E3	Pyruvate dehydrogenase complex E3 subunit
PEAR	Paired-end Read Merger
PEP	Phosphoenolpyruvate
PEPCK	Phosphoenolpyruvate carboxykinase
PERMANOVA	Permutational multivariate analysis of variance
PGAP	Prokaryotic Genome Annotation Pipeline
P_i	Inorganic phosphate
PP_i	Inorganic pyrophosphate
PTFE	Polytetrafluoroethene-lined
Q	Ubiquinone
QH_2	Ubiquinol
qPCR	Quantitative PCR
RAST	Rapid Annotation using Subsystem Technology
RDP	Ribosomal Database Project

RNA	Ribonucleic acid
ROS	Reactive oxygen species
rpm	Revolutions per minute
rRNA	Ribosomal RNA
SDS	Sodium dodecyl sulphate
SIP	Stable-isotope probing
SOA	Secondary organic aerosol
SSM	Sea-surface microlayer
TAPSO	3-[N-Tris(hydroxymethyl)methylamino]-2-hydroxypropanesulfonic acid
TCA	Tricarboxylic acid
TRIS	Tris(hydroxylmethyl)aminomethane
UniProtKB	UniProt Knowledgebase database
US EPA	United States Environmental Protection Agency
VOC	Volatile organic compound
WGS	Whole genome shotgun

Declaration

This thesis is submitted to the University of Essex in support of my application for the degree of Doctor of Philosophy. I declare that the work presented in this thesis was conducted by me, under the supervision of Professor Terry McGenity, Dr Boyd McKew, Dr Joanna Dixon, and Professor J. Colin Murrell, with the exception of those instances where the contribution of others has been specifically acknowledged.

The work presented, including data generated and data analysis, was carried out by the author except in the cases outlined below:

○ An in-gel trypsin digest was performed on extracted proteins and the resulting peptide fragments prepared for LC-MS/MS analysis (Chapter 4) by Dr Gergana Metodieva (University of Essex).

○ Initial peptide data analysis in MaxQuant and protein identification and validation (Chapter 4) were performed by Dr Metodi Metodiev (University of Essex).

○ Supporting data from the rivers, estuaries and coastal regions of south-west England during summer (Chapter 5) were collected by Christopher Webb (as reported in Webb C (2016) Turnover of acetaldehyde in natural waters. MSc thesis, Plymouth University). This included summer rates of microbial acetaldehyde assimilation, dissimilation, total uptake, turnover times, and bacterial growth efficiencies. Data were provided with permissions from Dr Joanna Dixon (Plymouth Marine Laboratory).

Chapter 1:

Introduction

1.1 Volatile organic compounds and the atmosphere

Volatile organic compounds (VOCs) are organic chemicals which easily volatilise or become vapour at temperatures between 0 - 250°C, and are found in all living organisms (Guenther et al. 1994). The United States Environmental Protection Agency (US EPA) define VOCs as carbon compounds "excluding carbon monoxide, carbon dioxide, carbonic acid, metallic carbides or carbonates and ammonium carbonate, which participate in atmospheric photochemical reactions" (U.S. Environmental Protection Agency 2016), and comprise of a wide range of compound classes including the isoprenoids (e.g. hemiterpenes; monoterpenes; sesquiterpenes) (Atkinson & Arey 2003), alkanes, alkenes, carbonyls, alcohols, esters, ethers and acids (Kesselmeier & Staudt 1999). Because of the large variety of classes within this system of classification, there exists a considerable number of defined subgroups, each based on the source, functionality, and/or general characteristics of VOCs. The most commonly used include biogenic VOC (BVOC), microbial VOC (MVOC), non-methane VOC (NMVOC), oxygenated VOC (OVOC) and non-methane hydrocarbons (NMHC).

For the last few decades much research effort concerning VOCs has focused on methane (CH_4); an acyclic saturated alkane hydrocarbon. Initially, this research effort was the result of increasing interest surrounding the overall composition of the atmosphere (Moss et al. 2000), and how VOCs influenced tropospheric chemistry and associated weather conditions (Cicerone & Oremland 1988; Koppmann et al. 2005). However, after the revelation that methane emissions play a significant part in global warming and the "greenhouse effect" (Lashof & Ahuja 1990; Kirschke et al. 2013; Yvon-Durocher et al. 2014), much like that observed for atmospheric carbon dioxide (CO_2), the focus of investigations shifted towards

the role of methane in regulating Earth's climate and global temperatures. Such studies identified methane as the second largest anthropogenic contributor to global warming (Jorgenson 2006), and demonstrated that methane has 20 - 25 times the global warming potential of CO_2 (Milich 1999; Yvon-Durocher et al. 2014). Consequently, the atmospheric effect of methane gained substantial attention in scientific circles and within society, and gathered the momentum necessary for methane to become a focal point of VOC research.

Through the study of methane, it became apparent that other VOCs were abundant in the atmosphere (Singh et al. 2003) and also had the potential to influence tropospheric chemical reactions, global atmospheric processes and climate (Guenther et al. 1995). Isoprene, for example, is a highly reactive hydrocarbon (Shaw et al. 2010) with an atmospheric concentration comparable to that of methane (Sharkey et al. 2008). Globally, isoprene constitutes 61% of total annual BVOC emissions (Lathìere et al. 2006), which equates to an estimated 500 - 750 Tg a^{-1} based on emission models such as MEGAN (Model of Emissions of Gases and Aerosols from Nature) (Guenther et al. 2006). The photooxidation of isoprene within the atmosphere results in the formation of low-volatile intermediates such as methylerythritol (Paulot et al. 2009), which act as a source of secondary organic aerosol (SOA) (Brégonzio-Rozier et al. 2016) and subsequently have an indirect role in cloud formation (Riipinen et al. 2011). Moreover, under the correct conditions, these intermediates can induce the formation of tropospheric ozone and increase the residence time of prominent greenhouse gases (Poisson et al. 2000). As a result, isoprene and its derivatives bring about significant changes to the radiative balance of the atmosphere, which in turn mediates the global climate and weather patterns. As pointed out by Guenther et al. (1995), this demonstrates an important and unambiguous relationship between VOC emissions and Earth's climate system, but also emphasises the importance of not overlooking other VOCs and their role in tropospheric chemistry, even if their relative atmospheric abundances are considerably lower than methane and isoprene.

Carbonyl compounds, such as formaldehyde and acetaldehyde, represent one such class of understudied VOCs when compared to methane and isoprene, despite the growing evidence which suggests that this compound class plays an important role in atmospheric chemistry (Shepson et al. 1991; Zhou & Mopper 1993; Kesselmeier & Staudt 1999; Singh et al. 2003; Rodigast et al. 2015). This can be attributed to isoprene and other reactive VOCs being globally ubiquitous and having substantially larger atmospheric concentrations (Atkinson 2000), whilst also acting as precursor molecules to carbonyls (Yu et al. 2008). Consequentially, aldehydes and other compounds within the carbonyl group are often the secondary focus of research, and research exclusively examining individual carbonyls in the atmosphere is few and far between. This has resulted in a comparative paucity of information regarding the role of carbonyl compounds in tropospheric chemistry and climate regulation, and has led to difficulties related to atmospheric modelling, as highlighted by Zhou & Mopper (1993). However, despite having low atmospheric concentrations (Zhou & Mopper 1993), carbonyl compounds have been shown to have a distinct effect on tropospheric chemistry (Singh et al. 2004), and also represent a useful proxy for photochemical activity and an important indicator of the presence of specific precursor VOCs (Shepson et al. 1991).

Acetaldehyde (C_2H_4O) (Figure 1.1), for instance, is a carbonyl compound which falls within the OVOC subgroup, and has a significant impact on the troposphere. Firstly, it has been shown that acetaldehyde acts as a source of ozone (O_3), peroxyacetyl nitrate (PAN), hydrogen oxide radicals (HO_x) and carbon monoxide (CO) via oxidation and photochemical degradation pathways (Millet et al. 2010). These secondary compounds drive the oxidative status of the atmosphere, and consequently change its "self-cleaning" capacity (Lelieveld et al. 2008). In particular, HO_x, which includes hydrogen (H), hydroxy ($\cdot OH$) and peroxy radicals, play a central role in the removal of VOCs from the troposphere and are the main chemical source of O_3 (Wennberg et al. 1998; Lelieveld et al. 2008; Mao et al. 2010). The latter is particularly important given that tropospheric O_3 is a powerful greenhouse gas, and

therefore has a considerable influence on global warming and the climate. Additionally, acetaldehyde, like many other carbonyl compounds, can be absorbed by wet aerosol particles and in the process undergo aqueous-phase reactions which result in the formation of SOA (Sareen et al. 2013). As empirically demonstrated by Sareen et al. (2013), these SOA have a reduced surface tension resulting from the surface-active properties of acetaldehyde, which causes a significant increase in hygroscopicity, or the ability to absorb moisture, and a subsequent enhancement of cloud condensation nuclei (CCN) activity. Under the correct conditions, this can result in increased cloud density and albedo, and simultaneously limit solar irradiance (Latham et al. 2008); having an important effect on local and global climate (Latham et al. 2008; Sareen et al. 2013).

Further exacerbating these climatic effects is the indirect activity of acetaldehyde on the residence times of greenhouse gases. Ozone, resulting from the atmospheric oxidation and photodegradation of acetaldehyde, can itself undergo photodegradation to produce more ·OH radicals (Mao et al. 2010), which at high concentrations increases the oxidising capacity of the atmosphere. This increased "cleaning" capacity causes a subsequent reduction of the lifetimes of methane and halogenated halocarbons (Wigley et al. 2002; Naik et al. 2005), culminating in substantial impacts to global radiative forcing. Conversely, the initial oxidation of acetaldehyde causes a reduction in the concentration of ·OH radicals, as seen with other VOCs (Poisson et al. 2000). Under low NO_x (nitric oxide (NO) + nitrogen dioxide (NO_2)) conditions, this results in a net loss of ·OH radicals (Lelieveld et al. 2008) and a decline in the atmosphere's oxidising potential. As such, the residence time of greenhouse gases increases, with the lifetime of methane shown to increase by as much as 15% (Poisson et al. 2000). Accordingly, despite having a considerably lower atmospheric concentration than methane and isoprene, acetaldehyde has significant effects on global climate and weather, both directly and indirectly, and further demonstrates the importance of extensive research into VOCs and their role in tropospheric chemistry.

1.2 Acetaldehyde synthesis

Acetaldehyde is an extremely volatile carbon compound belonging to the OVOC subgroup, and is distinguished as a carbonyl compound through its carbon-oxygen double bond (Figure 1.1). It is estimated that as much as 150 - 500 Tg C moves through the atmosphere in the form of OVOCs every year, with acetaldehyde accounting for as much as 115 - 286 Tg C (Singh et al. 2004). As previously stated, carbonyl compounds can be derived from precursor VOCs. In the case of acetaldehyde, it is understood that alkanes, alkenes and ethanol represent the main precursor molecules, with their oxidation providing the largest source of acetaldehyde in the atmosphere; corresponding to 128 Tg a^{-1}, based on the 3-D chemical transport model GEOS-Chem CTM (Millet et al. 2010).
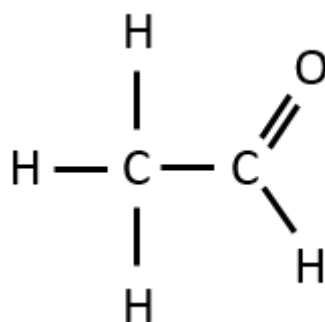
Figure 1.1 Molecular structure of acetaldehyde (C_2H_4O). Acetaldehyde is a carbonyl compound, as shown by its carbon-oxygen double bond.

Additionally, it is now thought that isoprene also acts as a minor source of acetaldehyde through the photolysis of its oxidation products, such as methyl vinyl ketone (C_4H_6O) (Atkinson et al. 2006), resulting in atmospheric yields of 6 - 8 Tg a^{-1} depending on global NO_x conditions (Millet et al. 2010). The acetaldehyde produced from these tropospheric reactions is subjected to further oxidation and photodegradation which equates to an atmospheric lifetime of 0.8 - 1.0 day (Singh et al. 2004; Millet et al. 2010) (Table 1.1). These reactions are summarised in Figure 1.2.

$$VOC \text{ (e.g. } C_2H_6O) + 2 \cdot OH \quad \rightarrow \quad C_2H_4O + 2\ H_2O \quad\quad\quad (R1)$$

$$VOC \text{ (e.g. } C_5H_8) + \cdot OH \quad \rightarrow \quad MACR + MVK + HCHO + HO_2 \quad (R2)$$
$$+ \text{ other products}$$

$$MVK + hv \quad \rightarrow \quad C_2H_4O$$

$$C_2H_4O + \cdot OH \text{ or } hv \quad \rightarrow \quad O_3 + PAN + HO_x + CO \quad\quad (R3)$$
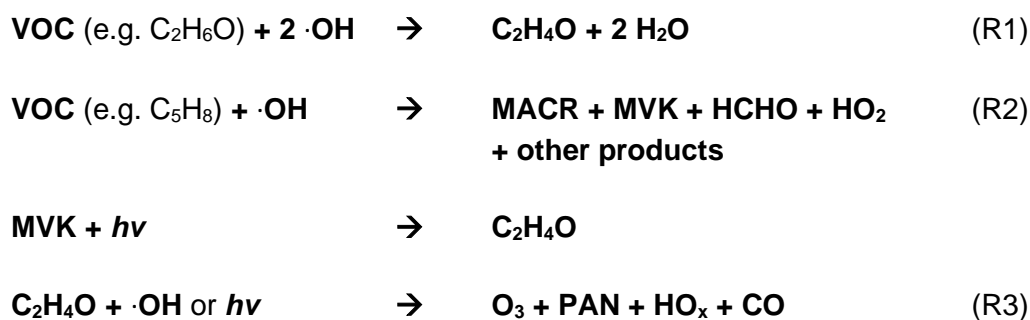
Figure 1.2 Summary of the reactions between volatile organic compounds (VOC) and the hydroxy radical ($\cdot$OH) in the atmosphere, and the production of acetaldehyde (C_2H_4O). C_2H_6O: ethanol; H_2O: water; C_5H_8: isoprene; MACR: methacrolein; MVK: methyl vinyl ketone; HCHO: formaldehyde; HO_2: hydroperoxyl; *hv*: light-associated photolysis reactions; O_3: ozone; PAN: peroxyacetyl nitrate; HO_x: hydrogen oxide radicals; CO: carbon monoxide.

Whilst continually formed in the atmosphere, acetaldehyde is also produced biogenically via enzymatic activity (Homann et al. 2000). The oxidation of ethanol (C_2H_6O) to acetaldehyde in living organisms is catalysed by the action of alcohol dehydrogenase enzymes (Figure 1.3), and has received particular attention in human biology due to the recognised carcinogenic and mutagenic effects of acetaldehyde (Ghica et al. 2007; Lachenmeier et al. 2009). Research within the last few years has shown that acetaldehyde produced from this enzyme-catalysed reaction can form adducts with DNA (Brooks & Zakhari 2014). In some cases, where repair is not possible, the presence of adducts can lead to DNA mutation during replication and the eventual development of cancer (Balbo & Brooks 2015). In addition to alcohol dehydrogenases, cytochrome P450 isoenzymes found in the endoplasmic reticulum of liver cells have been shown to have a role in the conversion of ethanol to acetaldehyde (Figure 1.3), especially under high ethanol conditions (Brooks & Zakhari 2014), as part of the microsomal ethanol oxidising system (Salaspuro 2003).

Moreover, the production of acetaldehyde from ethanol is not exclusive to eukaryotes (Homann et al. 1997; Jokelainen et al. 1997; Salaspuro 2003; Theruvathu et al. 2005). As shown by Homann et al. (1997), the microbiota of the human oral cavity can produce significant quantities of acetaldehyde after moderate ethanol ingestion. Within the study, it

was demonstrated that salivary acetaldehyde concentrations of healthy volunteers, who had consumed 0.5 g of ethanol per kg of body weight, ranged from 115 ± 28 µM to 136 ± 14 µM, whilst volunteers who used mouthwash, and therefore reduced the naturally occurring microbiota, had diminished salivary concentrations of 54 ± 18 µM. Furthermore, the sterile filtration of saliva through 0.22 µm filters, used to reduce the residual bacterial community, resulted in the complete prevention of acetaldehyde production. Consequently, these observations demonstrate a prokaryotic pathway of ethanol oxidation and simultaneously confirm the existence of bacterial alcohol dehydrogenase enzymes. This is further supported by observations made by Jokelainen et al. (1997), which highlighted that acetaldehyde production is not restricted to the oral microbiota but is also found in the resident bacterial gut community in rats. By applying the antibiotic ciprofloxacin (200 mg kg^{-1} day^{-1}) for four days, the faecal aerobic microbiota of rats was significantly reduced and lowered the associated bacterial alcohol dehydrogenase activity from 63 nmol min^{-1} mg^{-1} of faeces to 17 nmol min^{-1} mg^{-1} of faeces; resulting in a decreased rate of ethanol elimination (Jokelainen et al. 1997) and providing further evidence for a bacterial origin of acetaldehyde production.

Table 1.1 Physical and chemical properties of acetaldehyde.

Property	Acetaldehyde
IUPAC ID	Ethanal
Molecular formula	C_2H_4O or CH_3CHO
Molar mass (g·mol^{-1})	44.05
Boiling point (°C)	20.2
Melting point (°C)	-123.37
Atmospheric lifetime (days)	0.8 [1] - 1.0 [2]
Ocean mixed layer lifetime (hours)	0.3 – 12 [1]
Henry's constant (atm·m^3/mol) (25°C)	6.67 x 10^{-5}
Density (g·cm^{-3}) (20°C)	0.784

[1] Millet et al. (2010); [2] Singh et al. (2004)

Acetaldehyde produced from these enzymatic reactions is more toxic than ethanol (Ghica et al. 2007) and therefore requires further breakdown into nontoxic metabolites and removal from the systems of living organisms. This detoxification is performed by aldehyde dehydrogenase (ALDH) enzymes, such as mitochondrial class 2 aldehyde dehydrogenase (ALDH2) found in humans (Salaspuro 2003), which convert acetaldehyde to acetate (Figure 1.3). This oxidation is cofactor-dependent, requiring the presence of nicotinamide adenine dinucleotide (NAD$^+$), and in humans can be carried out by nineteen different ALDH enzymes (Moreb 2014); the primary enzyme responsible for this being ALDH2 (Salaspuro 2003).

$$\text{C}_2\text{H}_6\text{O} + \text{NAD}^+ \quad \xrightarrow{ALD} \quad \text{C}_2\text{H}_4\text{O} + \text{NADH} + \text{H}^+ \qquad (R1)$$

$$\text{C}_2\text{H}_6\text{O} + \text{NADPH} + \text{H}^+ + \text{O}_2 \quad \xrightarrow{CYT} \quad \text{C}_2\text{H}_4\text{O} + \text{NADP}^+ + 2\ \text{H}_2\text{O} \quad (R2)$$

$$\text{C}_2\text{H}_4\text{O} + \text{NAD}^+ \quad \xrightarrow{ALDH} \quad \text{C}_2\text{H}_3\text{O}_2 + \text{NADH} + \text{H}^+ \qquad (R3)$$
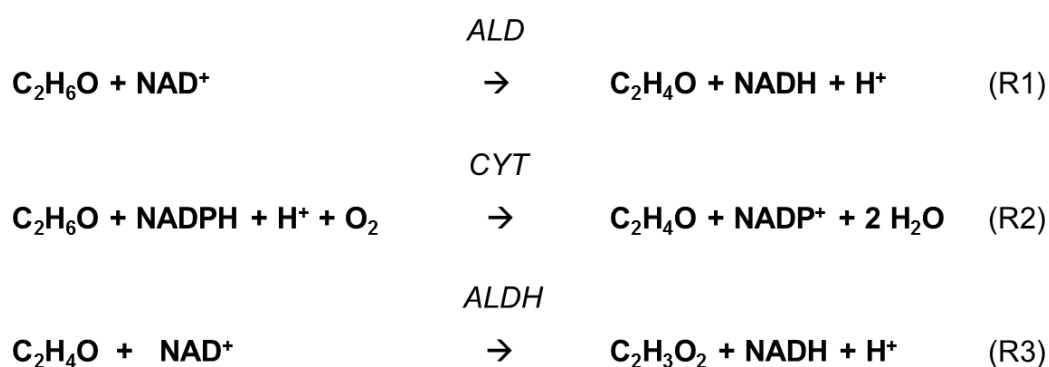
Figure 1.3 Production of acetaldehyde (C$_2$H$_4$O) from the enzymatic oxidation of ethanol (C$_2$H$_6$O) by alcohol dehydrogenase (*ALD*) and cytochrome P450 isoenzymes (*CYT*), and the production of acetate (C$_2$H$_3$O$_2$) from aldehyde dehydrogenase (*ALDH*) activity. NAD$^+$: Nicotinamide adenine dinucleotide (oxidised); NADH: Nicotinamide adenine dinucleotide (reduced); NADP$^+$: Nicotinamide adenine dinucleotide phosphate (oxidised); NADPH: Nicotinamide adenine dinucleotide phosphate (reduced); H$^+$: Proton; O$_2$: Oxygen; H$_2$O: Water.

The photodegradation of chromophoric dissolved organic matter (CDOM) also represents an important pathway for acetaldehyde synthesis (Kieber et al. 1990). CDOM is comprised of complex macromolecular coloured materials, including humic substances, which predominantly originate from degraded plant matter derived from terrestrial systems (de Bruyn et al. 2011), but are also produced via phytoplankton degradation, zooplankton grazing and viral activities (Zhang et al. 2009). The photoproduction of acetaldehyde and other low molecular weight carbonyl compounds, such as formaldehyde and pyruvate, is initiated by the absorption of ultraviolet light between 280 - 320 nm (UV-B) by CDOM found

in the sea-surface microlayer (Kieber et al. 1990; de Bruyn et al. 2011). This in turn causes destruction of the chromophores and CDOM photobleaching (Vecchio & Blough 2002), and simultaneously increases the bioavailability of dissolved organic carbon (Reche et al. 2000) in the form of acetaldehyde and other carbonyl compounds. These compounds can enter the atmosphere through air-sea gas exchange or are utilised by bacteria, resulting in an ocean mixed layer lifetime of 0.3 - 12 hours for acetaldehyde (Table 1.1; Millet et al. 2010).

1.3 Industrial and commercial significance

Whilst occurring widely in nature, acetaldehyde is frequently used in many industrial processes and is regularly found in commercial products that are consumed daily by the public (Table 1.2). Often, these industries are highly dependent on both the inherent properties and activities of acetaldehyde to make significant profits, and in some cases, the use of acetaldehyde can support multi-million or -billion dollar industries. For example, the estimated worth of the global alcoholic drinks market was valued at $979 billion in 2007 (Jernigan 2012), and is currently predicted to reach $1,452 billion by 2020 (P&S Market Research 2015). Acetaldehyde is a natural by-product of the fermentation and vinification processes that occur during the production of beer and wine (Osborne et al. 2000; Wang et al. 2013). In beer, acetaldehyde accounts for ~90% of all carbonyl compounds and is one of the main contributors to overall flavour (Wang et al. 2013), with excess concentrations resulting in grassy, off-tastes, while optimal concentrations exhibit fruity and pleasant qualities (Liu & Pilone 2000). Additionally, it is understood that the balance of aldehydes during beer storage is particularly important to overall shelf-life (Baert et al. 2015), and excessive acetaldehyde concentrations can promote beer staling (Wang et al. 2013).

Acetaldehyde is also critical to the development of flavour and aroma in wine, imparting strong, pungent odours at high concentrations and subtle fruity notes at low concentrations, but also has an important role in colour development and astringency (Osborne et al. 2000;

Sheridan & Elias 2015). The colour of red wine, for example, is brought about by the direct condensation between phenolic compounds such as anthocyanins and tannins, which is a very gradual process under normal conditions. However, as shown by Sheridan & Elias (2015), the presence of acetaldehyde catalyses this reaction and increases colour intensity and stability. Within the study, the application of a high exogenous acetaldehyde treatment accelerated the chemical ageing process of fermenting grapes, as a result of elevated tannin modification. Moreover, the high acetaldehyde treatment significantly reduced the formation of protein-tannin precipitates, suggesting fewer tannin interactions with salivary proteins and possible reductions in perceived astringency. These results, in combination with the recognised and established role of acetaldehyde in beer production, demonstrate the extent to which the alcohol industry, and its estimated value, is dependent on the activities and properties of acetaldehyde for success. Furthermore, this also illustrates how consumer perception of taste and aroma is greatly mediated by acetaldehyde.

Table 1.2 Summary of consumable products found to contain acetaldehyde. Data summarised from Liu & Pilone (2000) and Ghica et al. (2007).

Fruit & Vegetables	Dairy	Meats	Beverages
Apples	Butter	Cooked Beef	Apple Juice
Banana	Cheese (e.g. Cottage)	Cooked Chicken	Beer
Broccoli	Milk (heated)		Brandy
Grapefruit	Sour Cream		Cider
Grapes	Yoghurt		Coffee
Lemons			Cognac
Mushrooms			Perry
Onions			Red Wine
Oranges			Rum
Peaches			Saké
Pears			Sherry
Pineapples			Sweet Wine
Raspberries			Whiskey
Strawberries			White Wine

Acetaldehyde is also important to the dairy and coffee industries (Sanz et al. 2002; Weschenfelder et al. 2015; Zha et al. 2015), particularly for its effect on flavour. The taste and aroma of coffee, for example, can be attributed to the wide range of volatiles that are produced and lost during coffee bean processing; involving more than 800 volatiles, which must be delicately balanced to ensure quality and consumer preference (Weschenfelder et al. 2015). As shown by Semmelroch & Grosch (1995) using gas-chromatography headspace analysis, acetaldehyde is a major constituent of the popular Arabica and Robusta coffees and bestows fruity and pungent characteristics which enable clear distinctions between the two varieties. In this study, it was determined that brewed Arabica coffee had twice the acetaldehyde odour potency of brewed Robusta coffee (Semmelroch & Grosch 1995). These findings are supported by Sanz et al. (2002), who demonstrated that the volatile compound profile of Arabica coffee is dominated by aldehydes, including acetaldehyde, whilst Robusta coffee is mostly composed of sulphur compounds; accounting for differences in taste, aroma and commercial price (Sanz et al. 2002). Consequently, through its inherent

characteristics, acetaldehyde is essential to the coffee industry by enabling the production of a range of coffee varieties. This equates to substantial economic impacts and demonstrates the importance of acetaldehyde to a commodity ranked second only to petroleum in the world economy (Weschenfelder et al. 2015).

In addition to the industries previously mentioned, acetaldehyde is regularly used in the manufacture of goods including perfumes, basic dyes and construction materials such as polyester resins, and is often utilised as a food preservative, flavouring agent, and a solvent in the rubber and paper industries (U.S. Environmental Protection Agency 2000). Further highlighting its wide range of applications is the use of acetaldehyde in the fracking industry, where it is employed as a corrosion inhibitor in pipes used to remove fracking liquid containing shale gas (Meegoda et al. 2016). Accordingly, despite limited public awareness, acetaldehyde plays a central role in many everyday activities, and is integral to a considerable number of industries worth billions to the global economy. Due to the regular use of acetaldehyde, these industries also represent important anthropogenic sources of acetaldehyde to the atmosphere.

1.4 Health implications

Acetaldehyde is classified as a contaminant in drinking water by the US EPA and has a permissible exposure level of 200 ppm (National Institute for Occupational Safety and Health (2014)). Being found both naturally and artificially in many consumable products (Table 1.2), humans are continuously exposed to low levels of acetaldehyde. However, exposure can occasionally exceed safe limits (>2.5 mg kg^{-1} body weight day^{-1}; National Center for Biotechnology Information (2021)) and may become harmful. The severity of harm can vary enormously, with detrimental effects to the human body taking both acute and chronic forms. An evening of heavy alcohol consumption, for example, may bring about classic symptoms of a hangover such as tiredness, nausea and headache, due to the effect of acetaldehyde

on dopaminergic neurons in the brain (Stock et al. 2016). Alternatively, prolonged and excessive alcohol consumption, as seen in people exhibiting alcoholic behaviours, can result in more complex and life-threatening issues. These can include liver disease, resulting from the toxic effects of acetaldehyde on liver cell organelles such as mitochondria (Nuutinen et al. 1983; Setshedi et al. 2010), and the development of gastrointestinal, oesophageal and colorectal cancers due to the binding of acetaldehyde to DNA and cellular proteins (Jin et al. 2015). Such complications can also arise through a genetic polymorphism which effects the mitochondrial class 2 aldehyde dehydrogenase enzyme (ALDH2) found in humans, responsible for acetaldehyde metabolism. This polymorphism is caused by a point mutation in the ALDH2 gene, which subsequently induces a glutamic acid to lysine substitution, and a reduced ability of ALDH2 to metabolise acetaldehyde (Jin et al. 2015). The reduced efficiency of ALDH2 results in an accumulation of acetaldehyde, which aside from increasing the risk of liver disease and cancer, provokes a flushed and red appearance on the faces of affected drinkers termed "Asian flush syndrome"; thought to affect 40% of the East Asian population, and 500 million people worldwide (Väkeväinen et al. 2000; Jin et al. 2015)

The adverse health effects associated with acetaldehyde are not restricted to the consumption of alcohol, as shown in a study by Fujioka & Shibamoto (2006). Using gas chromatography it was demonstrated that cigarette smoke derived from 14 commercial brands contained a wide range of toxic carbonyl compounds including acetaldehyde and formaldehyde (Fujioka & Shibamoto 2006). Interestingly, acetaldehyde was shown to have the largest concentration of all carbonyl compounds analysed, with measurements ranging from 1110 μg to 2101 μg per cigarette: an order of magnitude larger than any other measured carbonyl. Due to its known involvement in carcinogenesis, such high concentrations of acetaldehyde pose a significant risk to smokers after inhalation. Moreover, smoking is associated with a variety of other diseases such as atherosclerosis (Siasos et al. 2014), and therefore a potential etiological role of acetaldehyde cannot be dismissed. Acetaldehyde is also recognised as an air pollutant, particularly in highly urbanised

environments (Altemose et al. 2015), and consequently poses similar health risks to smoking.

1.5 Terrestrial sources and sinks

The terrestrial biosphere represents an important source of carbon to the atmosphere, which primarily takes the form of CO_2 emissions (Guenther 2002). However, as previously mentioned, VOC emissions also constitute a considerable proportion of the total carbon that enters the atmosphere. Guenther et al. (1995), for example, reported global vegetative VOC emissions of 1150 Tg C a^{-1}, which is suggested to account for approximately 90% of global surface VOC emissions (Lathìere et al. 2006). OVOCs are thought to have a particularly large terrestrial source, and contribute as much as 150 - 500 Tg C to the atmosphere every year (Singh et al. 2004). Based on the global model of VOCs from natural sources developed by Guenther et al. (1995), a substantial quantity of terrestrial OVOCs are of biogenic origin, and acetaldehyde, which makes up a large fraction of the total OVOC flux (Singh et al. 2004), is also biogenically sourced (Guenther et al. 1995).

Estimates of the global acetaldehyde budget range between 205 - 213 Tg a^{-1} (Singh et al. 2004; Millet et al. 2010), most of which is attributed to atmospheric production. Within the last two decades, estimates of global annual biogenic acetaldehyde emissions have varied, but ultimately demonstrate a significant source of acetaldehyde from terrestrial plant growth and decay, with reported measurements ranging between 10 - 50 Tg a^{-1} (Singh et al. 2004; Wiedinmyer et al. 2004; Lathìere et al. 2006; Millet et al. 2010). In plants, acetaldehyde can be produced via the decarboxylation of pyruvate during ethanol fermentation, in response to environmental stressors such as anoxia (Tadege et al. 1999). In areas experiencing wet and dry seasons and in regions susceptible to flooding, this stress response is a large potential source of acetaldehyde. Moreover, it is suggested that acetaldehyde is synthesised and emitted by plants in response to a variety of other stressors such as herbivory, mechanical

wounding and disease (Jardine et al. 2009). Under these abiotic and biotic stresses acetaldehyde can act as an antimicrobial (Utama et al. 2002) and a herbivore deterrent (Loreto & Schnitzler 2010), which enhances overall plant survival. However, the exchange of acetaldehyde with the atmosphere is not unidirectional, and is dependent on the ambient acetaldehyde concentration (Jardine et al. 2008). When ambient acetaldehyde concentrations exceed those found within plant leaves, termed the "compensation point", acetaldehyde is taken up and terrestrial vegetation is recognised as an acetaldehyde sink (Seco et al. 2007). Compensation points vary between plant species and depend on factors such as leaf age and temperature (Jardine et al. 2008). Therefore, terrestrial vegetation can simultaneously represent a source and sink of acetaldehyde depending on local environmental conditions, plant health and species-specific compensation points.

Soils and leaf litter have also been identified as minor contributors to terrestrial biogenic acetaldehyde production, although experimental evidence in the literature is limited (Schade & Goldstein 2001; Seco et al. 2007). Schade & Goldstein (2001) demonstrated that acetaldehyde is emitted from bare soils at a rate of 0.05 mg C m^{-2} h^{-1}. Interestingly, emissions were maintained overnight, suggesting that acetaldehyde flux was unlikely to be the result of abiotic processes such as photodegradation. Furthermore, acetaldehyde emission exhibited a strong positive correlation with increasing temperature, and was enhanced by wet soil conditions, indicating that soil microorganisms may be responsible for production, however this was not investigated during the study.

Anthropogenic acetaldehyde emissions from terrestrial systems have been estimated to range up to 2 Tg a^{-1} (Singh et al. 2004; Millet et al. 2010). A significant proportion of these emissions can be attributed to exhaust fumes and other combustion sources such as fossil-fuelled power plant emissions (Atkinson 2000). In 2009, it was estimated that 700 million vehicles were in use around the world, and that by 2050 this number would reach over 2 billion (Balat & Balat 2009), suggesting that total anthropogenic acetaldehyde emissions will

substantially increase during the next 30 years. Reinforcing this prediction is the current rise in popularity of biofuels, particularly those based on ethanol, which are viewed as "greener" alternatives to conventional petrol and diesel fuels (Hansen et al. 2005), but have the disadvantage of increased acetaldehyde exhaust emissions (Balat & Balat 2009). A study by Jacobson (2007), for example, modelled the effects of converting all vehicles in the United States from gasoline to ethanol based fuels, and demonstrated that the use of E85 fuel (85% ethanol, 15% gasoline) would result in a 1250 - 4340% increase in acetaldehyde emissions compared to the use of gasoline (Jacobson 2007). Consequently, the current trend in encouraging the use of eco-friendly fuels as a fossil-fuel alternative may in fact have unforeseen negative impacts on atmospheric chemistry and the climate. Moreover, elevated acetaldehyde emissions associated with the use of bioethanol fuels could significantly affect urban air quality and public health, with Jacobson (2007) predicting a 4% increase in ozone-related mortality, hospitalisation and asthma in the United States alone due to the complete conversion to E85 fuel.

In addition to exhaust and combustion emissions, it is understood that industrial operations, fuel storage, landfills and solvent usage are all important anthropogenic sources of acetaldehyde (Atkinson 2000). Biomass burning, which involves the burning of live and dead vegetation, also represents a significant source of acetaldehyde, with the most recent emission estimates ranging between 3 - 10 Tg a^{-1} (Singh et al. 2004; Millet et al. 2010). Although biomass burning events can be initiated naturally, around 90% occur due to human activities, primarily for the purpose of deforestation, harvesting practices and clearing land for agriculture (Koppmann et al. 2005). With the global population increasing, and with it growing demands for food and land (Godfray et al. 2010), it is likely that biomass burning practices will become more frequent, particularly in developing countries (Koppmann et al. 2005). Accordingly, this will result in elevated emissions of acetaldehyde and an increase in the relative contribution of anthropogenic emissions to the global total.

1.6 Marine sources

The ocean covers around 70% of the Earth's surface and is recognised as a significant source and sink of volatile gases (Lewis et al. 2005; Andrews et al. 2015). In particular, the upper 1 mm of the ocean surface, termed the sea-surface microlayer (SSM) (Cunliffe & Murrell 2009), is key to the bidirectional exchange of volatile gases between the ocean and the atmosphere. This surface is in direct contact with a part of the atmosphere referred to as the marine boundary layer; a well-mixed atmospheric layer that exchanges heat, moisture and momentum with the ocean (Sikora & Ufermann 2004). Additionally, the SSM contains a complex mixture of inorganic and organic compounds (Carpenter & Nightingale 2015), which are regularly transferred between the air-sea interface. However, despite being identified as an important source of volatile gases, the SSM remains fairly unexplored, and knowledge regarding the magnitude of marine volatile emissions is limited (Nightingale et al. 2000).

The role of the ocean as a source of OVOCs is particularly understudied (Singh et al. 2003), and estimates of marine acetaldehyde flux are restricted to a small number of studies. Recent model estimates, based on the global distribution of CDOM light absorption, suggest that net ocean acetaldehyde emissions total 57 Tg a^{-1} and account for approximately 27% of all acetaldehyde emissions (Millet et al. 2010); making the ocean the second largest global source of acetaldehyde. This is further supported by Read et al. (2012), who reported a net ocean acetaldehyde source of 38 Tg a^{-1} using the CAM-Chem global chemical transport model (Read et al. 2012). In contrast, previous estimates by Singh et al. (2004) identified the ocean as the largest global source of acetaldehyde, with an oceanic flux of 125 Tg a^{-1}. This shows that there is considerable uncertainty regarding marine acetaldehyde emissions, which must be addressed if its total global source is to be accurately quantified, and to further establish how this influences atmospheric chemistry. However, from these studies it is evident that oceanic sources of acetaldehyde likely exceed those of terrestrial systems (Section 1.5), and this requires further investigation.

Empirical studies have demonstrated that marine acetaldehyde concentrations are found in the low nanomolar range (Table 1.3). Zhou & Mopper (1997) measured acetaldehyde concentrations of 1.38 nM in subsurface waters of the Sargasso Sea, and enriched concentrations of 16 - 38 nM in the SSM, as a result of reduced mixing (Zhou & Mopper 1997). Acetaldehyde concentrations also exhibited a diel cycle (Table 1.3), with subsurface and SSM concentrations reaching their maximum at 3pm local time, decreasing throughout the evening, and maintaining a constant level during the night and early morning; suggesting a strong photochemical influence. More recently, Kameyama et al. (2010) reported maximum acetaldehyde concentrations of 5.9 nM in surface waters of the western North Pacific Ocean, whilst Beale et al. (2013) measured concentrations ranging between 3 - 9 nM across a transect of the Atlantic Ocean. In contrast to previous studies, Beale et al. (2013) observed a weak correlation between acetaldehyde concentration and solar insolation, suggesting that a photochemical diurnal cycle does not exist below the SSM. Yang et al. (2014) measured similar surface concentrations of 4 - 9 nM in the Atlantic Ocean, but also demonstrated that acetaldehyde is supersaturated in seawater and is continuously emitted to the atmosphere. As previously mentioned (Section 1.2), CDOM photodegradation represents an important pathway for acetaldehyde synthesis in seawater (Kieber et al. 1990). Accordingly, a substantial proportion of acetaldehyde measured in surface waters can be attributed to this production process, with Dixon et al. (2013) reporting upper photochemical production values of 68% (Dixon et al. 2013). The remaining ~30% of surface acetaldehyde could result from the biodegradation of organic matter (Singh et al. 2003), or a steady supply from deep-ocean upwelling regions (Mopper & Kieber 1991; Beale et al. 2013), however, this has not been investigated in any study to date.

Seawater concentrations of acetaldehyde are comparable to those of dimethylsulfide (DMS) and dimethylsulfoxide (DMSO) but are significantly lower than surface seawater methanol concentrations (Table 1.3). In the Atlantic Ocean, DMS concentrations ranging from 0.9 nM to 2.1 nM have been reported (Williams et al. 2004; Bell et al. 2006), whilst higher

concentrations of 4.91 nM and 19.9 nM have been measured in the East China Sea and South Pacific Ocean, respectively (Lee et al. 2010; Yang et al. 2012). Similar DMSO concentrations have been reported in the Gulf of Mexico, with Kiene et al. (1994) reporting surface concentrations of 1 - 13 nM, whilst significantly higher DMSO concentrations of 4 - 160 nM were measured in the Southern Ocean (Asher et al. 2017). Methanol concentrations of 97 - 237 nM and 158.9 nM have been reported in surface waters of the Atlantic Ocean and North Pacific Ocean, respectively (Dixon et al. 2011; Read et al. 2012; Williams et al. 2004), demonstrating that acetaldehyde is considerably less abundant than methanol in the marine environment. This suggests that less acetaldehyde than methanol is produced in the open ocean or that a significant proportion of acetaldehyde is lost through microbial degradation, turbulent mixing, photochemical degradation, or exchange across the air-sea interface.

Acetaldehyde cycling in the marine environment involves both abiotic and biotic processes. Alongside CDOM photodegradation, which is recognised as the primary marine abiotic source of acetaldehyde, the demethylation pathway of dimethylsulfoniopropionate (DMSP) represents an important, yet less well known, biotic source of acetaldehyde. This pathway is initiated by the demethylation of DMSP to methylmercaptopropionate (MMPA) via the DMSP demethylase, DmdA (Curson et al. 2011); with the resulting methyl group accepted by tetrahydrofolate. MMPA is catabolised to the intermediates methylmercaptopropionate-CoA (MMPA-CoA) and methylthioacryloyl-CoA (MTA-CoA) by DmdB (3-methylmercapto-propionyl-CoA ligase) and DmdC (3-methylmercaptopropionyl-CoA dehydrogenase) enzyme activity, respectively (Curson et al. 2011). In the final reaction of the pathway, MTA-CoA is converted to acetaldehyde and CO_2 via the methylthioacryloyl-CoA hydratase, DmdD. The demethylation of DMSP to acetaldehyde has been observed in members of the Proteobacteria, including *Candidatus* Pelagibacter ubique (SAR11) and the *Roseobacter* clade, both of which are highly abundant and widely distributed in the marine environment (Morris et al. 2002; Wagner-Döbler & Biebl 2006) and thus have a potentially significant

impact on global acetaldehyde production. Marine acetaldehyde cycling is also significantly affected by the direct and indirect activities of phytoplankton. The diatom, *Thalassiosira pseudonana*, for example, has been shown to produce acetaldehyde in a light-dependent manner, with Halsey et al. (2017) measuring an acetaldehyde production rate of 160 μmol (g Chl α h)$^{-1}$ when cultures were exposed to a light intensity of 1500 μmol photons m^{-2} s^{-1}. This finding suggests that other phytoplankton species may also directly contribute to acetaldehyde production in the marine environment, although production is likely to vary by species and environmental conditions. Viral-induced lysis, senescence, and the grazing of phytoplankton by zooplankton have also been identified as important indirect sources of acetaldehyde through the release and subsequent bacterial degradation of DMSP (Curson et al. 2011).

Physicochemical and biological loss processes help to maintain the balance of the marine acetaldehyde cycle. As discussed in Section 1.7, the microbial degradation of acetaldehyde in the marine environment accounts for a significant proportion of acetaldehyde loss (Dixon et al. 2013; Halsey et al. 2017) and limits the exchange of acetaldehyde across the air-sea interface. This reduces the amount of acetaldehyde that reaches the atmosphere, which affects chemical reactions involved in maintaining the atmosphere's oxidative status, the residence time of greenhouse gases, and the formation of cloud condensation nuclei. Acetaldehyde may also be lost by turbulent mixing into the deep ocean (Carpenter et al. 2012) or by photochemical destruction in the marine boundary layer (Schlundt et al. 2017).

Importantly, acetaldehyde production is not restricted to the open ocean. Coastal and estuarine regions have also been identified as key sources of carbonyl compounds, including acetaldehyde, via CDOM photodegradation (Kerner & Edelkraut 1995; de Bruyn et al. 2011). Moreover, it is suggested that these sources are considerably underestimated in global models, and salt marshes in particular represent a significant source of carbonyl

compounds due to their high primary productivity (de Bruyn et al. 2011). The production of acetaldehyde in these environments may also be linked to the bacterial fermentation of organic matter in anoxic sediments that are typically found in estuaries and salt marshes. Furthermore, the bacterial demethylation of DMSP released by estuarine phytoplankton, such as diatoms, could be a potentially significant additional source of acetaldehyde that has not yet been considered in global models. Consequently, a potential acetaldehyde production gradient exists between the open ocean and coastal/estuarine environments, which could substantially alter future estimates of marine acetaldehyde emissions.

Table 1.3 Summary of seawater VOC concentrations (nM) measured from the surface (0.2 - 200 m) and sea-surface microlayer (SSM) of marine environments. Where available, data include the exact sampling depth below the surface and the time of sampling. DMS: dimethylsulfide; DMSO: Dimethylsulfoxide.

VOC	Open Ocean/Coastal Region	Sampling depth	Time of Day	Concentration (nM)	Source
Acetaldehyde	Whitewater Bay, Gulf of Mexico	Surface (0.3 m)	20:00-06:00	2-3	Mopper & Stahovec (1986)
		Surface (0.3 m)	14:00-15:00	20-30	Mopper & Stahovec (1986)
	Station BSK2, Black Sea	Surface (30 m)	NA	5.6	Mopper & Kieber (1991)
		Surface (200 m)	NA	6.1	Mopper & Kieber (1991)
	Hatchet Bay, Sargasso Sea	Surface (0.2 m)	20:00-06:00	1.38	Zhou & Mopper (1997)
		Surface (0.2 m)	14:30-15:00	7	Zhou & Mopper (1997)
		SSM (150 µM)	18:00-06:00	8-15	Zhou & Mopper (1997)
		SSM (150 µM)	09:00-16:00	16-38	Zhou & Mopper (1997)
	Pacific Ocean	Surface	NA	7	Singh et al. (2003)
	Western subarctic North Pacific Ocean	Surface (0.5-5 m)	NA	5.9*	Kameyama et al. (2010)
	Mauritanian upwelling, Atlantic Ocean	Surface	NA	4.9	Dixon et al. (2013)
		Surface (200 m)	NA	9.4	Dixon et al. (2013)
	Atlantic Ocean (Falmouth, UK - Punta Arenas, Chile)	Surface (5 m)	NA	3-9	Beale et al. (2013)
		Surface (17 m)	NA	3-12	Beale et al. (2013)
		Surface (200 m)	NA	3-16	Beale et al. (2013)
	Atlantic Ocean (Southampton, UK - Punta Arenas, Chile)	Surface (5 m)	NA	4-9	Yang et al. (2014)
DMS	Tropical North Atlantic Ocean	Surface (5 m)	NA	1.66	Williams et al. (2004)
	Atlantic Ocean	Surface (<10 m)	NA	0.9-2.1	Bell et al. (2006)
	South Pacific Ocean	Surface (3-200 m)	NA	0.1-19.9	Lee et al. (2010)
	Yellow Sea & East China Sea	Surface (126 m)	NA	4.91	Yang et al. (2012)
DMSO	Mobile Bay, Gulf of Mexico	Surface	NA	1-13	Kiene et al. (1994)
	Palmer Station, Southern Ocean	Surface	NA	4-160	Asher et al. (2017)
Methanol	Tropical North Atlantic Ocean	Surface (5 m)	NA	118.4	Williams et al. (2004)
	North Pacific Ocean	Surface (5 m)	NA	158.9	Kameyama et al. (2010)
	Western English Channel (coastal station L4)	Surface (55 m)	NA	97	Dixon et al. (2011)
	Atlantic Ocean	Surface (5 m)	NA	121-237	Read et al. (2012)

[*] Maximum value is reported, as majority of data below 4 nM detection limit. NA: Data not available.

1.7 Marine sinks

The role of the ocean as a sink for OVOCs is largely unexplored (Singh et al. 2003), and is particularly apparent with the exclusion of a marine sink term in the most recent global models of acetaldehyde. However, the marine environment possesses a considerable abundance of microbial life, estimated at 10^3 - 10^6 cells per mL in surface seawater (Zubkov et al. 2007), which is functionally diverse and capable of mediating global biogeochemical cycles, including the consumption of acetaldehyde (de Bruyn et al. 2017). By enriching surface seawater with ^{14}C-labelled acetaldehyde, Dixon et al. (2013) demonstrated that microbial consumption in the Atlantic Ocean reduced net surface acetaldehyde production rates by 49 - 92% and 60 - 100% in coastal and open ocean regions, respectively (Dixon et al. 2013). After correcting for rates of microbial oxidation measured in Atlantic Ocean surface waters, Beale et al. (2013) suggested that the global oceanic flux of acetaldehyde to the atmosphere may in fact equate to 17 Tg a^{-1}, which is markedly lower than previously modelled estimates (Singh et al. 2004; Millet et al. 2010; Read et al. 2012). Future modelling efforts therefore must include a microbial sink term to accurately predict marine emissions and reliably quantify the total global source of acetaldehyde. This will require further investigation of microbial oxidation in other marine environments to ensure that the rates of consumption compare to those observed in the Atlantic Ocean.

Although these findings indicate that marine acetaldehyde concentrations are under considerable microbial control, the identity and diversity of acetaldehyde degraders remains largely unknown. Liu et al. (2015) isolated *Shewanella mangrovi* from mangrove sediments collected from Zhangzhou, China, and reported acetaldehyde degradation at concentrations as high as 22.7 mM (1000 mg L^{-1}). Halsey et al. (2017) demonstrated that two strains of *Pelagibacter* SAR11, namely HTCC1062 and HTCC7211, could utilise acetaldehyde as a carbon and energy source, with ~70% of acetaldehyde dissimilated to CO_2 and the remaining ~30% assimilated into cell biomass. Due to the wide distribution and abundance

of the SAR11 clade in the marine environment, it was estimated that the global SAR11 community could oxidise more acetaldehyde than is currently estimated to be produced, and that the majority of acetaldehyde in the marine environment is prevented from reaching the atmosphere (Halsey et al. 2017). Gao et al. (2018) isolated 12 acetaldehyde-degrading bacteria from 2000 m deep seawater of the West Pacific Ocean, belonging to the genera *Vibrio, Halomonas, Pseudoalteromonas, Pseudomonas*, and *Bacillus*. Three strains with close identity to *Halomonas axialensis*, *Halomonas meridiana*, and *Vibrio parahaemolyticus* demonstrated the ability to degrade 7.9 mM (350 mg L^{-1}) of acetaldehyde in 24 hours and could tolerate concentrations of 34.1 mM (1500 mg L^{-1}) (Gao et al. 2018). These findings suggest that a diverse group of microorganisms contribute to acetaldehyde degradation in the marine environment, however, our knowledge of their diversity is far from complete and it is likely that a considerable number of acetaldehyde-degrading microorganisms have yet to be discovered.

1.8 Freshwater and estuarine sources and sinks

In comparison to the marine environment, the sources and sinks of acetaldehyde in freshwater rivers and estuaries have been severely understudied and current models of the global acetaldehyde budget do not include acetaldehyde emissions from these environments. Due to their close association with terrestrial systems, rivers and estuaries receive regular inputs of degraded plant matter that represent an important source of CDOM (de Bruyn et al. 2011). As mentioned in Section 1.2, the photodegradation of CDOM results in the formation of low molecular weight carbonyl compounds, including acetaldehyde (de Bruyn et al. 2011), suggesting that acetaldehyde emissions from rivers and estuaries may be considerable, particularly during summer. Roebuck et al. (2016) also identified the microbial breakdown of organic matter during fermentation as an important source of acetaldehyde in freshwater sediments, with slower production rates during autumn and winter allowing acetaldehyde to diffuse into the overlying water column. Metaldehyde, a cyclic-tetramer of

acetaldehyde (Figure 1.4) that is commonly used as a molluscicide in domestic gardens and agriculture (Castle et al. 2017; Thomas et al. 2017), has also been identified as a potentially important anthropogenic source of acetaldehyde in rivers. The microbial degradation of metaldehyde in soils has been shown to involve the oxidation of metaldehyde to a linear hemiacetal via the activity of 2-oxoglutarate-dependent oxidase enzymes, which cleave the metaldehyde ring (Castro-Gutiérrez et al. 2020). The hemiacetal intermediate is then iteratively degraded by a lyase enzyme to produce acetaldehyde (Castro-Gutiérrez et al. 2020). Although metaldehyde-degrading microorganisms have yet to be discovered in freshwater environments, it is possible that metaldehyde represents an important additional source of acetaldehyde in freshwater systems.
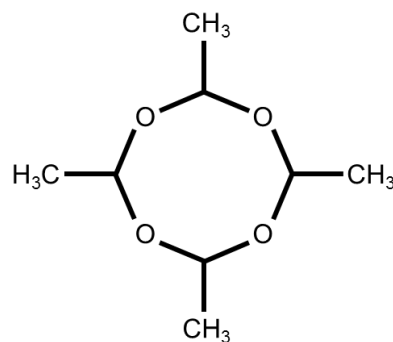
Figure 1.4 Molecular structure of metaldehyde ($C_8H_{16}O_4$). Metaldehyde is a cyclic-tetramer of acetaldehyde (C_2H_4O) that is commonly used as a molluscicide.

Current understanding of acetaldehyde sinks in freshwater rivers and estuaries is similar to our knowledge of sinks in the marine environment. Only a few acetaldehyde-degrading microorganisms have been isolated from freshwater and estuarine environments, all of which perform acetaldehyde degradation under anaerobic conditions. For example, Schmidt et al. (2014) identified the strictly anaerobic *Pelobacter carbinolicus* and *P. acetylenicus* as acetaldehyde degraders, with these species isolated from brackish water sediment and freshwater sewage sludge, respectively (Schmidt et al. 2014). Trifunović et al. (2020) also demonstrated that *Acetobacterium woodii*, an acetogenic bacterium isolated from marine

estuary sediments in Woods Hole, Massachusetts (Balch et al. 1977), could grow

anaerobically on 5 mM of acetaldehyde. To date, no aerobic acetaldehyde degraders have

been isolated from freshwater or estuarine environments, although it is well-established that

acetaldehyde degradation can occur via oxidative fermentation to produce acetic acid

(Matsushita & Matsutani 2016). This is performed by acetic acid bacteria, such as members

of the genus *Acetobacter*, which belong to the Acetobacteraceae and are widespread in

nature (Gomes et al. 2018). Acetic acid bacteria oxidise ethanol to acetaldehyde via a

membrane-bound pyrroloquinoline quinone-dependent alcohol dehydrogenase, with

acetaldehyde oxidised to acetic acid by a membrane-bound aldehyde dehydrogenase

(Gomes et al. 2018). These findings demonstrate that the microbial acetaldehyde sink

functions under both aerobic and anaerobic conditions and is likely to be considerably larger

and more diverse than is currently known. Significant research effort is required to improve

our knowledge of acetaldehyde degraders in freshwater and estuarine environments, as well

as the marine environment. This will help to develop a better understanding of the role of

microorganisms in the global acetaldehyde cycle.

1.9 Aims and objectives

VOCs have been extensively studied in the atmosphere and in terrestrial systems, with

research primarily focused on methane, isoprene and DMS. Comparatively, VOC emissions

from rivers, estuaries and the marine environment have been severely understudied, despite

suggestions that these environments may represent significant sources. Consequently, our

knowledge of sources and sinks in riverine, estuarine, and marine environments is limited,

and emission estimates of important VOCs remain somewhat unreliable. This is particularly

evident for acetaldehyde emissions in the marine environment, which range broadly between

17 - 125 Tg a^{-1}. These wide-ranging estimates are partly due to insufficient knowledge

regarding marine acetaldehyde sinks, including microbial degradation, which has been

shown to exert significant control over marine emissions. Despite this, the identification of

these microorganisms has been limited and our understanding of their diversity is almost completely unknown. Furthermore, the metabolic pathway(s) used by microbial acetaldehyde degraders is not fully understood and only a limited number of in-situ microbial acetaldehyde uptake rates have been reported. The uncertainty regarding acetaldehyde emissions in the marine environment is also a result of limited understanding and too few measurements of acetaldehyde production rates. Emission estimates are largely based on CDOM photodegradation, with less consideration given to alternative sources of acetaldehyde, such as the bacterial demethylation of DMSP released by phytoplankton following viral lysis, senescence or grazing by zooplankton. Moreover, it is unclear how production rates and microbial uptake rates are affected by environmental parameters such as temperature and how these rates are influenced by seasonal change. This has resulted in a poor understanding of marine acetaldehyde sources and sinks, culminating in broad emission estimates. As such, our knowledge of the acetaldehyde biogeochemical cycle (Figure 1.5) is limited.
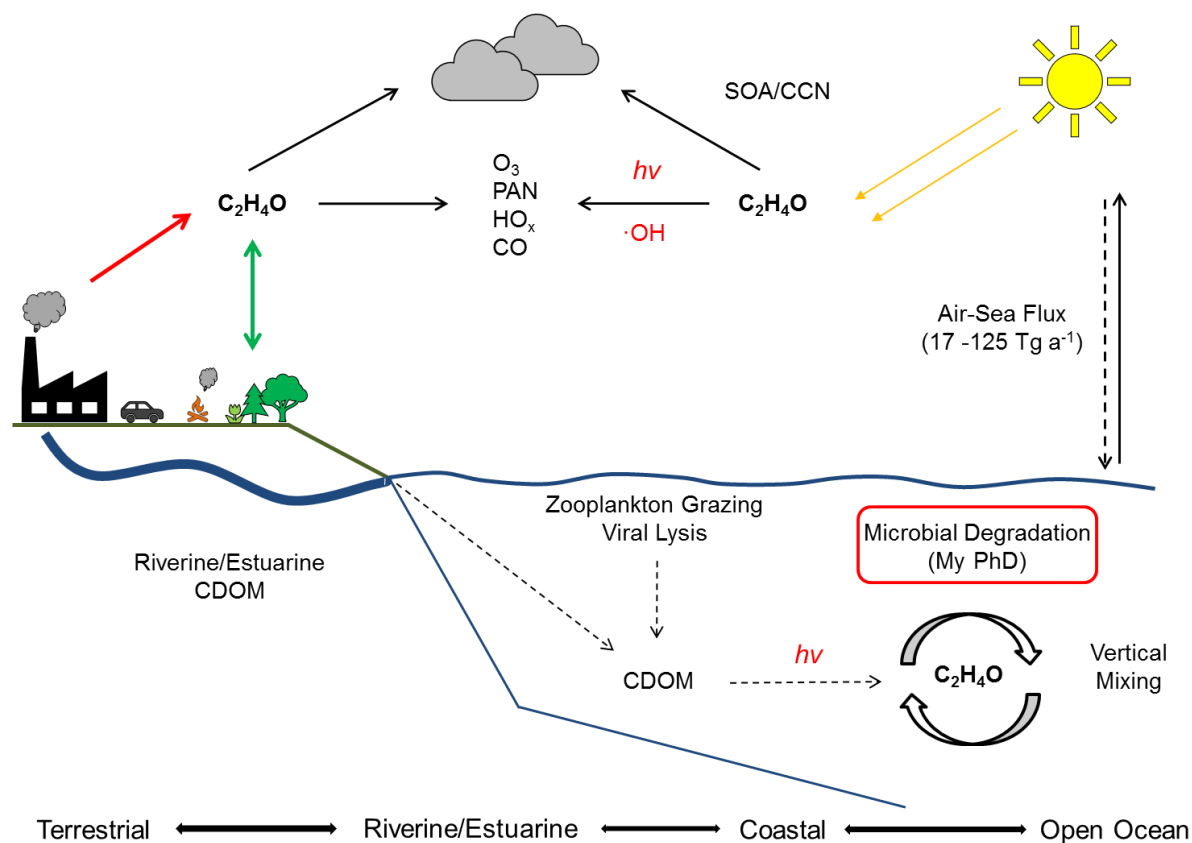
Figure 1.5 Schematic diagram illustrating the biogeochemical cycling of acetaldehyde (C_2H_4O). Dashed arrows represent processes within the pelagic environment, whilst bold arrows denote atmospheric processes. Red and green arrows represent anthropogenic and biogenic sources of acetaldehyde, respectively. O_3: Ozone; PAN: Peroxyacetyl nitrate; HO_x: Hydrogen oxide radicals; CO: Carbon monoxide; SOA: Secondary organic aerosol; CCN: Cloud condensation nuclei; CDOM: Chromophoric dissolved organic matter; ·OH: Oxidation via the hydroxy radical. *Hv*: Photodegradation processes.

Accordingly, the main aim of this research was to identify the microorganisms responsible for acetaldehyde degradation in freshwater, estuarine and marine environments. To achieve this aim, acetaldehyde enrichment experiments, containing water from the Colne Estuary, River Colne and River Gipping, were established and were monitored for degradation and growth. Microorganisms capable of degrading acetaldehyde were isolated, cultivated and

characterised. Following this, 16S rRNA gene amplicon sequencing and whole genome shotgun sequencing were used to conclusively identify these acetaldehyde degraders. Microbial community analysis via the Illumina MiSeq platform was used in conjunction with quantitative PCR (qPCR) to investigate the response of bacterial, archaeal and fungal communities to acetaldehyde. The second aim of this research was to elucidate the metabolic pathway(s) involved in acetaldehyde degradation. Genome annotation and proteomic analysis were used to identify the genetic and enzymatic tools used by a bacterial isolate to degrade acetaldehyde and to provide an insight into the pathway of acetaldehyde metabolism. The third aim of this research was to measure natural rates of acetaldehyde degradation in freshwater, estuarine and marine environments, and to establish the fate of acetaldehyde-derived carbon once utililsed by microorganisms. Uptake rates were measured using ^{14}C-radiolabelling techniques employing ^{14}C-acetaldehyde as a carbon source. Rates of microbial assimilation and dissimilation (oxidation) were calculated for rivers, estuaries and coastal regions of south-west England, in addition to the Colne Estuary. Collectively, the aim of this research was to enhance the current knowledge and understanding of microbial acetaldehyde degradation in the wider environment and to improve our understanding of the global acetaldehyde cycle.

1.10 References

Altemose B, Gong J, Zhu T, Hu M, Zhang L, Cheng H, Zhang L, Tong J, Kipen HM, Ohman-Strickland P, Meng Q, Robson MG, Zhang J (2015) Aldehydes in relation to air pollution sources: A case study around the Beijing Olympics. Atmos Environ 109:61–69

Andrews SJ, Hackenberg SC, Carpenter LJ (2015) Technical note: A fully automated purge and trap GC-MS system for quantification of volatile organic compound (VOC) fluxes between the ocean and atmosphere. Ocean Sci 11:313–321

Asher EC, Dacey JWH, Stukel M, Long MC, Tortell PD (2017) Processes driving seasonal variability in DMS, DMSP, and DMSO concentrations and turnover in coastal Antarctic waters. Limnol Oceanogr 62:104-124

Atkinson R (2000) Atmospheric chemistry of VOCs and NOx. Atmos Environ 34:2063–2101

Atkinson R, Arey J (2003) Gas-phase tropospheric chemistry of biogenic volatile organic compounds: a review. Atmos Environ 37:197–219

Atkinson R, Baulch DL, Cox RA, Crowley JN, Hampson RF, Hynes RG, Jenkin ME, Rossi MJ, Troe J (2006) Evaluated kinetic and photochemical data for atmospheric chemistry: Volume II -- gas phase reactions of organic species. Atmos Chem Phys 6:3625–4055

Baert JJ, De Clippeleer J, De Cooman L, Aerts G (2015) Exploring the binding behavior of beer staling aldehydes in model systems. J Am Soc Brew Chem 73:100–108

Balat M, Balat H (2009) Recent trends in global production and utilization of bio-ethanol fuel. Appl Energy 86:2273–2282

Balbo S, Brooks PJ (2015) Implications of acetaldehyde-derived DNA adducts for understanding alcohol-related carcinogenesis. Biological Basis of Alcohol-Induced Cancer. Springer, Cham, pp 71–88

Balch WE, Schoberth S, Tanner RS, Wolfe RS (1977) *Acetobacterium*, a new genus of

hydrogen-oxidizing, carbon dioxide-reducing, anaerobic bacteria. Int J Syst Bacteriol 27:355–361

Beale R, Dixon JL, Arnold SR, Liss PS, Nightingale PD (2013) Methanol, acetaldehyde, and acetone in the surface waters of the Atlantic Ocean. J Geophys Res Ocean 118:5412–5425

Bell TG, Malin G, McKee CM, Liss PS (2006) A comparison of dimethylsulphide (DMS) data from the Atlantic Meridional Transect (AMT) programme with proposed algorithms for global surface DMS concentrations. Deep-Sea Res PT II 53:1720-1735

Brégonzio-Rozier L, Giorio C, Siekmann F, Pangui E, Morales SB, Temime-Roussel B, Gratien A, Michoud V, Cazaunau M, DeWitt HL, Tapparo A, Monod A, Doussin J-F (2016) Secondary organic aerosol formation from isoprene photooxidation during cloud condensation–evaporation cycles. Atmos Chem Phys 16:1747–1760

Brooks PJ, Zakhari S (2014) Acetaldehyde and the genome: Beyond nuclear DNA adducts and carcinogenesis. Environ Mol Mutagen 55:77–91

de Bruyn WJ, Clark CD, Pagel L, Takehara C (2011) Photochemical production of formaldehyde, acetaldehyde and acetone from chromophoric dissolved organic matter in coastal waters. J Photochem Photobiol A Chem 226:16–22

de Bruyn WJ, Clark CD, Senstad M, Barashy O, Hok S (2017) The biological degradation of acetaldehyde in coastal seawater. Mar Chem 192:13–21

Carpenter LJ, Archer SD, Beale R (2012) Ocean-atmosphere trace gas exchange. Chem Soc Rev 41:6473-6506

Carpenter LJ, Nightingale PD (2015) Chemistry and release of gases from the surface ocean. Chem Rev 115:4015–4034

Castle GD, Mills GA, Gravell A, Jones L, Townsend I, Cameron DG, Fones GR (2017) Review of the molluscicide metaldehyde in the environment. Environ Sci Water Res Technol

3:415–428

Castro-Gutiérrez V, Fuller E, Thomas JC, Sinclair CJ, Johnson S, Helgason T, Moir JWB (2020) Genomic basis for pesticide degradation revealed by selection, isolation and characterisation of a library of metaldehyde-degrading strains from soil. Soil Biol Biochem 142:

Cicerone RJ, Oremland RS (1988) Biogeochemical aspects of atmospheric methane. Global Biogeochem Cycles 2:299–327

Cunliffe M, Murrell JC (2009) The sea-surface microlayer is a gelatinous biofilm. ISME J 3:1001–1003

Curson ARJ, Todd JD, Sullivan MJ, Johnston AWB (2011) Catabolism of dimethylsulphoniopropionate: Microorganisms, enzymes and genes. Nat Rev Microbiol 9: 849-859

Dixon JL, Beale R, Nightingale PD (2011) Microbial methanol uptake in northeast Atlantic waters. ISME J 5:704-716.

Dixon JL, Beale R, Nightingale PD (2013) Production of methanol, acetaldehyde, and acetone in the Atlantic Ocean. Geophys Res Lett 40:4700–4705

Fujioka K, Shibamoto T (2006) Determination of toxic carbonyl compounds in cigarette smoke. Environ Toxicol 21:47–54

Gao B, Shang X, Li L, Di W, Zeng R (2018) Phylogenetically diverse, acetaldehyde-degrading bacterial community in the deep sea water of the West Pacific Ocean. Acta Oceanol Sin 37:54–64

Ghica ME, Pauliukaite R, Marchand N, Devic E, Brett CMA (2007) An improved biosensor for acetaldehyde determination using a bienzymatic strategy at poly(neutral red) modified carbon film electrodes. Anal Chim Acta 591:80–86

Godfray HCJ, Beddington JR, Crute IR, Haddad L, Lawrence D, Muir JF, Pretty J, Robinson S, Thomas SM, Toulmin C (2010) Food security: The challenge of feeding 9 billion people. Science 327:812–818

Gomes RJ, de Fatima Borges M, de Freitas Rosa M, Castro-Gómes RJH, Spinosa WA (2018) Acetic acid bacteria in the food industry: Systematics, characteristics and applications. Food Technol Biotech 56:139-151

Guenther A (2002) The contribution of reactive carbon emissions from vegetation to the carbon balance of terrestrial ecosystems. Chemosphere 49:837–844

Guenther A, Hewitt CN, Erickson D, Fall R, Geron C, Graedel T, Harley P, Klinger L, Lerdau M, Mckay WA, Pierce T, Scholes B, Steinbrecher R, Tallamraju R, Taylor J, Zimmerman P (1995) A global model of natural volatile organic compound emissions. J Geophys Res 100:8873–8892

Guenther A, Karl T, Harley P, Wiedinmyer C, Palmer PI, Geron C (2006) Estimates of global terrestrial isoprene emissions using MEGAN (Model of Emissions of Gases and Aerosols from Nature) Journal. Atmos Chem Phys 6:3181–3210

Guenther A, Zimmerman P, Wildermuth M (1994) Natural volatile organic compound emission rate estimates for U.S. woodland landscapes. Atmos Environ 28:1197–1210

Halsey KH, Giovannoni SJ, Graus M, Zhao Y, Landry Z, Thrash JC, Vergin KL, de Gouw J (2017) Biological cycling of volatile organic carbon by phytoplankton and bacterioplankton. Limnol Oceanogr 62:2650–2661

Hansen AC, Zhang Q, Lyne PWL (2005) Ethanol–diesel fuel blends: A review. Bioresour Technol 96:277–285

Homann N, Jousimies-Somer H, Jokelainen K, Heine R, Salaspuro M (1997) High acetaldehyde levels in saliva after ethanol consumption: Methodological aspects and

pathogenetic implications. Carcinogenesis 18:1739–1743

Homann N, Tillonen J, Salaspuro M (2000) Microbially produced acetaldehyde from ethanol may increase the risk of colon cancer via folate deficiency. Int J Cancer 86:169–173

Jacobson MZ (2007) Effects of ethanol (E85) versus gasoline vehicles on cancer and mortality in the United States. Environ Sci Technol 41:4150–4157

Jardine K, Harley P, Karl T, Guenther A, Lerdau M, Mak JE (2008) Plant physiological and environmental controls over the exchange of acetaldehyde between forest canopies and the atmosphere. Biogeosciences 5:1559–1572

Jardine K, Karl T, Lerdau M, Harley P, Guenther A, Mak JE (2009) Carbon isotope analysis of acetaldehyde emitted from leaves following mechanical stress and anoxia. Plant Biol 11:591–597

Jernigan DH (2012) Global alcohol producers, science, and policy: The case of the International Center for Alcohol Policies. Am J Public Health 102:80–89

Jin S, Chen J, Chen L, Histen G, Lin Z, Gross S, Hixon J, Chen Y, Kung C, Chen Y, Fu Y, Lu Y, Lin H, Cai X, Yang H, Cairns RA, Dorsch M, Su SM, Biller S, Mak TW, Cang Y (2015) ALDH2(E487K) mutation increases protein turnover and promotes murine hepatocarcinogenesis. Proc Natl Acad Sci USA 112:9088–93

Jokelainen K, Nosova T, Koivisto T, Väkeväinen S, Jousimies-Somer H, Heine R, Salaspuro M (1997) Inhibition of bacteriocolonic pathway for ethanol oxidation by ciprofloxacin in rats. Life Sci 61:1755–1762

Jorgenson AK (2006) Global warming and the neglected greenhouse gas: A cross-national study of the social causes of methane emissions intensity, 1995. Soc Forces 84:1779–1798

Kerner M, Edelkraut F (1995) Decomposition of organic matter in aggregated seston from the Elbe estuary: redox dependency and production of low molecular weight DOC

compounds. Mar Ecol Press Ser 123:281–293

Kesselmeier J, Staudt M (1999) Biogenic volatile organic compounds (VOC): An overview on emission, physiology and ecology. J Atmos Chem 33:23–88

Kieber RJ, Zhou X, Mopper K (1990) Formation of carbonyl compounds from UV-induced photodegradation of humic substances in natural waters: Fate of riverine carbon in the sea. Limnol Oceanogr 35:1503–1515

Kiene RP, Gerard G (1994) Determination of trace levels of dimethylsulfoxide (DMSO) in seawater and rainwater. Mar Chem 47:1-12

Kirschke S, Bousquet P, Ciais P, Saunois M, Canadell JG, Dlugokencky EJ, Bergamaschi P, Bergmann D, Blake DR, Bruhwiler L, Cameron-Smith P, Castaldi S, Chevallier F, Feng L, Fraser A, Heimann M, Hodson EL, Houweling S, Josse B, Fraser PJ, Krummel PB, Lamarque JF, Langenfelds RL, Le Quére C, Naik V, O'Doherty S, Palmer PI, Pison I, Plummer D, Poulter B, Prinn RG, Rigby M, Ringeval B, Santini M, Schmidt M, Shindell DT, Simpson IJ, Spahni R, Steele LP, Strode SA, Sudo K, Szopa S, van der Werf GR, Voulgarakis A, van Weele M, Weiss RF, Williams JE, Zeng G (2013) Three decades of global methane sources and sinks. Nat Geosci 6:813–823

Koppmann R, Von Czapiewski K, Reid JS (2005) A review of biomass burning emissions, part I: gaseous emissions of carbon monoxide, methane, volatile organic compounds, and nitrogen containing compounds. Atmos Chem Phys Discuss 5:10455–10516

Lachenmeier DW, Kanteres F, Rehm J (2009) Carcinogenicity of acetaldehyde in alcoholic beverages: risk assessment outside ethanol metabolism. Addiction 104:533–550

Lashof DA, Ahuja DR (1990) Relative contributions of greenhouse gas emissions to global warming. Nature 344:529–531

Latham J, Rasch P, Chen CC, Kettles L, Gadian A, Gettelman A, Morrison H, Bower K,

Choularton T (2008) Global temperature stabilization via controlled albedo enhancement of low-level maritime clouds. Phil Trans R Soc A 366:3969–3987

Lathìere J, Hauglustaine DA, Friend AD, De Noblet-Ducoudré N, Viovy N, Folberth GA (2006) Impact of climate variability and land use changes on global biogenic volatile organic compound emissions. Atmos Chem Phys 6:2129–2146

Lee G, Park J, Jang Y, Lee M, Kim KR, Oh JR, Kim D, Yi HI, Kim TY (2010) Vertical variability of seawater DMS in the South Pacific Ocean and its implication for atmospheric and surface seawater DMS. Chemosphere 78:1063-1070

Lelieveld J, Butler TM, Crowley JN, Dillon TJ, Fischer H, Ganzeveld L, Harder H, Lawrence MG, Martinez M, Taraborrelli D, Williams J (2008) Atmospheric oxidation capacity sustained by a tropical forest. Nature 452:737–40

Lewis AC, Hopkins JR, Carpenter LJ, Stanton J, Read KA, Pilling MJ (2005) Sources and sinks of acetone, methanol, and acetaldehyde in North Atlantic marine air. Atmos Chem Phys 5:1963–1974

Liu S, Pilone GJ (2000) An overview of formation and roles of acetaldehyde in winemaking with emphasis on microbiological implications. Int J Food Sci Technol 35:49–61

Liu Y, Shang X, Yi Z, Gu L, Zeng R (2015) *Shewanella mangrovi* sp. nov., an acetaldehyde-degrading bacterium isolated from mangrove sediment. Int J Syst Evol Microbiol 65:2630–2634

Loreto F, Schnitzler JP (2010) Abiotic stresses and induced BVOCs. Trends Plant Sci 15:154–166

Mao J, Jacob DJ, Evans MJ, Olson JR, Ren X, Brune WH, St. Clair JM, Crounse JD, Spencer KM, Beaver MR, Wennberg PO, Cubison MJ, Jimenez JL, Fried A, Weibring P, Walega JG, Hall SR, Weinheimer AJ, Cohen RC, Chen G, Crawford JH, McNaughton C,

Clarke AD, Jaeglé L, Fisher JA, Yantosca RM, Le Sager P, Carouge C (2010) Chemistry of hydrogen oxide radicals (HOx) in the Arctic troposphere in spring. Atmos Chem Phys 10:5823–5838

Matsushita K, Matsutani M (2016) Distribution, evolution, and physiology of oxidative fermentation. In: Matsushita K, Toyama H, Tonouchi N, Okamoto-Kainuma A (eds) Acetic acid bacteria: Ecology and physiology. Springer, Tokyo, pp 159–178

Meegoda JN, Rudy S, Zou Z, Agbakpe M (2016) Can fracking be environmentally acceptable? J Hazardous, Toxic, Radioact Waste 4:1–11

Milich L (1999) The role of methane in global warming: where might mitigation strategies be focused? Glob Environ Chang 9:179–201

Millet DB, Guenther A, Siegel DA, Nelson NB, Singh HB, de Gouw JA, Warneke C, Williams J, Eerdekens G, Sinha V, Karl T, Flocke F, Apel E, Riemer DD, Palmer PI, Barkley M (2010) Global atmospheric budget of acetaldehyde: 3-D model analysis and constraints from in-situ and satellite observations. Atmos Chem Phys 10:3405–3425

Mopper K, Kieber DJ (1991) Distribution and biological turnover of dissolved organic compounds in the water column of the Black Sea. Deep Res 38:S1021–S1047

Moreb JS (2014) Aldehyde dehydrogenases. Encycl Cancer 1:1–4

Morris RM, Rappé MS, Connon SA, Vergin KL, Siebold WA, Carlson CA, Giovannoni SJ (2002) SAR11 clade dominates ocean surface bacterioplankton communities. Nature 420:806-810

Moss AR, Jouany J-P, Newbold J (2000) Methane production by ruminants: its contribution to global warming. Ann Zootech 49:231–253

Naik V, Mauzerall D, Horowitz L, Schwarzkopf MD, Ramaswamy V, Oppenheimer M (2005) Net radiative forcing due to changes in regional emissions of tropospheric ozone precursors.

J Geophys Res 110:1–14

National Center for Biotechnology Information (2021). PubChem Compound Summary for CID 177, Acetaldehyde. Retrieved from https://pubchem.ncbi.nlm.nih.gov/compound/Acetaldehyde

National Institute for Occupational Safety and Health (2014) Acetaldehyde: Immediately dangerous to life or health concentration (IDLH). Retrieved from https://www.cdc.gov/niosh/idlh/75070.html

Nightingale PD, Malin G, Law CS, Watson AJ, Liss PS, Liddicoat MI, Boutin J, Upstill-Goddard RC (2000) In situ evaluation of air-sea gas exchange parameterizations using novel conservative and volatile tracers. Global Biogeochem Cycles 14:373–387

Nuutinen H, Lindros KO, Salaspuro M (1983) Determinants of blood acetaldehyde level during ethanol oxidation in chronic alcoholics. Alcohol Clin Exp Res 7:163–168

Osborne JP, de Orduña RM, Pilone GJ, Liu SQ (2000) Acetaldehyde metabolism by wine lactic acid bacteria. FEMS Microbiol Lett 191:51–55

P&S Market Research (2015) Global alcoholic drinks market is expected to grow at 3% CAGR during 2015 - 2020: P&S Market Research. Retrieved from http//www.prnewswire.com/news-releases/global-alcoholic-drinks-market-is-expected-to-grow-at-3-cagr-during-2015---2020-ps-market-research-563350881.html

Paulot F, Crounse JD, Kjaergaard HG, Kroll JH, Seinfeld JH, Wennberg PO (2009) Isoprene photooxidation: new insights into the production of acids and organic nitrates. Atmos Chem Phys 9:1479–1501

Poisson N, Kanakidou M, Crutzen PJ (2000) Impact of non-methane hydrocarbons on tropospheric chemistry and the oxidizing power of the global troposphere: 3-Dimensional modelling results. J Atmos Chem 36:157–230

Read KA, Carpenter LJ, Arnold SR, Beale R, Nightingale PD, Hopkins JR, Lewis AC, Lee JD, Mendes L, Pickering SJ (2012) Multiannual observations of acetone, methanol, and acetaldehyde in remote tropical Atlantic air: Implications for atmospheric OVOC budgets and oxidative capacity. Environ Sci Technol 46:11028–11039

Reche I, Pace ML, Cole JJ (2000) Modeled effects of dissolved organic carbon and solar spectra on photobleaching in lake ecosystems. Ecosystems 3:419–432

Riipinen I, Pierce JR, Yli-Juuti T, Nieminen T, Hakkinen S, Ehn M, Junninen H, Lehtipalo K, Petaja T, Slowik J, Chang R, Shantz NC, Abbatt J, Leaitch WR, Kerminen VM, Worsnop DR, Pandis SN, Donahue NM, Kulmala M (2011) Organic condensation: a vital link connecting aerosol formation to cloud condensation nuclei (CCN) concentrations. Atmos Chem Phys 11:3865–3878

Rodigast M, Mutzel A, Iinuma Y, Haferkorn S, Herrmann H (2015) Characterisation and optimisation of a sample preparation method for the detection and quantification of atmospherically relevant carbonyl compounds in aqueous medium. Atmos Meas Tech 8:2409–2416

Roebuck JA, Avery GB, Felix JD, Kieber RJ, Mead RN, Skrabal SA (2016) Biogeochemistry of ethanol and acetaldehyde in freshwater sediments. Aquat Geochemistry 22:177–195

Salaspuro MP (2003) Acetaldehyde, microbes, and cancer of the digestive tract. Crit Rev Clin Lab Sci 40:183–208

Sanz C, Maeztu L, Jose Zapelena M, Bello J, Cid C (2002) Profiles of volatile compounds and sensory analysis of three blends of coffee: Influence of different proportions of Arabica and Robusta and influence of roasting coffee with sugar. J Sci Food Agric 82:840–847

Sareen N, Schwier AN, Lathem TL, Nenes A, McNeill VF (2013) Surfactants from the gas phase may promote cloud droplet formation. Proc Natl Acad Sci USA 110:2723–8

Schade GW, Goldstein AH (2001) Fluxes of oxygenated volatile organic compounds from a ponderosa pine plantation. J Geophys Res 106:3111–3123

Schlundt C, Tegtmeier S, Lennartz ST, Bracher A, Cheah W, Krüger K, Quack B, Marandino CA (2017) Oxygenated volatile organic carbon in the western Pacific convective center: ocean cycling, air-sea gas exchange and atmospheric transport. Atmos Chem Phys 17: 10837-10854

Schmidt A, Frensch M, Schleheck D, Schink B, Müller N (2014) Degradation of acetaldehyde and its precursors by *Pelobacter carbinolicus* and *P. acetylenicus*. PLoS One 9:1–23

Seco R, Penelas J, Filella I (2007) Short-chain oxygenated VOCs: Emission and uptake by plants and atmospheric sources, sinks, and concentrations. Atmos Environ 41:2477–2499

Semmelroch P, Grosch W (1995) Analysis of roasted coffee powders and brews by gas chromatography-olfactometry of headspace samples. LWT - Food Sci Technol 28:310–313

Setshedi M, Wands JR, de la Monte SM (2010) Acetaldehyde adducts in alcoholic liver disease. Oxid Med Cell Longev 3:178–185

Sharkey TD, Wiberley AE, Donohue AR (2008) Isoprene emission from plants: Why and how. Ann Bot 101:5–18

Shaw SL, Gantt B, Meskhidze N (2010) Production and emissions of marine isoprene and monoterpenes: A review. Adv Meteorol 1–24

Shepson PB, Hastie DR, Schiff HI, Polizzi M, Bottenheim JW, Anlauf K, Mackay GI, Karecki DR (1991) Atmospheric concentrations and temporal variations of C1-C3 carbonyl compounds at two rural sites in central Ontario. Atmos Environ 25A:2001–2015

Sheridan MK, Elias RJ (2015) Exogenous acetaldehyde as a tool for modulating wine color and astringency during fermentation. Food Chem 177:

Siasos G, Tsigkou V, Kokkou E, Oikonomou E, Vavuranakis M, Vlachopoulos C, Verveniotis

A, Limperi M, Genimata V, Athanasios GP, Christodoulos S, Tousoulis D (2014) Smoking and atherosclerosis: mechanisms of disease and new therapeutic approaches. Curr Med Chem 21:3936–48

Sikora TD, Ufermann S (2004) Marine atmospheric boundary layer cellular convection and longitudinal roll vortices. In: Jackson CR, Apel JR (eds) Synthetic aperture radar marine user's manual. NOAA, Washington, DC, pp 321–330

Singh HB, Salas LJ, Chatfield RB, Czech E, Fried A, Walega J, Evans MJ, Field BD, Jacob DJ, Blake D, Heikes B, Talbot R, Sachse G, Crawford JH, Avery MA, Sandholm S, Fuelberg H (2004) Analysis of the atmospheric distribution, sources, and sinks of oxygenated volatile organic chemicals based on measurements over the Pacific during TRACE-P. J Geophys Res 109:1–20

Singh HB, Tabazadeh A, Evans MJ, Field BD, Jacob DJ, Sachse G, Crawford JH, Shetter R, Brune WH (2003) Oxygenated volatile organic chemicals in the oceans: Inferences and implications based on atmospheric observations and air-sea exchange models. Geophys Res Lett 30:1862

Stock A, Hoffman S, Beste C (2016) Effects of binge drinking and hangover on response selection sub-processes - a study using EEG and drift diffusion modeling. Addict Biol 22:1–11

Tadege M, Dupuis I, Kuhlemeier C (1999) Ethanolic fermentation: new functions for an old pathway. Trends Plant Sci 4:320–325

Theruvathu JA, Jaruga P, Nath RG, Dizdaroglu M, Brooks PJ (2005) Polyamines stimulate the formation of mutagenic 1,N2-propanodeoxyguanosine adducts from acetaldehyde. Nucleic Acids Res 33:3513–3520

Thomas JC, Helgason T, Sinclair CJ, Moir JWB (2017) Isolation and characterization of metaldehyde-degrading bacteria from domestic soils. Microb Biotechnol 10:1824–1829

Trifunović D, Berghaus N, Müller V (2020) Growth of the acetogenic bacterium *Acetobacterium woodii* by dismutation of acetaldehyde to acetate and ethanol. Environ Microbiol Rep 12:58–62

U.S. Environmental Protection Agency (2000) Acetaldehyde hazard summary. Retrieved from https://www.epa.gov/sites/production/files/2016-09/documents/acetaldehyde.pdf

U.S. Environmental Protection Agency (2016) Technical overview of volatile organic compounds. Retrieved from https://www.epa.gov/indoor-air-quality-iaq/technical-overview-volatile-organic-compounds#definition

Utama S, Wills RBH, Ben-Yehoshua S, Kuek C (2002) In vitro efficacy of plant volatiles for inhibiting the growth of fruit and vegetable decay microorganims. J Agric Food Chem 50:6371–6377

Väkeväinen S, Tillonen J, Agarwal DP, Srivastava N, Salaspuro M (2000) High salivary acetaldehyde after a moderate dose of alcohol in ALDH2-deficient subjects: strong evidence for the local carcinogenic action of acetaldehyde. Alcohol Clin Exp Res 24:873–7

Vecchio RD, Blough NV (2002) Photobleaching of chromophoric dissolved organic matter in natural waters: kinetics and modeling. Mar Chem 78:231–253

Wagner-Döbler I, Biebl H (2006) Environmental biology of the marine *Roseobacter* lineage. Annu Rev Microbiol 60:255-280

Wang J, Shen N, Yin H, Liu C, Li Y, Li Q (2013) Development of industrial brewing yeast with low acetaldehyde production and improved flavor stability. Appl Biochem Biotechnol 169:1016–1025

Wennberg PO, Hanisco TF, Jaeglé L, Jacob DJ, Hintsa EJ, Lanzendorf EJ, Anderson JG, Gao RS, Keim ER, Donnelly SG, Del Negro LA, Fahey DW, McKeen SA, Salawitch RJ, Webster CR, May RD, Herman RL, Proffitt MH, Margitan JJ, Atlas EL, Schauffler SM, Flocke

F, McElroy CT, Bui TP (1998) Hydrogen radicals, nitrogen radicals, and the production of O3 in the upper troposphere. Science (80-) 279:49–53

Weschenfelder TA, Lantin P, Viegas MC, de Castilhos F, de Paula Scheer A (2015) Concentration of aroma compounds from an industrial solution of soluble coffee by pervaporation process. J Food Eng 159:57–65

Wiedinmyer C, Guenther A, Harley P, Hewitt N, Geron C, Artaxo P, Steinbrecher R, Rasmussen R (2004) Global organic emissions from vegetation. In: Granier C, Artaxo P, Reeves CE (eds) Emissions of Atmospheric Trace Compounds. Springer, Dordrecht, pp 115–170

Wigley TML, Smith SJ, Prather MJ (2002) Radiative forcing due to reactive gas emissions. J Clim 15:2690–2696

Williams J, Holzinger R, Gros V, Xu X, Atlas E, Wallace DWR (2004) Measurements of organic species in air and seawater from the tropical Atlantic. Geophys Res Lett 31:L23S06

Yang GP, Zhuang GC, Zhang HH, Dong Y, Yang J (2012) Distribution of dimethylsulfide and dimethylsulfoniopropionate in the Yellow Sea and the East China Sea during spring: Spatio-temporal variability and controlling factors. Mar Chem 138-139:21-31

Yu Y, Wen S, Lü H, Feng Y, Wang X, Sheng G, Fu J (2008) Characteristics of atmospheric carbonyls and VOCs in Forest Park in South China. Environ Monit Assess 137:275–285

Yvon-Durocher G, Allen AP, Bastviken D, Conrad R, Gudasz C, St-Pierre A, Thanh-Duc N, del Giorgio PA (2014) Methane fluxes show consistent temperature dependence across microbial to ecosystem scales. Nature 507:488–91

Zha M, Yu J, Zhang Y, Wang H, Bai N, Qin Y, Liangliang D, Liu W, Zhang H, Bilige M (2015) Study on *Streptococcus thermophilus* isolated from Qula and associated characteristic of acetaldehyde and diacetyl in their fermented milk. J Gen Appl Microbiol 61:50–56

Zhang Y, van Dijk MA, Liu M, Zhu G, Qin B (2009) The contribution of phytoplankton degradation to chromophoric dissolved organic matter (CDOM) in eutrophic shallow lakes: Field and experimental evidence. Water Res 43:4685–4697

Zhou X, Mopper K (1993) Carbonyl compounds in the lower marine troposphere over the Caribbean Sea and Bahamas. J Geophys Res 98:2385–2392

Zhou X, Mopper K (1997) Photochemical production of low-molecular-weight carbonyl compounds in seawater and surface microlayer and their air-sea exchange. Mar Chem 56:201–213

Zubkov MV, Mary I, Woodward EMS, Warwick PE, Fuchs BM, Scanlan DJ, Burkill PH (2007) Microbial control of phosphate in the nutrient-depleted North Atlantic subtropical gyre. Environ Microbiol 9:2079–2089

Chapter 2:

Microbial Degradation of Acetaldehyde in Freshwater and Estuarine Environments

2.1 Introduction

Volatile organic compounds (VOCs) constitute a diverse group of compound classes that are produced by biotic and abiotic processes (Halsey et al. 2017). The carbonyl compound, acetaldehyde (C_2H_4O), belongs to a subdivision of VOCs termed the oxygenated volatile organic compounds (OVOCs), which play a fundamental role in tropospheric chemistry and Earth's climate system. It is estimated that 150 - 500 Tg of carbon (Tg C) moves through the atmosphere in the form of OVOCs every year, with acetaldehyde contributing 115 - 286 Tg C (Singh et al. 2004). Within the troposphere, acetaldehyde acts as a source of ozone (O_3), peroxyacetyl nitrate (PAN), hydrogen oxide radicals (·OH), and carbon monoxide (CO) via oxidation and photochemical degradation pathways (Millet et al. 2010). These secondary compounds determine the oxidative status or "self-cleaning capacity" of the atmosphere, and consequently regulate the removal of other atmospheric VOCs, including important greenhouse gases such as methane (Wigley et al. 2002). The interaction of acetaldehyde with wet aerosol particles also indirectly enhances cloud condensation nuclei formation (Sareen et al. 2013), increasing overall cloud density, albedo, and limiting solar irradiance (Latham et al. 2008). Accordingly, the atmospheric activity of acetaldehyde can indirectly cause significant changes to local and global climate.

Modelled estimates of global acetaldehyde emissions vary considerably (Singh et al. 2004; Millet et al. 2010) and are highly dependent on the modelling approach taken; either top-down or bottom-up. Nonetheless, previously published models generally recognise atmospheric production as the largest global source of acetaldehyde (Millet et al. 2010).

However, there is considerable debate regarding the magnitude of acetaldehyde emissions from the marine environment, with estimates ranging broadly between 17 - 125 Tg C a^{-1} (Singh et al. 2004; Millet et al. 2010; Read et al. 2012; Beale et al. 2013). This wide range of estimates is, in part, due to limited knowledge of microbial acetaldehyde sinks and how they influence the flux of acetaldehyde from the marine environment to the atmosphere. Considerably less is known about acetaldehyde emissions from estuarine and freshwater environments and how these emissions may be influenced by microbial activity. As a result, estuarine and freshwater acetaldehyde emissions have not yet been included in global emission models, despite evidence to suggest that these systems may represent important sources of acetaldehyde (Roebuck et al. 2016; Giubbina et al. 2017). The photodegradation of chromophoric dissolved organic matter (CDOM) originating from degraded plant matter, for example, results in the formation of low molecular weight carbonyl compounds including acetaldehyde, acetone, and formaldehyde (de Bruyn et al. 2011). Both riverine and estuarine environments receive regular inputs of degraded plant matter (de Bruyn et al. 2011), suggesting that emissions of acetaldehyde and other carbonyl compounds may be particularly high in these systems, although the effect of microbial communities on these emissions is not clear.

The identity and diversity of acetaldehyde-degrading microorganisms is poorly understood, with only a handful of acetaldehyde degraders isolated, identified, and characterised. Most of these microorganisms have been isolated from marine or mangrove environments, while only one acetaldehyde degrader has been cultivated from estuarine sediments. *Shewanella mangrovi*, for example, was isolated from mangrove sediments collected from Zhangzhou, China, and demonstrated the ability to degrade 22.7 mM of acetaldehyde (Liu et al. 2015). An acetaldehyde concentration of ≥7.8 mM (342 mg L^{-1}) is reported to be the limit of toxicity for bacteria, with Curtis et al. (1982) using a 50% decrease in bioluminescence by the marine bacterium *Photobacterium phosphoreum* in response to acetaldehyde as a proxy for toxicity. This suggests that *S. mangrovi* and other acetaldehyde degraders are exceptionally

tolerant to acetaldehyde and may possess physiological adaptations, such as microcompartments, to counteract the toxic effects of this volatile compound. Twelve acetaldehyde-degrading Bacteria, belonging to the genera *Vibrio*, *Halomonas*, *Pseudoalteromonas*, *Pseudomonas*, and *Bacillus*, were also isolated from deep seawater of the West Pacific Ocean, with 3 isolates utilising 7.9 mM of acetaldehyde (Gao et al. 2018). *Acetobacterium woodii*, an acetogenic bacterium exhibiting the ability to grow anaerobically on 5 mM of acetaldehyde (Trifunović et al. 2020), represents the only acetaldehyde degrader to be isolated from an estuarine environment, having been cultivated from marine estuary sediments in Woods Hole, Massachusetts (Balch et al. 1977). To date, no acetaldehyde-degrading microorganisms have been isolated from freshwater environments. Accordingly, our knowledge of microbial acetaldehyde degradation and the microorganisms responsible in estuarine and freshwater environments is poor and significant research effort is required to gain an understanding of these microorganisms and their importance in the global acetaldehyde cycle.

It is important to note that our current knowledge of acetaldehyde degraders is not only limited to the Bacteria. Fungi, such as yeast, have also been reported to produce and degrade acetaldehyde during the wine fermentation process, with Li & de Orduña (2011) reporting acetaldehyde degradation by 26 different yeast strains. In that study, non-*Saccharomyces* yeast strains displayed acetaldehyde degradation rates of 0.24 ± 0.01 to 0.50 ± 0.01 mg g^{-1} min^{-1}, whilst degradation rates of 0.49 ± 0.04 to 0.77 ± 0.02 mg g^{-1} min^{-1} were measured for *Saccharomyces* strains (Li & de Orduña 2011). Although these strains are applied in industrial settings, they also constitute a part of natural microbial communities and have been found in association with deciduous tree bark, exudates and associated soils, and wild fruits (Charron et al. 2014). This suggests that Fungi may significantly contribute to the microbial acetaldehyde sink, although it is uncertain whether acetaldehyde-degrading Fungi, such as the genus *Saccharomyces*, inhabit freshwater, estuarine, and marine environments. It is also unknown whether Archaea also contribute to microbial acetaldehyde

degradation. Furthermore, it is unclear whether acetaldehyde-degrading microorganisms in estuarine and freshwater environments preferentially utilise acetaldehyde as a source of energy, via dissimilation to CO_2, or assimilate acetaldehyde-derived carbon into biomass for growth. Recent findings from the marine environment suggest that acetaldehyde is predominantly used as an energy source, with Dixon et al. (2013) demonstrating that microbial dissimilation accounted for 49 - 100% of acetaldehyde losses in the Atlantic Ocean. Halsey et al. (2017) also showed that two strains of *Pelagibacter* SAR11 primarily oxidised acetaldehyde to CO_2 and incorporated 30% of the utilised acetaldehyde into biomass. Measurements of acetaldehyde dissimilation and assimilation in estuarine and freshwater environments are restricted to a singular study of the temperate rivers and estuaries of South-West England (Webb 2016; J. Dixon, pers. comm.), which reported that microbial dissimilation rates were higher than rates of microbial assimilation. This suggests that acetaldehyde is also primarily used as a source of energy by acetaldehyde degraders in estuaries and freshwater rivers, however, further investigations are needed to corroborate these findings in other estuarine and freshwater systems.

Metaldehyde is a cyclic-tetramer of acetaldehyde that is commonly used as a molluscicide in domestic gardens and agricultural settings (Thomas et al. 2017). Its widespread application, mobility in soils, and recalcitrance to degradation has resulted in the accumulation of metaldehyde in freshwater systems, including potable water supplies (Castle et al. 2017). As a highly polar compound, metaldehyde is difficult to remove from freshwater using standard water treatment processes, such as granular or powdered activated carbon beds (Castle et al. 2018), which are particularly expensive to implement (Castle et al. 2017). Consequently, metaldehyde concentrations regularly exceed the European Union's regulatory drinking water standard for individual pesticides of 0.1 µg L^{-1} (Castle et al. 2017). This is a particularly significant issue in East Anglia due to the farming practices that occur in Norfolk, Suffolk, and Cambridgeshire, with 12% of Anglian Water test sites exceeding the regulatory limit in 2015 (Castle et al. 2017). Bioremediation has been suggested as a cheaper and more

efficient alternative in the management of freshwater metaldehyde concentrations. Metaldehyde-degrading bacteria with the potential for implementation in future bioremediation strategies have been isolated from metaldehyde-exposed soils from domestic gardens, allotments, and agricultural farms (Thomas et al. 2017; Castro-Gutiérrez et al. 2020). Thomas et al. (2017), for example, isolated the first metaldehyde-degrading bacteria from domestic garden soils, namely *Acinetobacter calcoaceticus* strain E1 and *Variovorax* strain E3, which could degrade metaldehyde at a concentration of 850 μM. Despite the accumulation of metaldehyde in freshwater systems, metaldehyde-degrading microorganisms have not been detected or isolated from freshwater rivers. Consequently, it is uncertain whether metaldehyde-degrading microorganisms are present and active in these environments and whether bioremediation strategies will be effective in removing metaldehyde. It is also unclear whether the degradation of metaldehyde represents a potentially important source of acetaldehyde to microbial acetaldehyde degraders in freshwater environments and whether the same microorganisms are responsible for both metaldehyde and acetaldehyde degradation.

The first aim of this study was to determine the potential for microbial acetaldehyde degradation in the Colne Estuary, the River Colne, and the River Gipping. This will enhance our knowledge of acetaldehyde cycling in estuarine and freshwater environments and improve our understanding of the role that microorganisms play in the global acetaldehyde cycle. A second aim was to identify the microorganisms potentially responsible for acetaldehyde degradation in estuarine and freshwater environments, which will improve our current understanding of the diversity of acetaldehyde degraders and may help to elucidate the role of fungi and archaea in microbial acetaldehyde degradation. The third aim was to measure in-situ degradation in the Colne Estuary and identify whether acetaldehyde is predominantly used by microorganisms as an energy source (i.e. dissimilation) or as a carbon source for growth (i.e. assimilation). The findings of previous investigations suggest that acetaldehyde is primarily dissimilated to CO_2, whilst a small proportion of acetaldehyde-

derived carbon is assimilated into biomass. The final aim of this study was to measure the potential for microbial metaldehyde degradation in freshwater rivers and to identify the microorganisms responsible. The following hypotheses were tested:

H1. Bacteria will be the primary acetaldehyde degraders in the Colne Estuary, the River Colne, and the River Gipping, as there is currently no evidence to suggest that fungi and archaea can utilise acetaldehyde as a carbon and energy source.

H2. Rates of microbial acetaldehyde dissimilation will be higher than rates of microbial assimilation, indicating that acetaldehyde is predominantly used as an energy source rather than being assimilated into biomass for growth.

H3. Bacteria inhabiting the River Colne and the River Gipping will utilise metaldehyde as a sole source of carbon and energy, demonstrating that metaldehyde-degrading microorganisms are present and active in freshwater environments.

2.2 Methodology

2.2.1 Sampling

Sediment samples were collected from the Colne Estuary, Essex (UK) on the 29th March 2017 during low tide. Sediment corers (6.5 cm diameter; 10 cm length) were used to extract sediment from the exposed mudflat surface, which is inundated twice daily. In total, 12 sediment cores were extracted from three sampling sites located along the Colne Estuary, namely Hythe (estuary head), Wivenhoe (estuary mid-point), and Brightlingsea (estuary mouth) (Figure 2.1). At each sampling site, four sediment cores were extracted from the mudflat surface, approximately 5 m from the estuary bank, at 5 m intervals, parallel to the shoreline. Sediment cores were stored in the dark at ~15°C for 24 hours before being processed. Surface water samples (5 L) were collected from Hythe, Wivenhoe, and Brightlingsea on the 15th February 2020 during high tide. The surface water samples were stored in the dark and were transported to Plymouth Marine Laboratory, Plymouth, to investigate the microbial assimilation and dissimilation of ^{14}C-labelled acetaldehyde. Surface water samples were stored in the dark at 9°C prior to analysis.

Samples of river water were collected from the River Colne (East Mills, Essex) and the River Gipping (Sproughton Intake, Suffolk) on the 13th September 2017 (Figure 2.2). A total of 6 L of river water was sampled from each site using two 10 L carboys (Nalgene). To increase the microbial load, 15 g of sediment was extracted from the bed of each river using 15 mL Falcon tubes and was added to the corresponding river water. Sampled river water was stored in the dark at ~15°C for 24 hours prior to processing.
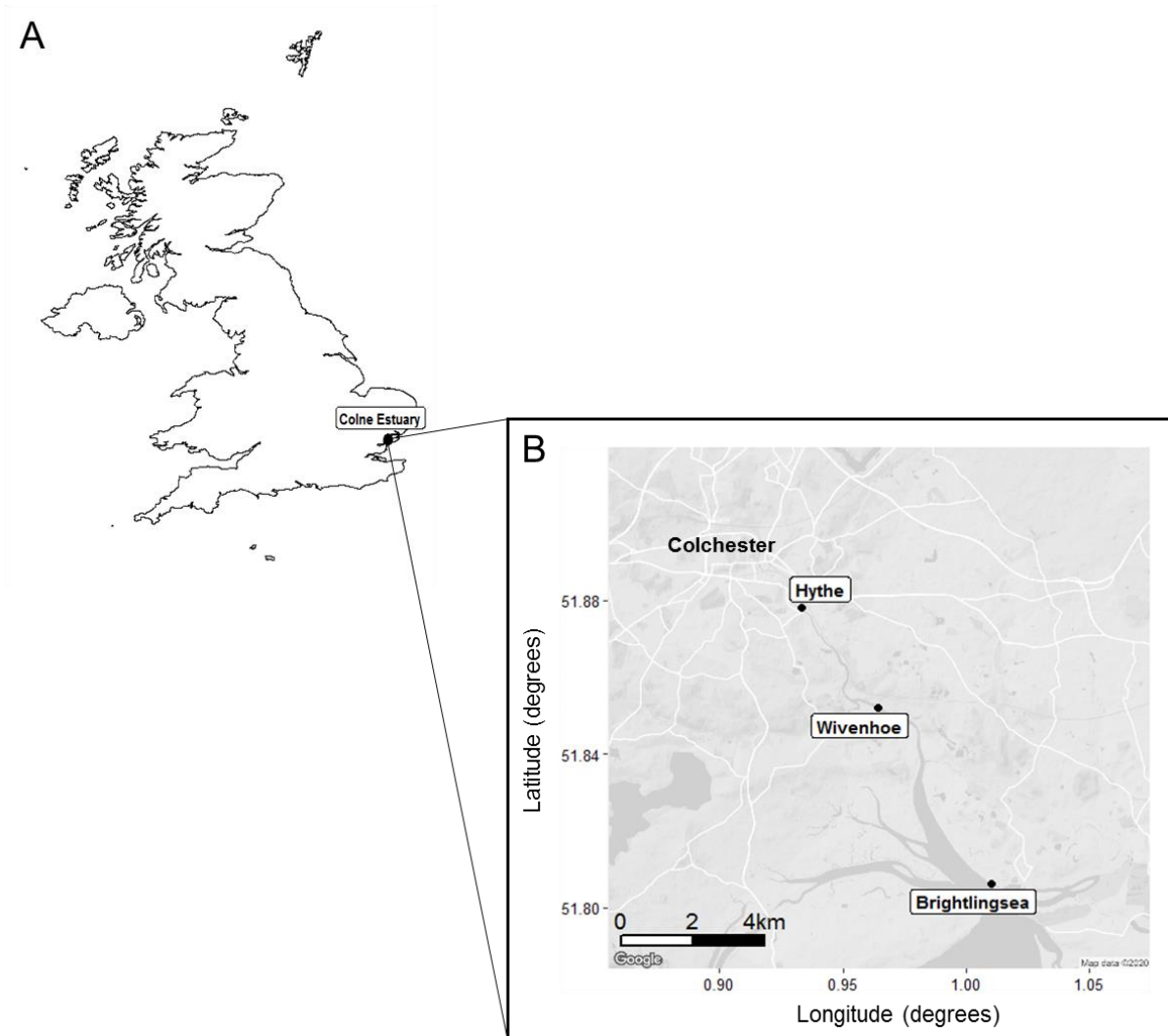
Figure 2.1 Map showing A) the location of the Colne Estuary in the United Kingdom and B) the sampling sites located at Hythe (estuary head), Wivenhoe (estuary midpoint), and Brightlingsea (estuary mouth).
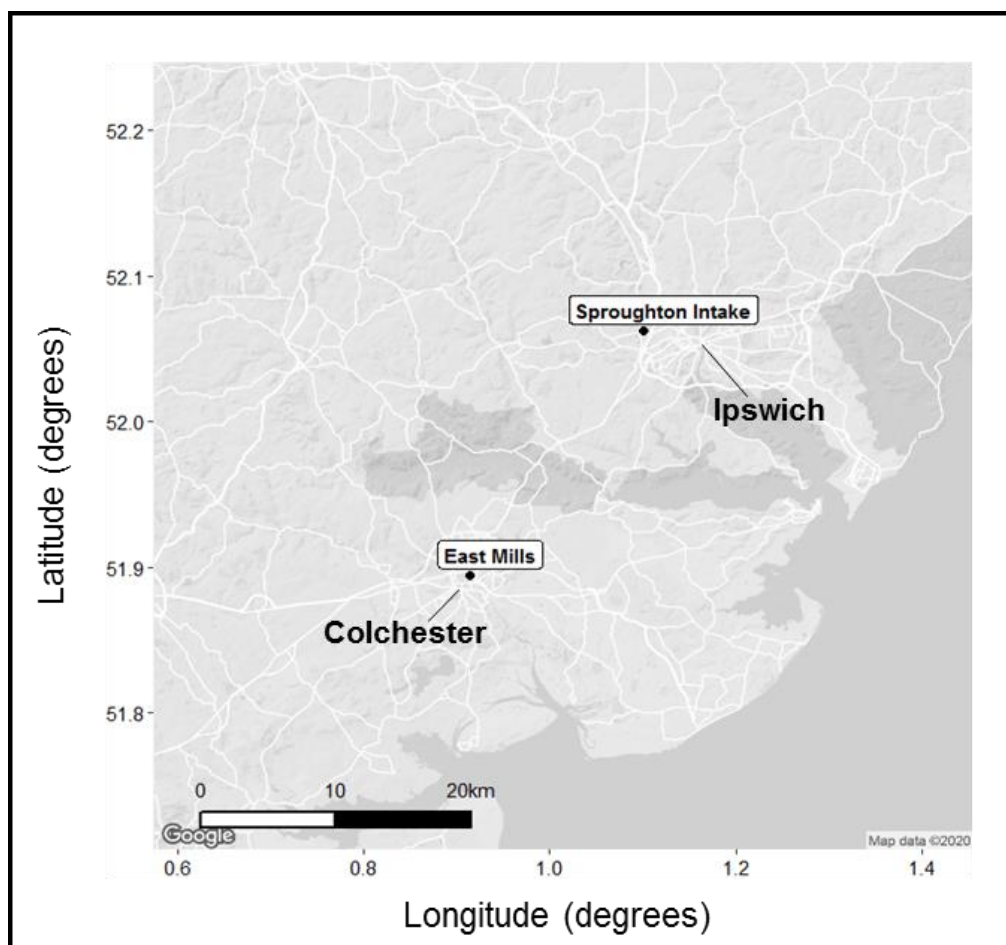
Figure 2.2 Map showing the location of East Mills on the River Colne, Colchester and Sproughton Intake on the River Gipping, Ipswich.

2.2.2 Enrichment preparation

The top 1.5 cm of each sediment core was removed with a flamed metal spatula, weighed, and mixed with ONR7a seawater-nutrient medium (Dyksterhouse et al. 1995) to produce a slurry with a sediment-medium weight ratio of 1:10. ONR7a seawater-nutrient medium used throughout this study was composed of 3 separate solutions. Solution 1 was composed of 22.79 g of NaCl, 3.98 g of Na_2SO_4, 1.30 g of TAPSO (3-[N-Tris(hydroxymethyl)methylamino] -2-hydroxypropanesulfonic acid; Sigma-Aldrich), 0.72 g of KCl, 0.27 g of NH_4Cl, 89.0 mg of Na_2HPO_4, 83.0 mg of NaBr, 31.0 mg of $NaHCO_3$, 27.0 mg of H_3BO_3 and 2.60 mg of NaF in 500 mL of Milli-Q water. Solution 2 was composed of 11.18 g of $MgCl_2$, 1.46 g of $CaCl_2$ and 24.0 mg of $SrCl_2$ in 450 mL of Milli-Q water. Solution 3 was composed of 2.0 mg of $FeCl_2$ in 50 mL of Milli-Q water. These solutions were autoclaved separately and mixed.

To prepare a 227 mM acetaldehyde working stock, 1.275 mL of acetaldehyde (≥99.5% purity; Sigma-Aldrich) was added to 98.725 mL of Milli-Q water in a 100 mL serum bottle. The serum bottle was immediately capped with a polytetrafluoroethene (PTFE) -lined butyl septum (Agilent) to ensure gas-tight conditions and was inverted several times to mix. To prepare a 22.7 mM acetaldehyde working stock, 10 mL of the 227 mM acetaldehyde stock solution was injected into a pre-sealed serum bottle containing 90 mL of Milli-Q water. The serum bottle was inverted several times to mix.

A total of 9 mL of sediment slurried in ONR7a was added to a sterile serum bottle (125 ml) and was capped with a PTFE-lined butyl septum (Agilent). A 1 mL aliquot of the 227 mM acetaldehyde working stock was injected into the serum bottle, yielding a final acetaldehyde concentration of 22.7 mM. This was performed in quadruplicate for Hythe, Wivenhoe, and Brightlingsea sediment slurries. Enrichments with a final acetaldehyde concentration of 2.27 mM were prepared in quadruplicate following the same protocol, although 1 mL of the 22.7 mM acetaldehyde working stock solution was injected into each serum bottle. To prepare no-acetaldehyde controls, 10 mL of sediment slurry was added to a sterile serum bottle and was sealed with a PTFE-lined butyl septum (Agilent). This was performed in triplicate for each sampling site. No-inoculum controls were set up in triplicate by injecting pre-sealed serum bottles containing 9 mL of ONR7a seawater-nutrient medium with 1 mL of the 227 mM acetaldehyde working stock solution. No-inoculum controls were also prepared in triplicate for the lower acetaldehyde concentration treatment by injecting pre-sealed serum bottles with 1 mL of the 22.7 mM acetaldehyde working stock. All serum bottles were incubated in the dark at 20°C for the duration of the experiment.

Three litres of freshwater from the River Colne and the River Gipping were subsampled from the 10 L carboys (Nalgene) and supplemented with 3 mL of autoclaved 300 mM NH_4Cl and 20 mM Na_2HPO_4, yielding final concentrations of 300 μM NH_4Cl and 20 μM Na_2HPO_4. To

prepare acetaldehyde-enriched microcosms, 18 mL of nutrient-enriched river water was aliquoted into a 40 mL serum bottle and sealed with a PTFE-lined butyl septum (Agilent). A 2 mL aliquot of the 22.7 mM acetaldehyde working stock solution was injected into the serum bottle, yielding a final acetaldehyde concentration of 2.27 mM. To prepare no-acetaldehyde controls, 20 mL of nutrient-enriched river water was aliquoted into a 40 mL serum bottle and sealed with a PTFE-lined butyl septum (Agilent). Metaldehyde-enriched microcosms were prepared by adding 1.1 g of metaldehyde (>99% purity; Acros Organics) to the remaining 2.43 L of nutrient-enriched river water, yielding a final metaldehyde concentration of 2.59 mM; considerably higher than concentrations generally found in UK drinking water, which have been reported to range from 2.3 - 3.4 nM (0.4 - 0.6 µg L^{-1}) in winter months (Kay & Grayson 2014), although a maximum concentration of 6.1 nM (1.03 µg L^{-1}) has previously been recorded (Water UK 2013). A total of 20 mL of metaldehyde-enriched river water was aliquoted into a 40 mL serum bottle and sealed with a PTFE-lined butyl septum (Agilent). Triplicate replicates of each treatment were prepared for five time points for each river using the nutrient-enriched river water from the River Colne and the River Gipping. To quantify background nutrient and acetaldehyde concentrations in the River Colne and the River Gipping, 20 mL of fresh river water was transferred from the 10 L carboys (Nalgene) into a 40 mL serum bottle and sealed with a PTFE-lined butyl septum (Agilent). Six replicates were prepared for each sampling site. The remaining freshwater sampled from each river was sterilised by autoclaving at 121°C. To prepare abiotic controls, 18 mL of sterilised river water was aliquoted into a 40 mL serum bottle and sealed with a PTFE-lined butyl septum (Agilent). A 2 mL aliquot of the 22.7 mM acetaldehyde working stock solution was injected into the serum bottle, yielding a final acetaldehyde concentration of 2.27 mM. A total of 12 replicates were prepared for each river using sterilised river water from the River Colne and the River Gipping. All serum bottles were incubated in the dark at 20°C for the duration of the experiment.

Headspace concentrations of acetaldehyde within Colne Estuary, River Colne, and River Gipping microcosms were measured 4 hours after initial set-up using an ATI Unicam 610 Series gas chromatograph with a 1.5 m packed column (10% Apiezon L on CarboWax (60 - 80 mesh)) and a flame-ionisation detector (GC-FID). A total of 100 μL of headspace was directly injected into the injector port using a 250 μL gas-tight syringe (SGE Analytical Science) and analysed. The injector and detector were set to 160°C and the column maintained at 120°C. Nitrogen was used as the carrier gas (40 mL min^{-1}) throughout the analysis. The retention time of acetaldehyde was measured as 0.731 ± 0.002 minutes (*n=21*). The relative level of detection for acetaldehyde was 100 μM. Headspace concentrations of acetaldehyde within Colne Estuary microcosms were measured every few days, whilst River Colne and River Gipping microcosms were measured on day 1, 4, 7, 14, and 21.

2.2.3 Successive enrichments

Secondary enrichments of Colne Estuary sediment slurries were set up after observing microbial growth or measuring ≥50% acetaldehyde degradation in acetaldehyde-enriched microcosms relative to the no-inoculum controls. To prepare secondary enrichments, 1 mL of sediment slurry from the corresponding primary enrichment was aliquoted into a sterile 125 mL serum bottle containing 8 mL of ONR7a seawater-nutrient medium and was sealed with a PTFE-lined butyl septum (Agilent). For the higher acetaldehyde concentration treatment, 1 mL of a freshly prepared 227 mM acetaldehyde working stock was injected into each serum bottle, yielding a final acetaldehyde concentration of 22.7 mM. For the lower acetaldehyde concentration treatment, 1 mL of a freshly prepared 22.7 mM acetaldehyde working stock was added to each serum bottle, resulting in a final acetaldehyde concentration of 2.27 mM. Secondary no-acetaldehyde controls were prepared by transferring 1 mL of sediment slurry from the primary no-acetaldehyde controls to serum bottles containing 9 mL of ONR7a seawater-nutrient medium and sealing with PTFE-lined

butyl septa (Agilent). No-inoculum controls were set up as described in Section 2.2.2. All serum bottles were incubated in the dark at 20°C and were monitored for acetaldehyde degradation via GC-FID as described in Section 2.2.2. Serum bottles were inspected for microbial growth every few days. Tertiary and quaternary enrichments of Colne Estuary sediment slurries were set up using the same protocol after measuring ≥50% acetaldehyde degradation or observing microbial growth in serum bottles from the previous enrichment.

Secondary enrichments of river water from the River Colne and the River Gipping were set up after observing microbial growth or measuring ≥50% acetaldehyde degradation in acetaldehyde-enriched microcosms relative to the abiotic controls. Artificial river water was prepared by adding 91.7 mg of $CaCl_2$, 69.0 mg of $MgSO_4$, 58.4 mg of $NaHCO_3$ and 15.4 mg of $KHCO_3$ to 1 L of Milli-Q water and was sterilised by autoclaving. To prepare secondary enrichments, 1 mL of primary enrichment was transferred to a 40 mL serum bottle containing 17 mL of artificial river water and was sealed with a PTFE-lined butyl septum (Agilent). A 2 mL aliquot of the 22.7 mM acetaldehyde working stock solution was injected into each serum bottle, yielding a final acetaldehyde concentration of 2.27 mM. Secondary abiotic controls were set up as described in Section 2.2.2, although artificial river water was used as the base medium. Serum bottles were incubated in the dark at 20°C and were inspected for microbial growth every few days. Acetaldehyde degradation was measured via GC-FID as described in Section 2.2.2.

At the conclusion of each enrichment, 1.5 mL of well-mixed enrichment from each Colne Estuary microcosm was transferred to a 1.5 mL microcentrifuge tube and centrifuged at 13,000 × g for 15 minutes. The supernatant was removed, and the pellets frozen at -20°C for downstream DNA extraction and microbial community analyses. Following GC-FID analysis, 5 mL of well-mixed enrichment was transferred from the River Colne and River Gipping primary enrichments into 15 mL Falcon tubes and centrifuged at 10,000 × g for 10 minutes.

The supernatant was transferred to a sterile 15 mL Falcon tube and stored at -20°C for downstream nutrient assimilation assays. Pellets were stored at -20°C for DNA extraction and microbial community analysis.

2.2.4 Nutrient assimilation assays

The assimilation of dissolved phosphate (PO_4^{3-}) in River Colne and River Gipping primary enrichments was determined following the protocol described by Strickland and Parsons (1968). Briefly, an ammonium molybdate solution was prepared by dissolving 15 g of ammonium paramolybdate in 500 mL of Milli-Q water. A sulfuric acid solution was prepared by adding 140 mL of concentrated sulfuric acid to Milli-Q water to a final volume of 900 mL, whilst an ascorbic acid solution was prepared by dissolving 2.7 g of ascorbic acid in 50 mL of Milli-Q water. A potassium antimonyl-tartrate solution was prepared by dissolving 0.34 g of potassium antimonyl-tartrate in 250 mL of Milli-Q water. To prepare a stock reagent, 2 mL of ammonium molybdate solution, 5 mL of sulfuric acid solution, 2 mL of ascorbic acid solution and 1 mL of potassium antimonyl-tartrate solution were mixed. To prepare a 20 μM sodium phosphate dibasic (Na_2HPO_4) stock solution, 10 μL of the 20 mM Na_2HPO_4 stock solution (Section 2.2.2) was added to 9.99 mL of Milli-Q water and autoclaved. Phosphate standards with a concentration range of 0, 5, 10, 15 and 20 μM were prepared in 1.6 mL cuvettes by diluting the 20 μM Na_2HPO_4 stock solution with Milli-Q water (Table S2.1) and adding 100 μL of the stock reagent. Phosphate standards were measured at 885 nm using a Jenway 7300 spectrophotometer 30 minutes after preparation, with the absorbance values plotted for each phosphate standard (Figure S2.1) (R^2 = 0.9989). To prepare samples from the River Colne and River Gipping primary enrichments, 250 μL of supernatant (Section 2.2.3) was diluted with 750 μL of Milli-Q water in a 1.6 mL cuvette and mixed with 100 μL of stock reagent. Samples were measured at 885 nm, with the final concentrations of dissolved phosphate multiplied by a factor of 4 to account for the dilution of supernatant with Milli-Q water.

Three reagents were prepared to quantify ammonium (NH_4^+) in River Colne and River Gipping primary enrichments. Reagent 1 was prepared by adding 6.25 g of trisodium citrate and 0.05 g of sodium nitroprusside to 50 mL of Milli-Q water. Reagent 2 was prepared by adding 0.5 g of phenol to 50 mL of Milli-Q water, whilst Reagent 3 was prepared by adding 0.34 g of sodium hydroxide and 0.1 g of dichloroisocyonuric acid to 50 mL of Milli-Q water. To prepare a 100 μM ammonium chloride (NH_4Cl) stock solution, 30 μL of the 300 mM NH_4Cl stock solution (Section 2.2.2) was added to 99.97 mL of Milli-Q water and autoclaved. Ammonium standards with a concentration range of 0, 25, 50, 75 and 100 μM were prepared in 1.6 mL cuvettes by diluting the 100 μM NH_4Cl stock solution with Milli-Q water (Table S2.2) and adding 200 μL of each reagent. Ammonium standards were incubated in the dark for 30 minutes and measured at 630 nm using a Jenway 7300 spectrophotometer. Absorbance values were plotted for each ammonium standard (Figure S2.2) (R^2 = 0.9992). To quantify ammonium assimilation in River Colne and River Gipping primary enrichments, 250 μL of supernatant (Section 2.2.3) was diluted with 750 μL of Milli-Q water in a 1.6 mL cuvette, mixed with 200 μL of each reagent, incubated in the dark for 30 minutes and measured at 630 nm. Final ammonium concentrations were multiplied by a factor of 4 to account for the dilution of supernatant with Milli-Q water.

2.2.5 Microbial community analysis

2.2.5.1 DNA extraction and quantitative-PCR

DNA was extracted from the pellets obtained in Section 2.2.3 using a DNeasy Powersoil Kit (Qiagen). Extracted DNA was separated by agarose gel electrophoresis (1.0% w/v), stained with SYBR™ Safe (Invitrogen), and was viewed on a Gel Doc™ EZ gel documentation system (Bio-Rad). Extracted DNA was stored at -20°C until use. Using the primer pairs 341F and 805R, 344F and 915R, and P5-fITS7 and P7-ITS4 (Table 2.1), the bacterial 16S rRNA gene, archaeal 16S rRNA gene, and fungal ITS2 region were PCR amplified from each DNA

extract, respectively. PCR was performed in a reaction volume of 25 μL, consisting of 1 μL of each primer (10 μM), 12.5 μL of app*Taq* DNA polymerase (Appleton Woods Ltd), 9.5 μL of PCR-grade water, and 1 μL of DNA extract. A negative control, using 1 μL of PCR-grade water as a template, was included in each PCR run. DNA extracts that had previously amplified using the same bacterial, archaeal, and fungal primers were used as positive controls. After an initial denaturation step at 95°C for 3 minutes, PCR amplification of the bacterial 16S rRNA gene and fungal ITS2 region was performed with 35 cycles as follows: denaturation at 95°C for 15 seconds, annealing at 57°C for 15 seconds, and extension at 72°C for 30 seconds. A final extension at 72°C was performed for 7 minutes. To amplify the archaeal 16S rRNA gene, an initial denaturation step was performed at 94°C for 3 minutes, followed by 35 cycles of denaturation at 94°C for 30 seconds, annealing at 60°C for 30 seconds, and extension at 72°C for 30 seconds. A final extension at 72°C was performed for 10 minutes. PCR products were visualised by agarose gel electrophoresis (1.2% w/v), stained with SYBR™ Safe (Invitrogen), and were viewed on a Gel Doc™ EZ gel documentation system (Bio-Rad). Samples with the highest amplification, indicated by increased band intensity on the agarose gel, were selected for use as quantitative-PCR (qPCR) standards for each target gene or DNA region and were subjected to a post-PCR clean-up using a GenElute™ PCR Clean-up Kit (Sigma-Aldrich). To ensure that potential inhibitors had been removed, cleaned PCR products were visualised by agarose gel electrophoresis (1.2% w/v). The qPCR standards were quantified via Quant-IT™ PicoGreen dsDNA Assay Kit (Thermo Fisher Scientific) using a Nanodrop 3300 Fluorospectrometer (Thermo Fisher Scientific). Copy numbers of each target gene or DNA region in each qPCR standard were calculated by multiplying the concentration of amplicons (ng μL^{-1}) by the Avogadro constant (6.023×10^{14} Da ng^{-1}) and dividing by the total molecular mass of the amplicons (amplicon size (bp) × average molecular weight of dsDNA (660 g mol^{-1})). For example:

$$\frac{6.023 \times 10^{14} \text{ Da ng}^{-1} \times 5.0 \text{ ng } \mu L^{-1}}{(464 \text{ bp} \times 660 \text{ g mol}^{-1})}$$

$$= 9.83 \times 10^9 \text{ copies of target gene } \mu L^{-1}$$

A dilution series, representing 10^{10} - 10^1 copies of target DNA, was prepared using each qPCR standard to construct a standard curve. A total of 1 μL of each dilution was added to a 384-well optical plate (Bio-Rad) in triplicate. Triplicate 1 μL aliquots of DNA extract from the Colne Estuary, River Colne or River Gipping enrichments were added to the 384-well optical plate. No-template controls (NTCs) were prepared by adding 1 μL of PCR-grade water to the remaining wells. To prepare a mastermix, 5 μL of 2 × SensiFAST™ SYBR No-ROX Mix (Bioline), 0.2 μL of each primer (10 μM), and 3.6 μL of PCR-grade water was mixed for each reaction. A total of 9 μL of mastermix was added to each well. The 384-well plate was sealed with optical film, centrifuged at 11,000 × g for 30 seconds to remove bubbles, and loaded onto a CFX384 real-time PCR detection system (Bio-Rad). After an initial denaturation and polymerase activation step at 95°C for 3 minutes, qPCR was performed with 40 cycles as follows: denaturation at 95°C for 5 seconds and combined annealing and extension at 60°C for 30 seconds. A final denaturation step was performed at 95°C for 5 seconds, whilst a melt-peak analysis, increasing by 0.5°C every 5 seconds, was performed at 65 - 95°C to produce a dissociation curve (melt curve). Quantification cycle (C_Q) values and standard curve construction were performed in CFX Manager Version 3.1 (Bio-Rad). The number of original templates in each sample was automatically calculated from the standard curve using the mean of 3 technical replicates. The average copy number of biological replicates was calculated for each sampling site at each time point (± S.D.). Separate qPCR analyses were performed for each target gene or DNA region using DNA extracts from the Colne Estuary, River Colne, and River Gipping enrichments.

Chapter 2

Table 2.1 Primers used for PCR amplification, quantitative-PCR (qPCR), and Illumina MiSeq metagenetic sequencing.

Target gene/region	Primer	Sequence (5'-3')	Method
16S rRNA (Bacteria)	341F	CCTACGGGNGGCWGCAG	PCR/qPCR
	805R	GACTACHVGGGTATCTAATCC	
	341F	TCGTCGGCAGCGTCAGATGTGTATAAGAGA CAGCCTACGGGNGGCWGCAG	MiSeq
	805R	GTCTCGTGGGCTCGGAGATGTGTATAAGAG ACAGGACTACHVGGGTATCTAATCC	
16S rRNA (Archaea)	344F	ACGGGGYGCAGCAGGCGCGA	PCR/qPCR
	915R	GTGCTCCCCCGCCAATTCCT	
	344F	TCGTCGGCAGCGTCAGATGTGTATAAGAGA CAGACGGGGYGCAGCAGGCGCGA	MiSeq
	915R	GTCTCGTGGGCTCGGAGATGTGTATAAGAG ACAGGTGCTCCCCCGCCAATTCCT	
ITS2 (Fungi)	P5-fITS7	GTGARTCATCGAATCTTTG	PCR/qPCR
	P7-ITS4	TCCTCCGCTTATTGATATGC	
	P5-fITS7	TCGTCGGCAGCGTCAGATGTGTATAAGAGA CAGGTGARTCATCGAATCTTTG	MiSeq
	P7-ITS4	GTCTCGTGGGCTCGGAGATGTGTATAAGAG ACAGTCCTCCGCTTATTGATATGC	

2.2.5.2 Metagenetic sequencing

Microbial community analysis was performed on DNA extracts from the Colne Estuary, River Colne, and River Gipping enrichments using the Illumina MiSeq platform. Using the primer pairs 341F and 805R, 344F and 915R, and P5-fITS7 and P7-ITS4 with Illumina overhang adapter sequences (Table 2.1), the bacterial 16S rRNA gene, archaeal 16S rRNA gene, and fungal ITS2 region were PCR amplified from each DNA extract, respectively. PCR was performed in a 96-well plate using a reaction volume of 25 μL, consisting of 0.5 μL of each primer (10 μM), 12.5 μL of app*Taq* DNA polymerase (Appleton Woods Ltd), 9 μL of PCR-grade water, and 2.5 μL of DNA extract. A negative control was prepared by using 2.5 μL of

PCR-grade water as a template in the PCR reagent mixture instead of DNA extract. After sealing the 96-well plate with a Microseal A film (Bio-Rad), PCR amplification was performed using the cycling conditions described in Section 2.2.5.1, although the bacterial 16S rRNA gene, archaeal 16S rRNA gene, and fungal ITS2 region were amplified following 24, 31, and 35 cycles, respectively. PCR products were visualised as described in Section 2.2.5.1. To remove primers and primer dimers from the amplified PCR products, 20 μL of AMPure XP beads was added to each sample well, mixed, and incubated at room temperature without shaking for 5 minutes. The 96-well plate was placed on a magnetic stand (Thermo Fisher Scientific) for 2 minutes to allow the supernatant to clear. The supernatant was removed and the AMPure XP beads washed with 200 μL of freshly prepared ethanol (80% v/v) for 30 seconds. This wash step was repeated and the AMPure XP beads allowed to air-dry for 10 minutes. The 96-well plate was removed from the magnetic stand and 52.5 μL of 10 mM Tris (pH 8.5) was added to each sample well and mixed. After incubating at room temperature for 2 minutes, the 96-well plate was placed on the magnetic stand for 2 minutes to allow the supernatant to clear. A total of 50 μL of supernatant from each well was transferred to a new 96-well plate and stored at -20°C. Purified amplicons were visualised by agarose gel electrophoresis (1.2% w/v) as described in Section 2.2.5.1. Using a Nextera XT Index Kit v2 (Illumina), dual indices and Illumina sequencing adapters were attached to the purified amplicons. Briefly, 5 μL of Nextera XT Index Primer 1 (N7XX), 5 μL of Nextera XT Index Primer 2 (S5XX), 25 μL of app*Taq* DNA polymerase (Appleton Woods Ltd), and 10 μL of PCR-grade water were added to 5 μL of purified amplicons in a new 96-well plate. The plate was covered with a Microseal A film (Bio-Rad), centrifuged at 1,000 × *g* for 1 minute, and PCR amplified. An initial denaturation step was performed at 95°C for 3 minutes, followed by 8 cycles of denaturation at 95°C for 30 seconds, annealing at 55°C for 30 seconds, and extension at 72°C for 30 seconds. A final extension was performed at 72°C for 5 minutes. Indexed PCR products were run on an agarose gel (1.0% w/v) next to the equivalent non-indexed amplicons to ensure that dual indices and Illumina sequencing adapters had

successfully attached. A second PCR clean-up step was performed on the indexed

amplicons following the protocol outlined above, although 56 μL of AMPure XP beads was

added to each sample well, washed twice with ethanol (80% v/v), and resuspended with

27.5 μL of 10 mM Tris (pH 8.5). A total of 25 μL of clear supernatant from each well was

transferred to a new 96-well plate and stored at -20°C. Purified amplicons were visualised by

agarose gel electrophoresis (1.2% w/v) as described in Section 2.2.5.1 and quantified via

Quant-IT™ PicoGreen assay (Thermo Fisher Scientific) at 520 nm using a FLUOstar Omega

microplate reader (BMG Labtech Ltd). Individual gene libraries were prepared by pooling

quantified amplicons in equal concentrations and were quantified via Quant-IT™ PicoGreen

assay (Thermo Fisher Scientific) using a Nanodrop 3300 Fluorospectrometer (Thermo

Fisher Scientific). DNA concentration (nM) in each gene library was calculated by multiplying

the DNA concentration (ng μL^{-1}) by 10^6 and dividing by the average library size multiplied by

the average molecular weight of dsDNA (660 g mol^{-1}). The bacterial 16S rRNA, archaeal

16S rRNA, and fungal ITS2 gene libraries were pooled using a ratio of 4:1:1, respectively.

The final amplicon library was quantified twice via 1) Quant-IT™ PicoGreen assay (Thermo

Fisher Scientific) using a Nanodrop 3300 Fluorospectrometer and 2) NEBNext Library Quant

Kit (Illumina) using a CFX96 real-time PCR detection system (Bio-Rad). The final amplicon

library was diluted to 4 nM with elution buffer (Qiagen). In preparation for cluster generation

and sequencing, 5 μL of the final amplicon library was denatured with 5 μL of 0.2 N NaOH,

mixed, and centrifuged at 280 × g for 1 minute. A 20 pM denatured library (1 mM NaOH)

was prepared by diluting 10 μL of the denatured amplicon library with 990 μL of hybridisation

buffer. To prepare a 4 pM denatured library, 120 μL of the 20 pM denatured library was

mixed with 480 μL of hybridisation buffer. A total of 570 μL of 4 pM denatured amplicon

library was mixed with 30 μL of 4 pM denatured PhiX control, incubated at 96°C for 2

minutes, mixed, and incubated on ice for 5 minutes. The final library was loaded onto a

MiSeq reagent cartridge and sequenced on the Illumina MiSeq system using the MiSeq

Reporter Metagenomics workflow.

2.2.5.3 MiSeq bioinformatics

Raw paired-end reads were quality filtered using Sickle Version 1.33 (Joshi & Fass 2011), with the 3' and 5'-end of reads trimmed based on quality and length thresholds. Trimmed reads were error corrected using the BayesHammer algorithm (Nikolenko et al. 2013) in SPAdes Version 3.7 (Bankevich et al. 2012). Error-corrected, paired-end reads were assembled into single contigs using PEAR (Zhang et al. 2014) within PANDAseq (Masella et al. 2012). Assembled sequences were dereplicated and sorted by their abundance. Operational taxonomic unit (OTU) centroid sequences were selected at the 97% similarity level using VSEARCH (Rognes et al. 2016). Singleton OTUs were removed, along with all chimeric sequences using reference-based chimera checking in UCHIME (Edgar et al. 2011). Taxonomy was assigned to OTU centroid sequences using the RDP Naïve Bayesian Classifier algorithm (Wang et al. 2007) by comparing sequences with the Ribosomal Database Project (RDP) database. OTU data, taxonomy data and read abundances were combined to produce an OTU table. OTU data was rarefied (Figure S2.3) in R Version 4.0.2 (R Core Team 2020) and diversity indices and OTU richness were calculated. Rarefied OTU data was explored and analysed in STAMP Version 2.1.3 (Parks et al. 2014) and R Version 4.0.2 (R Core Team 2020) using the "vegan" (Oksanen et al. 2020) and "ggplot2" (Wickham 2016) packages.

2.2.6 ^{14}C-acetaldehyde enrichments

Surface water samples from Hythe, Wivenhoe and Brightlingsea were pumped directly into 305 mL acid-washed, quartz Duran bottles (*n=3*) using a peristaltic pump and were incubated in the dark at 9°C. Killed controls (*n=1*) were prepared by adding trichloroacetic acid (≥99% purity, Acros Organics) (5% final concentration) to filtered surface water from each site, as described in Section 5.2.3. Killed controls and surface water samples were spiked with 20 μL of ^{14}C-acetaldehyde stock (10 nM final concentration) and were incubated at 9°C for 3 hours. Incubations were performed at 9°C to correspond to the in-situ surface

temperature at the time of sampling. The microbial assimilation and dissimilation of ^{14}C-acetaldehyde was measured using a Tri-Carb 2910TR liquid scintillation counter (PerkinElmer, Inc.) following the methods described in Section 5.2.2. Rates of microbial assimilation and dissimilation were calculated using the equations in Section 5.2.6.

2.2.7 Statistical analysis

Differences in the extent of acetaldehyde degradation between microcosms containing Colne Estuary sediment slurry and the no-inoculum controls were identified by one-way repeated measures analysis of variance (ANOVA) with Tukey's Honestly Significant Difference (HSD) post-hoc test for pairwise comparisons. This analysis was also used to identify differences in the extent of acetaldehyde degradation measured in microcosms containing Hythe, Wivenhoe, and Brightlingsea sediment slurries. A one-way analysis of covariance (ANCOVA) with Tukey's HSD post-hoc test for pairwise comparisons was performed to identify differences in the extent of acetaldehyde degradation between microcosms containing freshwater from the River Colne or the River Gipping and the abiotic controls. Differences in ammonium and phosphate assimilation in the River Colne and River Gipping microcosms were identified by one-way ANCOVA with Tukey's HSD post-hoc test for pairwise comparisons. All analyses were performed in R Version 4.0.2 (R Core Team 2020) using the R standard libraries.

2.3 Results

2.3.1 Acetaldehyde degradation and microbial abundance

2.3.1.1 Colne Estuary microcosms

Microbial acetaldehyde degradation was observed in Colne Estuary microcosms enriched with 2.27 mM of acetaldehyde (Figure 2.3). Complete acetaldehyde degradation was

measured in microcosms containing Hythe, Wivenhoe, and Brightlingsea sediment slurry during the primary enrichment, whilst >95% of acetaldehyde was degraded during the secondary, tertiary, and quaternary enrichments. Bacteria were identified as the most abundant microorganisms, with 16S rRNA gene copies more than 100-fold higher than archaeal 16S rRNA gene copies and more than 1000-fold higher than fungal ITS2 copies. Bacterial 16S rRNA gene copies in the acetaldehyde-enriched microcosms were similar to their respective no-acetaldehyde controls during the primary, secondary, and tertiary enrichments. At the conclusion of the quaternary enrichment, bacterial 16S rRNA gene copies in the acetaldehyde-enriched microcosms increased and were more than three orders of magnitude higher than bacterial 16S rRNA gene copies in the no-acetaldehyde controls ($p < 0.001$). This increase in bacterial abundance may indicate a transition from the co-metabolism of acetaldehyde and other organic matter during the primary, secondary, and tertiary enrichments, to the sole metabolism of acetaldehyde in the quaternary enrichment following the dilution and utilisation of organic matter. In this scenario, other organic matter would represent the primary metabolites for bacterial growth. Following the dilution and utilisation of this organic matter, only those bacteria capable of utilising acetaldehyde as a carbon and energy source increased in abundance. Alternatively, the increase in bacterial abundance observed in the quaternary enrichment may represent primary acetaldehyde metabolism. Primary metabolism may have occurred in the previous enrichments but was obscured by bacterial growth on other available substrates. The archaeal community exhibited a similar trend to the Bacteria during the four successive acetaldehyde enrichments. Archaeal 16S rRNA gene copies in the acetaldehyde-enriched microcosms remained similar to gene copies measured in the respective no-acetaldehyde controls during the primary, secondary, and tertiary enrichments. During the quaternary enrichment, archaeal 16S rRNA gene copies increased in the acetaldehyde-enriched microcosms and were more than two orders of magnitude higher than archaeal 16S rRNA gene copies in the no-acetaldehyde controls ($p < 0.001$). No differences in fungal ITS2 copies were detected between the acetaldehyde-enriched microcosms and the no-acetaldehyde controls

throughout the experiment. During the tertiary and quaternary enrichments, fungal ITS2 copies in the acetaldehyde-enriched microcosms and the no-acetaldehyde controls were lower than the negative controls, suggesting that fungi were in low abundance in these enrichments. Bacterial and archaeal 16S rRNA gene copies and fungal ITS2 copies were detected in the no-inoculum controls throughout the experiment, albeit at lower abundances than in the inoculated microcosms, despite being considered as sterile. This was thought to originate from the DNeasy Powersoil Kit (Qiagen) reagents used for DNA extraction or from the PCR mastermix used for qPCR (Section 2.2.5.1). The contamination of DNA extraction kits and PCR master mix reagents with microbial DNA has previously been reported (Salter et al. 2014), with the introduction of contaminating DNA during sample preparation termed the "kitome" (Stinson et al. 2018). Attempts to eliminate this contamination have included the use of UV irradiation, restriction endonuclease digestion, and DNase treatment (Stinson et al. 2018), although these attempts have been unreliable and non-reproducible. Stinson et al. (2018), however, demonstrated that the majority of contaminating DNA was found in PCR master mix reagents and that a dsDNase treatment could reduce contaminating bacterial reads by 99%. Consequently, experiments involving PCR amplification should include a dsDNase treatment of PCR reagents to minimise the introduction of contaminating microbial DNA, as detected in the Colne Estuary no-inoculum controls (Figure 2.3). Despite the detection of bacterial and archaeal 16S rRNA gene copies and fungal ITS2 copies in the no-inoculum controls, these findings suggest that bacteria are primarily responsible for microbial acetaldehyde degradation in the Colne Estuary, whilst archaea also play an important, albeit secondary, role. Conversely, these results suggest that fungi are not involved in acetaldehyde degradation.

Figure 2.3 Acetaldehyde degradation (%) and the associated abundance of bacteria (16S rRNA gene copies ml^{-1}), fungi (ITS2 copies ml^{-1}) and archaea (16S rRNA gene copies ml^{-1}) within Colne Estuary microcosms containing sediment slurries (primary to quaternary enrichment). Microcosms were enriched with 2.27 mM of acetaldehyde (lower concentration treatment), incubated in the dark at 20°C and monitored for degradation. Degradation within enrichments is relative to the mean of the no-inoculum controls (*n=4*) at each time point. The mean of four replicates is plotted for each sampling site (± S.E.). Successive enrichments were established after measuring ≥50% acetaldehyde degradation in the previous enrichment. Bacterial, fungal, and archaeal abundance was quantified at the conclusion of each successive enrichment. The initial abundance (day 0) of microorganisms within the secondary, tertiary, and quaternary enrichments was estimated by applying a 10-fold dilution factor to the final number of gene copies (16S rRNA or ITS2) quantified in the previous enrichment. The mean of four replicates is plotted for each sampling site (± S.E.). NoAA: No-acetaldehyde control.

Microbial acetaldehyde degradation was also detected in Colne Estuary microcosms enriched with the 10-fold higher concentration (22.7 mM) of acetaldehyde (Figure 2.4). During the primary enrichment, 51.3 ± 16.9%, 25.5 ± 7.2%, and 48.5 ± 17.9% of the added acetaldehyde was degraded in microcosms containing Hythe, Wivenhoe, and Brightlingsea sediment slurries, respectively, after 50 days of incubation. The extent of degradation in these microcosms was significantly different to the no-inoculum controls (p <0.001). Acetaldehyde degradation was not detected in microcosms containing Hythe or Wivenhoe sediment slurries during the secondary, tertiary, and quaternary enrichments, suggesting that the high concentration of acetaldehyde inhibited microbial growth and metabolism. This is reflected by the overall decrease in bacterial, fungal, and archaeal abundance in microcosms containing Hythe and Wivenhoe sediment slurries following four successive acetaldehyde enrichments. Furthermore, copies of the bacterial and archaeal 16S rRNA gene and fungal ITS2 region in the acetaldehyde-enriched microcosms were often comparable or lower than copies in their respective no-acetaldehyde controls. During the quaternary enrichment, for example, bacterial and archaeal 16S rRNA gene copies in acetaldehyde-enriched Hythe and Wivenhoe microcosms were significantly lower than the no-acetaldehyde controls. Acetaldehyde degradation was detected in microcosms containing Brightlingsea sediment slurry during the secondary, tertiary, and quaternary enrichments (Figure 2.4), however, this was driven by the activity of acetaldehyde-degrading microorganisms in one replicate, namely bottle B1 (Figure 2.5). Complete acetaldehyde degradation was measured in bottle B1 during the tertiary and quaternary enrichments, and microbial growth in the form of fungal-like biomass was observed (Figure 2.5; inset photos). Acetaldehyde degradation and microbial growth were not detected in replicates B2, B3 or B4 during the tertiary and quaternary enrichments. Fungal ITS2 copies in acetaldehyde-enriched Brightlingsea microcosms increased during the secondary and quaternary enrichments and were significantly higher than copies in the no-acetaldehyde controls (p <0.001), corresponding with the observations of fungal-like biomass in bottle B1. Bacterial and archaeal 16S rRNA gene copies in acetaldehyde-enriched Brightlingsea microcosms

were not significantly different to gene copies in the no-acetaldehyde controls and generally decreased following four successive enrichments. These findings suggest that some fungi can tolerate artificially high concentrations of acetaldehyde and grow, possibly utilising this compound as a carbon and energy source. The overall decrease in 16S rRNA gene copies suggests that the higher acetaldehyde concentration inhibits the growth of both bacteria and archaea found in the Colne Estuary. Similar to the lower concentration treatment (Figure 2.3), bacterial and archaeal 16S rRNA gene copies and fungal ITS2 copies were detected in the no-inoculum controls of the higher concentration treatment (Figure 2.4), further suggesting that the process of DNA extraction and/or qPCR introduced contaminating microbial DNA. As previously discussed, the "kitome" likely accounts for the low abundance of microorganisms detected in the no-inoculum controls, despite efforts to prevent contamination.
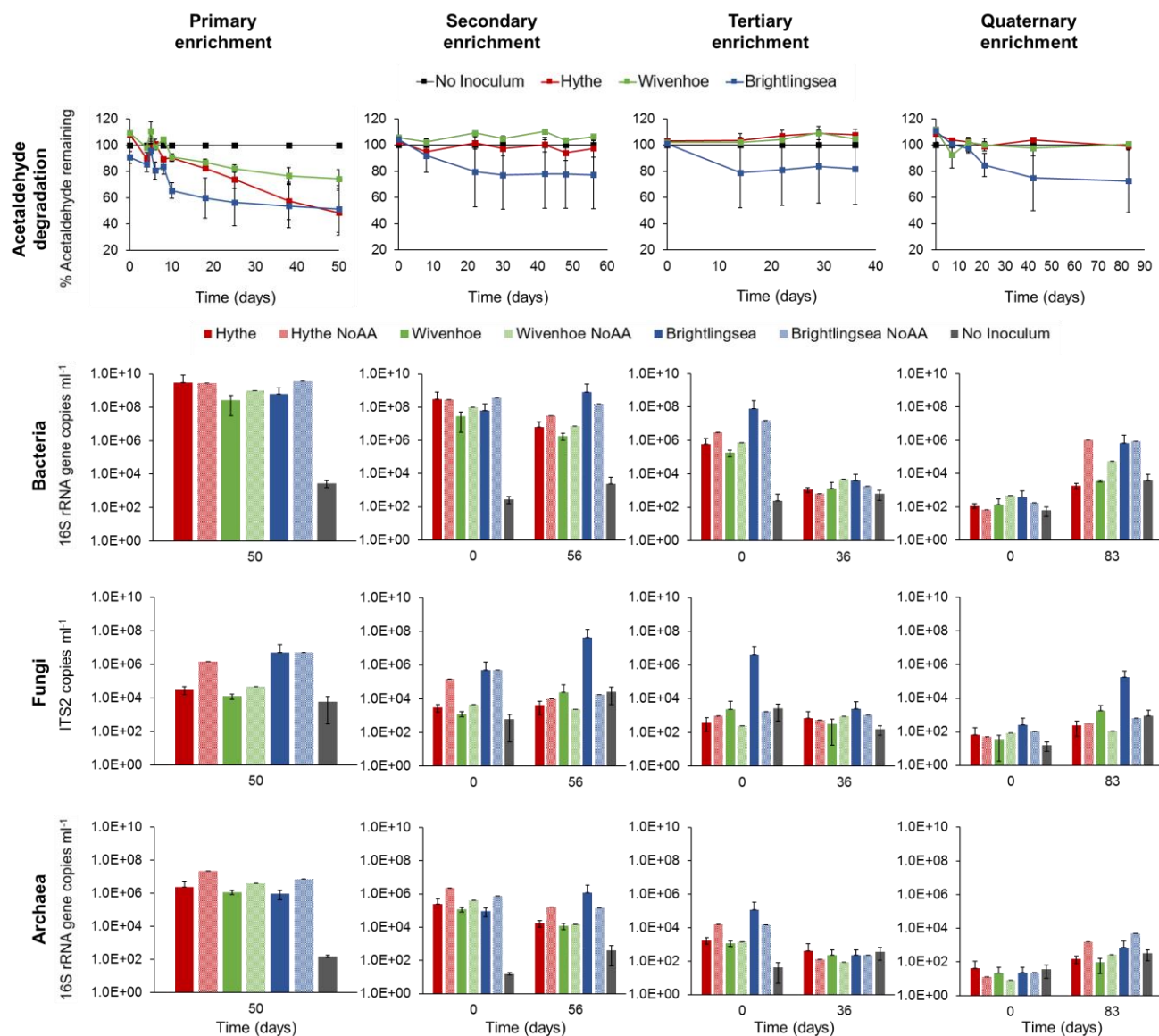
Figure 2.4 Acetaldehyde degradation (%) and the associated abundance of bacteria (16S rRNA gene copies ml^{-1}), fungi (ITS2 copies ml^{-1}) and archaea (16S rRNA gene copies ml^{-1}) within Colne Estuary microcosms containing sediment slurries (primary to quaternary enrichment). Microcosms were enriched with 22.7 mM of acetaldehyde (higher concentration treatment), incubated in the dark at 20°C and monitored for degradation. Degradation within enrichments is relative to the mean of the no-inoculum controls (*n=4*) at each time point. The mean of four replicates is plotted for each sampling site (± S.E.). Successive enrichments were established after observing microbial growth or measuring ≥50% acetaldehyde degradation in the previous enrichment. Bacterial, fungal, and archaeal abundance was quantified at the conclusion of each successive enrichment. The initial abundance (day 0) of microorganisms within the secondary, tertiary, and quaternary enrichments was estimated by applying a 10-fold dilution factor to the final number of gene copies (16S rRNA or ITS2) quantified in the previous enrichment. The mean of four replicates is plotted for each sampling site (± S.E.). NoAA: No-acetaldehyde control.
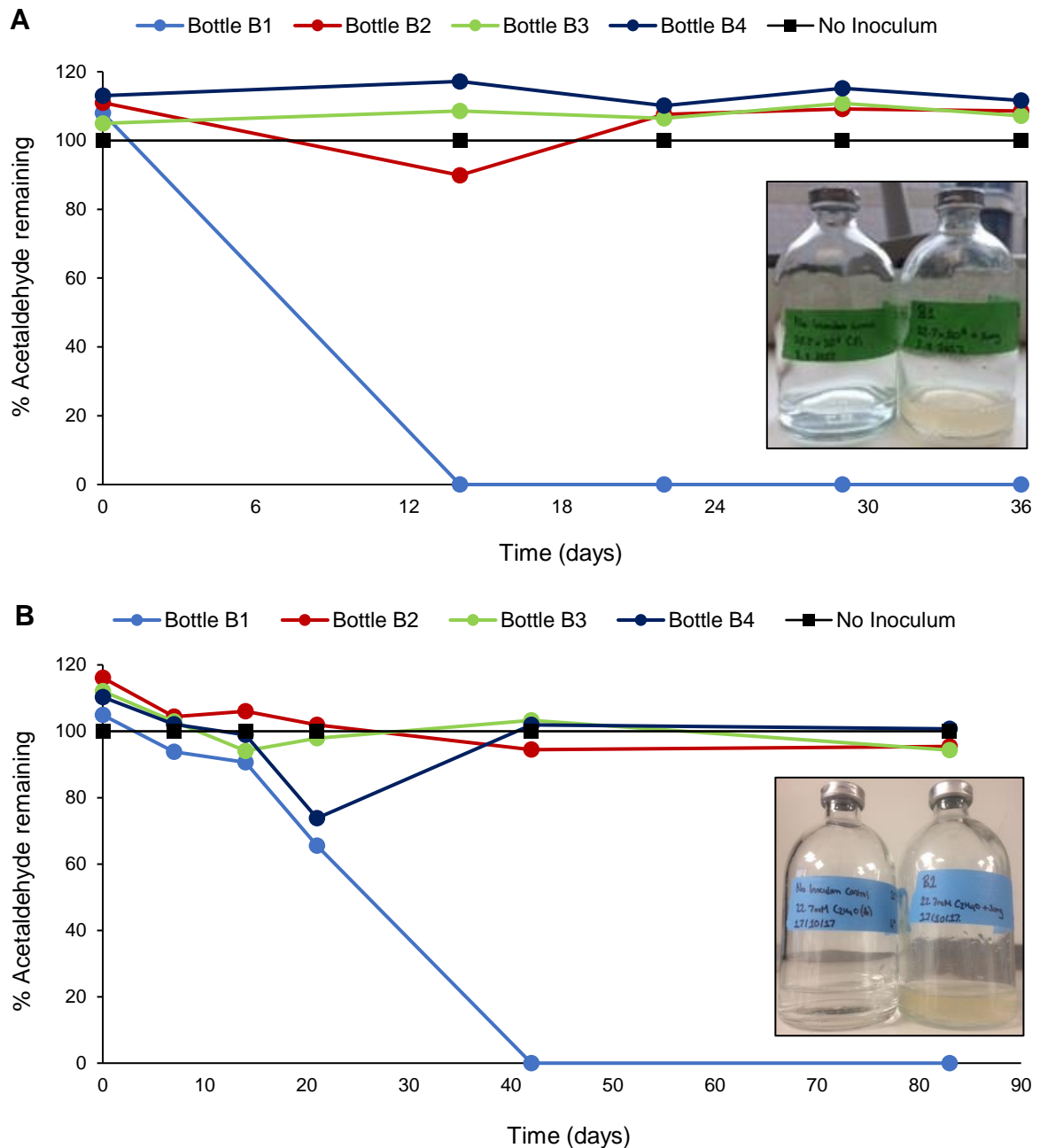
Figure 2.5 Acetaldehyde degradation (%) in microcosms containing Brightlingsea sediment slurry following (A) tertiary and (B) quaternary acetaldehyde enrichment. Microcosms were enriched with 22.7 mM of acetaldehyde (higher treatment), incubated in the dark at 20°C and monitored for degradation. Degradation within enrichments is relative to the mean of the no-inoculum controls (*n=4*) at each time point. Successive enrichments were established after measuring ≥50% acetaldehyde degradation in the previous enrichment or observing microbial growth. Microbial growth in replicate B1 compared to the no-inoculum control is shown in the inset photos.

2.3.1.2 River Colne and River Gipping microcosms

Acetaldehyde degradation was detected in microcosms containing freshwater from the River Colne and the River Gipping following enrichment with 2.27 mM of acetaldehyde (Figure 2.6). After 1 day of incubation, the concentration of acetaldehyde in River Colne and River Gipping microcosms increased, indicating the equilibration of acetaldehyde between the gas (headspace) and liquid phase. Microbial acetaldehyde degradation was initially detected after 4 days of incubation, with 26% and 44% of the added acetaldehyde degraded in River Colne and River Gipping microcosms, respectively. The onset of acetaldehyde degradation corresponded with a significant increase in bacterial 16S rRNA gene copies in River Colne and River Gipping microcosms ($p < 0.001$), and a significant increase in fungal ITS2 copies in River Gipping microcosms ($p < 0.05$). The increase in bacterial abundance in River Colne microcosms coincided with decreases in phosphate (PO_4^{3-}) and ammonium (NH_4^+) concentrations (Figure 2.7). Increases in bacterial and fungal abundance in River Gipping microcosms also coincided with a decrease in phosphate concentrations, however, ammonium concentrations remained constant. Complete acetaldehyde degradation was seen in River Colne and River Gipping microcosms by 7 days of incubation, with microbial growth, in the form of flocs, also observed (Figure 2.6; inset photos). The degradation of acetaldehyde and observations of microbial growth coincided with significant increases in bacterial and archaeal 16S rRNA gene and fungal ITS2 copies in the acetaldehyde-enriched microcosms after 7 days of incubation, whilst bacterial, archaeal, and fungal abundance remained constant in the no-acetaldehyde controls. The increase in bacterial and archaeal 16S rRNA gene and fungal ITS2 copies also corresponded with a significant decrease in phosphate and ammonium concentrations in the acetaldehyde-enriched microcosms (Figure 2.7), providing further support for acetaldehyde degradation being the result of microbial activity rather than physical or chemical loss. Bacteria were identified as the most abundant microorganisms in the River Colne and River Gipping acetaldehyde-enriched microcosms, with bacterial 16S rRNA gene copies more than 100-fold higher than fungal ITS2 copies and

more than 1000-fold higher than archaeal 16S rRNA gene copies. These findings suggest that bacteria are primarily responsible for microbial acetaldehyde degradation in freshwater rivers, whilst fungi and archaea also contribute to acetaldehyde degradation in these environments, either directly or indirectly, but likely play a lesser role than bacteria.

Bacterial, archaeal, and fungal abundance remained constant in microcosms enriched with 2.59 mM of metaldehyde (Figure 2.6), suggesting that the in-situ microorganisms were unable to utilise metaldehyde as a carbon and energy source or that the elevated concentration of metaldehyde was toxic and inhibited growth. Concentrations of phosphate and ammonium in metaldehyde-enriched River Colne microcosms decreased steadily throughout the experiment, demonstrating the presence and activity of microorganisms growing on dissolved or particulate organic matter derived from suspended sediment (Figure 2.7). Phosphate concentrations also decreased steadily in metaldehyde-enriched River Gipping microcosms, whilst ammonium was completely utilised following 7 days of incubation. The rapid utilisation of ammonium indicates the possible presence of ammonia-oxidising bacteria in metaldehyde-enriched River Gipping microcosms, with ammonium oxidised to nitrite (NO_2^-). Nitrite-oxidising bacteria could oxidise NO_2^- to nitrate (NO_3^-), whilst complete ammonia oxidisers (comammox) could perform both oxidation reactions. This may also explain the utilisation of ammonium in the River Colne and River Gipping no-acetaldehyde controls (Figure 2.7), despite the abundance of bacteria in the no-acetaldehyde controls remaining constant (Figure 2.6).

During the secondary acetaldehyde enrichment, acetaldehyde degradation was initially detected after 4 days of incubation, with River Colne and River Gipping microcosms exhibiting 78% and 23% degradation, respectively (Figure S2.4). Complete acetaldehyde degradation was measured in River Colne and River Gipping microcosms after 14 days of incubation and microbial growth, in the form of flocs, was observed.
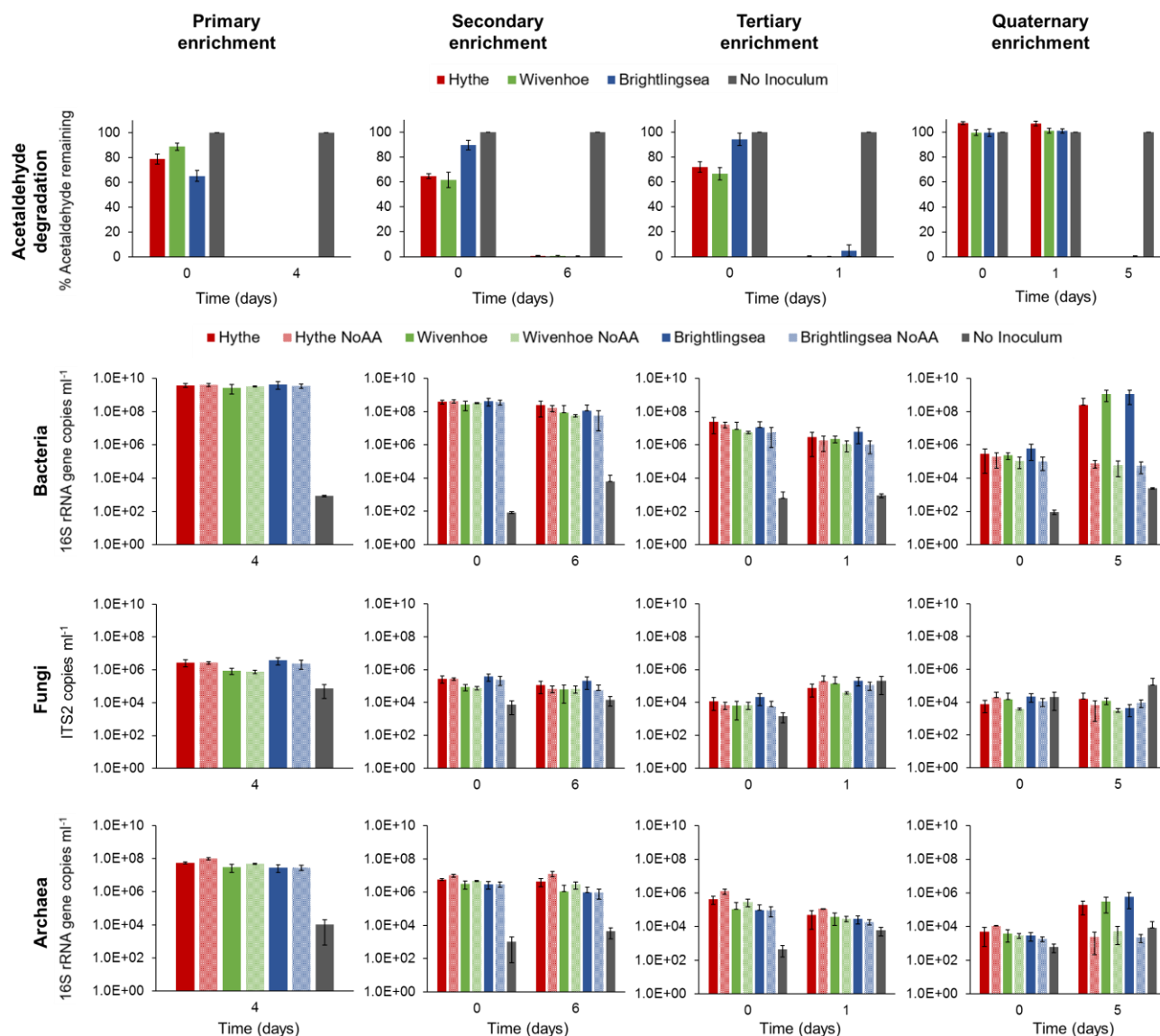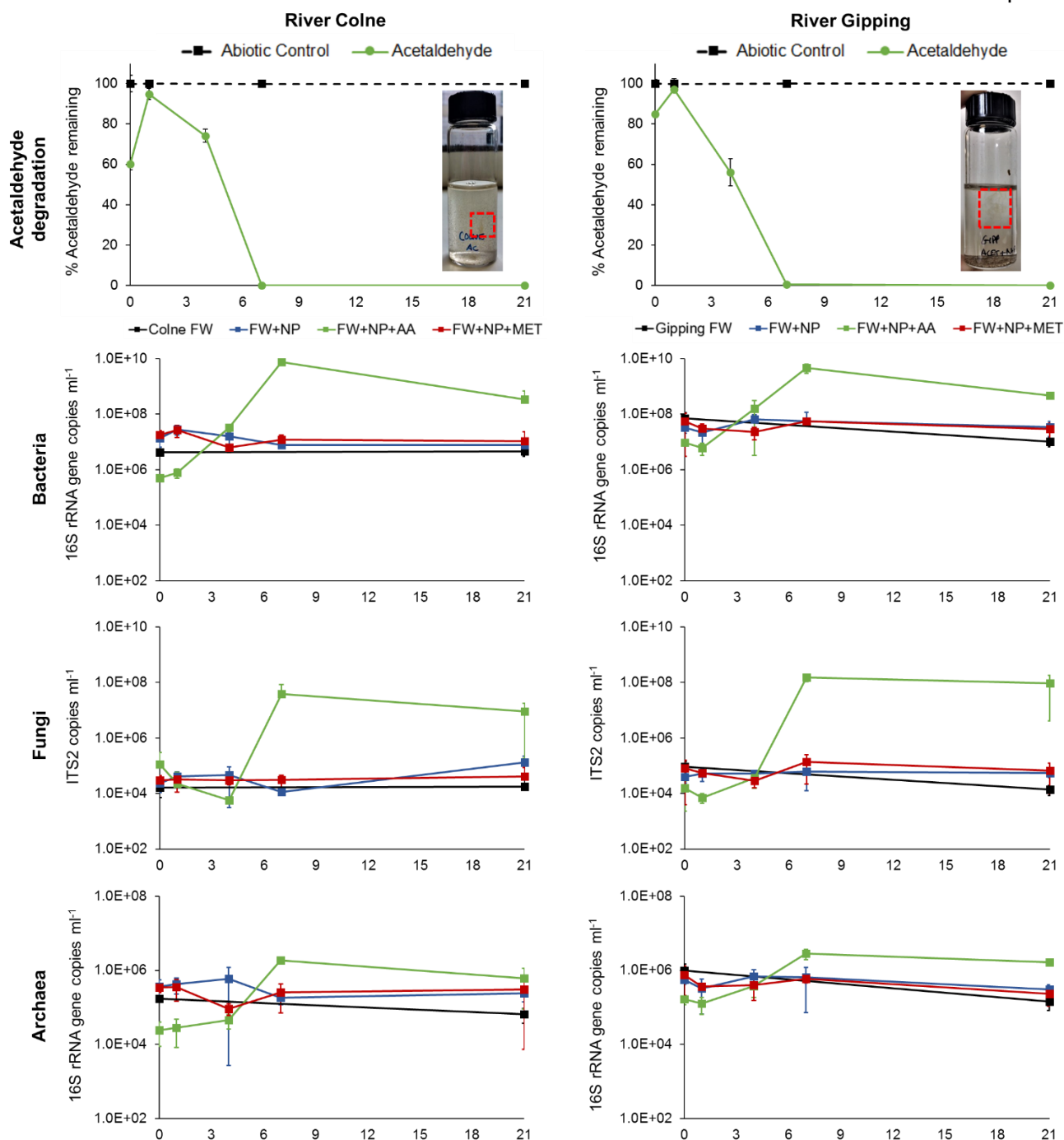
Figure 2.6 Acetaldehyde degradation (%) and the associated abundance of bacteria (16S rRNA gene copies ml^{-1}), fungi (ITS2 copies ml^{-1}) and archaea (16S rRNA gene copies ml^{-1}) within River Colne and River Gipping primary enrichments. Microcosms were enriched with 2.27 mM of acetaldehyde, incubated in the dark at 20°C and monitored for degradation. Degradation within enrichments is relative to the mean of the abiotic controls (*n=3*) at each time point. The mean of three replicates is plotted for each treatment (± S.E.). Bacterial, fungal, and archaeal abundance within individual replicates was quantified at each time point. The mean of three replicates is plotted for each treatment (± S.E.). FW: untreated freshwater; NP: freshwater treated with ammonium chloride and sodium phosphate dibasic; AA: freshwater enriched with 2.27 mM of acetaldehyde; MET: freshwater enriched with 2.59 mM of metaldehyde. Microbial growth in River Colne and River Gipping microcosms enriched with acetaldehyde is shown in the inset photos.
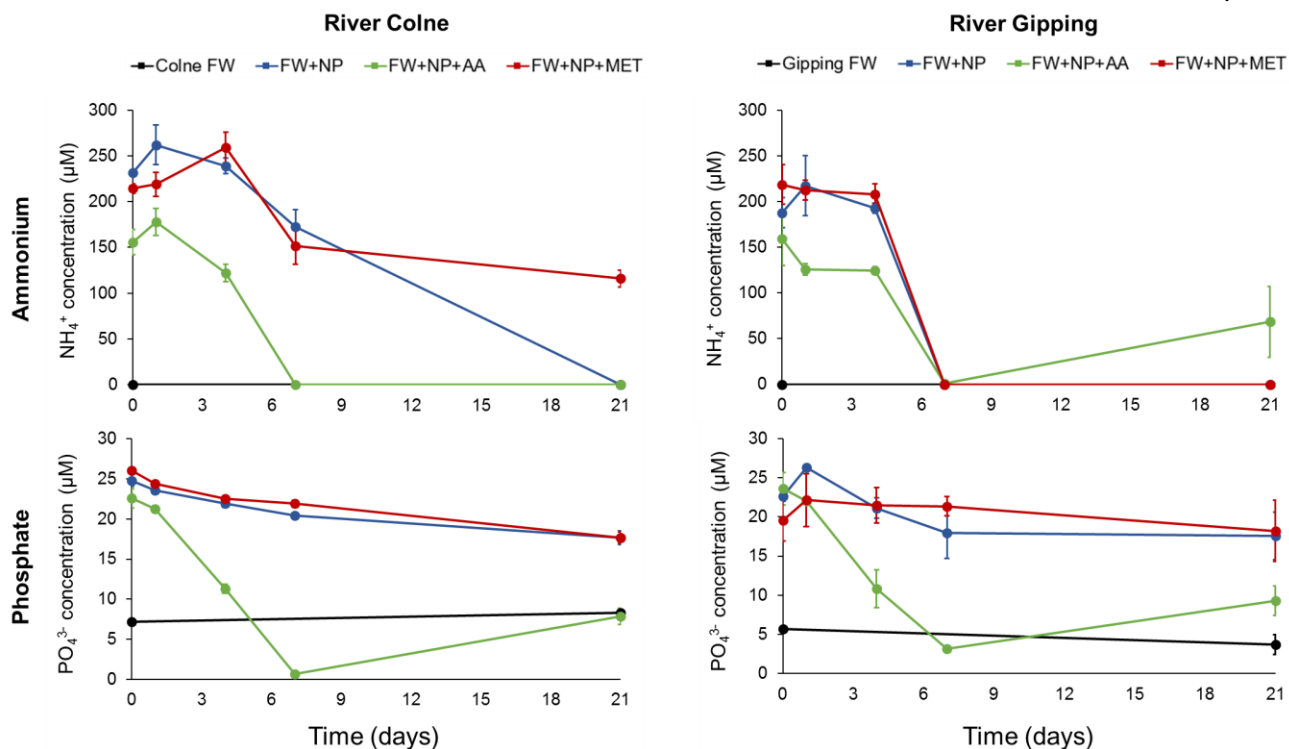
Figure 2.7 The assimilation of ammonium (NH_4^+) and phosphate (PO_4^{3-}) in River Colne and River Gipping primary enrichments. The mean of three replicates is plotted for each treatment (± S.E.). FW: untreated freshwater; NP: freshwater treated with ammonium chloride and sodium phosphate dibasic; AA: freshwater enriched with 2.27 mM of acetaldehyde; MET: freshwater enriched with 2.59 mM of metaldehyde.

2.3.2 Microbial community analysis

2.3.2.1 Microbial communities of the Colne Estuary

Distinct bacterial communities were identified in the no-acetaldehyde controls containing sediment slurry from Hythe, Wivenhoe, and Brightlingsea (Figure 2.8a), demonstrating that bacterial community composition varies along the Colne Estuary. Bacterial communities in Hythe, Wivenhoe, and Brightlingsea enrichments remained distinct following an initial enrichment of 2.27 mM of acetaldehyde but were different to the bacterial communities in the no-acetaldehyde controls. This difference resulted from a significant increase in the mean proportion of sequences within OTUs assigned to the genera *Pseudomonas* and *Arcobacter* (Figure 2.9a). Following the initial acetaldehyde enrichment, *Pseudomonas* sequences represented 19%, 16%, and 2% of all bacterial sequences in Hythe, Wivenhoe, and

Brightlingsea enrichments, respectively (Figure 2.9c), whilst *Arcobacter* sequences represented 1%, 8%, and 11% of all bacterial sequences, respectively (Figure 2.9c). At the conclusion of the quaternary acetaldehyde enrichment, the composition of bacterial communities in Hythe, Wivenhoe, and Brightlingsea enrichments became highly similar in response to successive acetaldehyde enrichments (Figure 2.8a), which corresponded with a significant decrease in bacterial OTU richness (Figure 2.8b), suggesting that a limited number of bacteria utilised acetaldehyde as a carbon and energy source. These changes primarily resulted from a significant increase in the mean proportion of *Pseudomonas* sequences (Figure 2.9b), which represented 39%, 87%, and 84% of all bacterial sequences in Hythe, Wivenhoe, and Brightlingsea enrichments, respectively (Figure 2.9c). Conversely, *Arcobacter* sequences represented less than 0.05% of the bacterial communities of Hythe, Wivenhoe, and Brightlingsea enrichments following the quaternary acetaldehyde enrichment (Figure 2.9c), suggesting that this genus was outcompeted by members of the *Pseudomonas* genus. The significant increase in the relative abundance of *Pseudomonas* following the quaternary acetaldehyde enrichment was primarily driven by OTU6 (Figure 2.10), which represented 96%, 99%, and 54% of the genus in Hythe, Wivenhoe, and Brightlingsea enrichments, respectively. OTU6 was identified as a close relative of *Pseudomonas benzenivorans* DSM 8628, and represented the majority of all bacterial sequences in Hythe (38%), Wivenhoe (86%), and Brightlingsea (45%) enrichments (Figure 2.10). OTU60, identified as a close relative of *P. zhaodongensis* YZGP305 and *P. stutzeri* SO240BG38 (Figure 2.10), represented 44% of the genus and 38% of all bacterial sequences in Brightlingsea enrichments, suggesting that this OTU is a potentially important acetaldehyde degrader in the mouth of the Colne Estuary. During the primary acetaldehyde enrichment, OTU4249, a close relative of *P. koreensis* MLS2-1, represented 42%, 53%, and 15% of the genus *Pseudomonas* in Hythe, Wivenhoe, and Brightlingsea enrichments, respectively (Figure 2.10), suggesting that this OTU may be an important acetaldehyde degrader towards the estuary head. The relative increase in *Arcobacter* sequences during the primary acetaldehyde enrichment was predominantly driven by OTU142 (Figure 2.10),

representing 36%, 90%, and 98% of the genus in Hythe, Wivenhoe, and Brightlingsea

enrichments, respectively. OTU142 was most closely related to *Arcobacter nitrofigilis* DSM

7299, sharing 97.05% sequence similarity, and represented 0.5%, 8%, and 11% of all

bacterial sequences in Hythe, Wivenhoe, and Brightlingsea enrichments, respectively.

Figure 2.8 Principal component analysis (PCA) plot (A) showing the similarity of bacterial communities in Colne Estuary microcosms enriched with 2.27 mM or 22.7 mM of acetaldehyde and the no-acetaldehyde controls. Numbers in parentheses indicate enrichment number (either enrichment 1 or 4). No-acetaldehyde controls for the lower (2.27 mM) and higher (22.7 mM) acetaldehyde concentration experiments are represented by 0 (Lower) and 0 (Higher), respectively, indicating that serum bottles had an acetaldehyde concentration of 0 mM and belonged to the lower or higher acetaldehyde concentration experiment. Bacterial OTU richness (B) in the acetaldehyde-enriched microcosms and the no-acetaldehyde controls is shown for Hythe, Wivenhoe, and Brightlingsea. The mean of two, three, and three replicates (± S.E.) is plotted for Hythe, Wivenhoe, and Brightlingsea no-acetaldehyde controls from the lower concentration experiment (0 Lower), respectively, whilst the mean of four replicates (± S.E.) is plotted for primary enrichments from the lower concentration experiment (2.27 mM (1)). The mean of two, three, and four replicates (± S.E.) is plotted for Hythe, Wivenhoe, and Brightlingsea quaternary enrichments from the lower concentration experiment (2.27 mM (4)), respectively. One replicate is plotted for the no-acetaldehyde controls from the higher concentration experiment (0 Higher), whilst the mean of two, three, and three replicates (± S.E.) is plotted for Hythe, Wivenhoe, and Brightlingsea primary enrichments from the higher concentration experiment (22.7 mM (1)), respectively.
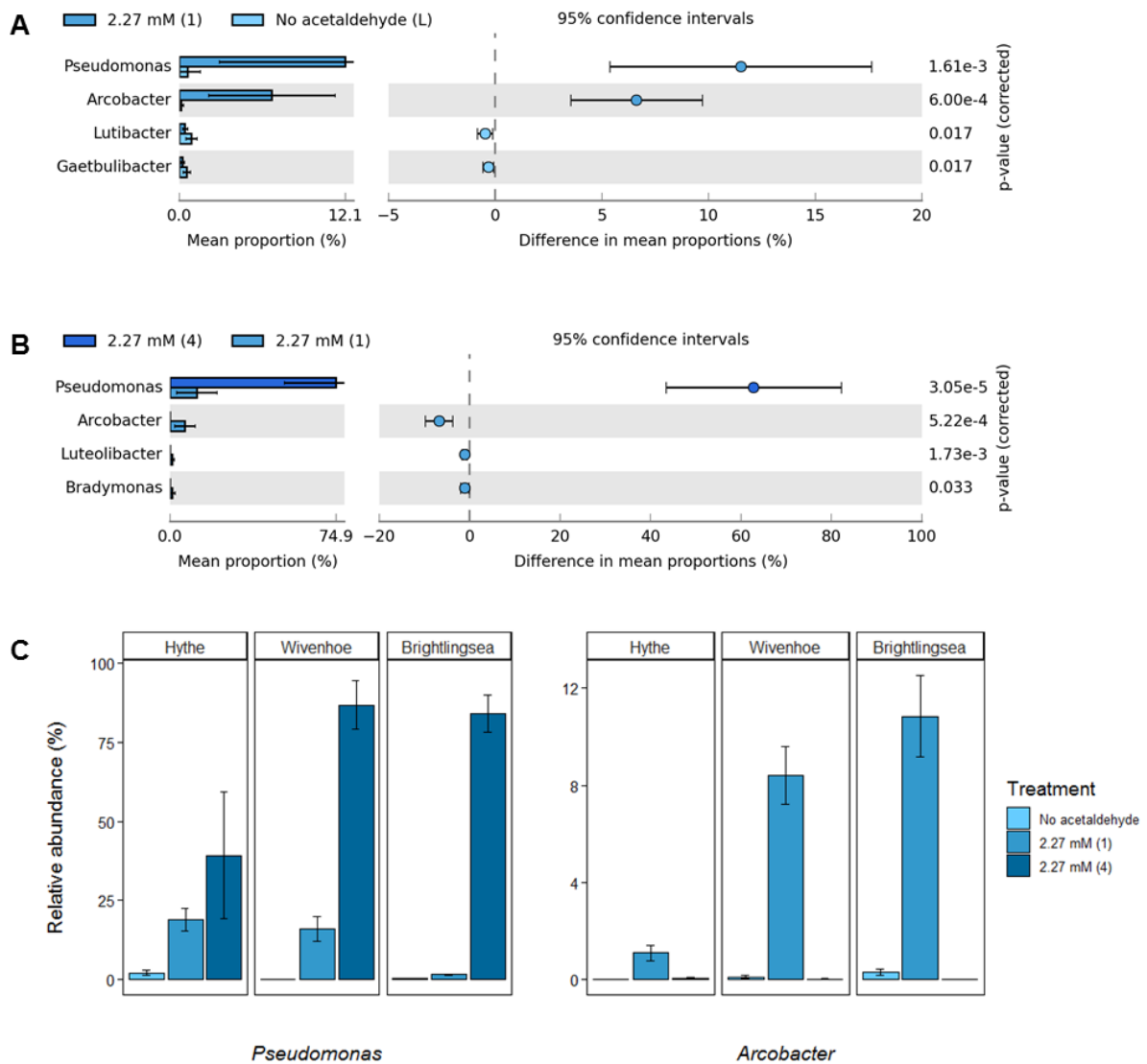
Figure 2.9 The mean proportion of *Pseudomonas* and *Arcobacter* sequences in microcosms enriched with 2.27 mM of acetaldehyde. (A) Colne Estuary primary enrichments and the no-acetaldehyde controls and (B) Colne Estuary primary and quaternary enrichments. (C) Relative abundance (%) of *Pseudomonas* and *Arcobacter* sequences relative to all bacterial sequences in Hythe, Wivenhoe, and Brightlingsea enrichments. Numbers in parentheses indicate enrichment number (either enrichment 1 or 4).
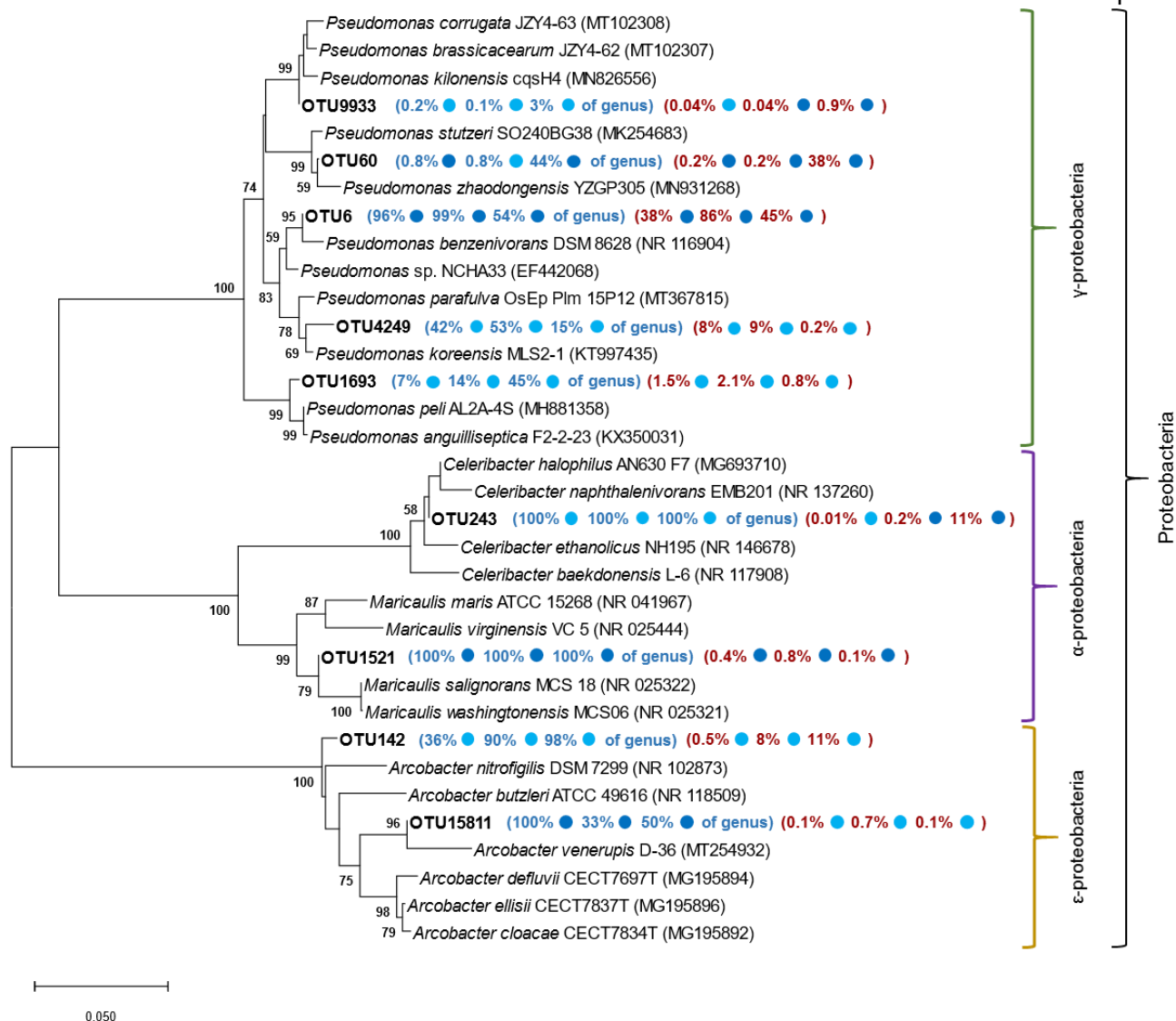
Figure 2.10 Phylogenetic tree showing the relationship between bacterial OTUs identified in Colne Estuary microcosms enriched with 2.27 mM of acetaldehyde and closely related strains within the phylum Proteobacteria, based on partial 16S rRNA gene sequences. The evolutionary history of OTUs was inferred using the Neighbour-Joining method (Saitou & Nei 1987). The percentage of replicate trees in which the associated taxa clustered together in the bootstrap test (1000 replicates) is shown next to the branches when ≥50%. Evolutionary distances were computed using Kimura's two-parameter model (Kimura 1980) and are in the units of the number of base substitutions per site (horizontal scale bar represents 5% nucleotide differences per site). Accession numbers of the type strains are shown in round brackets. The maximum proportion of the OTU within the genus (%) is shown in blue brackets, in the order Hythe, Wivenhoe, and Brightlingsea. The maximum proportion of the OTU relative to all bacterial sequences (%) is shown in red brackets, in the same order. Light blue circles indicate that the maximum proportion of the OTU within the genus (%), or the maximum proportion of the OTU relative to all bacterial sequences (%) was measured in the primary enrichment, whilst dark blue circles indicate that the maximum proportion was measured in the quaternary enrichment. Associated classes of the Proteobacteria are shown to the right of the tree.

Following an initial enrichment of 22.7 mM of acetaldehyde, bacterial communities in Hythe, Wivenhoe, and Brightlingsea enrichments were distinct from their respective no-acetaldehyde controls (Figure 2.8a) and were more similar to the bacterial communities in Hythe, Wivenhoe, and Brightlingsea enrichments following the quaternary 2.27 mM acetaldehyde enrichment. This shift in community composition coincided with decreases in bacterial OTU richness in Hythe, Wivenhoe, and Brightlingsea enrichments (Figure 2.8b), in addition to significant increases in the mean proportion of sequences assigned to the genera *Lutimonas* and *Loktanella* (Figure 2.11a). Following acetaldehyde enrichment, *Lutimonas* sequences represented 0.4%, 2%, and 6% of all bacterial sequences in Hythe, Wivenhoe, and Brightlingsea enrichments, respectively (Figure 2.11b), whilst *Loktanella* sequences represented 0.04%, 2%, and 4% of all bacterial sequences, respectively (Figure 2.11b). The significant increase in the relative abundance of the *Lutimonas* genus in Wivenhoe and Brightlingsea enrichments was primarily driven by OTU2502 (Figure 2.11c), a close relative of *Lutimonas halocynthiae* RSS3-C1, which represented 78% and 74% of the genus, and accounted for 1.6% and 4.6% of bacterial sequences, respectively. Increases in the relative abundance of the *Loktanella* genus in Wivenhoe and Brightlingsea enrichments was mostly driven by OTU1440 (Figure 2.11c), which was closely related to *Loktanella acticola* OISW-6. Following enrichment with 22.7 mM of acetaldehyde, OTU1440 represented 97% and 99% of the genus in Wivenhoe and Brightlingsea enrichments, respectively, equating to 2% and 4% of all bacterial sequences.

Differences in the bacterial communities of Hythe, Wivenhoe, and Brightlingsea enrichments following enrichment with 2.27 mM or 22.7 mM of acetaldehyde (Figure 2.8a) were primarily driven by successive enrichments (PERMANOVA: $p <0.001$, 24% of variance), acetaldehyde concentration (PERMANOVA: $p <0.001$, 19% of variance), and sampling site (PERMANOVA: $p <0.001$, 17% of variance).
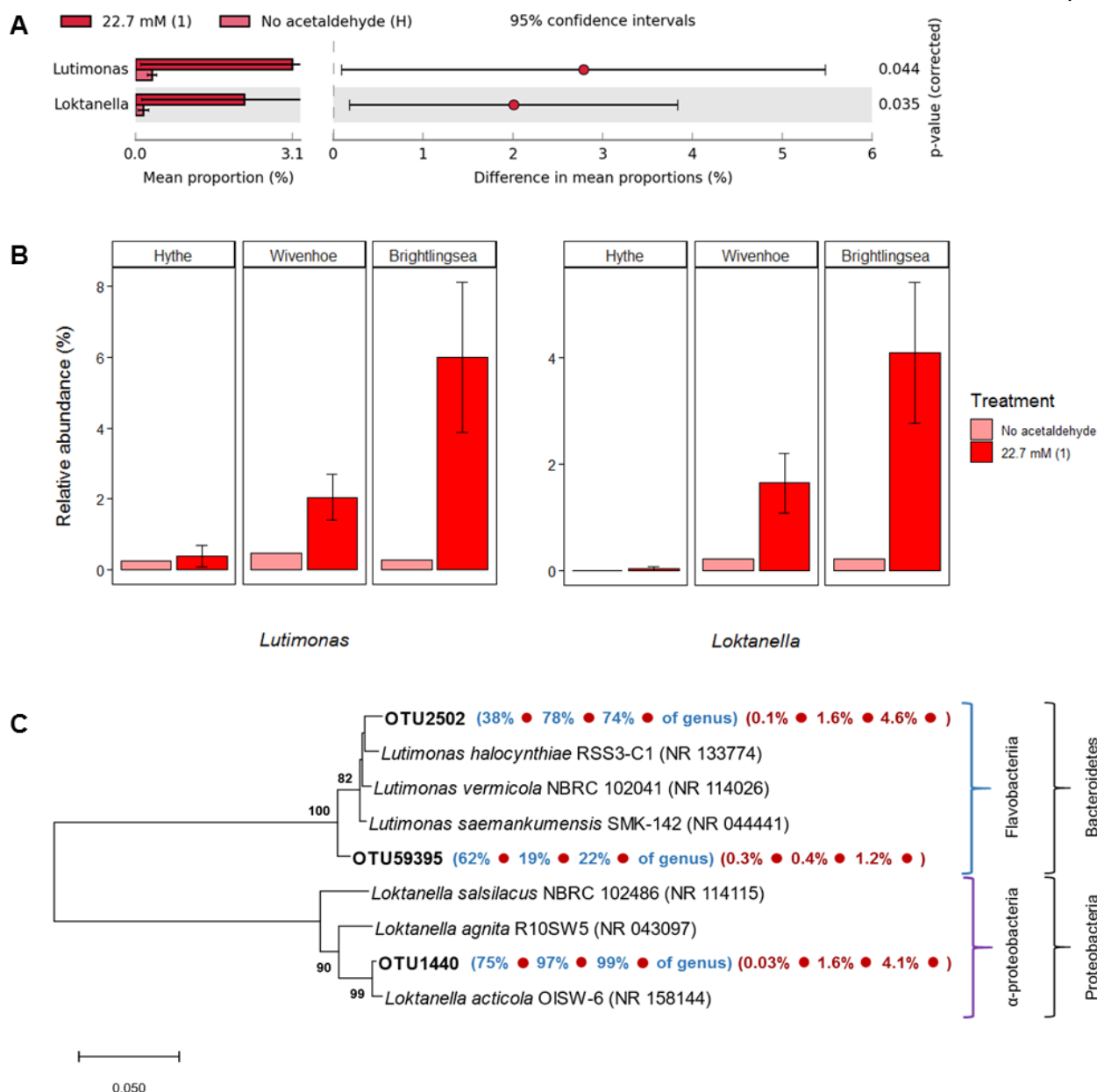
Figure 2.11 The mean proportion of *Lutimonas* and *Loktanella* sequences in Colne Estuary primary enrichments enriched with 22.7 mM of acetaldehyde and the no-acetaldehyde controls (A) and the relative abundance (%) of *Lutimonas* and *Loktanella* sequences relative to all bacterial sequences in Hythe, Wivenhoe, and Brightlingsea enrichments (B). The relationship between *Lutimonas* and *Loktanella* OTUs and closely related strains within the Bacteroidetes and Proteobacteria, based on partial 16S rRNA gene sequences, is shown in the phylogenetic tree (C). The evolutionary history of OTUs was calculated using the Neighbour-Joining method (Saitou & Nei 1987). The percentage of replicate trees in which the associated taxa clustered together in the bootstrap test (1000 replicates) is shown next to the branches when ≥50%. Evolutionary distances were computed using Kimura's two parameter model (Kimura 1980) and are in the units of the number of base substitutions per site (horizontal scale bar represents 5% nucleotide differences per site). Accession numbers of the type strains are shown in round brackets. The maximum proportion of the OTU within the genus (%) is shown in blue brackets, in the order Hythe, Wivenhoe, and Brightlingsea. The maximum proportion of the OTU relative to all bacterial sequences (%) is shown in red brackets, in the same order. Red circles indicate that the maximum proportion of the OTU within the genus (%), or the maximum proportion of the OTU relative to all bacterial sequences (%) was measured in the primary enrichment. Taxonomic classifications are shown to the right of the tree.

Fungal communities in the no-acetaldehyde controls containing Hythe, Wivenhoe, and Brightlingsea sediment slurries were distinct (Figure 2.12a), further demonstrating spatial differences in microbial community composition along the Colne Estuary; albeit based on single samples from each location that contained sufficient fungi to obtain sequence data. Following an initial enrichment of 22.7 mM of acetaldehyde, fungal communities in Hythe, Wivenhoe, and Brightlingsea enrichments became highly similar. The convergence of fungal communities at the conclusion of the primary enrichment corresponded with significant decreases in OTU richness (Figure 2.12b), indicating that a small proportion of fungi found in the Colne Estuary could tolerate unnaturally high and potentially toxic concentrations of acetaldehyde or utilise this compound as a carbon and energy source. The decrease in OTU richness and the convergence of fungal communities also corresponded with a significant increase in the mean proportion of sequences assigned to *Sordariaceae* sp. SH213056.06FU (Figure 2.13a), which represented 34%, 32%, and 17% of all fungal sequences in Hythe, Wivenhoe, and Brightlingsea enrichments, respectively (Figure 2.13b). With exception to Brightlingsea microcosms, fungal community data from the quaternary acetaldehyde enrichment was removed from the final data set following rarefaction (Figure S2.3c). At the conclusion of the quaternary acetaldehyde enrichment, the fungal community in Brightlingsea enrichments remained similar to the fungal communities observed at the conclusion of the primary enrichment (Figure 2.12a), however, fungal OTU richness decreased (Figure 2.12b). This coincided with a significant decrease in the mean proportion of *Sordariaceae* sp. SH213056.06FU sequences, but also corresponded with a significant increase in the mean proportion of sequences belonging to Sordariomycetes sp. SH232118.06FU (Figure 2.13c). The increase in Sordariomycetes sp. SH232118.06FU in the quaternary acetaldehyde enrichment of Brightlingsea sediment slurry suggests that this fungus contributed to the acetaldehyde degradation measured in bottle B1 (Figure 2.5) and was responsible for the spike in fungal ITS2 copies measured via qPCR (Figure 2.4). Differences in the fungal communities of Hythe, Wivenhoe, and Brightlingsea enrichments following enrichment with 22.7 mM of acetaldehyde (Figure 2.12a) were driven by sampling

site (PERMANOVA: $p < 0.05$, 19% of variance), successive enrichments (PERMANOVA: $p < 0.01$, 17% of variance), and acetaldehyde concentration (PERMANOVA: $p < 0.05$, 15% of variance).
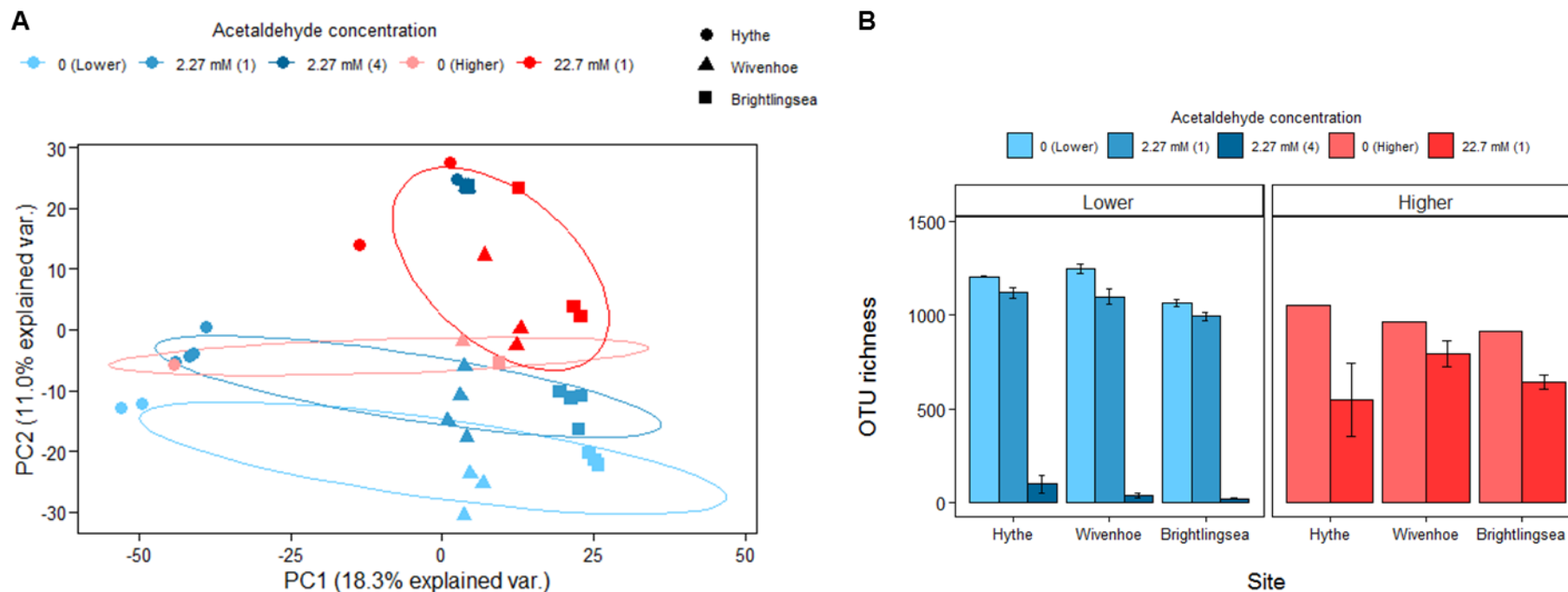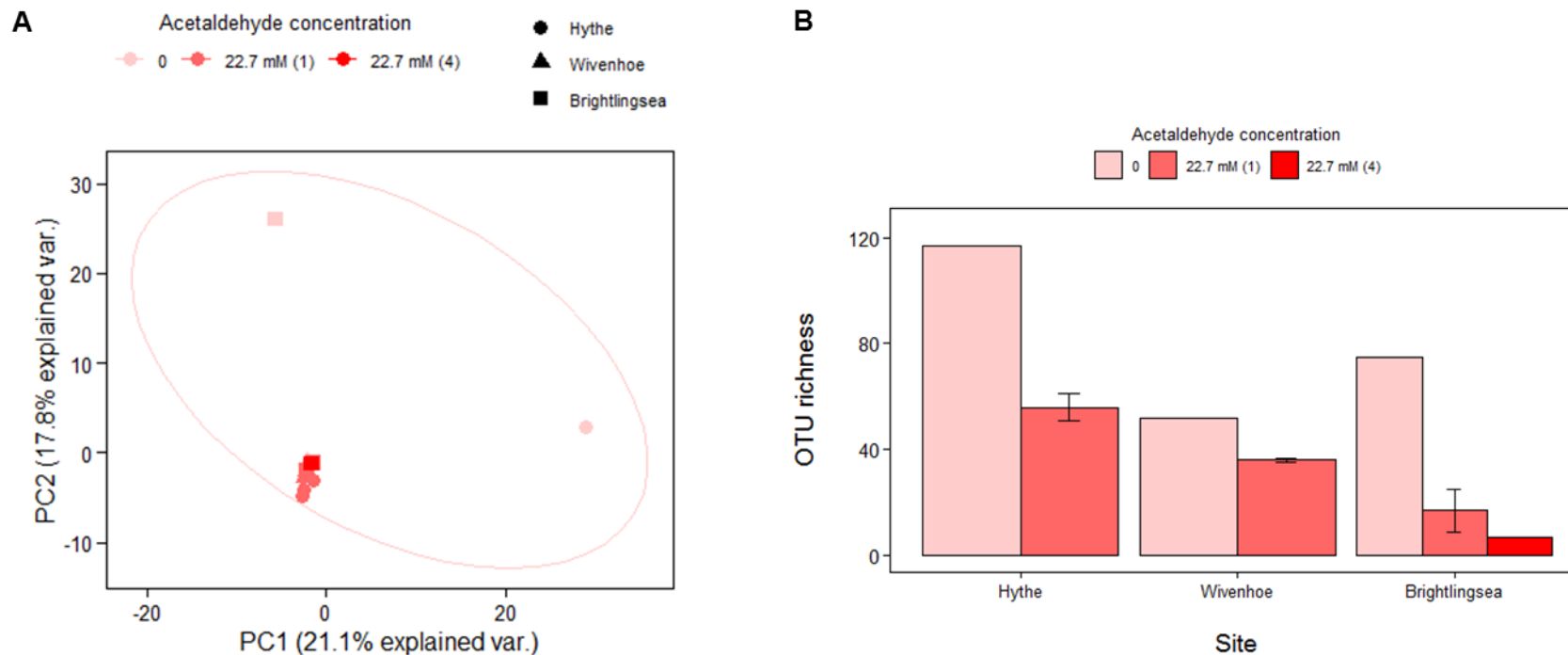
Figure 2.12 Principal component analysis plot (A) showing the similarity of fungal communities in Colne Estuary microcosms enriched with 22.7 mM of acetaldehyde and the no-acetaldehyde controls. Numbers in parentheses indicate enrichment number (either enrichment 1 or 4). No-acetaldehyde controls are represented by an acetaldehyde concentration of zero (0). Fungal OTU richness (B) in the acetaldehyde-enriched microcosms and the no-acetaldehyde controls is shown for Hythe, Wivenhoe, and Brightlingsea. The mean of four, three, and two replicates (± S.E.) is plotted for Hythe, Wivenhoe, and Brightlingsea primary enrichments (22.7 mM (1)), respectively. One replicate is plotted for Hythe, Wivenhoe, and Brightlingsea no-acetaldehyde controls (0) and Brightlingsea quaternary enrichments (22.7 mM (4)).
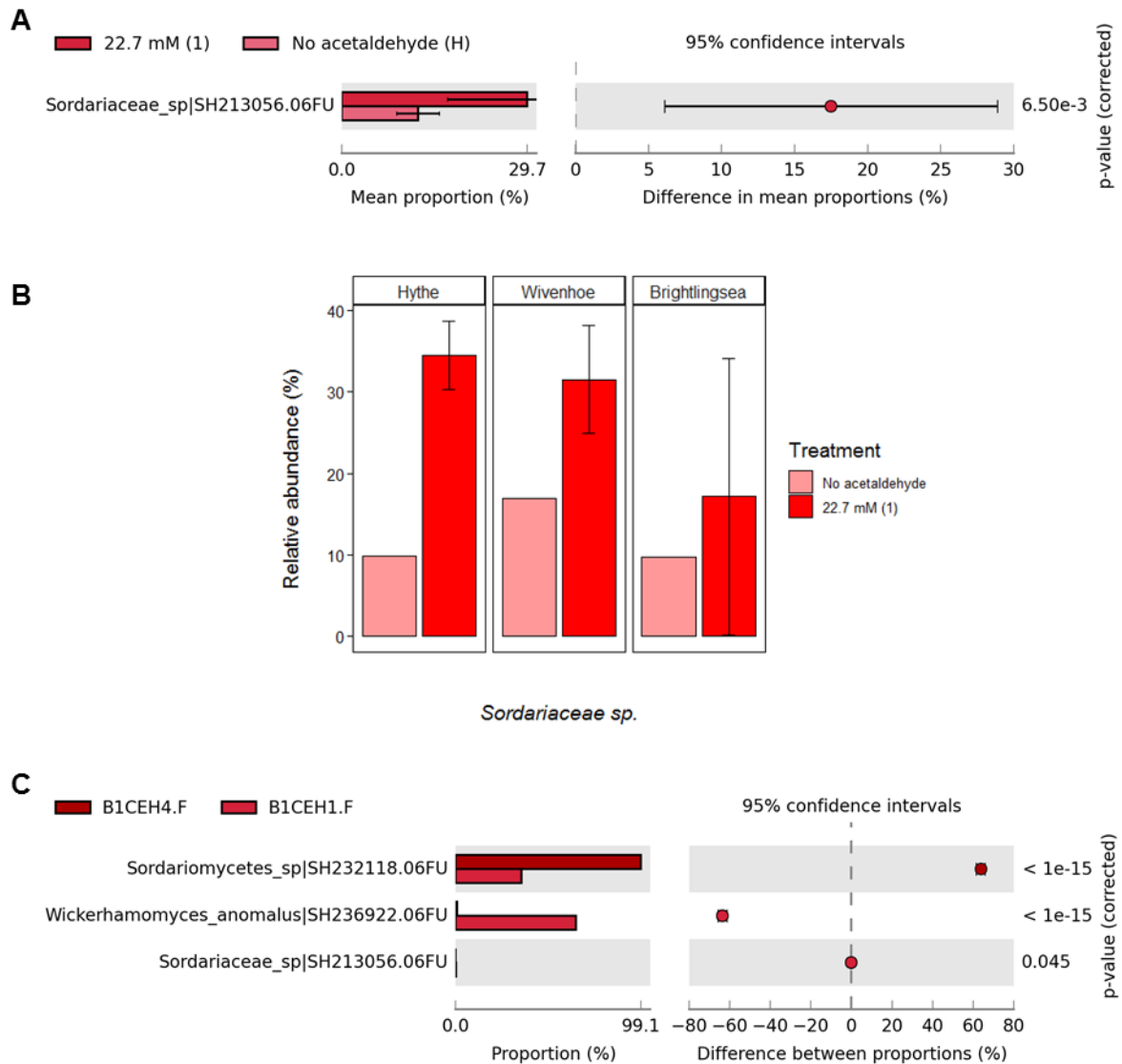
Figure 2.13 The mean proportion of *Sordariaceae* sp. SH213056.06FU sequences in (A) Colne Estuary primary enrichments enriched with 22.7 mM of acetaldehyde and the no-acetaldehyde controls. (B) Relative abundance (%) of *Sordariaceae* sp. SH213056.06FU sequences relative to all fungal sequences in Hythe, Wivenhoe, and Brightlingsea enrichments. (C) The mean proportion of Sordariomycetes sp. SH232118.06FU sequences in Brightlingsea replicate Bottle B1 primary and quaternary enrichments.

Prior to acetaldehyde enrichment, archaeal communities in Hythe, Wivenhoe, and Brightlingsea sediment slurries were near-identical (Figure 2.14a). Following four successive enrichments with 2.27 mM of acetaldehyde, archaeal communities diverged and increasing variability was observed amongst Hythe, Wivenhoe, and Brightlingsea replicates. OTU richness (data not shown) was below 8 following acetaldehyde enrichment. The divergence and variability of archaeal communities resulted from a decrease in the mean proportion of sequences belonging to the *Haloferax, Methanobrevibacter, Methanomassiliicoccus*, and *Nitrosopumilus* genera (Figure 2.14b), although differences between the quaternary acetaldehyde enrichment and the no-acetaldehyde controls were not significant ($p > 0.1$). These results suggest that Archaea cannot utilise acetaldehyde as a carbon and energy source and do not contribute to microbial acetaldehyde degradation. This contradicts the results of the qPCR analysis (Figure 2.3) and suggests that the archaeal primers 344F and 915R were non-specific and possibly amplified regions of the bacterial 16S rRNA gene. Following further analysis of the metagenetic sequencing data, 83 OTUs identified as "unclassified" were discovered amongst archaeal OTUs. A BLAST (Basic Local Alignment Search Tool) (Altschul et al. 1990) homology search revealed that 56 of these OTUs were assigned to the Bacteria, with the majority belonging to the genus *Pseudomonas*, indicating that the archaeal primers 344F and 915R amplified non-specific products. The remaining 27 "unclassified" OTUs did not match with sequences in the BLASTn NCBI sequence database and were considered to be amplification artifacts. These non-specific amplified products were removed during the MiSeq bioinformatics pipeline but would have been present during qPCR analysis, accounting for the significant increase in archaeal 16S rRNA gene copies during the quaternary acetaldehyde enrichment. Differences in the archaeal communities of Hythe, Wivenhoe, and Brightlingsea enrichments were driven by sampling site (PERMANOVA: $p < 0.05$, 18% of variance) and acetaldehyde concentration (PERMANOVA: $p < 0.01$, 14% of variance).
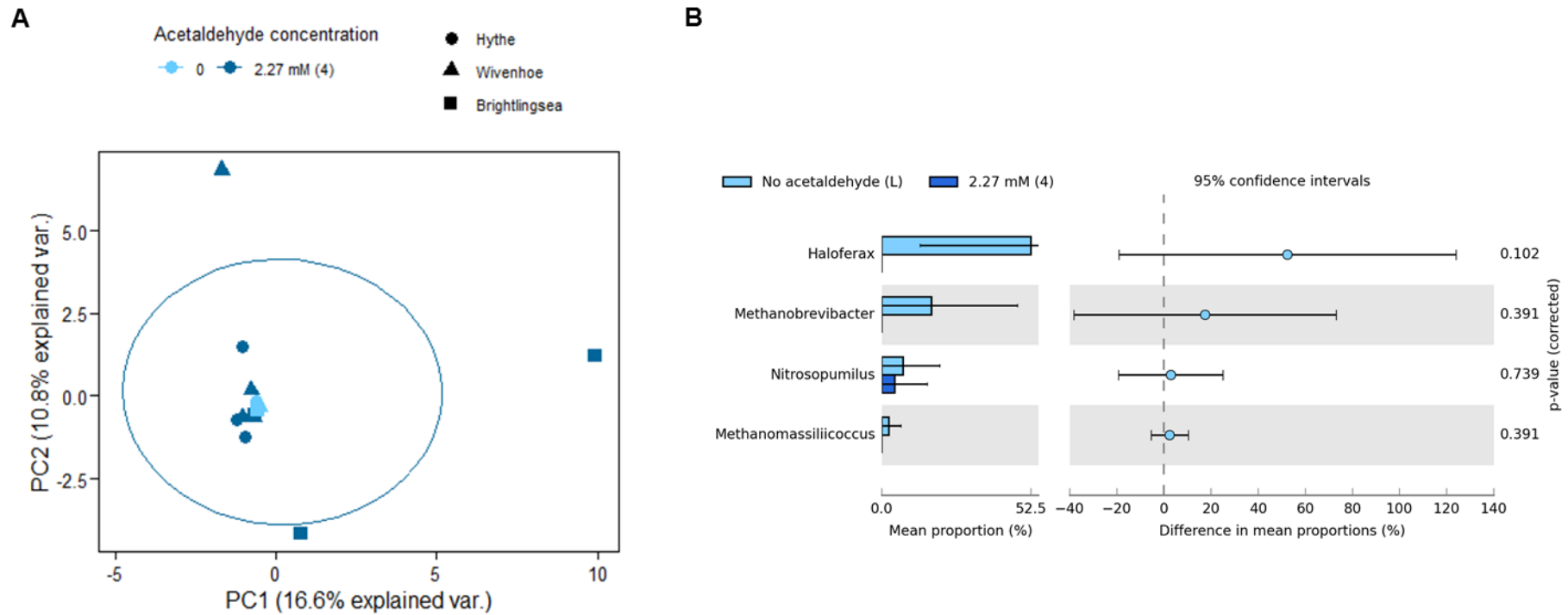
Figure 2.14 Principal component analysis plot (A) showing the similarity of archaeal communities in Colne Estuary microcosms enriched with 2.27 mM of acetaldehyde and the no-acetaldehyde controls. Numbers in parentheses indicate enrichment number (enrichment 4). No-acetaldehyde controls are represented by an acetaldehyde concentration of zero (0). (B) The mean proportion of *Haloferax*, *Nitrosopumilus*, *Methanobrevibacter*, and *Methanomassiliicoccus* sequences in Colne Estuary quaternary enrichments (2.27 mM (4)) and the no-acetaldehyde controls (No acetaldehyde (L)).

2.3.2.2 Microbial communities of freshwater rivers

The bacterial communities of the River Colne and the River Gipping were distinct, with

principal component analysis showing separate groupings of River Colne and River Gipping

no-acetaldehyde controls (Figure 2.15a). Also, bacterial OTU richness was significantly

higher in the River Gipping than the River Colne (Figure 2.15b), further highlighting the

differences between the bacterial communities of the two rivers. Microcosms enriched with

2.59 mM of metaldehyde clustered with the no-acetaldehyde controls of each respective

river, suggesting that bacteria could not utilise metaldehyde as a carbon and energy source,

and/or that the high concentration of metaldehyde was toxic and inhibited growth. This was

supported by similar counts of bacterial OTU richness in metaldehyde-enriched microcosms

and the no-acetaldehyde controls of both rivers (Figure 2.15b). Conversely, River Colne and

River Gipping microcosms enriched with 2.27 mM of acetaldehyde converged and clustered

separately from metaldehyde-enriched microcosms and the no-acetaldehyde controls

(Figure 2.15a), indicating that distinct bacterial communities had established in the

acetaldehyde-enriched microcosms. The addition of acetaldehyde coincided with a

significant decrease in bacterial OTU richness in both River Colne and River Gipping

microcosms (Figure 2.15b), indicating the selection of acetaldehyde-degrading or tolerant

bacteria in these enrichments. The mean proportion of *Pseudomonas* and *Arcobacter*

sequences increased significantly in the acetaldehyde-enriched microcosms relative to the

no-acetaldehyde controls (Figure 2.16a) and metaldehyde-enriched microcosms (Figure

2.16b), indicating that members of these genera may be key acetaldehyde-degraders in

freshwater rivers. Significant increases in the mean proportion of *Curvibacter, Acidovorax,*

Aquaspirillum, Cloacibacterium, and *Duganella* sequences were also observed in the

acetaldehyde-enriched microcosms (Figure 2.16), however, these genera represented a

considerably lower mean proportion of bacterial sequences than *Pseudomonas* and

Arcobacter. No significant differences in the mean proportion of bacterial sequences were

identified between the no-acetaldehyde controls and metaldehyde-enriched microcosms

(data not shown). Following 4 days of incubation, *Pseudomonas* sequences represented 57% and 54% of all bacterial sequences in River Colne and River Gipping acetaldehyde-enriched microcosms, respectively (Figure 2.16c), and represented 37% and 43% of all bacterial sequences after 7 days of acetaldehyde enrichment. During the same period, *Arcobacter* sequences represented 14 - 16% and 10 - 11% of all bacterial sequences in the acetaldehyde-enriched microcosms of the River Colne and River Gipping, respectively (Figure 2.16d).

Figure 2.15 Principal component analysis plot (A) showing the similarity of bacterial communities in River Colne and River Gipping microcosms enriched with 2.27 mM of acetaldehyde or 2.59 mM of metaldehyde, and the no-acetaldehyde controls. All microcosms were supplemented with 300 µM of NH_4Cl and 20 µM of Na_2HPO_4 to support microbial growth. Bacterial OTU richness (B) in the no-acetaldehyde controls, metaldehyde-enriched microcosms and the acetaldehyde-enriched microcosms is shown for both rivers. The mean of three replicates (± S.E.) is plotted for River Colne no-acetaldehyde controls (day 4), River Colne acetaldehyde-enriched microcosms (day 7), River Colne metaldehyde-enriched microcosms (day 7), River Gipping no-acetaldehyde controls (day 7), River Gipping acetaldehyde-enriched microcosms (day 7), and River Gipping metaldehyde-enriched microcosms (day 4), whilst the mean of two replicates (± S.E.) is plotted for River Colne no-acetaldehyde controls (day 7), River Colne acetaldehyde-enriched microcosms (day 4), River Gipping acetaldehyde-enriched microcosms (day 4) and River Gipping metaldehyde-enriched microcosms (day 7). One replicate is plotted for River Colne metaldehyde-enriched microcosms (day 4) and River Gipping no-acetaldehyde controls (day 4).

Figure 2.16 The mean proportion of bacterial sequences in River Colne and River Gipping microcosms enriched with 2.27 mM of acetaldehyde and (A) the no-acetaldehyde controls and (B) microcosms enriched with 2.59 mM of metaldehyde. The relative abundance (%) of (C) *Pseudomonas* and (D) *Arcobacter* sequences relative to all bacterial sequences in the River Colne and River Gipping microcosms on day 4 and day 7 is also shown.

The significant increase in the relative abundance of *Pseudomonas* in the River Colne and River Gipping acetaldehyde-enriched microcosms was primarily driven by OTU6 and OTU72333 (Figure 2.17), which represented 43% and 33% of the genus, respectively. OTU6 was identified as a close relative of *P. benzenivorans* DSM 8628 and *P. glareae* KMM 9500 and represented 20% of all bacterial sequences in the acetaldehyde-enriched microcosms, compared to 0.4% and 0.5% in the no-acetaldehyde controls and metaldehyde-enriched microcosms, respectively (Figure 2.17). OTU72333 was most closely related to *P. putida* ATCC 12633 and *P. japonica* DSM 22348, and accounted for 16.5% of bacterial sequences in the acetaldehyde-enriched microcosms (Figure 2.17). In the no-acetaldehyde controls and metaldehyde-enriched microcosms, OTU72333 accounted for 0.03% and 0.02% of bacterial sequences, respectively. The relative increase in *Arcobacter* sequences in the acetaldehyde-enriched microcosms was predominantly driven by OTU299 (Figure 2.17), which represented 91% of the *Arcobacter* genus. OTU299 was identified as a close relative of *A. suis* CECT7833^T, *A. defluvii* CECT7697^T, and *A. ellisii* CECT7837^T, and represented 11.8% of bacterial sequences in the acetaldehyde-enriched microcosms, compared to <0.04% in the no-acetaldehyde controls and metaldehyde-enriched microcosms. These findings suggest that OTU6, OTU72333, and OTU299 are key acetaldehyde degraders enriched from freshwater rivers.

A total of 11 *Pseudomonas* OTUs were present in both the River Colne and Colne Estuary acetaldehyde-enriched microcosms (Figure 2.18). OTU6 accounted for 56.5% and 17.6% of all bacterial sequences in acetaldehyde-enriched microcosms of the Colne Estuary and River Colne, respectively, suggesting that this taxon is an important acetaldehyde degrader in both estuarine and freshwater environments. Similarly, OTU60 represented 12.8% and 1.1% of bacterial sequences in the Colne Estuary and River Colne acetaldehyde-enriched microcosms, respectively, indicating that this taxon may also be a key acetaldehyde degrader in both environments. Although OTU72333 was present in both environments, this taxon represented <0.01% of bacterial sequences in Colne Estuary acetaldehyde-enriched

microcosms. Conversely, in the River Colne, OTU72333 accounted for 18.2% of all bacterial sequences following acetaldehyde enrichment, suggesting that this taxon may be a specialist acetaldehyde degrader in freshwater environments. Two *Arcobacter* OTUs, namely OTU299 and OTU15811, were present in both the River Colne and Colne Estuary acetaldehyde-enriched microcosms (Figure 2.18). Although present in the Colne Estuary, OTU299 and OTU15811 accounted for <0.3% of all bacterial sequences, suggesting that these taxa are not involved in estuarine acetaldehyde degradation. Conversely, in the River Colne, OTU299 and OTU15811 represented 13.9% and 1.1% of all bacterial sequences, respectively, suggesting that these taxa are specialist freshwater acetaldehyde degraders.
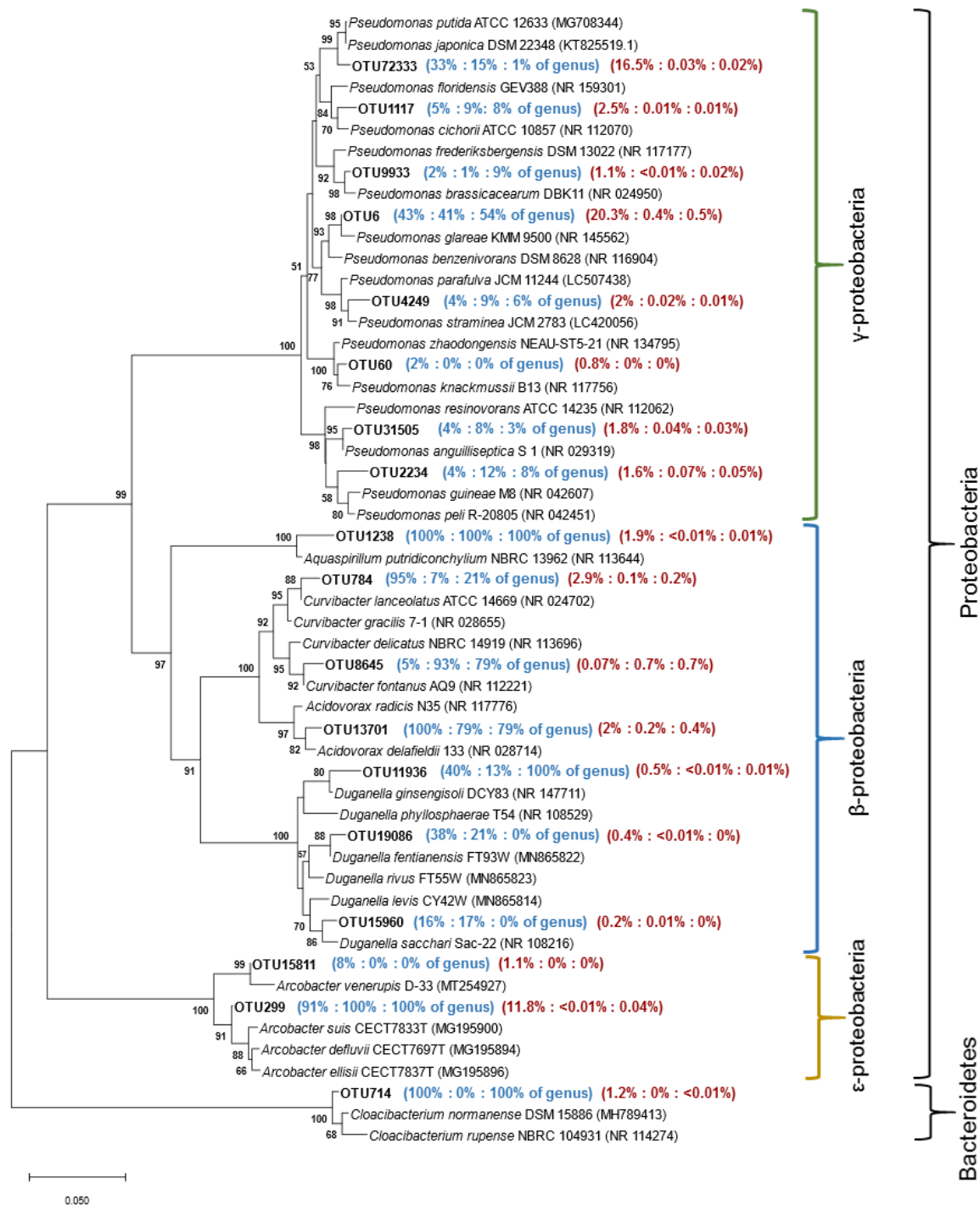
Figure 2.17 Phylogenetic tree showing the relationship between bacterial OTUs exhibiting increased relative abundance in the River Colne and River Gipping acetaldehyde-enriched microcosms and closely related strains within the Bacteroidetes and Proteobacteria, based on partial 16S rRNA gene sequences. The evolutionary history of OTUs was inferred using the Neighbour-Joining method (Saitou & Nei 1987). The percentage of replicate trees in which the associated taxa clustered together in the bootstrap test (1000 replicates) is shown next to the branches when ≥50%. Evolutionary distances were computed using Kimura's two-parameter model (Kimura 1980) and are in the units of the number of base substitutions per site (horizontal scale bar represents 5% nucleotide differences per site). Accession numbers of the type strains are shown in round brackets. The average (combined Colne and Gipping) proportion of the OTU within the genus (%) is shown in blue brackets, in the order of acetaldehyde-enriched, no-acetaldehyde controls, and metaldehyde-enriched microcosms. The average (combined Colne and Gipping) proportion of the OTU relative to all bacterial sequences (%) is shown in red brackets, in the same order.
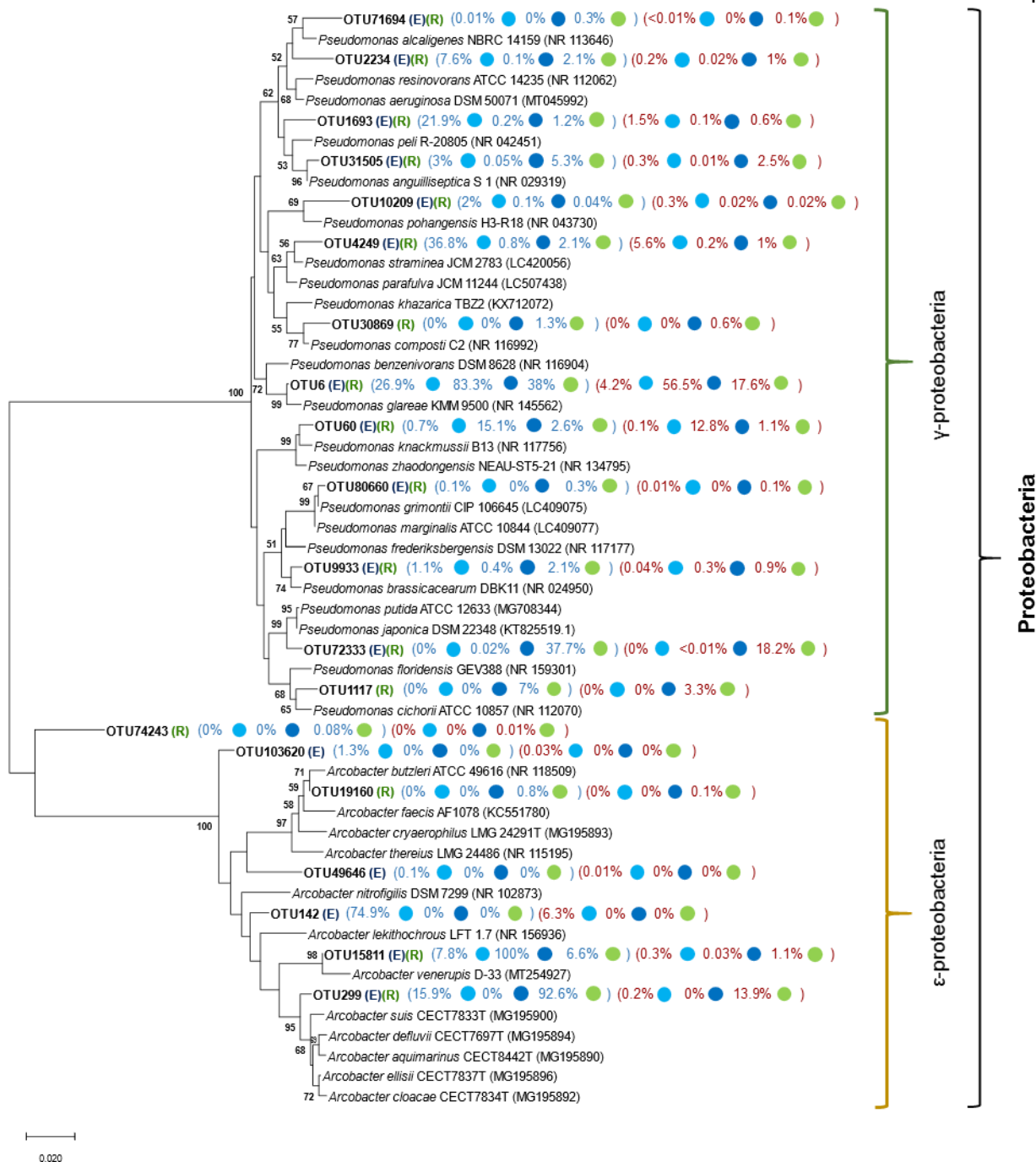
Figure 2.18 Phylogenetic tree showing the relationship between *Pseudomonas* and *Arcobacter* OTUs present in the River Colne and Colne Estuary acetaldehyde-enriched microcosms and closely related strains within the Proteobacteria. The evolutionary history of OTUs was inferred using the Neighbour-Joining method (Saitou & Nei 1987). The percentage of replicate trees in which the associated taxa clustered together in the bootstrap test (1000 replicates) is shown next to the branches when ≥50%. Evolutionary distances were computed using Kimura's two-parameter model (Kimura 1980) and are in the units of the number of base substitutions per site (horizontal scale bar represents 2% nucleotide differences per site). Accession numbers of the type strains are shown in round brackets. The average proportion of the OTU within the genus (%) is shown in blue brackets, in the order Colne Estuary primary enrichment (light blue circles), Colne Estuary quaternary enrichment (dark blue circles), and River Colne (green circles). The average proportion of the OTU relative to all bacterial sequences (%) is shown in red brackets, in the same order. Taxonomic classifications are shown to the right of the tree. (E): OTU present in Colne Estuary; (R): OTU present in River Colne.

Fungal communities in the River Gipping no-acetaldehyde controls were highly variable compared to the River Colne (Figure 2.19a) and exhibited higher fungal OTU richness (Figure 2.19b). In the acetaldehyde-enriched microcosms of the River Colne and River Gipping, fungal communities converged, indicating that communities had become increasingly similar in response to acetaldehyde, although these communities were not dissimilar from the fungal communities of the River Colne no-acetaldehyde controls (Figure 2.19a). The convergence of acetaldehyde-enriched fungal communities corresponded with a decrease in fungal OTU richness in River Colne microcosms on day 4, followed by an increase in OTU richness on Day 7 (Figure 2.19b). No significant change in OTU richness was detected in River Gipping microcosms enriched with acetaldehyde (Figure 2.19b). The mean proportion of fungal sequences assigned to the *Saccharomycetaceae* increased significantly in the acetaldehyde-enriched microcosms compared to the no-acetaldehyde controls (Figure 2.19c) and represented up to 1% of fungal sequences in the River Colne and River Gipping (Figure 2.19d). The increase in the relative abundance of the *Saccharomycetaceae* was driven by *Torulaspora delbrueckii* and *Williopsis* sp in the River Colne and River Gipping, respectively (data not shown), however, the relative abundance of these taxa in the acetaldehyde-enriched microcosms was not significantly different to the no-acetaldehyde controls (p >0.17) and significant increases in fungal relative abundance were only observed at the family level.

Distinct archaeal communities were identified in the River Colne and River Gipping no-acetaldehyde controls (Figure 2.20a), with archaeal OTU richness higher in the River Gipping (Figure 2.20b). Archaeal communities in the River Colne acetaldehyde-enriched microcosms clustered with their respective no-acetaldehyde controls, suggesting that communities did not significantly change in response to acetaldehyde. Conversely, acetaldehyde-enriched archaeal communities in the River Gipping diverged from their respective no-acetaldehyde controls, indicating that acetaldehyde influenced these archaeal communities. These changes coincided with a significant decrease in the mean proportion of

Nitrosopumilus sequences in the acetaldehyde-enriched microcosms compared to the no-acetaldehyde controls (Figure 2.20c), suggesting that the decrease of *Nitrosopumilus* was primarily responsible for differences between archaeal communities in the acetaldehyde-enriched microcosms and the no-acetaldehyde controls. *Nitrosopumilus* sequences were not present in River Colne microcosms (Figure 2.20d), contributing to the observed differences between the River Colne and River Gipping archaeal communities (Figure 2.20a). The relative abundance of *Nitrosopumilus* sequences significantly decreased in the River Gipping acetaldehyde-enriched microcosms on day 4 and day 7 (Figure 2.20d). In agreement with observations from the acetaldehyde-enriched microcosms of the Colne Estuary, these findings suggest that archaea cannot utilise acetaldehyde as a carbon and energy source or that the concentration of acetaldehyde was toxic and inhibited growth.
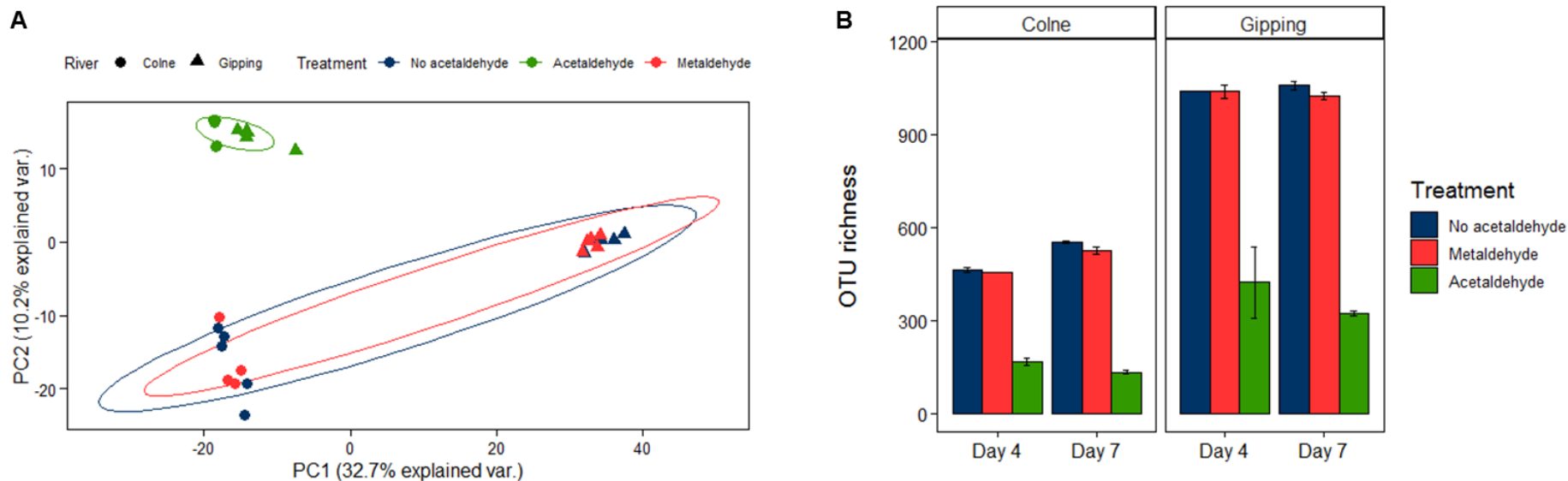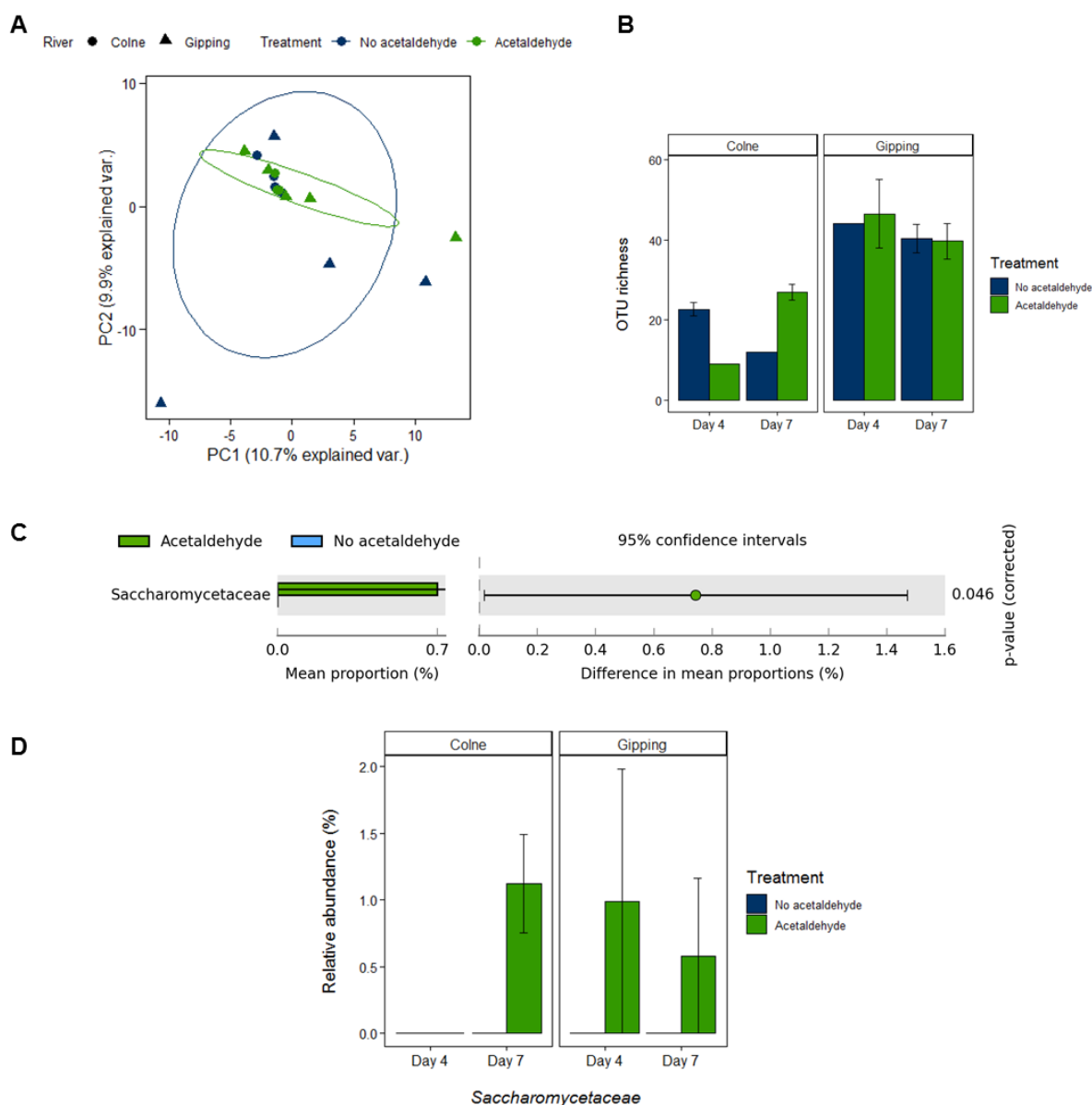
Figure 2.19 Principal component analysis plot (A) showing the similarity of fungal communities in River Colne and River Gipping microcosms enriched with 2.27 mM of acetaldehyde and the no-acetaldehyde controls on day four and seven. All microcosms were supplemented with 300 µM of NH_4Cl and 20 µM of Na_2HPO_4 to support microbial growth. Fungal OTU richness (B) and the mean proportion of *Saccharomycetaceae* sequences (C) in the acetaldehyde-enriched microcosms and the no-acetaldehyde controls is also shown. The relative abundance (%) of *Saccharomycetaceae* sequences (D) relative to all fungal sequences in the no-acetaldehyde controls and acetaldehyde-enriched microcosms is shown for the River Colne and River Gipping. The mean of three replicates (± S.E.) is plotted for River Colne no-acetaldehyde controls (day 4), River Gipping no-acetaldehyde controls (day 7), and River Gipping acetaldehyde-enriched microcosms (day 7), whilst the mean of two replicates (± S.E.) is plotted for River Colne acetaldehyde-enriched microcosms (day 7) and River Gipping acetaldehyde-enriched microcosms (day 4). One replicate is plotted for the River Colne no-acetaldehyde controls (day 7), River Colne acetaldehyde-enriched microcosms (day 4) and River Gipping no-acetaldehyde controls (day 4).
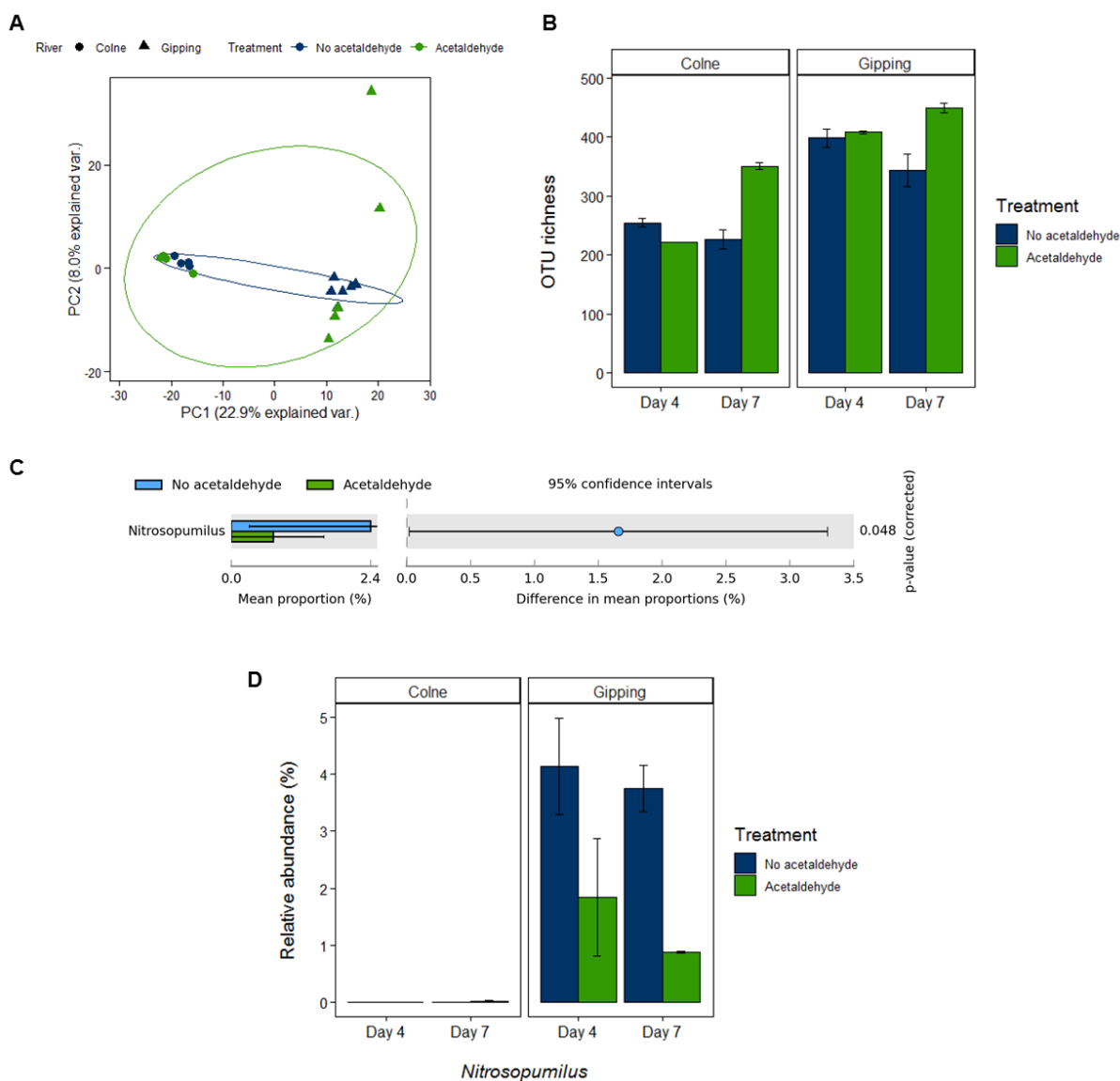
Figure 2.20 Principal component analysis plot (A) showing the similarity of archaeal communities in River Colne and River Gipping microcosms enriched with 2.27 mM of acetaldehyde and the no-acetaldehyde controls. All microcosms were supplemented with 300 µM of NH₄Cl and 20 µM of Na₂HPO₄ to support microbial growth. Archaeal OTU richness (B) and the mean proportion of *Nitrosopumilus* sequences (C) in the acetaldehyde-enriched microcosms and the no-acetaldehyde controls is also shown. The relative abundance (%) of *Nitrosopumilus* sequences (D) relative to all archaeal sequences in the acetaldehyde-enriched microcosms and the no-acetaldehyde controls of the River Colne and River Gipping is also shown. The mean of three replicates (± S.E.) is plotted for River Colne acetaldehyde-enriched microcosms (day 7), River Gipping no-acetaldehyde controls (day 4 and day 7),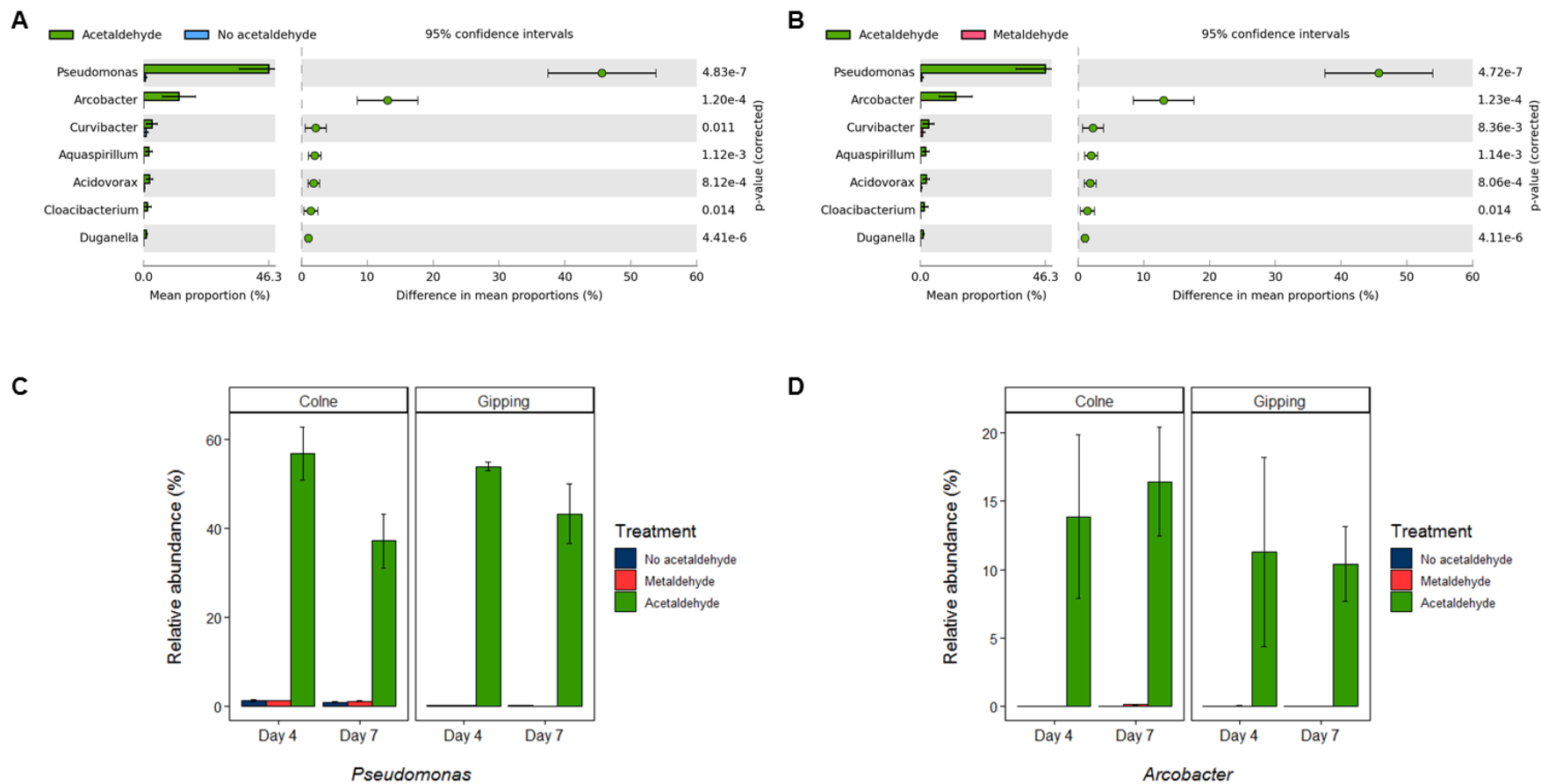 and River Gipping acetaldehyde-enriched microcosms (day 7), whilst the mean of two replicates (± S.E.) is plotted for River Colne no-acetaldehyde controls (day 4 and day 7) and River Gipping acetaldehyde-enriched microcosms (day 4). One replicate is plotted for the River Colne acetaldehyde-enriched microcosms (day 4).

2.3.3 Microbial ^{14}C-acetaldehyde uptake

Following 3 hours of incubation, microbial assimilation rates of 0.16 ± 0.01, 0.17 ± 0.02, and

0.11 ± 0.01 nmol L^{-1} day^{-1} were measured in surface water samples from Hythe, Wivenhoe,

and Brightlingsea, respectively (Table 2.2). Surface water samples from Hythe exhibited a

microbial dissimilation rate of 5.32 ± 1.22 nmol L^{-1} day^{-1}, whilst microbial dissimilation rates

of 4.93 ± 1.24 and 5.55 ± 1.04 nmol L^{-1} day^{-1} were measured in Wivenhoe and Brightlingsea

surface water samples, respectively. Total acetaldehyde uptake rates were calculated for

each site by summing microbial assimilation and dissimilation rates (Table 2.2). Total uptake

rates were highest in Brightlingsea surface water samples, with an acetaldehyde uptake rate

of 5.66 nmol L^{-1} day^{-1}. Microbial acetaldehyde turnover times ranged from 3.55 - 4.30 hours,

with the fastest turnover time measured in Wivenhoe surface water samples. Bacterial

growth efficiencies of 0.03, 0.03, and 0.02 were calculated for Hythe, Wivenhoe, and

Brightlingsea surface water samples, respectively.

Table 2.2 Microbial assimilation, dissimilation, total uptake, turnover time, and bacterial growth efficiency of ^{14}C-acetaldehyde in surface waters of the Colne Estuary, Essex. The mean of three replicates is shown for microbial assimilation and dissimilation rates at each sampling site (± S.E.).

Site	Assimilation (nmol L^{-1} d^{-1})	Dissimilation (nmol L^{-1} d^{-1})	Total uptake (nmol L^{-1} d^{-1})	Turnover time (hours)	Bacterial growth efficiency
Hythe	0.16 ± 0.01	5.32 ± 1.22	5.48	3.64	0.03
Wivenhoe	0.17 ± 0.02	4.93 ± 1.24	5.10	3.55	0.03
Brightlingsea	0.11 ± 0.01	5.55 ± 1.04	5.66	4.30	0.02

2.4 Discussion

2.4.1 Microbial acetaldehyde degradation

The findings of this study demonstrate that microbial communities play an important role in

acetaldehyde degradation in estuaries and freshwater rivers, but that bacteria, fungi, and

archaea do not equally contribute to acetaldehyde degradation in these environments.

As demonstrated by the significant increases in 16S rRNA gene copies and the relative

abundance of bacterial sequences in acetaldehyde-enriched microcosms, bacteria are the

primary acetaldehyde degraders in the Colne Estuary, the River Colne, and the River

Gipping. After four successive enrichments of 2.27 mM of acetaldehyde, bacterial 16S rRNA

gene copies significantly increased in Colne Estuary enrichments (Figure 2.3). This

coincided with a significant increase in the relative abundance of *Pseudomonas* and

Arcobacter sequences (Figure 2.9c), suggesting that members of these genera were

responsible for the acetaldehyde degradation measured in Hythe, Wivenhoe, and

Brightlingsea microcosms (Figure 2.3). Significant increases in bacterial 16S rRNA gene

copies were also measured in the acetaldehyde-enriched microcosms of the River Colne

and the River Gipping after 7 days of incubation (Figure 2.6), coinciding with complete

acetaldehyde degradation and significant increases in the relative abundance of

Pseudomonas (Figure 2.16c) and *Arcobacter* (Figure 2.16d) sequences. Furthermore, in the

acetaldehyde-enriched microcosms of the Colne Estuary, the River Colne, and the River

Gipping, bacterial 16S rRNA gene copies were generally two orders of magnitude more

abundant than fungal ITS2 copies and three orders of magnitude more abundant than

archaeal 16S rRNA gene copies, further implying that bacteria are primarily responsible for

acetaldehyde degradation.

Based on the significant increase in ITS2 copies and observations of fungal-like biomass in

Brightlingsea replicate B1 following enrichment with 22.7 mM of acetaldehyde (Figure 2.4 &

2.5), and the related increase in the mean proportion of Sordariomycetes sequences (Figure

2.13c), fungi were shown to contribute to acetaldehyde degradation in the Colne Estuary,

although they play a secondary role to bacteria. ITS2 copies also significantly increased in

the 2.27 mM acetaldehyde-enriched microcosms of the River Colne and the River Gipping

(Figure 2.6), coinciding with complete acetaldehyde degradation. Although

Saccharomycetaceae sequences significantly increased in response to acetaldehyde

enrichment (Figure 2.19c), the relative abundance of the two representative taxa in the acetaldehyde-enriched microcosms was not significantly different from the no-acetaldehyde controls. Accordingly, the members of the *Saccharomycetaceae* were not conclusively identified as acetaldehyde-degrading fungi in this study, and the fungal taxa putatively responsible for acetaldehyde degradation in the River Colne and the River Gipping remain unidentified. However, previous studies have also demonstrated that members of the *Saccharomycetaceae* are capable of acetaldehyde degradation. Li & Orduña (2011), for example, screened 26 yeast strains for the ability to produce and degrade acetaldehyde, including commercial *Saccharomyces* and non-*Saccharomyces* yeasts. All 26 strains were able to degrade 1.8 mM (80 mg L^{-1}) of acetaldehyde, with degradation rates ranging from 0.04 ± 0.00 to 0.77 ± 0.02 mg g^{-1} min^{-1} (Li & Orduña 2011). The highest rates of degradation were exhibited by *Saccharomyces* strains (0.49 ± 0.04 - 0.77 ± 0.02 mg g^{-1} min^{-1}), whilst non-*Saccharomyces* yeasts displayed acetaldehyde degradation rates of 0.04 ± 0.00 to 0.50 ± 0.01 mg g^{-1} min^{-1}. Although applied in industrial and commercial settings, these strains are also part of natural microbial communities and are often found in association with deciduous tree bark, exudates and associated soils, and wild fruits (Charron et al. 2014). These findings therefore provide strong evidence to suggest that the members of the *Saccharomycetaceae* that significantly increased in abundance during enrichment contributed to the acetaldehyde degradation measured in the River Colne and River Gipping microcosms. More generally, this also suggests that fungi contribute to the microbial acetaldehyde sink in freshwater systems.

It is possible that the increase in fungal abundance observed in the 2.27 mM acetaldehyde-enriched microcosms of the River Colne and the River Gipping resulted from secondary metabolism rather than primary acetaldehyde degradation. In this scenario, bacterial acetaldehyde degradation may have resulted in the production of metabolites or necromass that could support the growth of a fungal population in the acetaldehyde-enriched microcosms. This scenario seems unlikely to have occurred in the acetaldehyde-enriched

microcosms of the Colne Estuary, as increases in fungal ITS2 copies did not occur in microcosms enriched with 2.27 mM of acetaldehyde, despite significant increases in bacterial 16S rRNA gene copies. Moreover, increases in fungal ITS2 copies were observed in microcosms enriched with 22.7 mM of acetaldehyde when bacterial 16S rRNA gene copies in the acetaldehyde-enriched microcosms were lower than the no-acetaldehyde controls, suggesting that bacteria had not utilised acetaldehyde and had therefore not produced metabolites suitable for fungal growth. Instead, fungi may have been responsible for acetaldehyde degradation in these microcosms, although it is also possible that fungi may have utilised the cellular components from bacterial cells killed by the high concentration of acetaldehyde. It is also not clear whether fungi have a direct role in acetaldehyde degradation in the River Colne and the River Gipping enrichments, or if the observed increases in fungal abundance are the result of heterotrophic growth on leaked organic molecules or necromass. If fungi are partially responsible for acetaldehyde degradation, alongside bacteria, it is not clear which taxa are responsible, despite the significant increase in the relative abundance of *Saccharomycetaceae* and evidence to suggest that yeast strains belonging to this family can degrade acetaldehyde (Li & Orduña 2011). Further investigations are needed to ascertain the role that fungi play in acetaldehyde degradation in the River Colne and the River Gipping, and to clearly identify the fungal taxa responsible for acetaldehyde degradation. This could include the use of techniques such as DNA stable-isotope probing (SIP) to provide a clear link between phylogeny and function. Using this technique, environmental samples from the Colne Estuary, River Colne and River Gipping would be incubated with ^{13}C-labelled acetaldehyde to allow acetaldehyde-degrading microorganisms to incorporate the labelled carbon into biomass. Following DNA extraction, the heavier ^{13}C-DNA from the actively degrading microorganisms would be separated from the lighter ^{12}C-DNA of non-degrading microorganisms via caesium chloride buoyant density-gradient centrifugation. This heavier fraction would be subjected to PCR amplification using primers that amplify the specific gene or DNA region of interest, such as the 18S rRNA gene or ITS2 region. By sequencing these PCR products the fungi responsible for acetaldehyde

degradation could be identified. Furthermore, by using primers that amplify the 16S rRNA gene, this technique could also be used to conclusively identify bacteria and archaea as acetaldehyde degraders.

The results of this study provide no indication that archaea contribute to microbial acetaldehyde degradation in the Colne Estuary, the River Colne, and the River Gipping. Significant increases in archaeal 16S rRNA gene copies were seen in Colne Estuary quaternary microcosms enriched with 2.27 mM of acetaldehyde (Figure 2.3) and acetaldehyde-enriched microcosms of the River Colne and the River Gipping (Figure 2.6). However, compared to their respective no-acetaldehyde controls, the relative abundance of archaeal sequences decreased in acetaldehyde-enriched microcosms of the Colne Estuary (Figure 2.14b) and the River Gipping (Figure 2.20c). Whilst demonstrating that archaea did not contribute to microbial acetaldehyde degradation, these findings also show that the archaeal primers 344F and 915R are non-specific and also amplify regions of the bacterial 16S rRNA gene. Further analysis revealed that these primers amplified bacterial sequences assigned to the Alphaproteobacteria, Betaproteobacteria, and Gammaproteobacteria, with the majority belonging to the genus *Pseudomonas*. These non-specific amplified products were removed during the MiSeq bioinformatics pipeline but were present and could not be accounted for during qPCR analysis. Consequently, significant increases in archaeal 16S rRNA gene copies were likely the result of increases in bacterial abundance, rather than only archaeal abundance. These findings strongly suggest that archaea have no role in acetaldehyde degradation and may also help to improve the specificity of the archaeal primer set 344F and 915R.

It is important to note that the acetaldehyde concentrations used in this experiment were considerably higher than those found in nature, with in-situ acetaldehyde concentrations ranging from 1.38 - 38 nM in seawater (Section 1.6; Table 1.3) and 6 - 28.1 nM in freshwater rivers and open estuaries (Webb 2016). Consequently, it is likely that even the lower

concentration of acetaldehyde used here was toxic to many of the microorganisms present in the Colne Estuary, River Colne, and River Gipping microcosms, including taxa capable of utilising acetaldehyde at more environmentally relevant concentrations. The rates of microbial acetaldehyde assimilation and dissimilation reported for the Colne Estuary (Table 2.2) demonstrate that acetaldehyde is utilised as both a carbon and energy source at low nanomolar concentrations, with the higher rates of microbial dissimilation indicating that acetaldehyde is primarily used as an energy source. Based on the significant increase in bacterial 16S rRNA gene copies and the relative abundance of bacterial sequences in the acetaldehyde-enriched microcosms of the Colne Estuary, the River Colne, and the River Gipping, it is possible that bacteria are also primarily responsible for the degradation of ^{14}C-acetaldehyde, with the *Pseudomonas* and *Arcobacter* genera potentially representing the key acetaldehyde degraders. However, naturally occurring concentrations of acetaldehyde may also favour a greater diversity of acetaldehyde-degrading bacteria belonging to a range of genera and higher taxonomic rank. A review of isoprene-degrading bacteria by Carrión et al. (2020), for example, reported that the dominant genus in isoprene-degrading microbial communities was dependent on isoprene concentration, in addition to other environmental variables. Carrión et al. (2020) demonstrated that *Rhodococcus* regularly dominates environments with higher isoprene concentrations (150 - 5000 ppm), but that genera such as *Gordonia*, *Ramlibacter*, and *Pelomonas* dominated under lower isoprene concentrations (25 ppm). This suggests that under environmentally relevant concentrations of acetaldehyde, other genera may dominate bacterial communities and significantly contribute to acetaldehyde degradation, whilst those genera which dominate under high acetaldehyde concentrations, such as *Pseudomonas* and *Arcobacter*, may play more of a secondary role in acetaldehyde degradation. Furthermore, fungi and archaea may also be able to utilise acetaldehyde at environmentally relevant concentrations rather than the artificially high concentrations used for enrichment. Accordingly, the role of fungi, archaea, and other bacteria in microbial acetaldehyde degradation cannot be ruled out, and further research is necessary to determine the diversity of microbial acetaldehyde degraders. This could include

the use of microautoradiography-fluorescence in-situ hybridisation (MAR-FISH) to quantify the in-situ uptake of ^{14}C-labelled acetaldehyde at environmentally relevant concentrations, whilst simultaneously establishing the phylogenetic identity of individual cells (Okabe et al. 2004). This technique could help to conclusively identify bacteria, fungi, or archaea as acetaldehyde degraders and could improve our understanding of microbial acetaldehyde degradation in the natural environment. Similarly, other single-cell approaches, such as Raman-spectroscopy and NanoSIMS (nanoscale secondary ion mass spectrometry), could be used in combination with FISH (fluorescence in-situ hybridisation) to quantify and visualise the incorporation of ^{13}C-labelled acetaldehyde and identify individual microbial cells (Musat et al. 2012). These approaches may help to improve our knowledge of the diversity of acetaldehyde-degrading microorganisms.

2.4.2 Features of *Pseudomonas* species that facilitate acetaldehyde degradation

The genus *Pseudomonas* represented the majority of all bacterial sequences in microcosms enriched with 2.27 mM of acetaldehyde, suggesting that members of this genus are the primary acetaldehyde degraders in estuarine and freshwater environments. In the Colne Estuary, *Pseudomonas* sequences accounted for 39%, 87%, and 84% of all bacterial sequences in Hythe, Wivenhoe, and Brightlingsea microcosms, respectively (Figure 2.9c), and represented >50% of bacterial sequences in the River Colne and the River Gipping (Figure 2.16c). The dominance of *Pseudomonas* sequences in the acetaldehyde-enriched microcosms is perhaps unsurprising given the metabolic versatility of the genus, the wide range of environments in which *Pseudomonas* species live, and their persistence in nutrient-poor and hostile conditions (Frimmersdorf et al. 2010; Rojo 2010). Members of the genus, including the type species *P. aeruginosa* (Gomila et al. 2015), have been shown to utilise amino acids, polyamines, short-chain fatty acids, simple sugars, *n*-alkanes, aliphatic and aromatic hydrocarbons (including halogenated aromatic hydrocarbons), and xenobiotic compounds as sources of carbon and nitrogen (Moore et al. 2006; Frimmersdorf et al. 2010).

This metabolic versatility enables *Pseudomonas* species to live in soil and water ecosystems and to establish close associations with plants and animals, including humans (Moore et al. 2006; Rojo 2010), conferring advantages in the plant rhizosphere (Rainey 1999) but also behaving as opportunistic pathogens in plants (Xin et al. 2018) and humans (Klockgether & Tümmler 2017). The dominance of the *Pseudomonas* in the acetaldehyde-enriched microcosms may, in part, be due to a complex regulatory process termed carbon catabolite repression (CCR) (Rojo 2010), which has also been found to occur in the *Enterobacteriaceae* and members of the Firmicutes (Deutscher 2008). Carbon catabolite repression involves the preferential assimilation of a specific compound that is most efficient for growth, whilst simultaneously inhibiting the expression of genes required for the catabolism of other less preferred compounds (Stülke & Hillen 1999; Rojo 2010). This process optimises metabolism and prevents the synthesis of unnecessary enzymes involved in the degradation of other substrates. *P. aeruginosa*, for example, possesses a large number of genes involved in substrate uptake and catabolism that allow it to metabolise a variety of compounds (Frimmersdorf et al. 2010). Yet, in the presence of glucose, genes involved in the utilisation of other substrates, such as the amino acid histidine, are repressed to optimise glucose metabolism (Rojo 2010). In the regulatory process of carbon catabolite repression, gene expression inhibition is based on which substrates are the least efficient for growth. For *P. aeruginosa*, short-chain fatty acids, polyamines, and certain amino acids are preferred over glucose and other simple sugars, whilst *n*-alkanes and aromatic compounds such as naphthalene and toluene are least preferred (Frimmersdorf et al. 2010). It is important to note, however, that this hierarchy of compounds is not the same for all *Pseudomonas* species, with *P. putida* strain CSV86, for example, preferentially utilising aromatic hydrocarbons, such as naphthalene, ahead of glucose (Basu et al. 2006). Metabolic optimisation induced by carbon catabolite repression enhances the ability of bacteria to outcompete other taxa and provides bacteria with the advantage of being flexible to abrupt changes in substrate (Görke & Stülke 2008; Rojo 2010). This regulatory process may therefore optimise members of the *Pseudomonas* for acetaldehyde metabolism and

enable the *Pseudomonas* to outcompete other bacteria following the sudden availability of acetaldehyde.

The metabolic versatility of *Pseudomonas* species also results from the exchange of catabolic plasmids which typically contain all of the genes necessary for specific degradative pathways (Stephanopoulos et al. 1998). Catabolic plasmids are self-transmissible, encoding all four components of the conjugative apparatus (Smillie et al. 2010), and range from 80 to >300 kbp in size (Williams et al. 2004). These plasmids are commonly found in the genus *Pseudomonas* (Stephanopoulos et al. 1998) and often provide the genes necessary for the degradation of toxic compounds, such as aromatic hydrocarbons. The TOL plasmid pWW0 of *P. putida*, for example, carries the catabolic and regulatory genes encoding the biodegradation of toluene and xylenes (Greated et al. 2002), whilst the exchange of the NAH7 plasmid, also of *P. putida*, enables its host to utilise naphthalene or salicylate as a sole source of carbon and energy (Yen & Gunsalus 1985). The exchange of catabolic plasmids may also allow *Pseudomonas* to acquire genes encoding the necessary enzymes for acetaldehyde degradation, namely aldehyde dehydrogenases (ALDH), which may contribute to the significant increase of *Pseudomonas* in acetaldehyde-enriched microcosms of the Colne Estuary, River Colne, and River Gipping.

Of course, many *Pseudomonas* species already possess aldehyde dehydrogenase-encoding genes, as the majority of bacterial genomes contain 1 - 26 genes belonging to the ALDH superfamily (Sophos & Vasiliou 2003). However, little is known about the physiological roles of bacterial ALDH proteins which belong to a subgroup of the ALDH superfamily termed group X ALDH (Taniyama et al. 2012). The opportunistic pathogen *P. aeruginosa* PAO1, for example, synthesises a hydrazone dehydrogenase belonging to the X ALDH subgroup, which converts hydrazones to their corresponding hydrazides and acids, but also demonstrates the ability to oxidise acetaldehyde (Taniyama et al. 2012). This suggests that bacterial ALDH proteins are multi-functional and can be used in the catabolism

of more than one substrate. Accordingly, members of *Pseudomonas* may possess a range of enzymatic tools necessary for the utilisation of acetaldehyde as a carbon and energy source, rather than relying on the activity of individual enzymes with high substrate specificity. The ability to use multiple enzymes for acetaldehyde metabolism would likely provide the *Pseudomonas* with an advantage over other bacterial taxa.

The meta-cleavage pathway for the degradation of aromatic hydrocarbons, such as toluene, benzene, xylenes, and naphthalene, involves the conversion of catechol to pyruvate and acetyl-CoA (Platt et al. 1995), with the latter entering the tricarboxylic acid (TCA) cycle for energy production (Chapter 4; Figure 4.4). The genes involved in this pathway are located at the end of an operon in *P. putida* strain NCIMB9816, with the first gene encoding the enzymes necessary for the conversion of a stable compound, such as benzene, to catechol (Platt et al. 1995). Following a series of enzymatic reactions, catechol is converted to acetaldehyde and pyruvate, with the former subsequently oxidised to acetyl-CoA via an aldehyde or acetaldehyde dehydrogenase. This oxidation reaction represents the final step of the meta-cleavage pathway for the degradation of aromatic hydrocarbons. Consequently, bacteria demonstrating the ability to degrade aromatic compounds, including many *Pseudomonas* species, also possess the enzyme necessary for acetaldehyde degradation. The genes encoding the meta-cleavage pathway in the genus *Pseudomonas* are likely to only be switched on in the presence of aromatic hydrocarbons, such as toluene, benzene, and naphthalene, rather than being constitutively expressed. Accordingly, members of the *Pseudomonas* may only express aldehyde or acetaldehyde dehydrogenase-encoding genes, and therefore demonstrate the ability to degrade acetaldehyde, when aromatic hydrocarbons are available in their immediate environment. This raises the question as to whether acetaldehyde is exclusively degraded via co-metabolism or if pseudomonads can degrade acetaldehyde without first being primed by aromatic hydrocarbons. To investigate this, incubation experiments using aromatic hydrocarbon-degrading *Pseudomonas* strains should be performed. To determine the effect of priming, the selected *Pseudomonas* strains

should be enriched with an aromatic hydrocarbon, such as toluene. Having detected toluene degradation, the *Pseudomonas* strains should be enriched with acetaldehyde and monitored for degradation via gas-chromatography. Simultaneously, the same *Pseudomonas* strains should only be incubated with acetaldehyde, without initial priming with toluene, and monitored for degradation. These incubation experiments could also be coupled with qPCR to quantify the expression of key genes involved in toluene and acetaldehyde degradation, using specifically designed primers that target aldehyde dehydrogenase-encoding genes and other genes of interest. This would provide a clear indication as to whether acetaldehyde is co-metabolised and whether the necessary genes are only "switched-on" in response to the presence of aromatic hydrocarbons.

2.4.3 Physiology of *Pseudomonas* species related to abundant OTUs in acetaldehyde enrichments

Four *Pseudomonas* OTUs were identified as key acetaldehyde degraders in the Colne Estuary, the River Colne, and the River Gipping based on their significant increase in microcosms enriched with 2.27 mM of acetaldehyde. OTU6, a close relative of *P. benzenivorans* DSM 8628 and *P. glareae* KMM 9500 (Figure 2.10 & 2.17), accounted for the majority of bacterial sequences in acetaldehyde-enriched microcosms of the Colne Estuary (Figure 2.10), the River Colne, and the River Gipping (Figure 2.17). This suggests that OTU6 is primarily responsible for acetaldehyde degradation in estuarine and freshwater environments. Originally isolated from chlorobenzene-contaminated groundwater (Nishino et al. 1992), *P. benzenivorans* is able to utilise benzene, toluene, and *para*-cresol as sole sources of carbon and energy (Lang et al. 2010). The utilisation of these toxic compounds suggests that *P. benzenivorans* uses the meta-cleavage pathway for the degradation of aromatic hydrocarbons and likely possesses the aldehyde or acetaldehyde dehydrogenases necessary for acetaldehyde degradation. A review of the UniProt Knowledgebase (UniProtKB) database revealed that three putative acetaldehyde dehydrogenases have

previously been identified in *P. benzenivorans*, demonstrating that this *Pseudomonas* species has the necessary enzymes for acetaldehyde degradation, as discussed in Section 2.4.2.

OTU60, a close relative of *P. stutzeri* SO240BG38 and *P. zhaodongensis* YZGP305 (Figure 2.10), was highly abundant in Brightlingsea seawater sediment slurries enriched with acetaldehyde, representing 38% of all bacterial sequences (Figure 2.10). This suggests that OTU60 is an important acetaldehyde degrader at the mouth of the Colne Estuary and possibly in marine environments. *P. stutzeri* is considered to be a true marine *Pseudomonas* species (Lalucat et al. 2006), inhabiting both marine sediments and the water column, but is also found in close association with the cordgrass *Spartina alterniflora* in estuarine salt marshes (Lalucat et al. 2006). Strains of *P. stutzeri* can respire by denitrification (Peña et al. 2012) and are also metabolically versatile, utilising carbon compounds infrequently used by other pseudomonads, such as starch, and degrading aliphatic and aromatic hydrocarbons (Lalucat et al. 2006). *P. stutzeri* strain AN10, for example, can utilise naphthalene, 2-methylnaphthalene, and salicylate as sole sources of carbon and energy (Rossello-Mora et al. 1994). The operon encoding the naphthalene-degradation meta-cleavage pathway (*nahGTHINLOMKL*) is on the chromosome (Rossello-Mora et al. 1994), and includes the *nahO* gene encoding an acetaldehyde dehydrogenase (Bosch et al. 2000). Accordingly, it can be speculated that, as close relatives of OTU60 degrade acetaldehyde as an intermediate, that it can presumably also use it as a carbon and energy source.

OTU4249 was identified as a close relative of *P. koreensis* MLS2-1 and was particularly abundant in Hythe and Wivenhoe enrichments (Figure 2.10), suggesting that OTU4249 plays an important role in acetaldehyde degradation towards the head of the Colne Estuary. *P. koreensis* was originally isolated from Korean agricultural soils (Kwon et al. 2003) and regularly associates with agricultural crops, supressing disease and promoting plant growth through the production of lipopeptide biosurfactants (Hultberg et al. 2010a, 2010b). It has

also been shown to enhance heavy metal phytoremediation in soils, inhabiting the roots and rhizosphere of metalliferous plants and reducing metal toxicity, allowing plants to produce more biomass and accumulate larger amounts of metals (Babu et al. 2015). The close association of *P. koreensis* with agricultural plants and soils, in addition to its tolerance to toxic compounds, may explain the increase in abundance of OTU4249 in Hythe and Wivenhoe enrichments, as these sites are more influenced by agricultural land use than Brightlingsea. It should also be noted that Hythe sediments are also exposed to higher levels of urbanisation and industry and may receive increased amounts of toxic xenobiotic compounds than Wivenhoe or Brightlingsea. This may select for metabolically versatile and highly tolerant bacterial taxa such as *P. koreensis.*

OTU72333 was closely related to *P. putida* ATCC 12633 and *P. japonica* DSM 22348 (Figure 2.17) and was highly abundant in acetaldehyde-enriched microcosms of the River Colne and the River Gipping, representing 16.5% of the freshwater bacterial community (Figure 2.17). Comparatively, OTU72333 accounted for <0.01% of bacterial sequences in the Colne Estuary (Figure 2.18), suggesting that this taxon is a key acetaldehyde degrader in freshwater rivers. Like the majority of pseudomonads, *P. putida* is found in a variety of environments, including soils, freshwater, and plant rhizospheres (Jiménez et al. 2002; Wu et al. 2011), and is also metabolically versatile, degrading aromatic hydrocarbons including benzene, toluene, ethylbenzene, and p-cymene, and the halocarbon trichloroethene (Wu et al. 2011). This metabolic versatility is, in part, due to the proteins encoded by the TOL plasmid pWW0, which enable *P. putida* to utilise toluene and its derivatives (Jiménez et al. 2002). As previously mentioned, acetaldehyde is a key intermediate in the degradation of toluene and other aromatic hydrocarbons and is degraded by an acetaldehyde dehydrogenase enzyme encoded by *xylQ* located on the meta-cleavage pathway operon *xylXYZLTEGFJQKIH* of TOL plasmid pWW0 (Greated et al. 2002). Due to its close relationship with *P. putida*, OTU72333 likely possesses a catabolic plasmid carrying the degradative genes for toluene and its derivatives, including acetaldehyde.

2.4.4 Features of *Arcobacter* species that facilitate acetaldehyde degradation

The genus *Arcobacter* was the second most abundant bacterial genus in Colne Estuary, River Colne, and River Gipping microcosms following enrichment with 2.27 mM of acetaldehyde, suggesting that, alongside *Pseudomonas*, it is a key acetaldehyde degrader in estuarine and freshwater environments. At the conclusion of the primary enrichment, *Arcobacter* sequences represented 1%, 8%, and 11% of bacterial sequences in Hythe, Wivenhoe, and Brightlingsea microcosms, respectively, but accounted for <0.05% of bacterial sequences in the quaternary enrichment (Figure 2.9d). This decrease in abundance suggests that *Arcobacter* species may have been outcompeted by *Pseudomonas* species, as the relative abundance of *Pseudomonas* sequences increased significantly during the quaternary enrichment (Figure 2.9c).

Cultivated strains of *Arcobacter* are predominantly associated with human and animal disease (Ferreira et al. 2016), but uncultivated *Arcobacter* have been detected in several different environments, including seawater, rivers, hypersaline lagoons, ground water, and raw sewage (Diergaardt et al. 2004; Donachie et al. 2005; Snelling et al. 2006). *Arcobacter nitrofigilis*, a free-living nitrogen-fixing bacterium and type species of the genus, has also been found in association with the rhizosphere and roots of the salt marsh cordgrass *Spartina alterniflora* (McClung et al. 1983). Accordingly, the presence of the *Arcobacter* in the Colne Estuary, River Colne, and River Gipping is expected, as these environments provide suitable conditions for the proliferation of *Arcobacter* species. Notably, the Colne Estuary receives a regular supply of treated effluent from a sewage treatment works located upstream of Hythe, representing a potentially constant source of *Arcobacter* to the estuarine system. Moreover, species belonging to the *Spartina* genus of cordgrass, such as *S. maritima*, grow on the intertidal mudflats of the Colne Estuary, offering a potentially suitable environmental niche for the nitrogen-fixing *A. nitrofigilis* in their roots and surrounding rhizosphere. The metabolic capabilities of the genus *Arcobacter*, however, have not been

studied in detail (Campbell et al. 2006) and the ability to degrade acetaldehyde, as has been strongly suggested in this study, has not been previously identified.

Arcobacter have been isolated from hydraulically-fractured natural-gas wells in the Appalachian Basin and have been shown to persist in flowback fluids months after hydraulic fracturing (Evans et al. 2018), despite extremes of salinity and pressure, variations in temperature, and high concentrations of hydrocarbons. It has been suggested that these *Arcobacter* isolates are carbon opportunists, switching between heterotrophy and autotrophy depending on the availability of labile carbon sources (Evans et al. 2018). Furthermore, it has been proposed that *Arcobacter* species may be able to utilise a diverse range of carbon substrates, including the carboxylic acids L-malate, propionate, pyruvate, L-lactate, and succinate (Evans et al. 2018), however, the true metabolic versatility of the *Arcobacter* remains uncertain. There is currently no literature to suggest that *Arcobacter* species can utilise aromatic hydrocarbons such as toluene and benzene, however, the persistence of *Arcobacter* isolates in natural-gas wells containing high concentrations of hydrocarbons suggests that these isolates may be able to use these compounds as a carbon and energy source. Alternatively, and perhaps more likely, *Arcobacter* isolates may utilise the secondary compounds resulting from the degradation of hydrocarbons by known hydrocarbonoclastic microorganisms, such as *Marinobacter*, which have also been detected in the flowback fluids of hydraulically-fractured natural-gas wells (Evans et al. 2018). As previously mentioned in Section 2.4.2, acetaldehyde is an intermediate of the meta-cleavage pathway for the degradation of aromatic compounds, with catechol and 3-methylcatechol converted to acetaldehyde and pyruvate. Acetaldehyde is subsequently oxidised to acetate and acetyl-CoA via aldehyde dehydrogenase and acetate-CoA ligase activity, respectively. Accordingly, the ability of *Arcobacter* species to degrade acetaldehyde may result from the presence and activity of aldehyde dehydrogenase enzymes that constitute part of the meta-cleavage pathway for the degradation of aromatic hydrocarbons. Further research is necessary to determine if this metabolic pathway is present in the *Arcobacter* genus and to identify the

putative aldehyde dehydrogenase(s) involved in acetaldehyde degradation. Alternatively, members of the *Arcobacter* genus may utilise other metabolic pathways to degrade acetaldehyde. The ethanolamine degradation pathway, for example, involves the conversion of ethanolamine to acetaldehyde and ammonia via an ethanolamine ammonia-lyase encoded by *EutBC* (Chowdhury et al. 2014). Acetaldehyde is subsequently converted to acetyl-CoA via an acetaldehyde dehydrogenase encoded by *EutE* (Chowdhury et al. 2014). This suggests that the *Arcobacter*, and other acetaldehyde-degrading microorganisms, may use aldehyde dehydrogenases and acetaldehyde dehydrogenases that are not involved in the meta-cleavage pathway of aromatic hydrocarbons to degrade acetaldehyde, such as those reported to be involved in the ethanolamine degradation pathway.

The results of this study suggest that two *Arcobacter* OTUs are key acetaldehyde degraders in the Colne Estuary, the River Colne, and the River Gipping. OTU142 was identified as a close relative of *A. nitrofigilis* DSM 7299 (Figure 2.10) and represented 0.5%, 8%, and 11% of bacterial sequences in Hythe, Wivenhoe, and Brightlingsea microcosms, respectively, at the conclusion of the primary enrichment (Figure 2.10). OTU142 was not detected in the acetaldehyde-enriched microcosms of the River Colne or the River Gipping (Figure 2.18), suggesting that OTU142 is a specialist acetaldehyde degrader in estuarine environments. The absence of OTU142 in the River Colne and the River Gipping can be explained by the close association of *A. nitrofigilis* DSM 7299 with *Spartina* cordgrasses, which exclusively inhabit estuarine salt marshes. OTU299 was identified as a close relative of *A. suis* CECT7833^T (Levican et al. 2013), *A. defluvii* CECT7697^T (Collado et al. 2011), and *A. ellisii* CECT7837^T (Figueras et al. 2011) (Figure 2.17) and accounted for 11.8% of bacterial sequences in the acetaldehyde-enriched microcosms of the River Colne and the River Gipping (Figure 2.17). Although present in the Colne Estuary, OTU299 only accounted for <0.2% of bacterial sequences, indicating that this taxon is a key acetaldehyde degrader in freshwater rivers.

2.4.5 Putative acetaldehyde degraders

The relative abundance of *Lutimonas* and *Loktanella* sequences significantly increased in Brightlingsea microcosms enriched with 22.7 mM of acetaldehyde (Figure 2.11b), suggesting that members of these genera may have been responsible for the acetaldehyde degradation measured in Brightlingsea replicate Bottle B1 (Figure 2.5). However, the relative abundance of Sordariomycetes sp. SH232118.06FU also significantly increased in Bottle B1 following acetaldehyde enrichment (Figure 2.13c), coinciding with an increase in fungal ITS2 copies (Figure 2.4) and observations of fungal-like biomass (Figure 2.5). Consequently, it is difficult to determine which taxa were responsible for acetaldehyde degradation in this single replicate and to confidently identify these taxa as acetaldehyde degraders. OTU2502 and OTU1440 were identified as close relatives of *Lutimonas halocynthiae* RSS3-C1 and *Loktanella acticola* OISW-6, respectively, and individually represented >4% of bacterial sequences in Brightlingsea microcosms (Figure 2.11c). Neither of these species has been shown to utilise acetaldehyde as a carbon and energy source, although the metabolic versality of these taxa has not been studied in detail. Thus, as discussed for other OTUs earlier, the increase in the relative abundance of the *Lutimonas* and *Loktanella* may have been the result of acetaldehyde degradation or the use of carbon and energy released from dead cells resulting from the toxic concentration of acetaldehyde used for enrichment. There is some evidence to suggest that members of the genus *Loktanella* are capable of degrading dimethylsulfoniopropionate (DMSP) via the DMSP demethylation pathway (Liu et al. 2018), which results in the production of methanethiol and acetaldehyde. Liu et al. (2018) demonstrated that *Loktanella* sp. LDZ013 produced methanethiol following exposure to 0.5 and 5 mM of DMSP and possessed the DmdA gene encoding DMSP demethylase, suggesting that *Loktanella* sp. LDZ013 could demethylate DMSP and produce acetaldehyde. A review of the UniProt Knowledgebase (UniProtKB) database revealed that members of the *Loktanella* genus also possess aldehyde dehydrogenase encoding genes, indicating that the *Loktanella*, as well as producing acetaldehyde from DMSP, have the enzymatic tools

necessary for acetaldehyde degradation and could therefore be responsible for the acetaldehyde degradation measured in Brightlingsea replicate Bottle B1. Conversely, the ability of the *Lutimonas* genus to produce and degrade acetaldehyde is uncertain, with no indication that the *Lutimonas* are capable of DMSP demethylation and no genomes currently available to determine the presence of aldehyde dehydrogenase encoding genes.

The Sordariomycetes class belongs to the phylum Ascomycota, which constitutes the largest and most diverse group of Fungi (Bennet & Turgeon 2017). Members of the Ascomycota have been shown to metabolise aromatic hydrocarbons (Prenafeta-Boldú et al. 2006), although studies investigating fungal aromatic hydrocarbon degradation are limited and, in contrast to Bacteria, the metabolic pathways used are not well-understood (Prenafeta-Boldú et al. 2006; Lubbers et al. 2019). The fungal degradation of toluene, for example, has been shown to involve similar enzymatic reactions to those used by bacteria, with toluene subsequently metabolised to catechol (Prenafeta-Boldú et al. 2006). As observed in bacterial toluene degradation, catechol is converted to acetyl-CoA through a series of enzymatic reactions, in which acetaldehyde is an intermediate. Accordingly, Sordariomycetes sp. SH232118.06FU may possess the acetaldehyde dehydrogenase enzymes necessary for acetaldehyde degradation as part of an aromatic hydrocarbon degradation pathway, which may explain the significant increase in the abundance of Sordariomycetes sp. SH232118.06FU and the acetaldehyde degradation measured in Bottle B1. However, further research is necessary to confirm that Sordariomycetes sp. SH232118.06FU possesses genes encoding acetaldehyde dehydrogenase enzymes and to confidently identify this taxon as an acetaldehyde-degrading fungi. Furthermore, investigations are needed to ensure that *Lutimonas* and *Loktanella* species contribute to acetaldehyde degradation and to identify the aldehyde dehydrogenase enzymes that are potentially involved.

2.4.6 Microbial degradation of metaldehyde in freshwater rivers

The findings of this study suggest that metaldehyde was not utilised as a carbon and energy source by bacteria in the River Colne and River Gipping enrichments. Following enrichment with 2.59 mM of metaldehyde, bacterial communities in the River Colne and the River Gipping were similar to their respective no-acetaldehyde controls, which did not receive an additional source of carbon (Figure 2.15a), whilst bacterial OTU richness counts were comparable between the two treatments (Figure 2.15b). The inability to utilise metaldehyde may have resulted from the high concentrations used for enrichment, which may have been toxic to bacteria with the potential for metaldehyde degradation. Metaldehyde-degrading bacteria have previously been isolated from the soils of domestic gardens (Thomas et al. 2017), allotments, and agricultural farms (Castro-Gutiérrez et al. 2020) exposed to metaldehyde, demonstrating that this compound, a cyclic-tetramer of acetaldehyde, can be utilised by bacteria as a sole source of carbon and energy. Thomas et al. (2017), for example, isolated the first bacterial strains capable of metaldehyde degradation, namely *Acinetobacter calcoaceticus* strain E1 and *Variovorax* strain E3, which demonstrated the ability to degrade metaldehyde at a concentration of 850 µM. Eight metaldehyde-degrading bacterial strains, including *Rhodococcus globerulus* strain HMET-A, were also isolated by Castro-Gutiérrez et al. (2020) and degraded metaldehyde at a concentration of 85 µM (150 mg L^{-1}). The concentration of metaldehyde used in the current study was considerably higher than those previously used to isolate metaldehyde degraders, suggesting that this concentration was not conducive for the growth of metaldehyde-degrading bacteria. The ability to degrade metaldehyde has been shown to result from the expression of the *mahX* gene, which encodes a 2-oxoglutarate-dependent oxygenase that oxidises metaldehyde to a linear hemiacetal by cleavage of the metaldehyde ring (Castro-Gutiérrez et al. 2020). The hemiacetal intermediate is iteratively degraded by a lyase encoded by the *mahY* gene, producing acetaldehyde which is subsequently converted to acetate via aldehyde dehydrogenase activity (Castro-Gutiérrez et al. 2020). The River Colne and the River

Gipping flow through areas of heavy agricultural activity, suggesting that metaldehyde may regularly enter these rivers, particularly during periods of heavy rainfall when slug pellets containing metaldehyde dissolve and run into freshwater bodies (Castle et al. 2017). This may support a metaldehyde-degrading bacterial community in the River Colne and the River Gipping, however, it seems likely that the concentration of metaldehyde used for enrichment during this study was toxic and prevented growth. Metaldehyde is not easily removed by conventional drinking water treatment processes, including the use of granular or powdered activated carbon adsorption (Castle et al. 2017), both of which are particularly expensive and have poor removal efficiencies at typical environmental concentrations (Castle et al. 2017). Accordingly, bioremediation has been identified as a potentially cost effective and efficient strategy to manage metaldehyde concentrations in freshwater rivers, particularly where these are used for potable water supplies. The results presented here suggest that the upper concentration limit for bioremediation is considerably lower than 2.59 mM of metaldehyde, however, it is important to note that these concentrations are not achieved in freshwater systems.

2.5 Conclusion

The findings of this study show that microbial acetaldehyde degraders are present and active in the Colne Estuary, the River Colne, and the River Gipping. Bacteria are primarily responsible for acetaldehyde degradation in estuarine and freshwater environments, with members of the genera *Pseudomonas* and *Arcobacter* representing the majority of the bacterial community following acetaldehyde enrichment. The ability of the *Pseudomonas* and *Arcobacter* to degrade acetaldehyde is dependent on the activity of acetaldehyde dehydrogenase enzymes, which often represent the final enzyme in the meta-cleavage pathway for the degradation of aromatic hydrocarbons such as benzene, toluene, and naphthalene. This suggests that bacteria capable of utilising aromatic hydrocarbons as sources of carbon and energy may also contribute to acetaldehyde degradation and that the

diversity of acetaldehyde-degrading bacteria is considerably larger than previously thought. Fungi, such as the Sordariomycetes, also contribute to acetaldehyde degradation, although play a secondary role to bacteria, whilst archaea have no clear role in microbial acetaldehyde degradation. Acetaldehyde-degrading bacteria and fungi utilised 2.27 mM of acetaldehyde but were sensitive to acetaldehyde concentrations of 22.7 mM, suggesting that the higher acetaldehyde concentration was toxic and inhibited growth. Acetaldehyde is predominantly dissimilated to CO_2 for energy production by acetaldehyde degraders, whilst a small proportion of acetaldehyde is assimilated into biomass for growth. Metaldehyde was not utilised as a carbon and energy source by bacteria in the River Colne and River Gipping enrichments, however, the concentrations used in this study were considerably higher than those used to isolate metaldehyde-degrading bacteria from soils, suggesting that conditions were not conducive for the growth of metaldehyde-degraders. Further investigations are needed to improve our understanding of the diversity of acetaldehyde-degrading microorganisms and to identify the bacteria and fungi most responsible for acetaldehyde degradation in estuarine and freshwater environments. Further research is also necessary to establish whether metaldehyde-degrading bacteria are present in freshwater rivers, which may provide an indication as to whether freshwater metaldehyde-degraders can be used in future bioremediation strategies.

2.6 References

Babu AG, Shea PJ, Sudhakar D, Jung IB, Oh BT (2015) Potential use of *Pseudomonas koreensis* AGB-1 in association with *Miscanthus sinensis* to remediate heavy metal(loid)-contaminated mining site soil. J Environ Manage 151:160–166

Balch WE, Schoberth S, Tanner RS, Wolfe RS (1977) *Acetobacterium*, a new genus of hydrogen-oxidizing, carbon dioxide-reducing, anaerobic bacteria. Int J Syst Bacteriol 27:355–361

Bankevich A, Nurk S, Antipov D, Gurevich AA, Dvorkin M, Kulikov AS, Lesin VM, Nikolenko SI, Pham S, Prjibelski AD, Pyshkin AV, Sirotkin AV, Vyahhi N, Tesler G, Alekseyev MA, Pevzner PA (2012) SPAdes: A new genome assembly algorithm and its applications to single-cell sequencing. J Comput Biol 19:455–477

Basu A, Apte SK, Phale PS (2006) Preferential utilization of aromatic compounds over glucose by *Pseudomonas putida* CSV86. Appl Environ Microbiol 72:2226–2230

Beale R, Dixon JL, Arnold SR, Liss PS, Nightingale PD (2013) Methanol, acetaldehyde, and acetone in the surface waters of the Atlantic Ocean. J Geophys Res Ocean 118:5412–5425

Bennet RJ, Turgeon BG (2017) Fungal sex: The Ascomycota. The Fungal Kingdom. pp 117–145

Bosch R, García-Valdés E, Moore ERB (2000) Complete nucleotide sequence and evolutionary significance of a chromosomally encoded naphthalene-degradation lower pathway from *Pseudomonas stutzeri* AN10. Gene 245:65–74

de Bruyn WJ, Clark CD, Pagel L, Takehara C (2011) Photochemical production of formaldehyde, acetaldehyde and acetone from chromophoric dissolved organic matter in coastal waters. J Photochem Photobiol A Chem 226:16–22

Campbell BJ, Engel AS, Porter ML, Takai K (2006) The versatile ε-proteobacteria: Key players in sulphidic habitats. Nat Rev Microbiol 4:458–468

Carrión O, McGenity TJ, Murrell JC (2020) Molecular ecology of isoprene-degrading bacteria. Microorganisms 8:1–15

Castle GD, Mills GA, Bakir A, Gravell A, Schumacher M, Snow K, Fones GR (2018) Measuring metaldehyde in surface waters in the UK using two monitoring approaches. Environ Sci Process Impacts 20:1180–1190

Castle GD, Mills GA, Gravell A, Jones L, Townsend I, Cameron DG, Fones GR (2017) Review of the molluscicide metaldehyde in the environment. Environ Sci Water Res Technol 3:415–428

Castro-Gutiérrez V, Fuller E, Thomas JC, Sinclair CJ, Johnson S, Helgason T, Moir JWB (2020) Genomic basis for pesticide degradation revealed by selection, isolation and characterisation of a library of metaldehyde-degrading strains from soil. Soil Biol Biochem 142:107702

Charron G, Leducq JB, Bertin C, Dubé AK, Landry CR (2014) Exploring the northern limit of the distribution of *Saccharomyces cerevisiae* and *Saccharomyces paradoxus* in North America. FEMS Yeast Res 14:281–288

Chowdhury C, Sinha S, Chun S, Yeates TO, Bobik TA (2014) Diverse bacterial microcompartment organelles. Microbiol Mol Biol Rev 78:438–468

Collado L, Levican A, Perez J, Figueras MJ (2011) *Arcobacter defluvii* sp. nov., isolated from sewage samples. Int J Syst Evol Microbiol 61:2155–2161

Curtis C, Lima A, Lozano S, Veith G (1982) Evaluation of a bacterial bioluminescence bioassay as a method for predicting acute toxicity of organic chemicals to fish. In: Pearson J, Foster R, Bishop W (eds) Aquatic toxicology and hazard assessment. ASTM International, West Conshohocken, PA, pp 170–178

Deutscher J (2008) The mechanisms of carbon catabolite repression in bacteria. Curr Opin Microbiol 11:87–93

Diergaardt SM, Venter SN, Spreeth A, Theron J, Brözel VS (2004) The occurrence of campylobacters in water sources in South Africa. Water Res 38:2589–2595

Dixon JL, Beale R, Nightingale PD (2013) Production of methanol, acetaldehyde, and acetone in the Atlantic Ocean. Geophys Res Lett 40:4700–4705

Donachie SP, Bowman JP, On SLW, Alam M (2005) *Arcobacter halophilus* sp. nov., the first obligate halophile in the genus Arcobacter. Int J Syst Evol Microbiol 55:1271–1277

Dyksterhouse SE, Gray JP, Herwig RP, Lara JC, Staley JT (1995) *Cycloclasticus pugetii* gen. nov., sp. nov., an aromatic hydrocarbon-degrading bacterium from marine sediments. Int J Syst Bacteriol 45:116–123

Edgar RC, Haas BJ, Clemente JC, Quince C, Knight R (2011) UCHIME improves sensitivity and speed of chimera detection. Bioinformatics 27:2194–2200

Evans MV, Panescu J, Hanson AJ, Welch SA, Sheets JM, Nastasi N, Daly RA, Cole DR, Darrah TH, Wilkins MJ, Wrighton KC, Mouser PJ (2018) Members of *Marinobacter* and *Arcobacter* influence system biogeochemistry during early production of hydraulically fractured natural gas wells in the Appalachian Basin. Front Microbiol 9:1–17

Ferreira S, Queiroz JA, Oleastro M, Domingues FC (2016) Insights in the pathogenesis and resistance of *Arcobacter*: A review. Crit Rev Microbiol 42:364–383

Figueras MJ, Levican A, Collado L, Inza MI, Yustes C (2011) *Arcobacter ellisii* sp. nov., isolated from mussels. Syst Appl Microbiol 34:414–418

Frimmersdorf E, Horatzek S, Pelnikevich A, Wiehlmann L, Schomburg D (2010) How *Pseudomonas aeruginosa* adapts to various environments: A metabolomic approach. Environ Microbiol 12:1734–1747

Gao B, Shang X, Li L, Di W, Zeng R (2018) Phylogenetically diverse, acetaldehyde-degrading bacterial community in the deep sea water of the West Pacific Ocean. Acta Oceanol Sin 37:54–64

Giubbina FF, Scaramboni C, De Martinis BS, Godoy-Silva D, Nogueira RFP, Campos MLAM (2017) A simple method for simultaneous determination of acetaldehyde, acetone, methanol, and ethanol in the atmosphere and natural waters. Anal Methods 9:2915–2922

Gomila M, Peña A, Mulet M, Lalucat J, García-Valdés E (2015) Phylogenomics and systematics in *Pseudomonas*. Front Microbiol 6:1–13

Görke B, Stülke J (2008) Carbon catabolite repression in bacteria: Many ways to make the most out of nutrients. Nat Rev Microbiol 6:613–624

Greated A, Lambertsen L, Williams PA, Thomas CM (2002) Complete sequence of the IncP-9 TOL plasmid pWW0 from *Pseudomonas putida*. Environ Microbiol 4:856–871

Halsey KH, Giovannoni SJ, Graus M, Zhao Y, Landry Z, Thrash JC, Vergin KL, de Gouw J (2017) Biological cycling of volatile organic carbon by phytoplankton and bacterioplankton. Limnol Oceanogr 62:2650–2661

Hultberg M, Alsberg T, Khalil S, Alsanius B (2010a) Suppression of disease in tomato infected by *Pythium ultimum* with a biosurfactant produced by *Pseudomonas koreensis*. BioControl 55:435–444

Hultberg M, Bengtsson T, Liljeroth E (2010b) Late blight on potato is suppressed by the biosurfactant-producing strain *Pseudomonas koreensis* 2.74 and its biosurfactant. BioControl 55:543–550

Jiménez JI, Miñambres B, García JL, Díaz E (2002) Genomic analysis of the aromatic catabolic pathways from *Pseudomonas putida* KT2440. Environ Microbiol 4:824–841

Joshi NA, Fass JN (2011) Sickle: A sliding-window, adaptive, quality-based trimming tool for FastQ files (Version 1.33) [Software]. https://github.com/najoshi/sickle

Kay P, Grayson R (2014) Using water industry data to assess the metaldehyde pollution problem. Water Environ J 28:410–417

Kimura M (1980) A simple method for estimating evolutionary rates of base substitutions through comparative studies of nucleotide sequences. J Mol Evol 16:111–120

Klockgether J, Tümmler B (2017) Recent advances in understanding *Pseudomonas aeruginosa* as a pathogen. F1000 Res 6:1–10

Kwon SW, Kim JS, Park IC, Yoon SH, Park DH, Lim CK, Go SJ (2003) *Pseudomonas koreensis* sp. nov., *Pseudomonas umsongensis* sp. nov. and *Pseudomonas jinjuensis* sp. nov., novel species from farm soils in Korea. Int J Syst Evol Microbiol 53:21–27

Lalucat J, Bennasar A, Bosch R, García-Valdés E, Palleroni NJ (2006) Biology of *Pseudomonas stutzeri*. Microbiol Mol Biol Rev 70:510–547

Lang E, Burghartz M, Spring S, Swiderski J, Spröer C (2010) *Pseudomonas benzenivorans* sp. nov. and *Pseudomonas saponiphila* sp. nov., represented by xenobiotics degrading type strains. Curr Microbiol 60:85–91

Latham J, Rasch P, Chen C, Kettles L, Gadian A, Gettelman A, Morrison H, Bower K, Choularton T (2008) Global temperature stabilization via controlled albedo enhancement of low-level maritime clouds. Phil Trans R Soc A 366:3969–3987

Levican A, Collado L, Figueras MJ (2013) *Arcobacter cloacae* sp. nov. and *Arcobacter suis* sp. nov., two new species isolated from food and sewage. Syst Appl Microbiol 36:22–27

Li E, de Orduña RM (2011) Evaluation of the acetaldehyde production and degradation potential of 26 enological *Saccharomyces* and non-*Saccharomyces* yeast strains in a resting cell model system. J Ind Microbiol Biotechnol 38:1391–1398

Liu J, Liu J, Zhang SH, Liang J, Lin H, Song D, Yang GP, Todd JD, Zhang XH (2018) Novel insights into bacterial dimethylsulfoniopropionate catabolism in the East China Sea. Front Microbiol 9:3206

Liu Y, Shang X, Yi Z, Gu L, Zeng R (2015) *Shewanella mangrovi* sp. nov., an acetaldehyde-degrading bacterium isolated from mangrove sediment. Int J Syst Evol Microbiol 65:2630–

2634

Lubbers RJM, Dilokpimol A, Visser J, Mäkelä MR, Hildén KS, de Vries RP (2019) A comparison between the homocyclic aromatic metabolic pathways from plant-derived compounds by Bacteria and Fungi. Biotechnol Adv 37:107396

Masella AP, Bartram AK, Truszkowski JM, Brown DG, Neufeld JD (2012) PANDAseq: PAired-eND Assembler for Illumina sequences. BMC Bioinformatics 13:

McClung CR, Patriquin DG, Davis RE (1983) *Campylobacter nitrofigilis* sp. nov., a nitrogen-fixing bacterium associated with roots of *Spartina alterniflora* Loisel. Int J Syst Bacteriol 33:605–612

Millet DB, Guenther A, Siegel DA, Nelson NB, Singh HB, de Gouw JA, Warneke C, Williams J, Eerdekens G, Sinha V, Karl T, Flocke F, Apel E, Riemer DD, Palmer PI, Barkley M (2010) Global atmospheric budget of acetaldehyde: 3-D model analysis and constraints from in-situ and satellite observations. Atmos Chem Phys 10:3405–3425

Moore ERB, Tindall BJ, Martins dos Santos VAP, Pieper DH, Ramos JL, Palleroni NJ (2006) Nonmedical: *Pseudomonas*. The Prokaryotes: A Handbook on the Biology of Bacteria. pp 646–703

Musat N, Foster R, Vagner T, Adam B, Kuypers MMM (2012) Detecting metabolic activities in single cells, with emphasis on nanoSIMS. FEMS Microbiol Rev 36:486-511

Nikolenko SI, Korobeynikov AI, Alekseyev MA (2013) BayesHammer: Bayesian clustering for error correction in single-cell sequencing. BMC Genomics 14:S7

Nishino SF, Spain JC, Belcher LA, Litchfield CD (1992) Chlorobenzene degradation by bacteria isolated from contaminated groundwater. Appl Environ Microbiol 58:1719–1726

Okabe S, Kindaichi T, Ito T (2004) MAR-FISH - An ecophysiological approach to link phylogenetic affiliation and *in situ* metabolic activity of microorganisms at a single-cell resolution. Microbes Environ 19:83–98

Oksanen J, Guillaume Blanchet F, Friendly M, Kindt R, Legendre P, McGlinn D, Minchin PR, O'Hara RB, Simpson GL, Solymos P, Stevens MHH, Szoecs E, Wagner H (2020). Vegan: Community Ecology Package. R package version 2.5-7. https://CRAN.R-project.org/package=vegan

Parks DH, Tyson GW, Hugenholtz P, Beiko RG (2014) STAMP: Statistical analysis of taxonomic and functional profiles. Bioinformatics 30:3123–3124

Peña A, Busquets A, Gomila M, Bosch R, Nogales B, Elena GV, Lalucat J, Bennasar A (2012) Draft genome of *Pseudomonas stutzeri* strain ZoBell (CCUG 16156), a marine isolate and model organism for denitrification studies. J Bacteriol 194:1277–1278

Platt A, Shingler V, Taylor SC, Williams PA (1995) The 4-hydroxy-2-oxovalerate aldolase and acetaldehyde dehydrogenase (acylating) encoded by the *nahM* and *nahO* genes of the naphthalene catabolic plasmid pWW60-22 provide further evidence of conservation of meta-cleavage pathway gene sequences. Microbiology 141:2223–2233

Prenafeta-Boldú FX, Summerbell R, Sybren de Hoog G (2006) Fungi growing on aromatic hydrocarbons: Biotechnology's unexpected encounter with biohazard? FEMS Microbiol Rev 30:109–130

R Core Team (2020) R: A language and environment for statistical computing. R foundation for statistical computing, Vienna, Austria. URL https://www.R-project.org/

Rainey PB (1999) Adaptation of *Pseudomonas fluorescens* to the plant rhizosphere. Environ Microbiol 1:243–257

Read KA, Carpenter LJ, Arnold SR, Beale R, Nightingale PD, Hopkins JR, Lewis AC, Lee JD, Mendes L, Pickering SJ (2012) Multiannual observations of acetone, methanol, and acetaldehyde in remote tropical Atlantic air: Implications for atmospheric OVOC budgets and oxidative capacity. Environ Sci Technol 46:11028–11039

Roebuck JA, Avery GB, Felix JD, Kieber RJ, Mead RN, Skrabal SA (2016) Biogeochemistry

of ethanol and acetaldehyde in freshwater sediments. Aquat Geochemistry 22:177–195

Rognes T, Flouri T, Nichols B, Quince C, Mahé F (2016) VSEARCH: A versatile open source tool for metagenomics. PeerJ 4:e2584

Rojo F (2010) Carbon catabolite repression in *Pseudomonas*: Optimizing metabolic versatility and interactions with the environment. FEMS Microbiol Rev 34:658–684

Rossello-Mora RA, Lalucat J, Garcia-Valdes E (1994) Comparative biochemical and genetic analysis of naphthalene degradation among *Pseudomonas stutzeri* strains. Appl Environ Microbiol 60:966–972

Saitou N, Nei M (1987) The neighbor-joining method: a new method for reconstructing phylogenetic trees. Mol Biol Evol 4:406–425

Salter SJ, Cox MJ, Turek EM, Calus ST, Cookson WO, Moffatt MF, Turner P, Parkhill J, Loman NJ, Walker AW (2014) Reagent and laboratory contamination can critically impact sequence-base microbiome analyses. BMC Biol 12:87

Sareen N, Schwier AN, Lathem TL, Nenes A, McNeill VF (2013) Surfactants from the gas phase may promote cloud droplet formation. Proc Natl Acad Sci USA 110:2723–8

Singh HB, Salas LJ, Chatfield RB, Czech E, Fried A, Walega J, Evans MJ, Field BD, Jacob DJ, Blake D, Heikes B, Talbot R, Sachse G, Crawford JH, Avery MA, Sandholm S, Fuelberg H (2004) Analysis of the atmospheric distribution, sources, and sinks of oxygenated volatile organic chemicals based on measurements over the Pacific during TRACE-P. J Geophys Res 109:1–20

Smillie C, Garcillán-Barcia MP, Francia MV, Rocha EPC, de la Cruz F (2010) Mobility of plasmids. Microbiol Mol Biol Rev 74:434–452

Snelling WJ, Matsuda M, Moore JE, Dooley JSG (2006) Under the microscope: *Arcobacter*. Lett Appl Microbiol 42:7–14

Sophos NA, Vasiliou V (2003) Aldehyde dehydrogenase gene superfamily: The 2002 update. Chem Biol Interact 143–144:5–22

Stephanopoulos GN, Aristidou AA, Nielsen J (1998) Examples of pathway manipulations: Metabolic engineering in practice. Metabolic Engineering. pp 203–283

Stinson LF, Keelan JA, Payne MS (2018) Identification and removal of contaminating microbial DNA from PCR reagents: impact on low-biomass microbiome analyses. Lett Appl Microbiol 68:2-8

Strickland JDH, Parsons TR (1968) Determination of reactive phosphorus. A Practical Handbook of Seawater Analysis. pp 49–56

Stülke J, Hillen W (1999) Carbon catabolite repression in bacteria. Curr Opin Microbiol 2:195–201

Taniyama K, Itoh H, Takuwa A, Sasaki Y, Yajima S, Toyofuku M, Nomura N, Takaya N (2012) Group X aldehyde dehydrogenases of *Pseudomonas aeruginosa* PAO1 degrade hydrazones. J Bacteriol 194:1447–1456

Thomas JC, Helgason T, Sinclair CJ, Moir JWB (2017) Isolation and characterization of metaldehyde-degrading bacteria from domestic soils. Microb Biotechnol 10:1824–1829

Trifunović D, Berghaus N, Müller V (2020) Growth of the acetogenic bacterium *Acetobacterium woodii* by dismutation of acetaldehyde to acetate and ethanol. Environ Microbiol Rep 12:58–62

Wang Q, Garrity GM, Tiedje JM, Cole JR (2007) Naïve Bayesian classifier for rapid assignment of rRNA sequences into the new bacterial taxonomy. Appl Environ Microbiol 73:5261–5267

Water UK (2013) Water UK Briefing Paper on Metaldehyde. Retrieved from http://www.water .org.uk/home/policy/positions/metaldehyde-briefing/water-uk-policy-briefing-metaldehyde-13-aug-2013.pdf

Webb C (2016) Turnover of acetaldehyde in natural waters. MSc thesis, Plymouth University

Wickham H (2016) ggplot2: Elegant graphics for data analysis. Springer-Verlag, New York. https://ggplot2.tidyverse.org

Wigley TML, Smith SJ, Prather MJ (2002) Radiative forcing due to reactive gas emissions. J Clim 15:2690–2696

Williams PA, Jones RM, Zylstra G (2004) Genomics of catabolic plasmids. *Pseudomonas*. pp 165–195

Wu X, Monchy S, Taghavi S, Zhu W, Ramos J, van der Lelie D (2011) Comparative genomics and functional analysis of niche-specific adaptation in *Pseudomonas putida*. FEMS Microbiol Rev 35:299–323

Xin XF, Kvitko B, He SY (2018) *Pseudomonas syringae*: what it takes to be a pathogen. Nat Rev Microbiol 16:316–328

Yen KM, Gunsalus IC (1985) Regulation of naphthalene catabolic genes of plasmid NAH7. J Bacteriol 162:1008–1013

Zhang J, Kobert K, Flouri T, Stamatakis A (2014) PEAR: A fast and accurate Illumina Paired-End reAd mergeR. Bioinformatics 30:614–620

2.7 Supplementary material

Table S2.1 Phosphate (PO_4^{3-}) calibration standards used to determine absolute quantities of dissolved phosphate in River Colne and River Gipping primary enrichments. Na_2HPO_4: sodium phosphate dibasic.

Standard No.	PO_4^{3-} concentration (µM)	20 µM Na_2HPO_4 stock addition (µL)	Milli-Q water addition (µL)
1	0	0	1000
2	5	250	750
3	10	500	500
4	15	750	250
5	20	1000	0

Table S2.2 Ammonium (NH_4^+) calibration standards used to determine absolute quantities of dissolved ammonium in River Colne and River Gipping primary enrichments. NH_4Cl: ammonium chloride.

Standard No.	NH_4^+ concentration (µM)	100 µM NH_4Cl stock addition (µL)	Milli-Q water addition (µL)
1	0	0	1000
2	25	250	750
3	50	500	500
4	75	750	250
5	100	1000	0
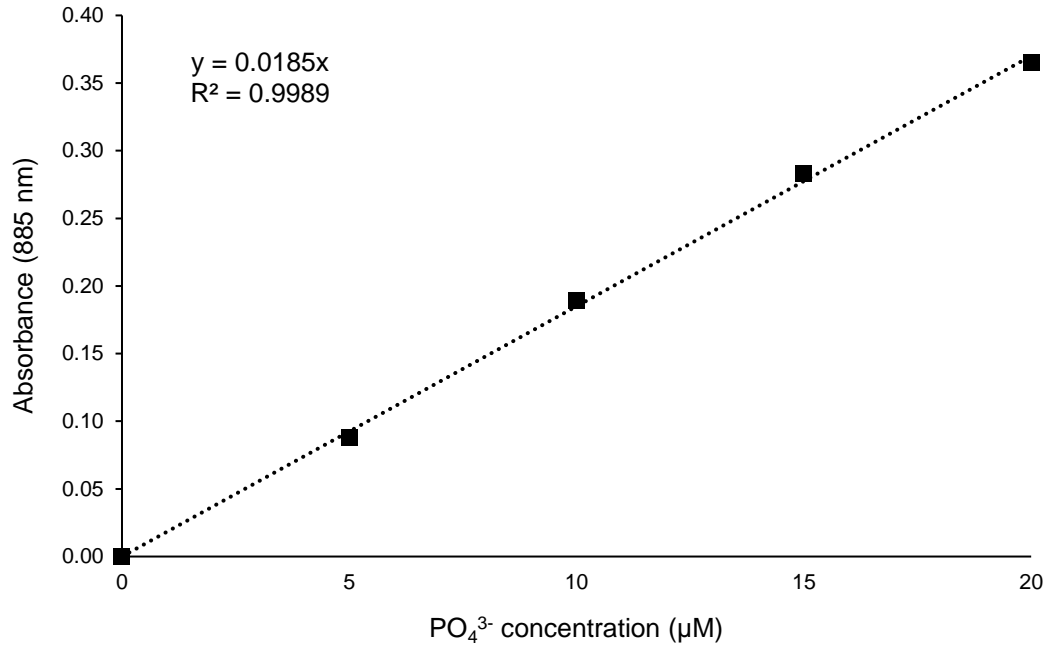
Figure S2.1 Five-point calibration curve used to quantify dissolved phosphate (PO_4^{3-}) concentrations in River Colne and River Gipping primary enrichments.
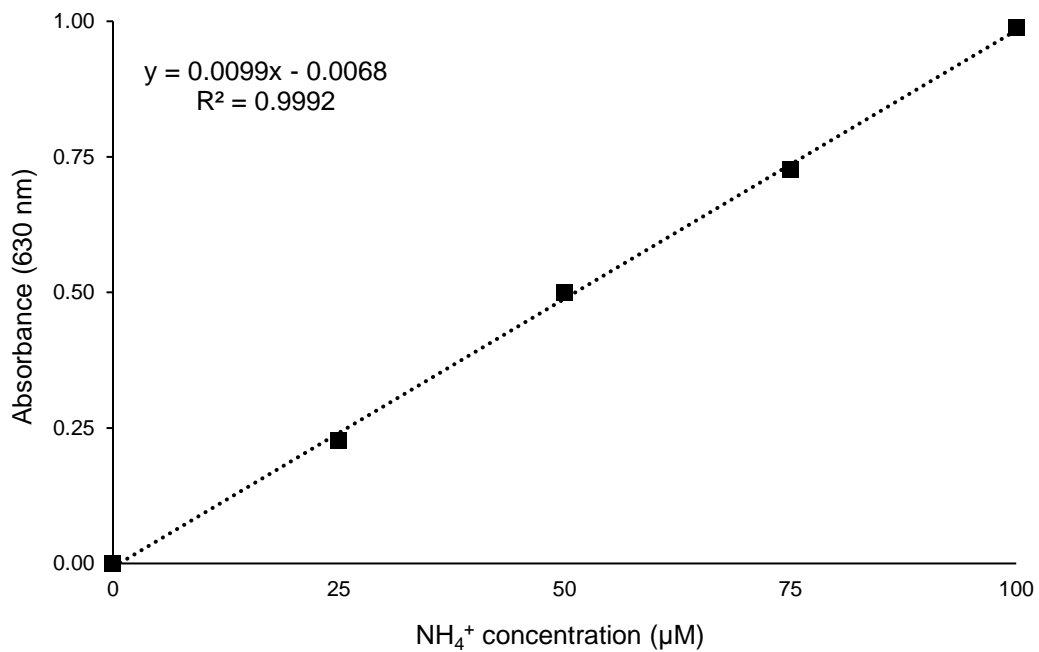
Figure S2.2 Five-point calibration curve used to quantify ammonium (NH_4^+) concentrations in River Colne and River Gipping primary enrichments.
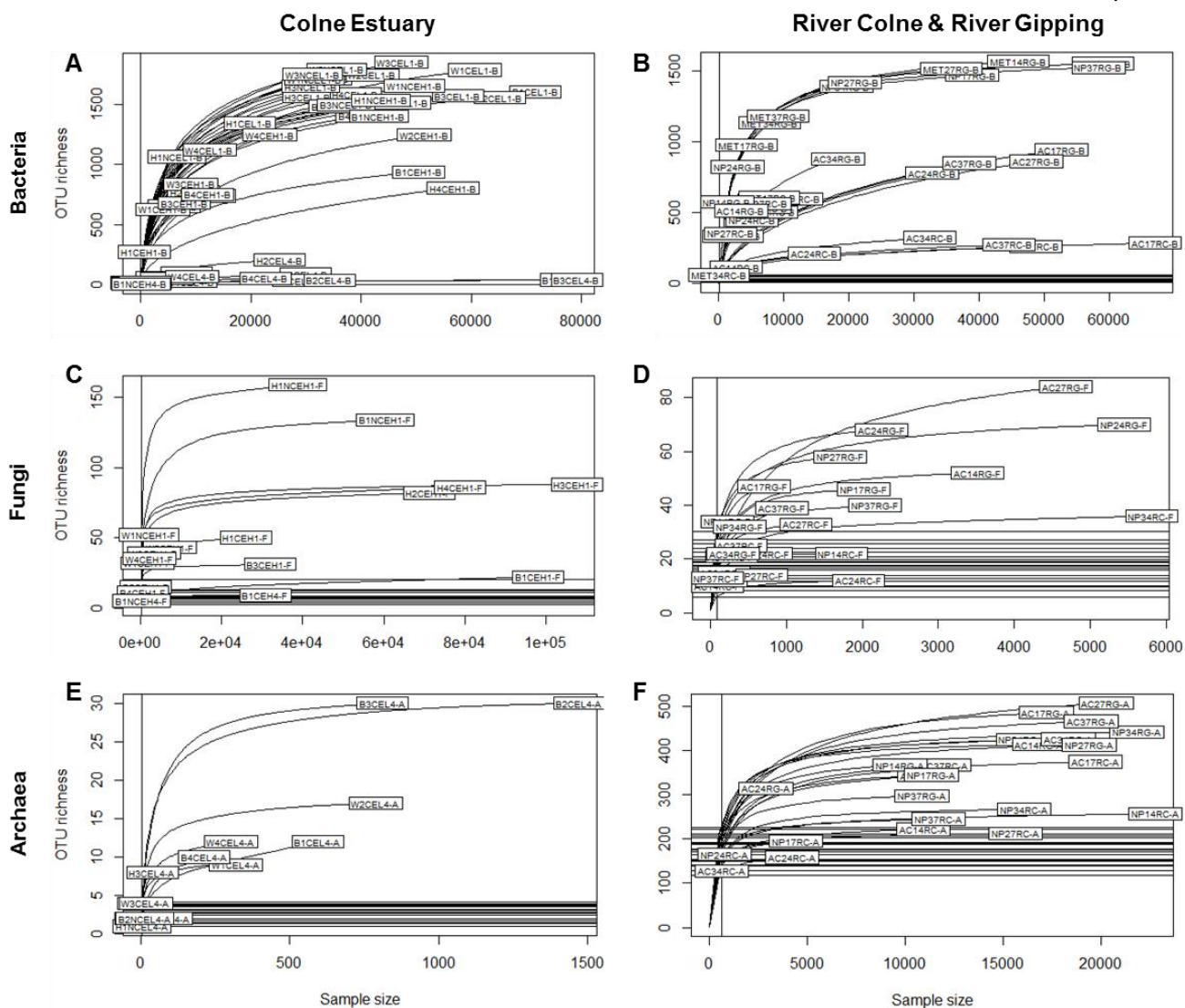
Figure S2.3 Rarefaction curves estimating the richness of bacterial (A - B), fungal (C - D), and archaeal (E - F) OTUs in samples collected from the Colne Estuary, River Colne, and the River Gipping.
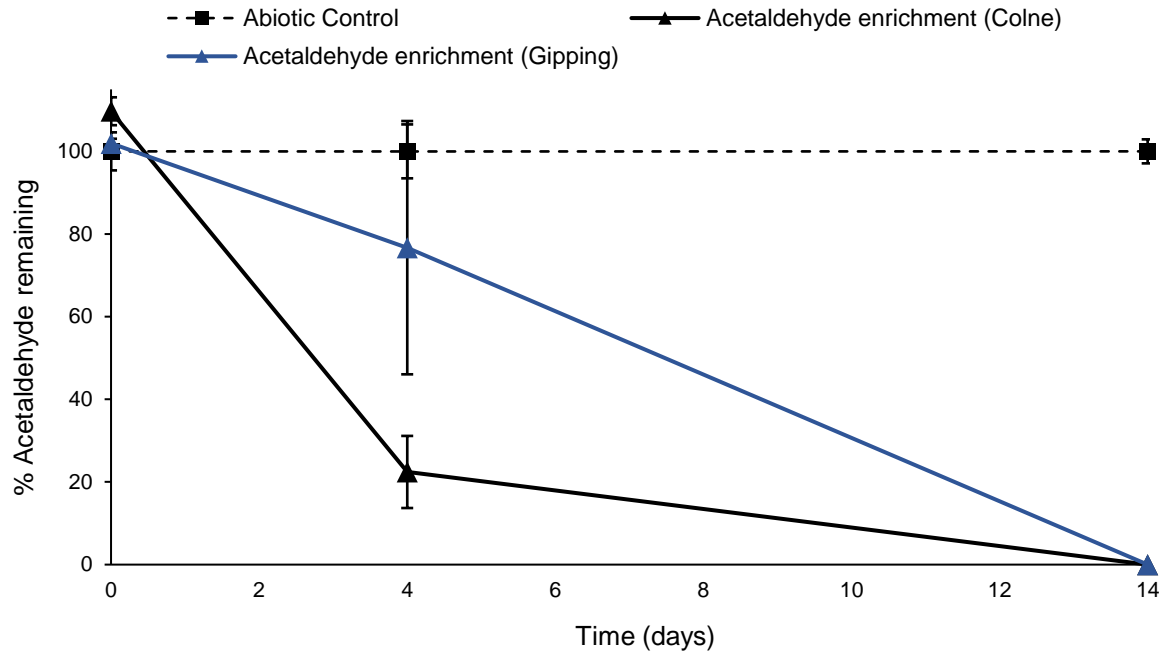
Figure S2.4 Acetaldehyde degradation (%) in River Colne and River Gipping secondary enrichments. Microcosms were enriched with 2.27 mM of acetaldehyde, incubated in the dark at 20°C and monitored for degradation. Degradation within enrichments is relative to the mean of the abiotic controls (*n=3*) at each time point. The mean of three replicates is plotted for each sampling site (± S.E.).

Chapter 3:

Identification and Characterisation of Acetaldehyde-Degrading Microorganisms from the Colne Estuary

3.1 Introduction

The microbial degradation of volatile organic compounds (VOCs) plays a fundamental role in the global carbon cycle and in regulating the Earth's climate. Accordingly, much attention has been given to the identification and characterisation of microorganisms that are responsible for degrading the most abundant VOCs, such as methane (CH_4) and of late, isoprene (C_5H_8). Our knowledge of these VOC-degrading microorganisms and their role in VOC biogeochemical cycling have therefore improved significantly in recent years. The diversity, abundance, and global distribution of methanotrophs, for example, has been explored in considerable detail in the past two decades and has demonstrated the important role that these microorganisms play in maintaining the global methane balance; with aerobic methanotrophic bacteria accounting for ~4% of the global methane sink (Kirschke et al. 2013). In terms of diversity, aerobic methane-oxidising bacteria have been shown to belong to three distinct lineages over a twenty-five year period, namely the Alphaproteobacteria, Gammaproteobacteria, and Verrucomicrobia (Hanson & Hanson, 1996; Op den Camp et al. 2009), and utilise methane monooxygenase, encoded by *pmo* genes, to initiate methane oxidation (Dean et al. 2018; Kalyuzhnaya et al. 2019).

More recently, the importance of isoprene-degrading microorganisms in the global isoprene cycle has also emerged, with terrestrial soils recognised as a significant biological isoprene sink (Gray et al. 2015), and marine environments also found to be populated by isoprene-degrading microorganisms (Acuña Alvarez et al. 2009). In both environments, members of the Actinobacteria were identified as key isoprene degraders, including species within the *Rhodococcus*, *Mycobacterium* and *Nocardia* genera (Acuña Alvarez et al. 2009; El Khawand

et al. 2016; McGenity et al. 2018). A closely related isolate cultivated from freshwater sediment, namely *Rhodococcus* strain AD45 (Van Hylckama Vlieg et al. 1998), has been used as a model isoprene degrader for over twenty years and has provided valuable insights into the mechanisms of isoprene metabolism. Most notably, this organism has been used to identify and characterise several genes involved in isoprene degradation, including the gene cluster *isoABCDEF* that encodes an isoprene monooxygenase, which catalyses the initial oxidation of isoprene to 1,2-epoxy-isoprene (Van Hylckama Vlieg et al. 2000; Crombie et al. 2015).

Comparatively, our knowledge of the microorganisms that utilise oxygenated volatile organic compounds (OVOCs), such as acetone and acetaldehyde, as a source of carbon is limited, particularly in terms of their identity, diversity, and the mechanisms used for OVOC degradation. This has restricted our understanding of the role that these microorganisms play in the global biogeochemical cycles of OVOCs, although it is thought that OVOC-degrading microorganisms represent an important biological sink in terrestrial and aquatic ecosystems. The microbial degradation of methanol by methylotrophic microorganisms has been studied more extensively than the microbial degradation of acetone and acetaldehyde, and much more than isoprene. This has led to a better understanding of the identities and diversity of methylotrophs, and the mechanisms of microbial methanol oxidation. In terrestrial soils, for example, at least 56 species of aerobic methanol-oxidising microorganisms have been isolated, belonging to a diverse group of phyla, including the Firmicutes, Actinobacteria, Verrucomicrobia, and the Proteobacteria (Kolb 2009). The activity of these isolates and non-cultivated methylotrophs in soils is estimated to prevent >80% of the methanol produced by plants from entering the atmosphere (Kolb 2009), which has a direct and significant impact on atmospheric chemistry (Galbally & Kirstine 2002; Stacheter et al. 2013). This includes increasing the oxidising capacity of the atmosphere due to an increased availability of hydroxyl radicals, which would otherwise react with the methanol released by plants. The enhanced oxidising capacity of the atmosphere reduces the residence time of

other VOCs and greenhouse gases, including methane, reducing the potential for atmospheric warming. Several methanol dehydrogenase enzymes, responsible for oxidising methanol to formaldehyde, have also been discovered in methanol-oxidising bacteria (Chistoserdova et al. 2009), highlighting the importance of isolating microorganisms from their environment for further investigation.

The identity and diversity of acetaldehyde-degrading microorganisms in aquatic ecosystems is poorly understood compared to our knowledge of methylotrophs. This lack of information is primarily due to limited research effort in the field of microbial acetaldehyde degradation, which has resulted in the identification of only a handful of acetaldehyde degraders in the past five years (Liu et al. 2015; Halsey et al. 2017; Gao et al. 2018; Trifunović et al. 2020). Besides highlighting the paucity of research effort, this also demonstrates the significant gulf in understanding and lack of information regarding acetaldehyde degraders compared to the microorganisms that utilise methane, isoprene, and other OVOCs. This is concerning when the importance of these discoveries is considered. Halsey et al. (2017), for example, demonstrated that two isolated strains of *Pelagibacter* SAR11, namely HTCC1062 and HTCC7211, could utilise acetaldehyde as a carbon and energy source. It was reported that these strains oxidised ~70% of utilised acetaldehyde to CO_2, whilst the remaining ~30% was assimilated into cell biomass. The SAR11 clade is widely distributed and highly abundant in the marine environment, with an estimated 2.4×10^{28} cells estimated in the world's oceans (Morris et al. 2002). Based on the acetaldehyde uptake rates exhibited by HTCC1062 and HTCC7211, it was estimated that the global SAR11 community could oxidise more acetaldehyde than is currently estimated to be produced, preventing the majority of acetaldehyde in the marine environment from reaching the atmosphere (Halsey et al. 2017). This finding demonstrates the importance of microorganisms in regulating the global biogeochemical cycle of acetaldehyde and highlights the need to isolate microorganisms from their environment for further investigation. Moreover, the estimated capacity of the SAR11 clade to oxidise acetaldehyde, although only based on the uptake rates of two

strains, suggests that microbial degradation is considerably underestimated as an acetaldehyde sink, not only in terms of its contribution to the global acetaldehyde cycle, but also in the global carbon cycle. Importantly, this does not consider the contributions of other acetaldehyde-degrading microorganisms, which will likely increase the magnitude of the microbial acetaldehyde sink.

The diversity and distribution of acetaldehyde-degrading microorganisms is poorly understood, although previous studies suggest that the ability to utilise acetaldehyde as a carbon and energy source is not restricted to specific groups of microorganisms, and that acetaldehyde degraders can be found in a variety of environments. Liu et al. (2015), for example, isolated *Shewanella mangrovi* from mangrove sediment collected from Zhangzhou, China. This isolate was shown to degrade acetaldehyde at a concentration of 1000 mg L^{-1} (22.7 mM), which is significantly higher than the naturally occurring concentrations reported in the marine environment (Section 1.6). This was also the first and only member of the genus *Shewanella* to be identified as an acetaldehyde degrader. Gao et al. (2018) isolated 12 acetaldehyde-degrading bacteria from 2000 m deep seawater of the West Pacific Ocean. These isolates were identified as members of the *Vibrio*, *Halomonas*, *Pseudoalteromonas*, *Pseudomonas*, and *Bacillus* genera, belonging to the Proteobacteria and Firmicutes phyla. *Halomonas axialensis*, *Halomonas meridiana*, and *Vibrio parahaemolyticus* could tolerate 1500 mg L^{-1} (34.1 mM) of acetaldehyde and could degrade as much as 350 mg L^{-1} (7.9 mM) in 24 hours. The findings of Gao et al. (2018) suggest that a diverse group of bacteria contribute to acetaldehyde degradation in the marine environment and that microbial communities in the deep-sea also utilise acetaldehyde for growth. Acetaldehyde degradation has also been shown to occur under anaerobic conditions, with *Acetobacterium woodii*, an acetogenic bacterium isolated from marine estuary sediments (Balch et al. 1977), exhibiting the ability to grow on 5 mM of acetaldehyde (Trifunović et al. 2020). Alongside the findings of Schmidt et al. (2014), which identified the strictly anaerobic *Pelobacter carbinolicus* and *P. acetylenicus* as acetaldehyde degraders, this suggests that anaerobic microorganisms

represent an important, yet understudied, acetaldehyde sink. Although these findings demonstrate that acetaldehyde is utilised by a variety of microorganisms, our knowledge of the diversity of microbial acetaldehyde degraders is far from complete and many acetaldehyde-degrading microorganisms have yet to be discovered. It is important, therefore, that isolated bacteria are screened for their ability to degrade acetaldehyde to determine the true diversity of acetaldehyde degraders, which may be considerably larger than currently thought.

The aim of this study was to identify and characterise acetaldehyde-degrading bacterial isolates from the Colne Estuary, Essex, that were cultivated from the acetaldehyde enrichment microcosms set up in Chapter 2. This will enhance our knowledge of the diversity of acetaldehyde-degrading microorganisms and may provide an indication of the microorganisms most responsible for acetaldehyde degradation in the Colne Estuary. A second aim of this study was to establish the ubiquity of acetaldehyde degradation amongst previously identified marine bacterial strains to understand the phylogenetic breadth of microbial acetaldehyde degradation. To achieve these aims, bacterial isolates from the Colne Estuary, the in-house culture collection at the University of Essex, and bacterial strains provided by Joseph Christie-Oleza (University of the Balearic Islands), were screened for their ability to degrade acetaldehyde. Using a range of biochemical, physiological, and molecular techniques, the bacterial isolates obtained from the Colne Estuary were characterised, providing a better understanding of the characteristics of bacterial acetaldehyde degraders.

3.2 Methodology

3.2.1 Isolation of microorganisms

Seventeen bacterial isolates were cultivated from the tertiary and quaternary acetaldehyde enrichments of Colne Estuary sediment slurries set up in Chapter 2. These enrichments had been exposed to the higher concentration of acetaldehyde (22.7 mM), which was selected based on the protocol used by Liu et al. (2015) to isolate *S. mangrovi*. To isolate microorganisms from the enriched Colne Estuary sediment slurries, 1 mL of well-mixed enrichment from each serum bottle containing sediment slurry from Hythe, Wivenhoe, and Brightlingsea was spread onto Difco™ marine agar 2216 medium. Difco™ marine agar 2216 medium used throughout this study was composed of 5.0 g of peptone, 1.0 g of yeast extract, 0.1 g of ferric citrate, 19.45 g of NaCl, 8.8 g of $MgCl_2$, 3.24 g of Na_2SO_4, 1.8 g of $CaCl_2$, 0.55 g of KCl, 0.16 g $NaHCO_3$, 0.08 g of KBr, 34.0 mg of $SrCl_2$, 22.0 mg of H_3BO_3, 4.0 mg of Na_2SiO_3, 2.4 mg of NaF, 1.6 mg of NH_4NO_3, 8.0 mg of Na_2HPO_4, and 15.0 g of Difco™ agar in 1 L of Milli-Q water. Inoculated plates were incubated at 20°C and monitored for growth every 24 hours. Colonies with distinct morphology or pigmentation were picked using a sterile inoculating loop and streaked onto fresh Difco™ marine agar 2216 plates to establish pure cultures of each isolate. Cultures were incubated at 20°C and monitored for growth every 24 hours. This procedure was repeated at least three times to ensure that cultures were pure. Growing cultures were maintained throughout this study by inoculating fresh Difco™ marine agar 2216 plates every two weeks, whilst glycerol stocks (15% v/v) were prepared and stored at -80°C. Ten bacterial isolates were cultivated from the tertiary acetaldehyde enrichments, whilst seven bacterial isolates were obtained from the quaternary acetaldehyde enrichments.

Twenty-two previously identified bacterial isolates were also screened for their ability to degrade acetaldehyde (Table 3.1), including 12 isolates provided by Joseph Christie-Oleza

(formerly University of Warwick, now University of the Balearic Islands). Cultures of each
isolate were set up by streaking colonies onto Difco™ marine agar 2216 plates and
incubating at 20°C. The purity of each culture was checked by subculturing onto fresh plates
at least three times. Cultures were maintained throughout this study by subculturing every
two weeks, and glycerol stocks (15% v/v) were set up and stored at -80°C.

Table 3.1 Bacterial isolates screened for their ability to degrade acetaldehyde (2.27 mM).

Bacterial isolate	Phylum/Class	Received from
Aeromicrobium marinum (T2)	Actinobacteria	Joseph Christie-Oleza
Salinispora tropica (CNB-440)	Actinobacteria	(University of the Balearic
Algoriphagus machipongonensis (PR1)	Bacteroidetes	Islands)
Formosa agariphila (KMM3901)	Bacteroidetes	
Gramella forsetii (KT0803)	Bacteroidetes	
Polaribacter sp. (MED152)	Bacteroidetes	
Dinoroseobacter shibae (DFL-12)	Alphaproteobacteria	
Roseobacter denitrificans (OCh114)	Alphaproteobacteria	
Ruegeria pomeroyi (DSS-3)	Alphaproteobacteria	
Alteromonas macleodii (ATCC27126)	Gammaproteobacteria	
Marinobacter adhaerens (HP15)	Gammaproteobacteria	
Verrucomicrobiae strain (DG1235)	Verrucomicrobia	
Shewanella mangrovi (JCM 30121^T)	Gammaproteobacteria	Japanese Collection of Microorganisms (RIKEN)
Pseudoalteromonas strain (43)	Gammaproteobacteria	In-house collection (Essex)
Pseudoalteromonas strain (50)	Gammaproteobacteria	(Chronopoulou et al. 2015)
Pseudoalteromonas strain (104)	Gammaproteobacteria	
Pseudoalteromonas strain (164)	Gammaproteobacteria	
Alcanivorax borkumensis (SK2)	Gammaproteobacteria	In-house collection (Essex)
Cycloclasticus zancles (78-ME)	Gammaproteobacteria	
Marinobacter hydrocarbonoclasticus (SP17)	Gammaproteobacteria	
Oleispira antarctica (RB-8)	Gammaproteobacteria	
Thalassolituus oleivorans (MIL-1)	Gammaproteobacteria	

3.2.2 Acetaldehyde screening

Liquid cultures of each isolate were prepared by inoculating 10 mL of Difco™ marine broth 2216 with a freshly picked bacterial colony from the Difco™ marine agar 2216 plates. Difco™ marine broth 2216 was prepared as outlined in Section 3.2.1, but without agar. Liquid cultures (10 ml) were incubated on an automated shaker (75 rpm) at 20°C and monitored for growth every 24 hours. After observing growth, liquid cultures were centrifuged at 4000 × g for 15 minutes and the supernatant carefully discarded. The pellet was resuspended with 10 mL of ONR7a seawater-nutrient medium (Section 2.2.2) to wash the bacterial cells of residual media, before being centrifuged at 4000 × g for 15 minutes. The supernatant was carefully discarded, and the pellet resuspended with 10 mL of ONR7a seawater-nutrient medium.

To prepare a 227 mM acetaldehyde stock solution, 98.725 mL of Milli-Q water was spiked with 1.275 mL of acetaldehyde (≥99.5% purity; Sigma-Aldrich) in a 125 mL serum bottle. The serum bottle was immediately capped with a polytetrafluoroethene (PTFE) -lined butyl septum (Agilent) to ensure gas-tight conditions and was inverted several times to mix. Following 3 hours of incubation at room temperature to allow the acetaldehyde to equilibrate between the headspace and liquid phase, a 10-fold serial-dilution was performed to prepare a 22.7 mM working stock of acetaldehyde. A total of 10 mL of the 227 mM acetaldehyde stock solution was injected into a pre-sealed serum bottle containing 90 mL of Milli-Q water. The working stock solution was inverted several times to mix.

A 200 µL aliquot of washed, liquid culture was added to a serum bottle (125 ml) containing 8.8 mL of ONR7a seawater-nutrient medium and was capped with a PTFE-lined butyl septum (Agilent). A 1 mL aliquot of acetaldehyde stock solution (22.7 mM) was injected into the serum bottle, resulting in a final acetaldehyde concentration of 2.27 mM. This was performed in duplicate for each bacterial isolate. The same protocol was used to set up

duplicate cultures of each isolate using Difco™ marine broth 2216 as the growth medium, instead of ONR7a seawater-nutrient medium. No-acetaldehyde controls were prepared in duplicate for each isolate by inoculating serum bottles containing 9.8 mL of Difco™ marine broth 2216 with 200 μL of washed, liquid culture and sealing with PTFE-lined butyl septa (Agilent). No-inoculum controls were set up in triplicate by injecting 1 mL of acetaldehyde stock solution into pre-sealed serum bottles containing 9 mL of ONR7a seawater-nutrient medium. No-inoculum controls using Difco™ marine broth 2216 as the growth medium were also set up in triplicate. All serum bottles were incubated in the dark at 20°C.

Headspace concentrations of acetaldehyde within each serum bottle were measured 4 hours after initial set up via gas chromatography, following the protocol outlined in Section 2.2.2. Headspace concentrations of acetaldehyde were measured every 1 - 10 days for the Colne Estuary bacterial isolates and every 1 - 16 days for the 22 previously identified bacterial isolates. Acetaldehyde loss (%) in the no-inoculum controls was subtracted from the final degradation values (%) measured in the inoculated serum bottles to correct for the physical, chemical, or photochemical loss of acetaldehyde, although this was considered to be negligible.

3.2.3 Calibration curve

To provide absolute quantities of acetaldehyde in each serum bottle, a seven-point acetaldehyde calibration curve was set up (Figure 3.1). A 100 mM acetaldehyde working stock solution was prepared by adding 562 μL of acetaldehyde (≥99.5% purity; Sigma-Aldrich) to a serum bottle (125 ml) containing 99.438 mL of Milli-Q water. The serum bottle was immediately capped with a PTFE-lined butyl septum (Agilent), inverted several times to mix, and left for several hours to equilibrate. To prepare serum bottles with an acetaldehyde concentration range of 0, 1, 5, 10, 15, 20, and 25 mM, a total of 0, 0.1, 0.5, 1.0, 1.5, 2.0, and 2.5 mL of the 100 mM acetaldehyde working stock solution was added to 10.0, 9.9, 9.5, 9.0,

8.5, 8.0, and 7.5 mL of Milli-Q water, respectively. Serum bottles were immediately capped with PTFE-lined butyl septa (Agilent) and were vortexed to mix. This was performed in triplicate for each concentration. Headspace concentrations of acetaldehyde within each serum bottle were measured 4 hours after initial set up via gas chromatography, following the protocol outlined in Section 2.2.2. The average peak area was plotted for each acetaldehyde concentration ($R^2 = 0.9993$).
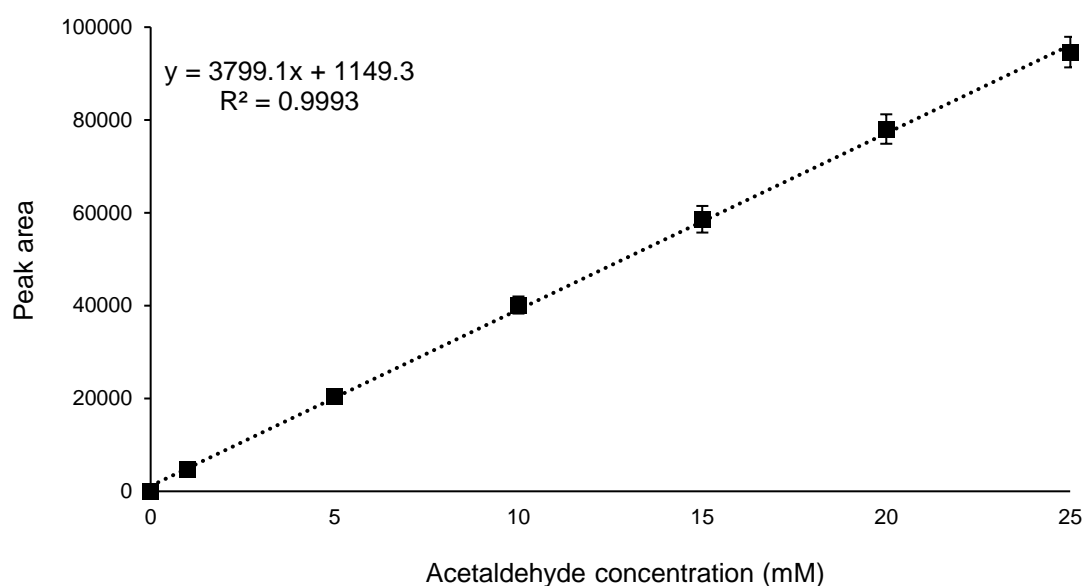
Figure 3.1 Seven-point acetaldehyde calibration curve used to quantify headspace concentrations of acetaldehyde in serum bottles. The mean of three replicates is plotted for each calibration point (± S.E.).

3.2.4 Sanger sequencing

DNA was extracted from the 17 bacterial isolates cultivated from the acetaldehyde-enriched Colne Estuary sediment slurries using a DNeasy Powersoil Kit (Qiagen). Extracted DNA was separated by agarose gel electrophoresis (1.0% w/v), stained with SYBR™ Safe (Invitrogen), and was viewed on a Gel Doc™ EZ gel documentation system (Bio-Rad). Extracted DNA was stored at -20°C until use. Using the bacterial primers 27F (5'- AGAGTTTGATCCTGGCTCAG -3') and 1492R (5'- GGTTACCTTGTTACGACTT -3'),

the 16S rRNA gene was PCR amplified from the DNA of each isolate. PCR was performed in a reaction volume of 50 μL, consisting of 2 μL of each bacterial primer (10 μM), 25 μL of app*Taq* DNA polymerase (Appleton Woods Ltd), 19 μL of PCR-grade water, and 2 μL of DNA extract. A negative control, using 2 μL of PCR-grade water as a template in the PCR reagent mixture, was included in the PCR run, whilst DNA extracted from *Alcanivorax borkumensis* (SK2) was used as a positive control. After an initial denaturation step at 94°C for 5 minutes, PCR amplification was performed with 35 cycles as follows: denaturation at 94°C for 30 seconds, annealing at 57°C for 30 seconds, and extension at 72°C for 90 seconds. A final extension at 72°C was performed for 7 minutes. All PCR amplification products were visualised by agarose gel electrophoresis (1.2% w/v), stained, and viewed as above. PCR products were quantified via Quant-IT™ PicoGreen assay (Thermo Fisher Scientific) using a Nanodrop 3300 Fluorospectrometer (Thermo Fisher Scientific) and were stored at -20°C.

PCR amplification products were subjected to a post-PCR clean-up using a GenElute™ PCR Clean-up Kit (Sigma-Aldrich), to remove excess primers, nucleotides, DNA polymerase, and salts. Cleaned PCR products were visualised as above and sent to Eurofins Genomics for Sanger sequencing. Chromatograms of the forward and reverse sequences of the 16S rRNA gene from each isolate were visualised and analysed using the chromatogram trace viewing program Chromas (version 2.6.6; Technelysium). Nucleotides with non-uniform traces and low quality scores were trimmed from both ends of the forward and reverse sequences to remove unreliable base calls. Base positions with incorrect nucleotide assignments were manually corrected by assessing the quality score and trace of each base call. To produce a consensus sequence, the corrected forward and reverse sequences of each isolate were exported to the sequence alignment editor, BioEdit (version 7.0.5.3). The reverse sequence was reverse complemented, and a pairwise alignment was performed between the forward and reverse sequences to concatenate the two reads.

IUPAC (International Union of Pure and Applied Chemistry) nucleotide codes in the resulting consensus sequence, indicating differences in the nucleotide base call between the forward and reverse sequences, were manually corrected by assessing the traces and quality scores within each chromatogram. To provide initial identification of each isolate, the sequences were subjected to a BLAST (Basic Local Alignment Search Tool) (Altschul et al. 1990) homology search using the BLASTn NCBI sequence database as reference.

To infer the phylogeny of the 17 bacterial isolates cultivated from the acetaldehyde-enriched Colne Estuary sediment slurries, phylogenetic trees based on the 16S rRNA gene were produced. Based on the top hits from the BLAST homology search, 16S rRNA gene sequences of closely related type strains and non-type strains within the NCBI sequence database were collated in FASTA format. A total of 55 16S rRNA gene sequences belonging to the Actinobacteria, including 6 isolates cultivated from the Colne Estuary, were collated as one FASTA file. An additional 68 16S rRNA gene sequences belonging to the Firmicutes, including 11 Colne Estuary isolates, were collated as a second FASTA file. Each FASTA file was imported into MEGA (Molecular Evolutionary Genetics Analysis; version 10.0.5) (Kumar et al. 2018) and the sequences aligned by MUSCLE (Edgar 2004). The aligned sequences were trimmed, resulting in maximum sequence lengths of 1446 bp and 1483 bp for the Actinobacteria and Firmicutes sequences, respectively. Phylogenetic trees were constructed using the neighbour-joining method (Saitou & Nei 1987), with evolutionary distances calculated using Kimura's two-parameter model (Kimura 1980). Bootstrap analysis (Felsenstein 1985) was performed for 1000 replications.

3.2.5 Characterisation of isolates

Four isolates demonstrating the ability to degrade acetaldehyde as a sole carbon source within 5 days of incubation, namely isolates A4, A5, A14, and A17, were selected for characterisation using morphological, biochemical, and physiological techniques. To

establish morphological characteristics, a colony of each isolate was spread onto a fresh Difco™ marine agar 2216 plate and was incubated at 20°C for 48 hours. After observing growth, bacterial colonies were visually inspected to determine colony morphology and pigmentation. Liquid cultures (10 ml) of each isolate were prepared as described in Section 3.2.2, although cultures were not washed with ONR7a seawater-nutrient medium. The hanging-drop method was used to determine the motility of each isolate. Briefly, 10 μL of liquid culture was transferred to a coverslip which had been prepared by placing petroleum jelly on each corner. With the depression facing downwards, a glass slide was placed over the drop of liquid culture, ensuring a seal was formed with the petroleum jelly. The glass slide was inverted to suspend the liquid culture from the coverslip. The prepared slide was visualised on a Primo Star LED microscope (Zeiss) at 40 × magnification, with the centre of the field focussed on the edge of the drop of liquid culture. True motility was differentiated from Brownian motion and the morphology of cells was also recorded. A Gram stain was performed for each isolate following the protocol outlined by Beveridge (2001), and oxidase tests were performed using oxidase strips (Millipore), according to the manufacturer's instructions. A catalase test was performed by mixing 10 μL of liquid culture with 10 μL of hydrogen peroxide (3% v/v) on a glass microscope slide. The production of bubbles within 5 to 10 seconds, resulting from the rapid evolution of oxygen, indicated a positive result. The ability of each isolate to utilise 195 different carbon sources was investigated using Phenotype Microarray™ 1 (PM1) and 2A (PM2A) microplates (Biolog Inc.) (Bochner et al. 2001) following the manufacturer's protocol. The formation of a strong purple colouration within a microplate well, resulting from the reduction of a tetrazolium dye via NADH production, indicated carbon-source utilisation. Colour formation within each well was quantified immediately after inoculation by measuring PM1 and PM2A microplates at 590 nm using a FLUOstar Omega microplate reader (BMG Labtech Ltd). Microplates were incubated in the dark at 30°C and were measured after 6, 12, 24, 48, and 72 hours of incubation. The optimum temperature for growth was determined for each isolate by incubating liquid

cultures at 4°C, 12°C, 20°C, 30°C, 37°C, and 45°C. Briefly, 50 mL Falcon tubes (Corning

Inc.) containing 15 mL of Difco™ marine broth 2216 medium were inoculated with 500 μL of

fresh liquid culture and were sealed with Parafilm™ (Bemis Company, Inc.). This was

performed in triplicate for each isolate at each temperature. No-inoculum controls, containing

15 mL of Difco™ marine broth 2216 medium only, were also prepared in triplicate for each

temperature. The optical density of each liquid culture was measured at a wavelength of 600

nm using a Jenway 7300 spectrophotometer immediately after inoculation. Optical densities

(OD_{600}) of the no-inoculum controls were used to blank-correct the Jenway 7300

spectrophotometer before measuring liquid cultures from each temperature regime. Liquid

cultures were incubated at the relevant temperature and the OD_{600} measured after 0.5, 1, 2,

4, 6, 8, 10, 12, and 14 days of incubation.

3.3 Results

3.3.1 Identification of Colne Estuary isolates

The 17 bacterial isolates cultivated from the acetaldehyde-enriched Colne Estuary sediment

slurries belonged to two phyla, namely the Firmicutes (Figure 3.2) and the Actinobacteria

(Figure 3.3). A total of 11 isolates were identified as members of the Firmicutes and

belonged to four genera within the *Bacillaceae* family (Figure 3.2). Isolates A2, A3, A4, and

A5 were most closely related to *Halobacillus* sp. FIB248 (EU308337), whilst the closest

relative of isolate A12 was *H. locisalis* (AY190534) (Table 3.2). Isolates A8 and A15 shared

the same clade as *Bacillus oceanisediminis* (GQ292772), whilst isolate A17 was most

closely related to *B. mycoides* (AB021192) (Table 3.2). *Lysinibacillus boronitolerans*

(AB199591) and *L. macroides* (AJ628749) were identified as the closest relatives to isolates

A1 and A11, respectively (Table 3.2). Isolate A16 was identified as a close relative of

Psychrobacillus psychrodurans (AJ277984) and *P. psychrotolerans* (AJ277983) (Table 3.2).

Six of the isolates cultivated from the Colne Estuary sediment slurries were identified as

members of the Actinobacteria and belonged to the *Microbacteriaceae* and *Nocardiaceae* (Figure 3.3). Isolates A6, A7, A9, A10, and A13 shared a distinct clade within the genus *Microbacterium* and were most closely related to *M. maritypicum* (AJ853910), *M. oxydans* (Y17227), and *M. liquefaciens* (X77444) (Table 3.2). Isolate A14 was identified as a close relative of *Rhodococcus wratislaviensis* (Z37138) (99.71% 16S rRNA sequence similarity; Table 3.2) and was monophyletic with *R. opacus* (X80630) (Figure 3.3).

Table 3.2 Closest relatives of the bacterial strains isolated from the acetaldehyde-enriched Colne Estuary sediment slurries based on 16S rRNA gene sequence similarity (%).

Isolate	Closest relative (16S rRNA gene sequence similarity)	Identity (%)
A1	*Lysinibacillus boronitolerans* strain Mix24	98.18%
A2	*Halobacillus* sp. FIB248	98.41%
A3	*Halobacillus* sp. FIB248	97.58%
A4	*Halobacillus* sp. FIB248	97.30%
A5	*Halobacillus* sp. FIB248	96.74%
A6	*Microbacterium oxydans* strain S41	98.71%
A7	*Microbacterium oxydans* strain S41	98.79%
A8	*Bacillus oceanisediminis* strain C26	99.58%
A9	*Microbacterium maritypicum* strain IMB16-019	99.86%
A10	*Microbacterium maritypicum* strain IMB16-039	99.86%
A11	*Lysinibacillus macroides* strain LNHL43	99.86%
A12	*Halobacillus locisalis* strain K-W48	99.93%
A13	*Microbacterium maritypicum* strain IMB16-039	99.86%
A14	*Rhodococcus wratislaviensis* strain I	99.71%
A15	*Bacillus oceanisediminis* strain C22	99.93%
A16	*Psychrobacillus psychrodurans* strain M414	99.93%
A17	*Bacillus mycoides* strain 18A-B9	99.85%

Figure 3.2 Phylogenetic tree showing the relationship between isolates cultivated from the Colne Estuary and representative type strains within the phylum Firmicutes, based on 16S rRNA gene sequences. The evolutionary history of isolates was inferred using the Neighbour-Joining method (Saitou & Nei 1987). The percentage of replicate trees in which the associated taxa clustered together in the bootstrap test (1000 replicates) are shown next to the branches when ≥50%. Evolutionary distances were computed using Kimura's two-parameter model (Kimura 1980) and are in the units of the number of base substitutions per site (horizontal scale bar represents 2% nucleotide differences per site). Accession numbers of the type strains are shown in round brackets. Associated family classifications are shown to the right of the tree.
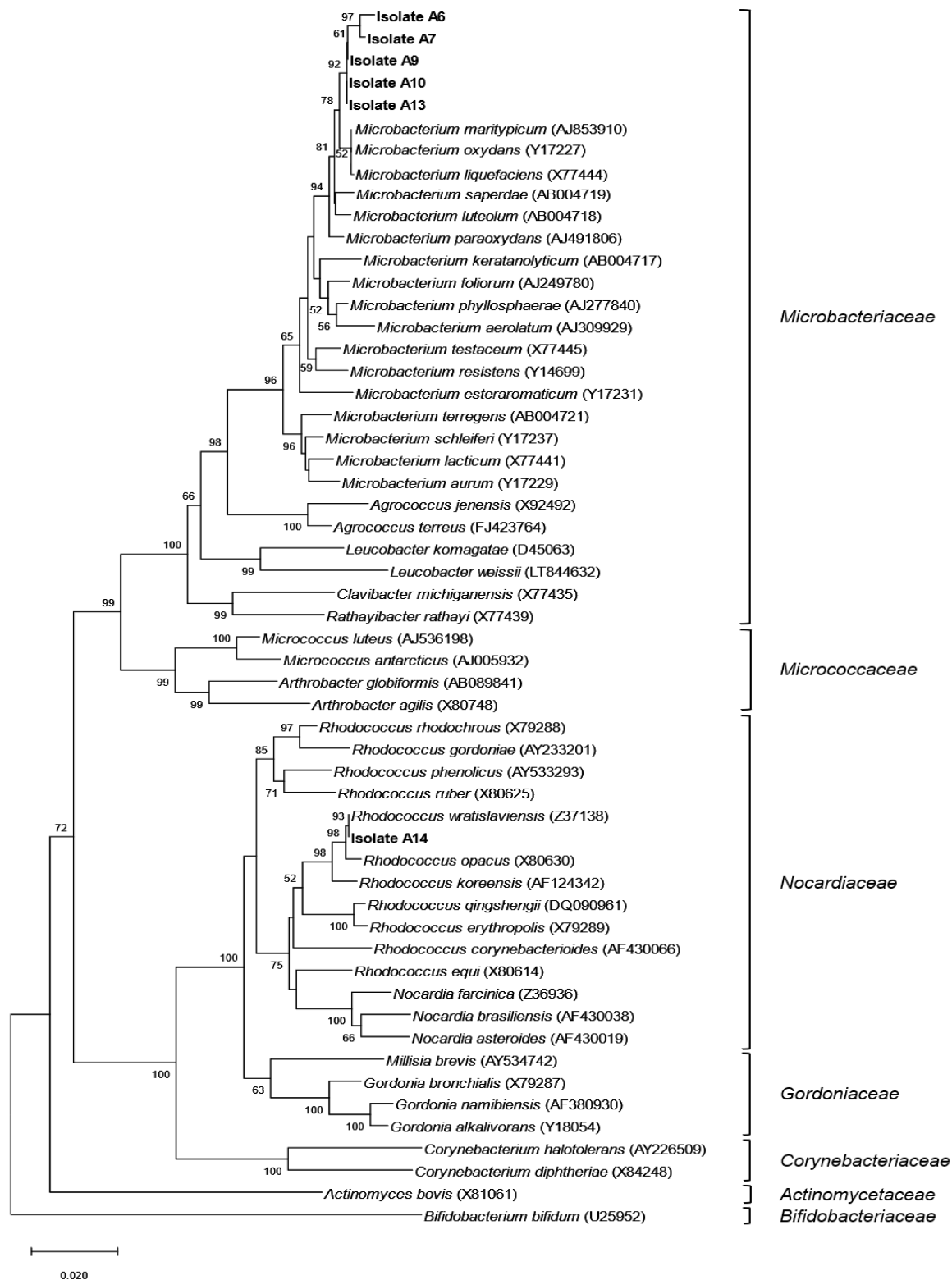
Figure 3.3 Phylogenetic tree showing the relationship between isolates cultivated from the Colne Estuary and representative type strains within the phylum Actinobacteria, based on 16S rRNA gene sequences. The evolutionary history of isolates was inferred using the Neighbour-Joining method (Saitou & Nei 1987). The percentage of replicate trees in which the associated taxa clustered together in the bootstrap test (1000 replicates) are shown next to the branches when ≥50%. Evolutionary distances were computed using Kimura's two-parameter model (Kimura 1980) and are in the units of the number of base substitutions per site (horizontal scale bar represents 2% nucleotide differences per site). Accession numbers of the type strains are shown in round brackets. Associated family classifications are shown to the right of the tree.

3.3.2 Acetaldehyde-biodegradation

Isolates cultivated from the tertiary acetaldehyde enrichment of Colne Estuary sediment slurries (A1 - A10) demonstrated the ability to utilise acetaldehyde as a sole carbon source (Figure 3.4a). After 1 day of incubation, isolates A4 and A5 utilised 51.8% and 59.4% of acetaldehyde, respectively. Both isolates completely degraded the remaining acetaldehyde within 4 days. Isolates A6, A7, A8, A9, and A10 degraded 43.7 - 47.9% of added acetaldehyde after 26 days of incubation (Table 3.3), whilst isolates A1, A2, and A3 degraded 12.1%, 26.1%, and 9.8% of added acetaldehyde, respectively. Acetaldehyde degradation was exhibited by all isolates growing on the nutrient-rich Difco™ marine broth 2216 medium (Figure 3.4b). After 1 day of incubation, isolates A4 and A5 utilised 42.6% and 44.4% of acetaldehyde, respectively, and degraded the remaining acetaldehyde within 4 days. Complete acetaldehyde degradation was also measured in serum bottles containing cultures of isolates A6, A7, A9, and A10 after 4 days of incubation, whilst isolates A1, A3, and A8 exhibited complete acetaldehyde degradation after 7 - 11 days. Isolate A2 utilised 35.3% of added acetaldehyde following 26 days of incubation (Table 3.3).

Seven isolates cultivated from the quaternary acetaldehyde enrichment of Colne Estuary sediment slurries (A11 - A17) utilised acetaldehyde as a sole carbon source (Figure 3.5a). Following 1 day of incubation, isolate A14 utilised 26.1% of acetaldehyde and degraded the remaining acetaldehyde within 5 days. Complete acetaldehyde degradation was measured in serum bottles containing cultures of isolates A12, A13, A16, and A17 after 19 days of incubation, whilst isolates A11 and A15 degraded 3.7% and 47.4% of added acetaldehyde, respectively (Table 3.3). All isolates demonstrated the ability to completely degrade acetaldehyde during growth on Difco™ marine broth 2216 medium (Figure 3.5b). After 1 day of incubation, isolate A17 utilised 89.7% of acetaldehyde and degraded the remaining acetaldehyde within 5 days. Isolates A13 and A14 also completely degraded acetaldehyde within 5 days of incubation. Complete acetaldehyde degradation was measured in serum

bottles containing cultures of isolates A11, A12, and A15 after 9 days of incubation, whilst

isolate A16 utilised the added acetaldehyde after 19 days.
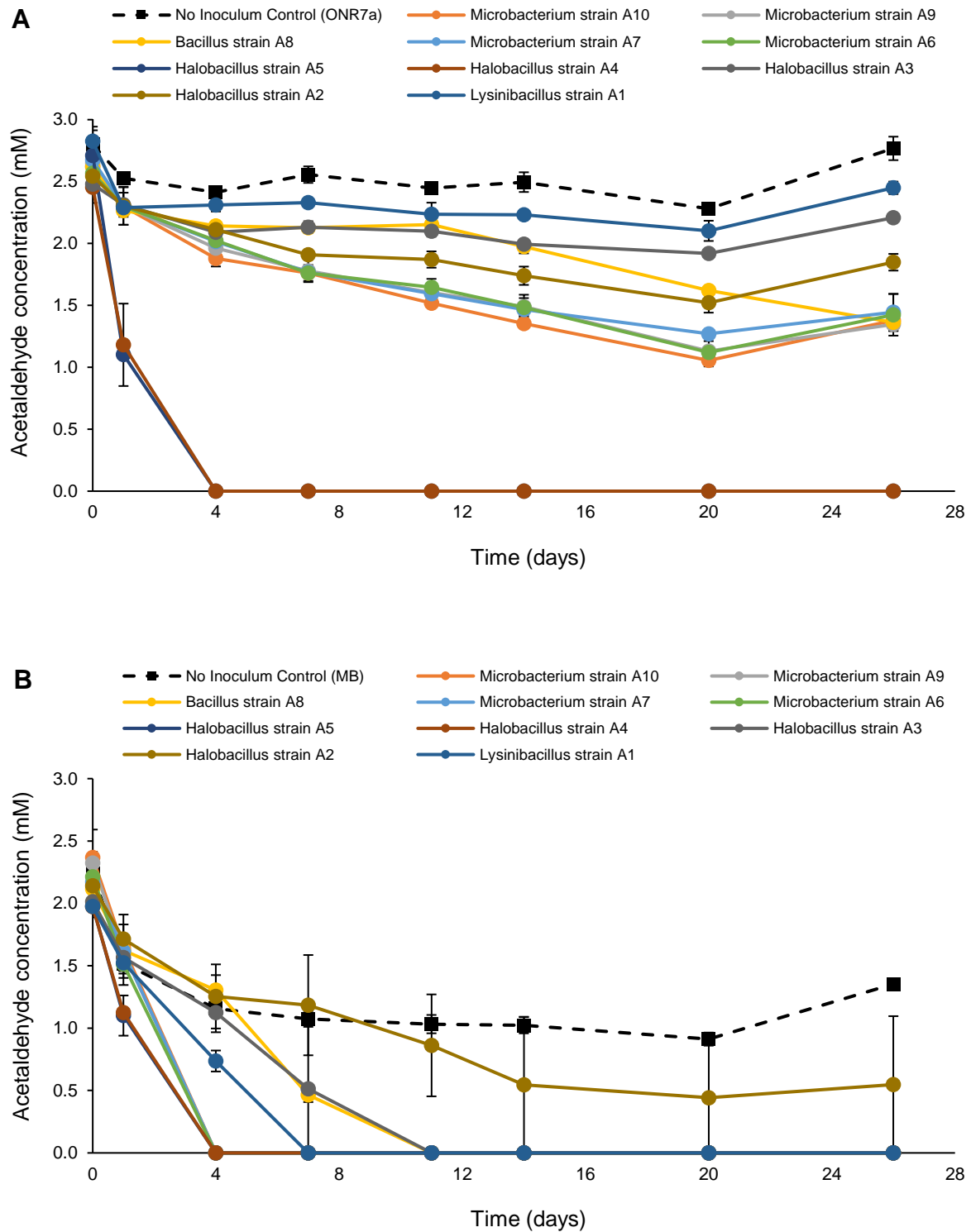
Figure 3.4 Acetaldehyde degradation measured in serum bottles containing (A) ONR7a seawater-nutrient medium and (B) Difco™ marine broth 2216 medium inoculated with isolates cultivated from the tertiary acetaldehyde enrichments of Colne Estuary sediment slurry. Serum bottles were enriched with 2.27 mM of acetaldehyde. The mean of two replicates is plotted for each isolate (± S.E.), while the mean of three replicates is plotted for the no-inoculum controls (± S.E.).
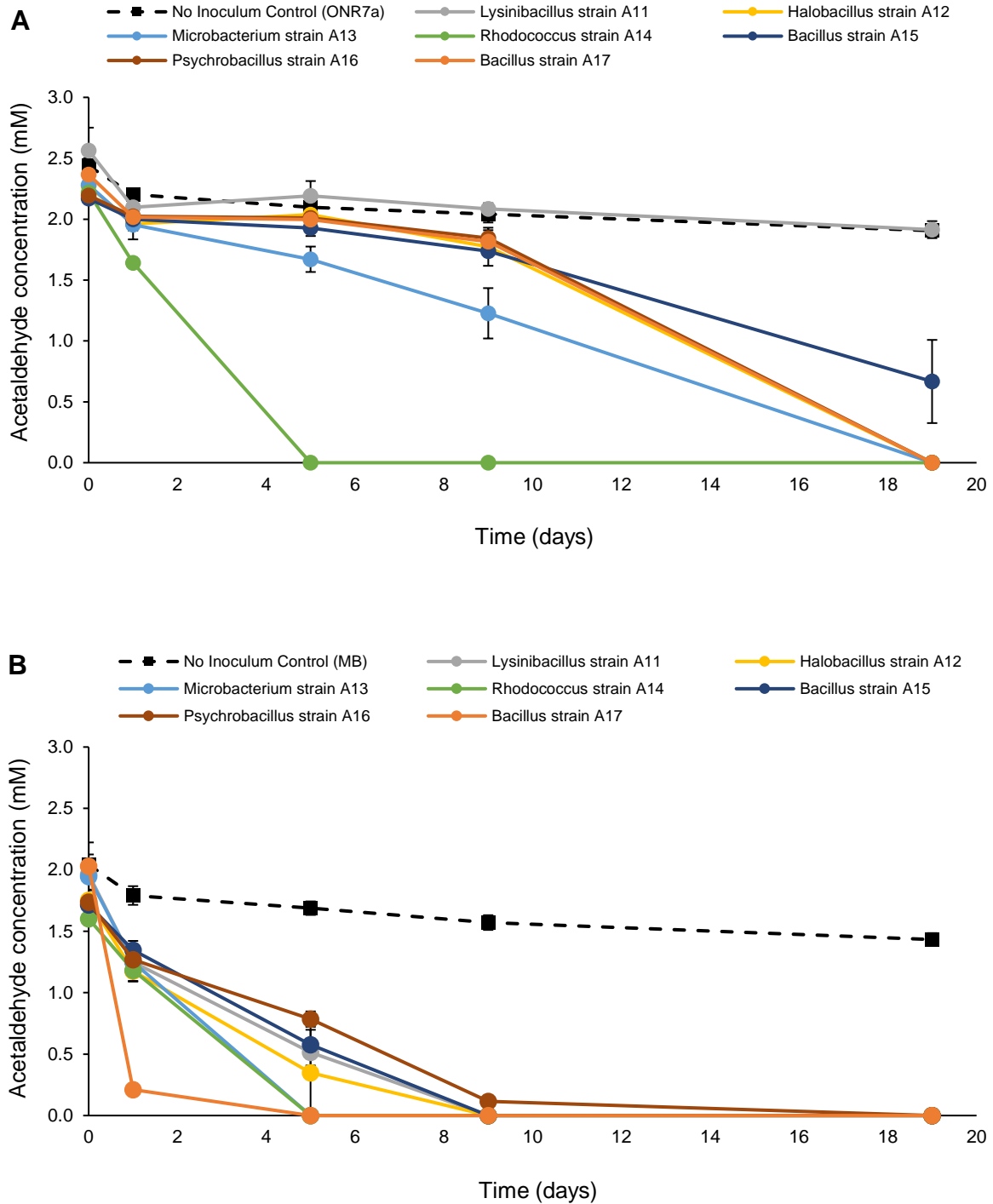
Figure 3.5 Acetaldehyde degradation measured in serum bottles containing (A) ONR7a seawater-nutrient medium and (B) Difco™ marine broth 2216 medium inoculated with isolates cultivated from the quaternary acetaldehyde enrichments of Colne Estuary sediment slurry. Serum bottles were enriched with 2.27 mM of acetaldehyde. The mean of two replicates is plotted for each isolate (± S.E.), while the mean of three replicates is plotted for the no-inoculum controls (± S.E.).

Isolates representing a wide range of marine taxa received from Joseph Christie-Oleza (University of the Balearic Islands) utilised acetaldehyde as a sole carbon source during growth on ONR7a seawater-nutrient medium (Table 3.3). *Aeromicrobium marinum* (T2), *Salinispora tropica* (CNB-440), *Algoriphagus machipongonensis* (PR1), *Formosa agariphila* (KMM3901), *Gramella forsetii* (KT0803), *Dinoroseobacter shibae* (DFL-12), *Roseobacter denitrificans* (OCh114), *Alteromonas macleodii* (ATCC27126), *Marinobacter adhaerens* (HP15), and Verrucomicrobiae strain (DG1235) completely degraded the added acetaldehyde within 7 - 10 days. After 10 days of incubation, *Polaribacter* sp. (MED152) utilised 33.7% of the added acetaldehyde, whilst 31.3% of added acetaldehyde was used by cultures of *Ruegeria pomeroyi* (DSS-3). With the exception of *A. machipongonensis* (PR1), which utilised 32.5% of the added acetaldehyde, all isolates demonstrated the ability to completely degrade acetaldehyde within 10 days of incubation during growth on Difco™ marine broth 2216 medium (Table 3.3).

Shewanella mangrovi (JCM 30121^T), a previously identified acetaldehyde degrader, utilised all of the available acetaldehyde after 1 day of incubation during growth on ONR7a seawater-nutrient medium and Difco™ marine broth 2216 medium (Table 3.3). Acetaldehyde was also used as a sole carbon source by four strains of *Pseudoalteromonas*, namely strains 43, 50, 104, and 164 (Table 3.3). Complete acetaldehyde degradation was exhibited by all 4 strains after 12 days of growth on ONR7a seawater-nutrient medium. During growth on Difco™ marine broth 2216 medium, *Pseudoalteromonas* strains 43, 104, and 164 also utilised all of the added acetaldehyde, whilst 65.4% of acetaldehyde was used by strain 50. Five hydrocarbon-degrading isolates, namely *Alcanivorax borkumensis* (SK2), *Cycloclasticus zancles* (78-ME), *Marinobacter hydrocarbonoclasticus* (SP17), *Oleispira antarctica* (RB-8), and *Thalassolituus oleivorans* (MIL-1), demonstrated a limited ability to utilise acetaldehyde as a carbon source (Table 3.3). During growth on ONR7a seawater-nutrient medium, *A. borkumensis* (SK2) utilised 20.7% of added acetaldehyde. Acetaldehyde loss was detected in serum bottles containing cultures of *T. oleivorans* (MIL-1), however, this

was considered a result of fluctuations in GC-FID measurements and not acetaldehyde biodegradation. Acetaldehyde degradation was not detected in serum bottles containing cultures of *C. zancles* (78-ME), *M. hydrocarbonoclasticus* (SP17), and *O. antarctica* (RB-8).

Table 3.3 Acetaldehyde degradation (%) exhibited by isolates cultivated from the Colne Estuary (A1 - A17) and isolates acquired from Joseph Christie-Oleza (University of the Balearic Islands), the Japanese Collection of Microorganisms (RIKEN), and the University of Essex in-house culture collection. * Degradation (%) in inoculated serum bottles was corrected for acetaldehyde loss (%) in the no-inoculum controls.

Isolate	Phylum/Class	ONR7a seawater-nutrient medium				Difco™ marine broth 2216 medium			
		Starting conc. (mM)	Final conc. (mM)	Degradation (%) *	Maximum days to complete degradation	Starting conc. (mM)	Final conc. (mM)	Degradation (%) *	Maximum days to complete degradation
Colne Estuary									
Halobacillus strain A4	Firmicutes	2.45	0	100	4	1.97	0	100	4
Halobacillus strain A5	Firmicutes	2.71	0	100	4	1.98	0	100	4
Halobacillus strain A12	Firmicutes	2.27	0	100	19	1.75	0	100	9
Psychrobacillus strain A16	Firmicutes	2.19	0	100	19	1.74	0	100	19
Bacillus strain A17	Firmicutes	2.37	0	100	19	2.03	0	100	5
Bacillus strain A15	Firmicutes	2.17	0.67	47.4	-	1.71	0	100	9
Bacillus strain A8	Firmicutes	2.62	1.36	47.0	-	2.11	0	100	11
Halobacillus strain A2	Firmicutes	2.54	1.85	26.1	-	2.14	0.55	35.3	-
Lysinibacillus strain A1	Firmicutes	2.82	2.45	12.1	-	1.97	0	100	7
Halobacillus strain A3	Firmicutes	2.48	2.21	9.8	-	2.01	0	100	11
Lysinibacillus strain A11	Firmicutes	2.56	1.91	3.7	-	1.96	0	100	9
Rhodococcus strain A14	Actinobacteria	2.22	0	100	5	1.60	0	100	5
Microbacterium strain A13	Actinobacteria	2.28	0	100	19	1.95	0	100	5
Microbacterium strain A9	Actinobacteria	2.65	1.35	48.0	-	2.32	0	100	4
Microbacterium strain A10	Actinobacteria	2.62	1.38	46.3	-	2.37	0	100	4
Microbacterium strain A7	Actinobacteria	2.67	1.44	45.0	-	2.17	0	100	4
Microbacterium strain A6	Actinobacteria	2.57	1.42	43.7	-	2.21	0	100	4
Marine strains (Christie-Oleza)									
Aeromicrobium marinum (T2)	Actinobacteria	2.56	0	100	10	2.26	0	100	7
Salinispora tropica (CNB-440)	Actinobacteria	2.68	0	100	10	2.30	0	100	7
Algoriphagus machipongonensis (PR1)	Bacteroidetes	2.48	0	100	7	2.26	0.92	32.5	-
Formosa agariphila (KMM3901)	Bacteroidetes	2.83	0	100	10	2.23	0	100	10
Gramella forsetii (KT0803)	Bacteroidetes	2.64	0	100	10	2.19	0	100	7
Polaribacter sp. (MED152)	Bacteroidetes	2.70	1.09	33.7	-	2.23	0	100	7
Roseobacter denitrificans (OCh114)	α-Proteobacteria	2.58	0	100	7	2.16	0	100	7
Dinoroseobacter shibae (DFL-12)	α-Proteobacteria	2.55	0	100	10	2.33	0	100	7
Ruegeria pomeroyi (DSS-3)	α-Proteobacteria	2.81	1.20	31.3	-	2.24	0	100	7
Alteromonas macleodii (ATCC27126)	γ-Proteobacteria	2.24	0	100	7	2.18	0	100	7
Marinobacter adhaerens (HP15)	γ-Proteobacteria	2.24	0	100	7	2.13	0	100	7
Verrucomicrobiae strain (DG1235)	Verrucomicrobia	2.28	0	100	7	2.01	0	100	7
Japanese Collection of Microorganisms									
Shewanella mangrovi (JCM 30121[T])	γ-Proteobacteria	2.19	0	100	1	1.96	0	100	1
University of Essex collection									
Pseudoalteromonas strain (43)	γ-Proteobacteria	2.11	0	100	12	1.79	0	100	12
Pseudoalteromonas strain (50)	γ-Proteobacteria	2.35	0	100	12	2.02	0.10	65.4	-
Pseudoalteromonas strain (104)	γ-Proteobacteria	2.01	0	100	12	1.83	0	100	12
Pseudoalteromonas strain (164)	γ-Proteobacteria	2.10	0	100	12	1.93	0	100	12
Alcanivorax borkumensis (SK2)	γ-Proteobacteria	2.16	1.19	20.7	-	-	-	-	-
Thalassolituus oleivorans (MIL-1)	γ-Proteobacteria	2.26	1.68	1.5	-	-	-	-	-
Cycloclasticus zancles (78-ME)	γ-Proteobacteria	1.91	1.62	0	-	-	-	-	-
Marinobacter hydrocarbonoclasticus (SP17)	γ-Proteobacteria	1.97	1.69	0	-	-	-	-	-
Oleispira antarctica (RB-8)	γ-Proteobacteria	2.17	1.84	0	-	-	-	-	-

3.3.3 Characterisation of acetaldehyde-degrading isolates

The morphological, biochemical, and physiological characteristics of *Halobacillus* strains A4 and A5, *Rhodococcus* strain A14, and *Bacillus* strain A17 were investigated due to their ability to rapidly degrade acetaldehyde. All isolates were Gram-positive, positive for catalase activity, and negative for oxidase activity (Table 3.4). All four isolates proved to be mesophilic, growing at 12°C, 20°C, 30°C, and 37°C, and also grew at 4°C (Figure 3.6). No growth was observed at 45°C (Figure 3.6). *Halobacillus* strains A4 and A5 grew optimally at 20°C and 30°C. Optimum growth was observed at 30°C and 37°C for *Rhodococcus* strain A14 and at 30°C for *Bacillus* strain A17 (Table 3.4). Colonies of *Halobacillus* strains A4 and A5 were circular and white-cream in colour (Table 3.4). Cells of both isolates were non-motile and cocci (Figure S3.1). *Rhodococcus* strain A14 grew on Difco™ marine agar 2216 as circular, cream, opaque colonies (Table 3.4). Cells were non-motile rods (Figure S3.1). Colonies of *Bacillus* strain A17 were white, opaque, and rhizoid (Table 3.4). Cells were non-motile, rod-shaped, and formed chains (Figure S3.1). *Rhodococcus* strain A14 utilised 187 different carbon sources from the PM1 (Table 3.5a & 3.5b) and PM2A microplates (Table 3.6a & 3.6b), with 164 of these carbon sources utilised within 24 hours. After 6 hours of incubation, *Rhodococcus* strain A14 utilised D-ribose, L-lyxose, and dihydroxy acetone as carbon sources, while L-arabinose, D-xylose, D-fructose, α-D-glucose, D-psicose, and 2-deoxy-D-ribose were used after 12 hours. *Bacillus* strain A17 utilised 189 different carbon sources from the PM1 (Table 3.5a & 3.5b) and PM2A microplates (Table 3.6a & 3.6b), with 173 of these carbon sources used within 12 hours of incubation. Comparatively, *Halobacillus* strains A4 and A5 exhibited a more restricted metabolism, utilising 26 and 25 different carbon sources after 72 hours of incubation, respectively. Within 6 hours of incubation, both isolates utilised D-ribose, L-lyxose, and dihydroxy acetone.

Table 3.4 Phenotypic characteristics of acetaldehyde-degrading isolates *Halobacillus* strain A4, *Halobacillus* strain A5, *Rhodococcus* strain A14, and *Bacillus* strain A17 cultivated from sediment slurries collected from the Colne Estuary, Essex. * Optimal growth was measured at this temperature.

Characteristic	*Halobacillus* strain A4	*Halobacillus* strain A5	*Rhodococcus* strain A14	*Bacillus* strain A17
Colony morphology	Circular	Circular	Circular	Rhizoid
Colony colour	White/cream	White/cream	Cream, opaque	White, opaque
Cell morphology	Cocci	Cocci	Rod-shaped	Rod-shaped (chains)
Motility	Non-motile	Non-motile	Non-motile	Non-motile
Gram reaction	+	+	+	+
Oxidase	-	-	-	-
Catalase	+	+	+	+
Growth at:				
4°C	+	+	+	+
12°C	+	+	+	+
20°C	+*	+*	+	+
30°C	+*	+*	+*	+*
37°C	+	+	+*	+
45°C	-	-	-	-

Figure 3.6 Growth curves of isolates *Halobacillus* strain A4, *Halobacillus* strain A5, *Rhodococcus* strain A14, and *Bacillus* strain A17 incubated at 4°C, 12°C, 20°C, 30°C, 37°C, and 45°C. The mean of three replicates is plotted for each isolate at each temperature (± S.E.).

Table 3.5a Utilisation of PM1™ Microplate (Biolog Inc.) carbon sources by isolates *Halobacillus* strain A4, *Halobacillus* strain A5, *Rhodococcus* strain A14, and *Bacillus* strain A17 cultivated from the Colne Estuary, Essex. Numbers denote hours taken for a specific carbon source to be utilised by each isolate. Dark purple denotes rapid carbon source utilisation, whilst light purple denotes slower utilisation of a specific carbon source. Blank spaces represent carbon sources not used by isolates during the 72 hour incubation period.

PM1™ Microplate

Carbon Source	*Halobacillus* strain A4	*Halobacillus* strain A5	*Rhodococcus* strain A14	*Bacillus* strain A17
L-Arabinose	24	12	12	12
N-Acetyl-D-Glucosamine			24	12
D-Saccharic Acid			24	12
Succinic Acid			24	12
D-Galactose	24	24	24	6
L-Aspartic Acid			24	12
L-Proline			24	12
D-Alanine			24	24
D-Trehalose			24	12
D-Mannose	24	24	24	12
Dulcitol			24	12
D-Serine			24	24
D-Sorbitol	48	48	24	12
Glycerol	48	48	24	12
L-Fucose			24	12
D-Glucuronic Acid			24	12
D-Gluconic Acid	72		24	12
D,L-α-Glycerol-Phosphate			24	12
D-Xylose	12	12	12	12
L-Lactic Acid			24	12
Formic Acid			24	12
D-Mannitol	48	48	24	12
L-Glutamic Acid	48		24	12
D-Glucose-6-Phosphate			24	12
D-Galactonic Acid-γ-Lactone			48	24
D-L-Malic Acid			24	12
D-Ribose	6	6	6	6
Tween 20			24	12
L-Rhamnose			24	6
D-Fructose	48	48	12	12
Acetic Acid			24	12
α-D-Glucose	24	24	12	6
Maltose			24	6
D-Melibiose			24	12
Thymidine			24	12
L-Asparagine			24	12
D-Aspartic Acid			48	48
D-Glucosaminic Acid			24	12
1,2-Propanediol			24	12
Tween 40			24	12
α-Keto-Glutaric Acid			24	12
α-Keto-Butyric Acid			24	12
α-Methyl-D-Galactoside			24	12
α-D-Lactose		48	24	12
Lactulose			24	12
Sucrose			24	12
Uridine			24	12
L-Glutamine			24	12

Table 3.5b Utilisation of PM1™ Microplate (Biolog Inc.) carbon sources by isolates *Halobacillus* strain A4, *Halobacillus* strain A5, *Rhodococcus* strain A14, and *Bacillus* strain A17 cultivated from the Colne Estuary, Essex. Numbers denote hours taken for a specific carbon source to be utilised by each isolate. Dark purple denotes rapid carbon source utilisation, whilst light purple denotes slower utilisation of a specific carbon source. Blank spaces represent carbon sources not used by isolates during the 72 hour incubation period.

PM1™ Microplate (continued)

Carbon Source	*Halobacillus* strain A4	*Halobacillus* strain A5	*Rhodococcus* strain A14	*Bacillus* strain A17
M-Tartaric Acid			24	12
D-Glucose-1-Phosphate			24	12
D-Fructose-6-Phosphate			24	12
Tween 80			24	12
α-Hydroxy Glutaric Acid-γ-Lactone			24	12
α-Hydroxy Butyric Acid			24	12
β-Methyl-D-Glucoside			24	12
Adonitol			24	12
Maltotriose			24	12
2-Deoxy Adenosine			72	12
Adenosine			24	12
Glycyl-L-Aspartic Acid			24	12
Citric Acid			24	12
M-Inositol			24	12
D-Threonine			24	24
Fumaric Acid			24	12
Bromo Succinic Acid			24	12
Propionic Acid			24	12
Mucic Acid			24	12
Glycolic Acid			24	12
Glyoxylic Acid			24	24
D-Cellubiose			24	12
Inosine			24	12
Glycyl-L-Glutamic Acid			24	12
Tricarballylic Acid			48	12
L-Serine			48	48
L-Threonine			24	12
L-Alanine			24	12
L-Alanyl-Glycine	72		24	12
Acetoacetic Acid			24	12
N-Acetyl-β-D-Mannosamine			24	12
Mono Methyl Succinate			24	12
Methyl Pyruvate			24	12
D-Malic Acid			24	12
L-Malic Acid			24	12
Glycyl-L-Proline			24	12
p-Hydroxy Phenyl Acetic Acid			24	12
m-Hydroxy Phenyl Acetic Acid			24	12
Tyramine			24	12
D-Psicose			12	12
L-Lyxose	6	6	6	6
Glucuronamide			24	6
Pyruvic Acid			24	12
L-Galactonic Acid-γ-Lactone			24	12
D-Galacturonic Acid			24	12
Phenylethylamine			48	12
2-Aminoethanol			24	12

Table 3.6a Utilisation of PM2A™ Microplate (Biolog Inc.) carbon sources by isolates *Halobacillus* strain A4, *Halobacillus* strain A5, *Rhodococcus* strain A14, and *Bacillus* strain A17 cultivated from the Colne Estuary, Essex. Numbers denote hours taken for a specific carbon source to be utilised by each isolate. Dark purple denotes rapid carbon source utilisation, whilst light purple denotes slower utilisation of a specific carbon source. Blank spaces represent carbon sources not used by isolates during the 72 hour incubation period.

PM2A™ Microplate

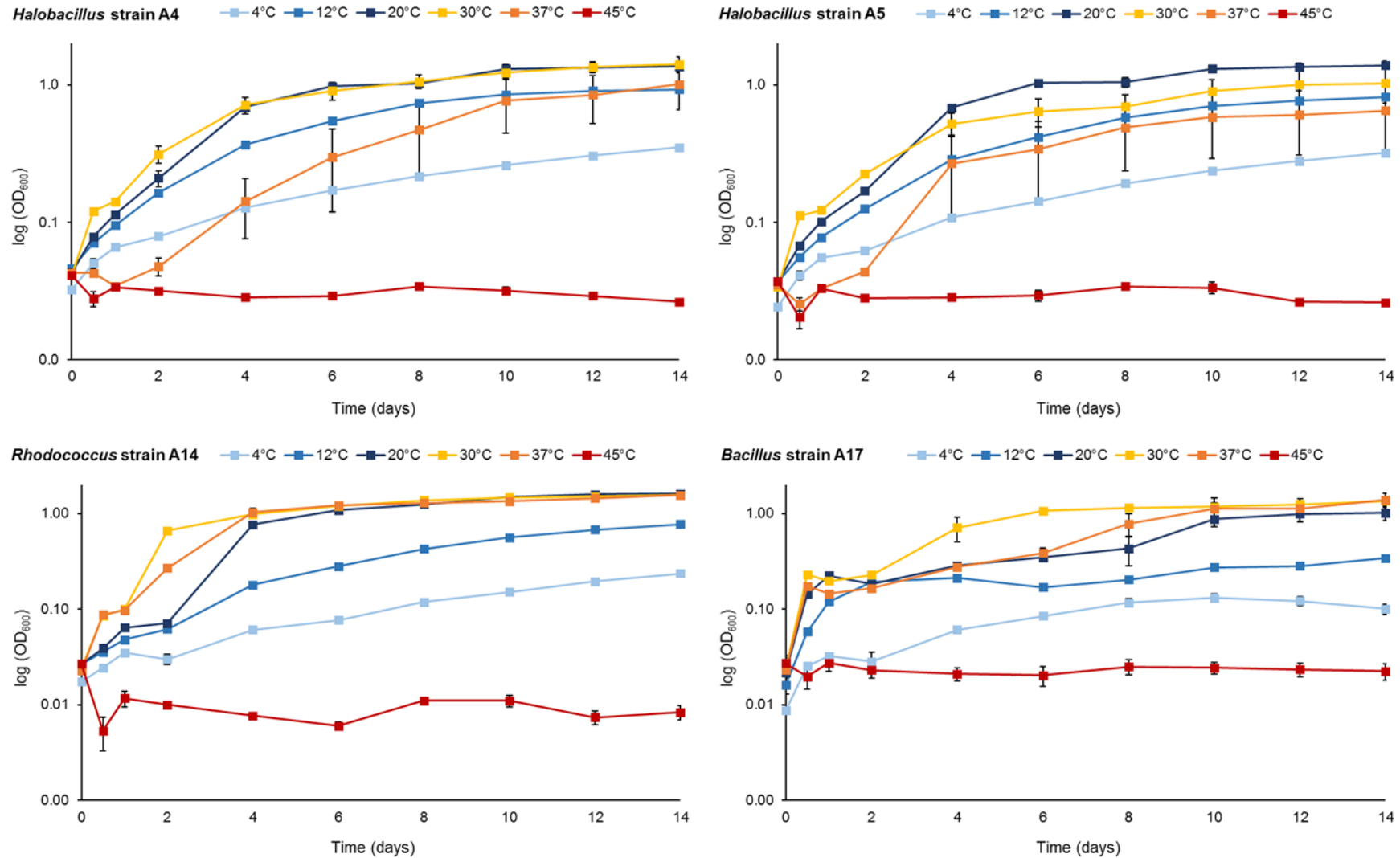| Carbon Source	*Halobacillus* strain A4	*Halobacillus* strain A5	*Rhodococcus* strain A14	*Bacillus* strain A17
Chondroitin Sulfate C			72	12
α-Cyclodextrin			24	12
β-Cyclodextrin				12
γ-Cyclodextrin				12
Dextrin			24	12
Gelatin			24	12
Glycogen			24	12
Inulin			24	12
Laminarin			24	12
Mannan			72	12
Pectin			24	12
N-Acetyl-D-Galactosamine			24	12
N-Acetyl-Neuraminic Acid				
β-D-Allose			24	
Amygdalin			24	12
D-Arabinose	72	72	24	12
D-Arabitol			24	12
L-Arabitol			24	12
Arbutin			24	72
2-Deoxy-D-Ribose	12	12	12	72
l-Erythritol			24	12
D-Fucose			24	12
3-0-β-D-Galactopyranosyl-D-Arabinose			48	72
Gentiobiose			24	12
L-Glucose			48	12
Lactitol			24	12
D-Melezitose			24	12
Maltitol			24	12
α-Methyl-D-Glucoside			24	12
β-Methyl-D-Galactoside			24	12
3-Methyl Glucose			24	12
β-Methyl-D-Glucuronic Acid			24	12
α-Methyl-D-Mannoside			24	12
β-Methyl-D-Xyloside			24	12
Palatinose			24	12
D-Raffinose			24	12
Salicin			48	12
Sedoheptulosan			24	12
L-Sorbose			24	12
Stachyose			24	12
D-Tagatose			24	12
Turanose	48	48	24	12
Xylitol	72	72	24	12
N-Acetyl-D-Glucosaminitol			24	24
γ-Amino Butyric Acid			24	12
δ-Amino Valeric Acid				24
Butyric Acid			24	12
Capric Acid				

Table 3.6b Utilisation of PM2A™ Microplate (Biolog Inc.) carbon sources by isolates *Halobacillus* strain A4, *Halobacillus* strain A5, *Rhodococcus* strain A14, and *Bacillus* strain A17 cultivated from the Colne Estuary, Essex. Numbers denote hours taken for a specific carbon source to be utilised by each isolate. Dark purple denotes rapid carbon source utilisation, whilst light purple denotes slower utilisation of a specific carbon source. Blank spaces represent carbon sources not used by isolates during the 72 hour incubation period.

PM2A™ Microplate (continued)

Carbon Source	*Halobacillus* strain A4	*Halobacillus* strain A5	*Rhodococcus* strain A14	*Bacillus* strain A17
Caproic Acid			24	24
Citraconic Acid			48	12
Citramalic Acid			24	12
D-Glucosamine	48	48	48	12
2-Hydroxy Benzoic Acid				
4-Hydroxy Benzoic Acid	48	48	48	
β-Hydroxy Butyric Acid			24	12
γ-Hydroxy Butyric Acid			24	12
α-Keto-Valeric Acid			24	12
Itaconic Acid				
5-Keto-D-Gluconic Acid	48	48	24	12
D-Lactic Acid Methyl Ester			24	12
Malonic Acid			24	12
Melibionic Acid			24	12
Oxalic Acid			48	12
Oxalomalic Acid	72	72	24	12
Quinic Acid	48	48	24	12
D-Ribono-1,4-Lactone				12
Sebacic Acid	72	72	24	48
Sorbic Acid	72	72		
Succinamic Acid		72	24	12
D-Tartaric Acid			24	12
L-Tartaric Acid			24	12
Acetamide			48	12
L-Alaninamide			48	12
N-Acetyl-L-Glutamic Acid			48	12
L-Arginine			24	12
Glycine			24	12
L-Histidine			48	12
L-Homoserine			72	24
Hydroxy-L-Proline			24	12
L-Isoleucine			24	12
L-Leucine			24	12
L-Lysine			24	12
L-Methionine			24	12
L-Ornithine			24	12
L-Phenylalanine			48	12
L-Pyroglutamic Acid			24	12
L-Valine			24	12
D,L-Carnitine			48	12
Sec-Butylamine			24	12
D,L-Octopamine			48	12
Putrescine			24	12
Dihydroxy Acetone	6	6	6	12
2,3-Butanediol			24	12
2,3-Butanone			24	24
3-Hydroxy 2-Butanone			24	12

3.4 Discussion

3.4.1 Importance of understanding acetaldehyde degrader diversity

The microbial degradation of OVOCs, such as methanol and acetaldehyde, is thought to play a significant role in the global carbon cycle by limiting the flux of these compounds to the atmosphere. Despite the proposed importance of microbial OVOC degradation, only a small number of OVOC-degrading microorganisms have been identified and our understanding of their diversity is severely limited. This has restricted our ability to accurately predict the magnitude of microbial OVOC sinks in terrestrial and aquatic ecosystems, which has considerable detrimental implications for global modelling approaches. Our limited knowledge of the identities and diversity of acetaldehyde-degrading microorganisms means that the magnitude of the microbial acetaldehyde sink is likely significantly underestimated, as the activity of currently unidentified acetaldehyde-degrading microorganisms is not yet recognised. Accordingly, it is also likely that previous estimates of acetaldehyde emissions from terrestrial and marine environments (Singh et al. 2004; Millet et al. 2010) are considerably overestimated, as these modelled estimates do not include a microbial sink term. The importance of identifying acetaldehyde-degrading microorganisms and the impact that these findings have on estimates of the magnitude of the microbial acetaldehyde sink are perhaps best demonstrated by Halsey et al. (2017), which identified two strains of *Pelagibacter* SAR11, namely HTCC1062 and HTCC7211, as acetaldehyde degraders. Based on the acetaldehyde uptake rates exhibited by these strains, it was estimated that the global SAR11 community could oxidise more acetaldehyde than is currently estimated to be produced, and that a large proportion of acetaldehyde in the marine environment is prevented from reaching the atmosphere. These findings, based on only two acetaldehyde-degrading strains, suggest that the microbial acetaldehyde sink is significantly underestimated, and that the identification of additional acetaldehyde degraders will increase the estimated magnitude of the microbial acetaldehyde sink. However, it is important to note

that the extrapolation of acetaldehyde uptake rates exhibited by only two SAR11 strains to the entire SAR11 community does not provide an entirely reliable or accurate estimate of the contribution of SAR11 to the microbial acetaldehyde sink. For example, it is very likely that not all members of the SAR11 clade are capable of acetaldehyde degradation and that these microorganisms do not constantly degrade acetaldehyde. Therefore the contribution of the entire SAR11 clade to the microbial acetaldehyde sink is likely to be lower than the projections of Halsey et al. (2017), although these estimates are useful indicators of the potential for acetaldehyde degradation and also suggest that the source of acetaldehyde from the marine environment is likely to be considerably lower than current estimates that do not consider the metabolic activity of microorganisms. To accurately estimate the magnitude of the microbial acetaldehyde sink, and therefore improve the accuracy of the global flux of acetaldehyde, a suite of techniques must be applied. Firstly, in-situ measurements of microbial acetaldehyde uptake using radiotracer techniques are necessary to reliably quantify rates of microbial acetaldehyde loss under natural conditions. In-situ rate measurements using ^{14}C-labelled acetaldehyde have previously been performed in the Atlantic Ocean (Dixon et al. 2013; Beale et al. 2015), providing an indication of the importance of microorganisms in mediating acetaldehyde flux from the marine environment. However, significantly more in-situ measurements are necessary to improve our understanding of how rates of microbial acetaldehyde uptake vary by location and season (see Chapter 5), and to determine the effect of a range of environmental conditions, such as temperature and nutrient availability. Following the suggestion in Chapter 2 that the meta-cleavage pathway for the degradation of aromatic hydrocarbons may enable genera such as the *Pseudomonas* to degrade acetaldehyde, the effect of nutrient availability is particularly important, as the presence of aromatic or aliphatic hydrocarbons may induce the co-metabolism of acetaldehyde. Furthermore, increasing the number of in-situ measurements of microbial acetaldehyde uptake in freshwater and estuarine systems, as well as the marine environment, will contribute to increasing the accuracy of global models of the acetaldehyde budget. Rates of acetaldehyde uptake should also be investigated at the single-cell level,

using techniques such as MAR-FISH (microautoradiography-fluorescence in-situ

hybridisation) and NanoSIMS (nanoscale secondary ion mass spectrometry), which can

provide high-resolution information regarding the metabolic activity of microorganisms, whilst

also establishing the identity of individual cells, thus simultaneously enhancing our

knowledge of the diversity of acetaldehyde-degrading microorganisms.

3.4.2 Expanding the diversity of acetaldehyde degraders

In this study, 17 bacterial isolates cultivated from the Colne Estuary exhibited the ability to

utilise acetaldehyde as a sole carbon source, albeit with different amounts of degradation

exhibited by each isolate. These isolates belonged to two distinct phyla, namely the

Firmicutes and the Actinobacteria. Eleven bacterial isolates were identified as members of

the Firmicutes, and belonged to four different genera, namely the *Bacillus* (3), *Halobacillus*

(5), *Lysinibacillus* (2), and *Psychrobacillus* (1) genera. Within the Actinobacteria, isolates

were identified as members of the *Microbacterium* (5) and *Rhodococcus* (1) genera.

Previous studies have identified 18 different acetaldehyde-degrading strains belonging to the

Proteobacteria and Firmicutes phyla, with the majority of isolates belonging to the

Gammaproteobacteria within the former (Liu et al. 2015; Gao et al. 2018). Acetaldehyde-

degrading Proteobacteria were not cultivated from the Colne Estuary sediment slurries in

this study, despite microbial community analysis, via the Illumina MiSeq platform, revealing

that the genus *Pseudomonas* represented 39 - 89% of the bacterial community at the

conclusion of the quaternary acetaldehyde enrichment (Section 2.3.2.1). This is likely a

result of the limited range of culture media used to isolate acetaldehyde-degrading

microorganisms, although Difco™ marine agar 2216 medium contains all of the nutrients

necessary for the growth of heterotrophic marine bacteria and is regularly used in their

isolation. Gao et al. (2018), for example, used the same medium to isolate 10 acetaldehyde-

degrading Proteobacteria from seawater of the West Pacific Ocean, collected at a depth of

2000 m, demonstrating that Difco™ marine agar 2216 medium was a suitable choice of

culture medium in this study. Alternatively, the concentration of acetaldehyde used to isolate acetaldehyde degraders from the Colne Estuary sediment slurries may have been toxic to a significant proportion of the microbial community, providing unfavourable conditions for growth and preventing successful isolation. The genus *Arcobacter*, for example, belonging to the Epsilonproteobacteria, represented 1 - 11% of the bacterial community in Colne Estuary sediment slurries following the primary acetaldehyde enrichment, but accounted for less than 0.05% of the bacterial community at the conclusion of the quaternary enrichment (Section 2.3.2.1). This significant decrease in relative abundance may be the result of *Arcobacter* species being outcompeted by the genus *Pseudomonas*, but also suggests that the genus *Arcobacter* could not tolerate repeated exposure to unnaturally high and potentially toxic acetaldehyde concentrations. In-situ acetaldehyde concentrations in the marine environment have been shown to range from 1.38 - 38 nM (Section 1.6), so it is conceivable that the concentration of acetaldehyde used to isolate microorganisms in this study (22.7 mM) was toxic to the majority of microorganisms and possibly to acetaldehyde-degraders with a low tolerance to high or repeated acetaldehyde exposure. However, both Gao et al. (2018) and Liu et al. (2015) used similarly high concentrations to isolate acetaldehyde-degrading members of the Gammaproteobacteria, with final concentrations of 16 mM and 22.7 mM used for isolation, respectively. Gao et al. (2018) also reported that three acetaldehyde-degrading isolates with close identity to *Vibrio parahaemolyticus*, *Halomonas axialensis*, and *Halomonas meridiana* could tolerate concentrations as high as 34.1 mM. These findings, combined with the high concentrations of acetaldehyde used for isolation, suggest that the conditions used for the isolation of acetaldehyde-degrading microorganisms from the Colne Estuary sediment slurries were favourable for the growth of acetaldehyde-degrading Proteobacteria. It may be possible that the high concentrations of acetaldehyde used for isolation in this study and by Gao et al. (2018) and Liu et al. (2015), favour the isolation of only the most tolerant acetaldehyde degraders and prevent the isolation of acetaldehyde-degraders with a tolerance to acetaldehyde concentrations that naturally occur in aquatic environments. This requires further investigation, but if correct, suggests that a considerable

number of acetaldehyde-degrading microorganisms remain unidentified due to the use of unnaturally high acetaldehyde concentrations during isolation and that a significant amount of microbial acetaldehyde degrader diversity has yet to be discovered. The findings from this study suggest that optimal acetaldehyde concentrations for the isolation and growth of most acetaldehyde degraders are below the millimolar range, with microbial abundance considerably higher (Chapter 2) and isolated bacterial strains exhibiting active growth and metabolism in the lower concentration treatment (2.27 mM). Future investigations should consider enrichments using more environmentally-relevant concentrations (nanomolar) to increase the number of isolated microorganisms and to potentially isolate the acetaldehyde degraders that dominate microbial communities under natural conditions. It is important to note, however, that the isolation of specific microorganisms may also relate to the initial starting communities in the Colne Estuary sediment slurries compared to environments such as the deep sea. Microbial community composition in these environments is likely to be significantly different, resulting in the isolation of different microorganisms.

The majority of acetaldehyde-degrading isolates cultivated from the Colne Estuary were identified as members of the Firmicutes phylum, including 3 isolates belonging to the genus *Bacillus*. Gao et al. (2018), also reported the isolation of two acetaldehyde-degrading strains of *Bacillus*, namely ACH-S-8 and ACH-S-9, which were closely related to *B. aquimaris* TF-12 and degraded 55.4% and 73.9% of an 11.35 mM acetaldehyde addition, respectively (equivalent to 6.29 and 8.39 mM of acetaldehyde). In this study, *Bacillus* strains A8, A15, and A17 degraded 47%, 47.4%, and 100% of added acetaldehyde, respectively, during growth on ONR7a seawater-nutrient medium (equivalent to 1.23, 1.03, and 2.37 mM of acetaldehyde), suggesting that *Bacillus* strains A8 and A15 have a lower capacity for acetaldehyde degradation than the two strains of *Bacillus* isolated by Gao et al. (2018). The complete degradation of acetaldehyde by *Bacillus* strain A17, a close relative of *Bacillus mycoides*, suggests that this strain may be able to tolerate and utilise higher acetaldehyde concentrations similar to isolates ACH-S-8 and ACH-S-9 and may be an important

acetaldehyde degrader in the Colne Estuary, although this requires further investigation. The identification of novel acetaldehyde-degrading strains of *Lysinibacillus*, *Psychrobacillus*, and *Halobacillus* within the Firmicutes phylum also suggests that the diversity of acetaldehyde-degrading microorganisms is considerably wider than previously thought. Two strains of *Halobacillus*, namely *Halobacillus* strains A4 and A5, utilised all of the added acetaldehyde within 4 days of incubation during growth on ONR7a seawater-nutrient medium, suggesting that these strains may be important members of the acetaldehyde-degrading community and may be key components of the microbial acetaldehyde sink. It is important to note, however, that microbial communities of the acetaldehyde-enriched Colne Estuary sediment slurries were dominated by two genera belonging to the Proteobacteria and not members of the Firmicutes (Section 2.3.2.1), suggesting that the contribution of *Halobacillus* strains A4 and A5 to microbial acetaldehyde degradation may be less than that of *Pseudomonas* and *Arcobacter* species.

Acetaldehyde degradation was also exhibited by isolates belonging to the *Microbacterium* and *Rhodococcus* genera. To the best of my knowledge, this is only the second study to identify acetaldehyde-degrading isolates within the Actinobacteria, with the work of Yoshida (2019) suggesting that the oligotrophic *Rhodococcus erythropolis* N9T-4 can utilise acetaldehyde as a carbon source under nutrient limited conditions by upregulating the expression of genes encoding aldehyde dehydrogenases and enzymes involved in the glyoxylate shunt. *Rhodococcus* strain A14, a close relative of *Rhodococcus wratislaviensis* and *Rhodococcus opacus*, utilised acetaldehyde as a sole carbon source during growth on ONR7a seawater-nutrient medium and degraded all of the available acetaldehyde within 5 days of incubation. Members of the genus *Rhodococcus* are metabolically versatile due to a variety of advantageous genetic attributes, including the possession of a large genome, the presence of large linear plasmids containing a diverse range of catabolic genes, and the ability to acquire genes via linear plasmid-mediated horizontal gene transfer (Bell et al. 1998; Van Der Geize & Dijkhuizen 2004; Larkin et al. 2005; Tischler et al. 2009; Cappelletti et al.

2019). It is therefore unsurprising that *Rhodococcus* strain A14 exhibited the ability to degrade acetaldehyde, and perhaps more surprising that additional members of the genus *Rhodococcus* have not been identified as acetaldehyde degraders. Based on its ability to rapidly utilise acetaldehyde as a sole carbon source, *Rhodococcus* strain A14 is likely a key acetaldehyde degrader in the Colne Estuary, and, given the metabolic versatility of the genus *Rhodococcus*, this group is likely an important component of the microbial acetaldehyde sink.

The screening of 22 previously identified bacterial isolates demonstrated that the diversity of acetaldehyde-degrading microorganisms is significantly underestimated. As expected, *Shewanella mangrovi* (JCM 30121^T), a known acetaldehyde degrader (Liu et al. 2015), completely degraded acetaldehyde during growth on ONR7a seawater-nutrient medium and Difco™ marine broth 2216 medium after only 1 day of incubation. Complete acetaldehyde degradation was also exhibited by 14 bacterial isolates belonging to a diverse group of genera within the Actinobacteria, Bacteroidetes, Proteobacteria, and Verrucomicrobia. To the best of my knowledge, this is the first study to identify acetaldehyde-degrading bacterial isolates within the Bacteroidetes and Verrucomicrobia, whilst the identification of *Aeromicrobium marinum* (T2) and *Salinispora tropica* (CNB-440) as acetaldehyde degraders further suggests that the Actinobacteria may play an important role in the microbial acetaldehyde sink. Importantly, acetaldehyde degradation was not exhibited by all of the bacterial isolates that were screened. The hydrocarbon degraders *Thalassolituus oleivorans* (MIL-1), *Cycloclasticus zancles* (78-ME), *Marinobacter hydrocarbonoclasticus* (SP17), and *Oleispira antarctica* (RB-8) did not utilise acetaldehyde during growth on ONR7a seawater-nutrient medium, suggesting that these isolates cannot use acetaldehyde as a sole carbon source. Although 1.5% acetaldehyde loss was measured in serum bottles inoculated with *T. oleivorans* (MIL-1), this was attributed to fluctuations in GC-FID measurements rather than acetaldehyde biodegradation. These findings also show that the ability to degrade acetaldehyde is not conserved amongst all members of a particular phylum or class, such as

the Proteobacteria and Gammaproteobacteria, and that a diverse group of microorganisms constitute the acetaldehyde-degrading community. This diversity is perhaps unsurprising, as the majority of microorganisms possess the enzymatic tools necessary for the initial step of acetaldehyde degradation, namely aldehyde dehydrogenases. Based on the sequencing of entire microbial genomes, Sophos & Vasiliou (2003) reported that bacterial genomes contain 1 - 26 aldehyde dehydrogenase-encoding genes and that these genes are also found in both fungal and archaeal genomes. Not only does this suggest that the diversity of acetaldehyde-degrading bacteria is significantly underestimated, this also implies that both fungi and archaea may contribute to the microbial acetaldehyde sink, however, the findings from Chapter 2 suggest that archaea have no role in acetaldehyde degradation and further investigations are necessary to isolate acetaldehyde-degrading fungi. It is also important to note that the obligate hydrocarbon-degrading bacteria examined in this study also possess aldehyde dehydrogenase-encoding genes but did not utilise acetaldehyde as a sole carbon and energy source, suggesting that the ability to degrade acetaldehyde is not solely based on the presence of aldehyde dehydrogenases and may be dependent on the specific function or substrate affinities of these enzymes. Alternatively, this may also result from the lack of a suitable growth substrate, such as aromatic hydrocarbons, which may induce the aldehyde dehydrogenase enzymes necessary for the co-metabolism of acetaldehyde as part of the meta-cleavage pathway for the degradation of aromatic hydrocarbons, as discussed in Chapter 2. Collectively, the findings of this study suggest that a significant number of previously identified bacteria may be able to utilise acetaldehyde as a carbon source and that the microbial acetaldehyde sink may be considerably larger than is currently thought. The identification of acetaldehyde-degrading bacteria belonging to a variety of genera within the Actinobacteria, Bacteroidetes, Firmicutes, Proteobacteria, and Verrucomicrobia demonstrates that a diverse group of microorganisms constitute the microbial acetaldehyde sink and that the ability to utilise acetaldehyde as a carbon source is not restricted to a specialist group of microorganisms. The findings reported here show that further research is necessary to improve our understanding of the diversity of acetaldehyde-degrading

microorganisms and the impact of the microbial acetaldehyde sink on the global

biogeochemical cycle of acetaldehyde.

3.4.3 Nutrient availability and acetaldehyde degradation

Acetaldehyde degradation was generally more extensive and occurred more rapidly when

isolates were grown on Difco™ marine broth 2216 medium compared to growth on ONR7a

seawater-nutrient medium. This suggests that acetaldehyde degradation is enhanced by the

availability of other essential nutrients and is therefore co-metabolic, whilst also implies that

most isolates preferentially use other sources of carbon for growth ahead of acetaldehyde.

Isolates cultivated from the Colne Estuary, for example, exhibited an increase in

acetaldehyde degradation during growth on Difco™ marine broth 2216 medium, with 16

isolates utilising all of the available acetaldehyde within 19 days of incubation, compared to 7

isolates during growth on ONR7a seawater-nutrient medium (Table 3.3). The Colne Estuary

exhibits strong gradients of nutrient concentrations, including nitrate, ammonium, and

phosphate, from the estuary head towards the estuary mouth (Nedwell et al. 2016). This

suggests that acetaldehyde degradation may be more extensive at the head of the Colne

Estuary, with acetaldehyde-degrading microorganisms capitalising on the increased

availability of essential nutrients. Conversely, in the relatively oligotrophic waters of the

estuary mouth, the extent and rate of acetaldehyde degradation may be considerably lower.

Acuña Alvarez et al. (2009) reported the fastest rates of microbial isoprene degradation at

the head of the Colne Estuary and the slowest rates of degradation towards the estuary

mouth. Importantly, the increase in isoprene degradation was attributed to the elevated

production of isoprene by microalgae in response to higher nutrient concentrations at the

estuary head (Acuña Alvarez et al. 2009), rather than a direct relationship between nutrient

concentrations and microbial isoprene degradation. It is therefore uncertain whether

acetaldehyde degradation rates would be higher at the head of the Colne Estuary in

response to elevated nutrient concentrations and this requires further investigation in future

studies. Interestingly, Halsey et al. (2017) demonstrated that the diatom, *Thalassiosira pseudonana*, could produce acetaldehyde in a light-dependent manner. This suggests that diatoms and other microalgae in the Colne Estuary may be able to support a community of acetaldehyde degraders in a similar manner to the relationship observed between isoprene-producing microalgae and the microbial isoprene-degrading community. Higher nutrient concentrations at the estuary head may result in elevated rates of microalgal acetaldehyde production, possibly resulting in increased rates of acetaldehyde degradation. Future studies should investigate the relationship between nutrient availability, microalgal acetaldehyde production, and microbial acetaldehyde degradation in the Colne Estuary to determine whether the findings of Acuña Alvarez et al. (2009) for isoprene also apply to acetaldehyde.

3.5 Conclusion

The findings of this study suggest that the diversity of acetaldehyde-degrading microorganisms is significantly underestimated and that a considerable number of bacteria can utilise acetaldehyde as a carbon source. The screening of bacterial isolates demonstrated that acetaldehyde-degraders belong to a diverse group of genera within the Actinobacteria, Bacteroidetes, Firmicutes, Proteobacteria, and the Verrucomicrobia, and that the ability to degrade acetaldehyde is not restricted to a specific phylum or class. To the best of my knowledge, this is the first study to identify acetaldehyde-degrading bacteria within the Bacteroidetes and Verrucomicrobia. These findings highlight the importance of screening previously identified bacterial isolates for the ability to degrade acetaldehyde and it is likely that a considerable number of acetaldehyde-degrading bacteria have yet to be discovered. Accordingly, our current knowledge and understanding of acetaldehyde degraders remains limited. This has significant implications for estimates of the microbial acetaldehyde sink, which is likely to be significantly larger than previously thought and may exert considerable control over global acetaldehyde emissions. Microbial acetaldehyde degradation may also be enhanced by the availability of essential nutrients, with the extent and rate of

acetaldehyde degradation exhibited by bacterial isolates increasing during growth on a nutrient-rich culture medium. This suggests that aquatic environments with high nutrient concentrations, such as the Colne Estuary, may also experience higher rates of microbial acetaldehyde degradation, although this requires further investigation. Based on their ability to rapidly utilise acetaldehyde as a sole carbon source, four bacterial isolates belonging to the *Halobacillus*, *Rhodococcus*, and *Bacillus* genera were identified as key acetaldehyde degraders in the Colne Estuary. As the majority of bacteria possess aldehyde dehydrogenase enzymes, it is likely that a diverse group of bacteria are responsible for acetaldehyde degradation in the Colne Estuary and in other aquatic systems, although the presence of aldehyde dehydrogenases does not necessarily guarantee that bacteria can utilise acetaldehyde as a carbon source. Further work is needed to identify these microorganisms and to improve our knowledge of the diversity of acetaldehyde degraders. This will improve our understanding of the microbial acetaldehyde sink and the global biogeochemical cycle of acetaldehyde.

3.6 References

Acuña Alvarez L, Exton DA, Timmis KN, Suggett DJ, McGenity TJ (2009) Characterization of marine isoprene-degrading communities. Environ Microbiol 11:3280–3291

Altschul SF, Gish W, Miller W, Myers EW, Lipman DJ (1990) Basic local alignment search tool. J Mol Biol 215:403–410

Balch WE, Schoberth S, Tanner RS, Wolfe RS (1977) *Acetobacterium*, a new genus of hydrogen-oxidizing, carbon dioxide-reducing, anaerobic bacteria. Int J Syst Bacteriol 27:355–361

Beale R, Dixon JL, Smyth TJ, Nightingale PD (2015) Annual study of oxygenated volatile organic compounds in UK shelf waters. Mar Chem 171:96–106

Bell KS, Philp JC, Aw DWJ, Christofi N (1998) The genus *Rhodococcus*. J Appl Microbiol 85:195–210

Beveridge TJ (2001) Use of the Gram stain in microbiology. Biotech Histochem 76:111–118

Bochner BR, Gadzinski P, Panomitros E (2001) Phenotype microarrays for high-throughput phenotypic testing and assay of gene function. Genome Res 11:1246–1255

Cappelletti M, Zampolli J, Di Gennaro P, Zannoni D (2019) Genomics of *Rhodococcus*. In: Biology of *Rhodococcus*. pp 23–60. H. M. Alvarez (Ed.). Microbiology Monographs 16. Springer Nature Switzerland AG

Chistoserdova L, Kalyuzhnaya MG, Lidstrom ME (2009) The expanding world of methylotrophic metabolism. Annu Rev Microbiol 63:477–499

Chronopoulou PM, Sanni GO, Silas-Olu DI, van der Meer JR, Timmis KN, Brussaard CPD, McGenity TJ (2015) Generalist hydrocarbon-degrading bacterial communities in the oil-polluted water column of the North Sea. Microb Biotechnol 8:434–447

Crombie AT, El Khawand M, Rhodius VA, Fengler KA, Miller MC, Whited GM, McGenity TJ,

Murrell JC (2015) Regulation of plasmid-encoded isoprene metabolism in *Rhodococcus*, a representative of an important link in the global isoprene cycle. Environ Microbiol 17:3314–3329

Dean JF, Middelburg JJ, Röckmann T, Aerts R, Blauw LG, Egger M, Jetten MSM, de Jong AEE, Meisel OH, Rasigraf O, Slomp CP, in't Zandt MH, Dolman AJ (2018) Methane feedbacks to the global climate system in a warmer world. Rev Geophys 56:207–250

Dixon JL, Beale R, Nightingale PD (2013) Production of methanol, acetaldehyde, and acetone in the Atlantic Ocean. Geophys Res Lett 40:4700–4705

Edgar RC (2004) MUSCLE: Multiple sequence alignment with high accuracy and high throughput. Nucleic Acids Res 32:1792–1797

El Khawand M, Crombie AT, Johnston A, Vavlline DV, McAuliffe JC, Latone JA, Primak YA, Lee SK, Whited GM, McGenity TJ, Murrell JC (2016) Isolation of isoprene degrading bacteria from soils, development of *isoA* gene probes and identification of the active isoprene-degrading soil community using DNA-stable isotope probing. Environ Microbiol 18:2743–2753

Felsenstein J (1985) Confidence limits on phylogenies: An approach using the bootstrap. Evolution (N Y) 39:783–791

Galbally IE, Kirstine W (2002) The production of methanol by flowering plants and the global cycle of methanol. J Atmos Chem 43:195–229

Gao B, Shang X, Li L, Di W, Zeng R (2018) Phylogenetically diverse, acetaldehyde-degrading bacterial community in the deep sea water of the West Pacific Ocean. Acta Oceanol Sin 37:54–64

Gray CM, Helmig D, Fierer N (2015) Bacteria and fungi associated with isoprene consumption in soil. Elementa 3:1–10

Halsey KH, Giovannoni SJ, Graus M, Zhao Y, Landry Z, Thrash JC, Vergin KL, de Gouw J

(2017) Biological cycling of volatile organic carbon by phytoplankton and bacterioplankton. Limnol Oceanogr 62:2650–2661

Hanson RS, Hanson TE (1996) Methanotrophic bacteria. Microbiol Rev 60:439–471

Kalyuzhnaya MG, Gomez OA, Murrell JC (2019) The methane-oxidizing bacteria (Methanotrophs). Taxonomy, genomics and ecophysiology of hydrocarbon-degrading microbes. pp 245–278

Kimura M (1980) A simple method for estimating evolutionary rates of base substitutions through comparative studies of nucleotide sequences. J Mol Evol 16:111–120

Kirschke S, Bousquet P, Ciais P, Saunois M, Canadell JG, Dlugokencky EJ, Bergamaschi P, Bergmann D, Blake DR, Bruhwiler L, Cameron-Smith P, Castaldi S, Chevallier F, Feng L, Fraser A, Heimann M, Hodson EL, Houweling S, Josse B, Fraser PJ, Krummel PB, Lamarque JF, Langenfelds RL, Le Quére C, Naik V, O'Doherty S, Palmer PI, Pison I, Plummer D, Poulter B, Prinn RG, Rigby M, Ringeval B, Santini M, Schmidt M, Shindell DT, Simpson IJ, Spahni R, Steele LP, Strode SA, Sudo K, Szopa S, van der Werf GR, Voulgarakis A, van Weele M, Weiss RF, Williams JE, Zeng G (2013) Three decades of global methane sources and sinks. Nat Geosci 6:813–823

Kolb S (2009) Aerobic methanol-oxidizing bacteria in soil. FEMS Microbiol Lett 300:1–10

Kumar S, Stecher G, Li M, Knyaz C, Tamura K (2018) MEGA X: Molecular evolutionary genetics analysis across computing platforms. Mol Biol Evol 35:1547–1549

Larkin MJ, Kulakov LA, Allen CCR (2005) Biodegradation and *Rhodococcus* - Masters of catabolic versatility. Curr Opin Biotechnol 16:282–290

Liu Y, Shang X, Yi Z, Gu L, Zeng R (2015) *Shewanella mangrovi* sp. nov., an acetaldehyde-degrading bacterium isolated from mangrove sediment. Int J Syst Evol Microbiol 65:2630–2634

McGenity TJ, Crombie AT, Murrell JC (2018) Microbial cycling of isoprene, the most

abundantly produced biological volatile organic compound on Earth. ISME J 12:931–941

Millet DB, Guenther A, Siegel DA, Nelson NB, Singh HB, de Gouw JA, Warneke C, Williams J, Eerdekens G, Sinha V, Karl T, Flocke F, Apel E, Riemer DD, Palmer PI, Barkley M (2010) Global atmospheric budget of acetaldehyde: 3-D model analysis and constraints from in-situ and satellite observations. Atmos Chem Phys 10:3405–3425

Morris RM, Rappé MS, Connon SA, Vergin KL, Siebold WA, Carlson CA, Giovannoni SJ (2002) SAR11 clade dominates ocean surface bacterioplankton communities. Nature 420:806–810

Nedwell DB, Underwood GJC, McGenity TJ, Whitby C, Dumbrell AJ (2016) The Colne Estuary: A long-term microbial ecology observatory. Adv Ecol Res 55:227–281

Op den Camp HJM, Islam T, Stott MB, Harhangi HR, Hynes A, Schouten S, Jetten MSM, Birkeland NK, Pol A, Dunfield PF (2009) Environmental, genomic and taxonomic perspectives on methanotrophic Verrucomicrobia. Environ Microbiol Rep 1:293–306

Saitou N, Nei M (1987) The neighbor-joining method: a new method for reconstructing phylogenetic trees. Mol Biol Evol 4:406–425

Schmidt A, Frensch M, Schleheck D, Schink B, Müller N (2014) Degradation of acetaldehyde and its precursors by *Pelobacter carbinolicus* and *P. acetylenicus*. PLoS One 9:1–23

Singh HB, Salas LJ, Chatfield RB, Czech E, Fried A, Walega J, Evans MJ, Field BD, Jacob DJ, Blake D, Heikes B, Talbot R, Sachse G, Crawford JH, Avery MA, Sandholm S, Fuelberg H (2004) Analysis of the atmospheric distribution, sources, and sinks of oxygenated volatile organic chemicals based on measurements over the Pacific during TRACE-P. J Geophys Res 109:1–20

Sophos NA, Vasiliou V (2003) Aldehyde dehydrogenase gene superfamily: The 2002 update. Chem Biol Interact 143–144:5–22

Stacheter A, Noll M, Lee CK, Selzer M, Glowik B, Ebertsch L, Mertel R, Schulz D, Lampert

N, Drake HL, Kolb S (2013) Methanol oxidation by temperate soils and environmental determinants of associated methylotrophs. ISME J 7:1051–1064

Tischler D, Eulberg D, Lakner S, Kaschabek SR, Van Berkel WJH, Schlömann M (2009) Identification of a novel self-sufficient styrene monooxygenase from *Rhodococcus opacus* 1CP. J Bacteriol 191:4996–5009

Trifunović D, Berghaus N, Müller V (2020) Growth of the acetogenic bacterium *Acetobacterium woodii* by dismutation of acetaldehyde to acetate and ethanol. Environ Microbiol Rep 12:58–62

van der Geize R, Dijkhuizen L (2004) Harnessing the catabolic diversity of rhodococci for environmental and biotechnological applications. Curr Opin Microbiol 7:255–261

van Hylckama Vlieg JET, Kingma J, van den Wijngaard AJ, Janssen DB (1998) A glutathione S-transferase with activity towards cis-1,2- dichloroepoxyethane is involved in isoprene utilization by *Rhodococcus* sp. strain AD45. Appl Environ Microbiol 64:2800–2805

van Hylckama Vlieg JET, Leemhuis H, Lutje Spelberg JH, Janssen DB (2000) Characterization of the gene cluster involved in isoprene metabolism in *Rhodococcus* sp. strain AD45. J Bacteriol 182:1956–1963

Yoshida N (2019) Oligotrophic growth of *Rhodococcus*. pp 87–101. In: Alvarez HM (Ed.). Biology of *Rhodococcus*. Microbiology Monographs 16. Springer Nature Switzerland AG

3.7 Supplementary material
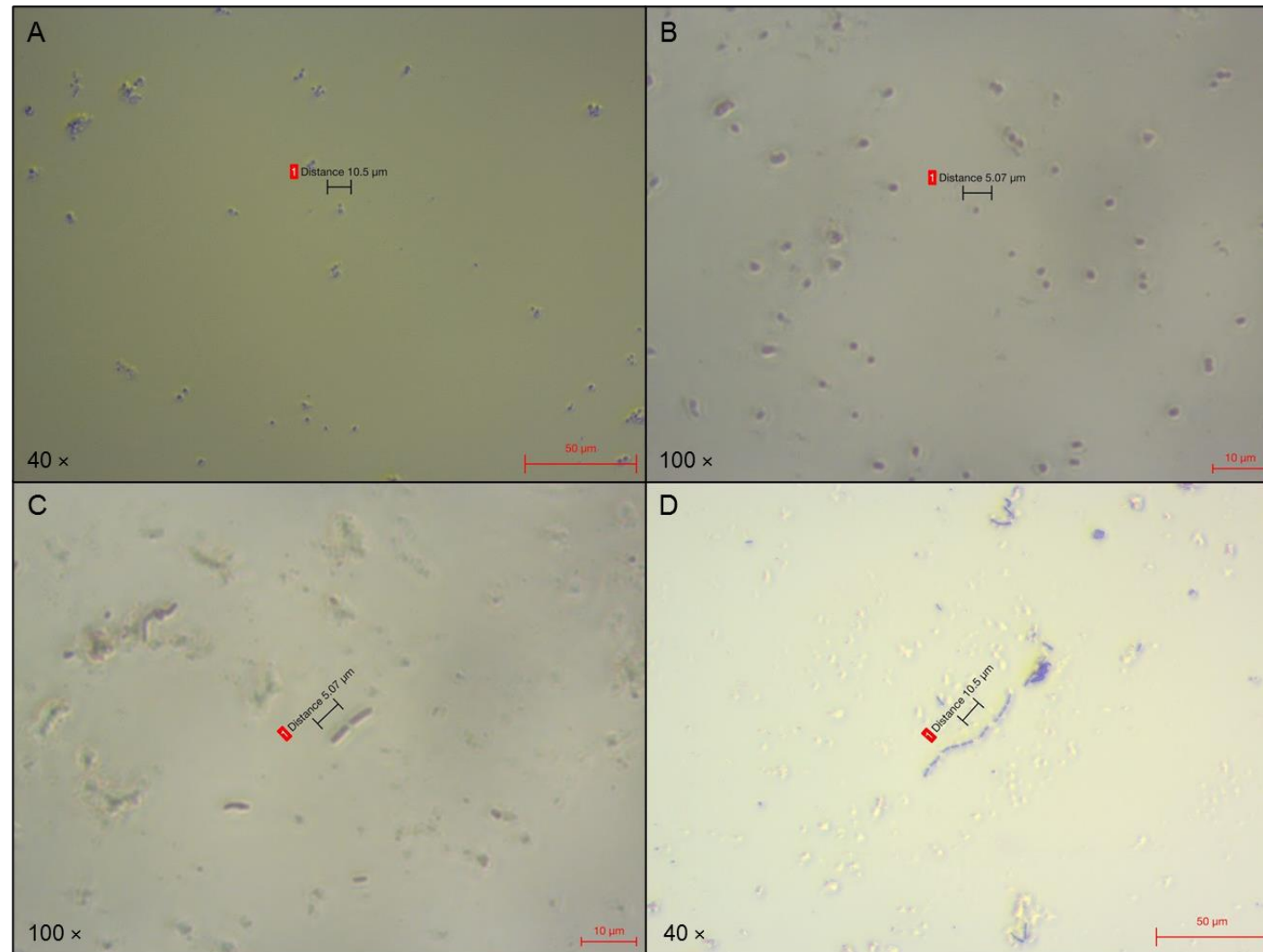
Figure S3.1 Cellular morphology of isolates (**A**) *Halobacillus* strain A4, (**B**) *Halobacillus* strain A5, (**C**) *Rhodococcus* strain A14, and (**D**) *Bacillus* strain A17. Isolates were visualised using a Primo Star LED microscope (Zeiss). *Halobacillus* strain A4 and *Bacillus* strain A17 were visualised at 40 × magnification. *Halobacillus* strain A5 and *Rhodococcus* strain A14 were viewed at 100 × magnification.

Chapter 4:

Insights into the Mechanism of Acetaldehyde Degradation by Genomics and Proteomics

4.1 Introduction

The ability to accurately identify and characterise prokaryotes has been, and continues to be, essential in establishing and maintaining a precise taxonomy for Bacteria and Archaea. Historically, DNA-DNA hybridisation has been used as the primary method for distinguishing species based on the genetic similarity between microbial strains, and for over fifty years has been considered as the "gold standard" for species delineation (Richter & Rosselló-Móra 2009; Barco et al. 2020). Based on this technique, a value of ≥70% similarity between strains was proposed as the standard for circumscribing species (Wayne et al. 1987) and, until recently, this was recognised as the best method for species distinction. This was primarily because DNA-DNA hybridisation offered the first numerical and relatively stable species boundary (Richter & Rosselló-Móra 2009), which was more reliable than classifications based on phenotypic similarities (Rosselló-Mora 2006). However, limitations of this technique, combined with the increasing availability of genomic tools has led to the use of alternative methods to establish bacterial and archaeal taxonomy with greater resolution and robustness. Notably, DNA-DNA hybridisation requires large quantities of high quality DNA, making the technique both labour-intensive and protracted (Stackebrandt 2003; Goris et al. 2007). Furthermore, it cannot be used for uncultured microorganisms (Gevers et al. 2005), which represent the major fraction of the existing microbial diversity (Amann et al. 1995). Perhaps most detrimental, however, is the inability to build databases using the resulting DNA-DNA hybridisation data that would enable comparisons to be drawn between individual strains and previously submitted data (Richter & Rosselló-Móra 2009).

Accordingly, methods that employ the use of sequence databases have become popular

alternatives for defining prokaryotic taxonomy. Classification using ribosomal RNA (rRNA) gene sequencing, for example, is commonly used due to the speed and low costs associated with this technique (Gevers et al. 2005). Moreover, the ability to compare the rRNA gene sequence of an isolate with sequences of all previously identified prokaryotic species has enabled rapid identification of novel microorganisms. However, despite these advantages, the isolated use of rRNA gene sequencing for species delineation also presents limitations. Most notably, due to its highly conserved nature, the 16S rRNA gene provides lower taxonomic resolution than DNA-DNA hybridisation (Richter & Rosselló-Móra 2009) and necessitates further investigation using additional techniques to confidently assign microorganisms to particular species (Gevers et al. 2005). As such, techniques such as multilocus sequence typing (MLST), which characterises microorganisms based on the allelic mismatches of several housekeeping genes, have been used in combination with rRNA gene sequencing for identification to species and subspecies level (Gevers et al. 2005; Richter & Rosselló-Móra 2009). Moreover, the relationship between 16S rRNA gene homology and DNA-DNA hybridisation has been shown to be non-linear (Stackebrandt & Goebel 1994), meaning that microorganisms which share near-identical 16S rRNA gene sequences (>99%) may exhibit DNA-DNA hybridisation scores that are significantly lower than the 70% similarity threshold, and therefore represent distinct species. In this respect, DNA-DNA hybridisation remains the superior method for establishing the relatedness between highly related microorganisms.

More recently, as genome sequencing has become increasingly accessible and common, genome-relatedness indices have replaced DNA-DNA hybridisation as the "gold standard" for species delineation (Richter & Rosselló-Móra 2009; Kim et al. 2014; Barco et al. 2020). This has included average nucleotide identity (ANI) (Konstantinidis et al. 2006), genome BLAST distance phylogeny (GBDP) (Henz et al. 2005) and the maximal unique matches (MUM) index (Deloger et al. 2009). Notably, ANI has been most widely accepted as the new "gold standard" for species delineation (Kim et al. 2014; Lee et al. 2016) and is calculated

from two genome sequences. One genome sequence is treated as a query, whilst the other genome is considered the subject. The query genome sequence is fragmented in-silico into 1020 bp fragments, which are searched against the subject genome to identify homologous regions and are given identity values (Yoon et al. 2017). The mean of these identity values is used to calculate the final ANI score. An ANI value of ≥95%, corresponding to 70% similarity via DNA-DNA hybridisation (Konstantinidis et al. 2006) and equivalent to 98.65% 16S rRNA gene sequence similarity (Kim et al. 2014), indicates that queried genomes belong to the same species. Comparatively, species delineation via GBDP begins with an "all-against-all" pairwise comparison of multiple genomes using BLASTN (Henz et al. 2005), a variant of the BLAST algorithm used for DNA sequence comparison (Altschul 2014). A distance matrix is then calculated before being processed by a distance-based phylogenetic method, such as the neighbour-joining method (Saitou & Nei 1987), to produce a phylogenetic tree. The MUM index, which is particularly sensitive to intraspecies variability, calculates genomic distances based on the number of unique and exact matches (MUMs) of a given minimal length shared by two genomes (Deloger et al. 2009). This index ranges between 0 to 1, with closely related genomes scoring closer to 0. To date, the ANI method is considered the best option for establishing species boundaries and for accurately identifying microorganisms (Ciufo et al. 2018), and has been used here to classify two bacterial isolates.

Once identified, the ability to further interrogate the genome of an isolated microorganism is fundamental in understanding the potential role the microorganism may play in the environment and how it may respond to certain conditions. Genome annotation, the process of identifying and labelling features on a genome sequence (Richardson & Watson 2013; Seemann 2014), can therefore significantly contribute to the characterisation of an isolated microorganism. Automated genome annotation tools, such as the Rapid Annotation using Subsystem Technology (RAST) server (Aziz et al. 2008) and the Prokaryotic Genome Annotation Pipeline (PGAP) (Tatusova et al. 2016) from the National Center for Biotechnology Information (NCBI), can be used to predict the function of many genes and

provide an insight into the biochemical and physiological potential of a microorganism.

Importantly, the use of automated genome annotation tools has somewhat reduced the need for manual curation, and to some extent, the expertise required for genome annotation. This has made genome annotation more accessible to the scientific community. Furthermore, these tools have significantly increased the speed of genome annotation, which is now possible in a few days (Seemann 2014), contributing to the rapid growth of annotated genome databases. However, automated genome annotation pipelines should not be viewed as infallible, as they may introduce erroneous annotation (Richardson & Watson 2013), highlighting the importance and purpose of manual curation. This is perhaps best demonstrated when considering the basis of automated annotation, which is homology. Often, automated genome annotation pipelines transfer annotation to a newly discovered strain based on the closest annotated relative within a database (Richardson & Watson 2013). As a result, areas of interest within the newly discovered strain may not be annotated, as they are not always present in the closest relative (i.e. reference genome). Accordingly, the purpose of initially sequencing a strain, which is to establish how it differs genetically from its closest relatives, is somewhat limited, as the differences between query and subject strain are determined using a similarity-based method (Richardson & Watson 2013). Furthermore, previous misannotations or errors can be passed on to a newly annotated strain using automated pipelines (Loman et al. 2012). This can perpetuate indefinitely unless it is addressed via manual curation, causing erroneous annotation for multiple, possibly hundreds, of genomes. Even seemingly small errors, such as spelling mistakes, can cause difficulties, particularly for the users of genome databases searching for specific genes of interest. Unless resolved by manual curation, misspellings can go unnoticed and may result in the artificial separation of genes with identical function (Richardson & Watson 2013). The importance of manual curation is highlighted by the findings of Schnoes et al. (2009), which reported the lowest levels of misannotation and error in the manually curated Swiss-Prot database and the highest levels in databases primarily containing auto-annotated genome

sequences (e.g. TrEMBL). However, manual curation is labour-intensive, expensive, and cannot keep up with the quantity of genomic information currently being produced (Baumgartner Jr et al. 2007), highlighting the need for automated genome annotation pipelines, despite their disadvantages.

Automated genome annotation pipelines generally operate in a similar way. Prior to annotation, raw sequence reads from a microbial genome are assembled into contiguous sequences to form a draft genome (Markowitz et al. 2009). The draft genome is uploaded to the annotation pipeline in FASTA format. Gene prediction software, such as GLIMMER (Gene Locator and Interpolated Markov ModelER) (Delcher et al. 1999), is used to predict coding regions in the draft genome, based on a set of reference sequences. The coding regions are aligned to a previously annotated reference genome or an entire genome database, such as UniProt (UniProt Consortium 2019). The top hits are accepted and the annotation is transferred to genes that display high similarity (Richardson & Watson 2013). Manual curation provides quality control and involves the editing of annotated genomes in a genome browser. Gene structure is often reviewed first to ensure the coding region is correct before the identity of a gene is verified by comparing to a reference gene. Following successful identification, a function is assigned to the gene of interest. These curations are heavily informed by experimental evidence derived from a variety of techniques (Schnoes et al. 2009) such as transcriptomics, proteomics and the use of knock-out mutants. Provided annotation via the multitude of available tools is successful and is error-free, genome annotation provides a basis upon which other analytical techniques can be applied to further our understanding of the functioning of microorganisms and therefore improve their characterisation.

Proteomics, the large-scale analysis of proteins (Pandey & Mann 2000; Graves & Haystead 2002), is highly complementary to annotated genome data and is a technique that can be used to determine how protein expression within a microorganism changes in response to

different conditions. Individual microorganisms express an entire set of proteins, termed the proteome, at any given time in response to changes in their environment and following exposure to various stressors or nutrients. This can include sudden changes in temperature, salinity, and nutrient availability. Accordingly, proteomics can be used to provide an insight into the actual expression of genes and translation of mRNA in response to environmental change, rather than the potential expression of genes identified via genomic analyses (Karlsson et al. 2015). This can significantly improve our understanding of the metabolic and regulatory pathways that microorganisms use to function and survive. Genome annotation is a useful pre-requisite to proteomic analysis, as it provides information regarding the identity and function of protein-encoding genes in the organism of interest. It is also important to note that proteomic analysis can contribute to genome annotation by verifying a gene product (Pandey & Mann 2000; Ansong et al. 2008). Hypotheses regarding the presence and function of a particular gene can be formulated based on the outcome of a preliminary proteomic experiment. These hypotheses can be validated by performing a knockout experiment, whereby the gene of interest is made inoperative and a secondary proteomic experiment is performed to determine if the associated protein is expressed, and/or via relevant phenotypic assays. This type of analysis can be used to verify coding regions of a genomic sequence (Ansong et al. 2008) and conclusively assign a function to a gene.

Our current knowledge and understanding of the metabolic pathways used by microorganisms to utilise acetaldehyde as a carbon source are limited to a handful of studies. Halsey et al. (2017) proposed a potential pathway of acetaldehyde metabolism for SAR11, a clade of highly abundant and globally distributed Alphaproteobacteria represented by the type strain "*Candidatus* Pelagibacter ubique HTCC1062" (Tripp 2013). This pathway is initiated by the oxidation of acetaldehyde to acetate by the enzyme aldehyde dehydrogenase (ALDH) and results in acetaldehyde-derived carbon being oxidised to carbon dioxide or being assimilated into biomass (Halsey et al. 2017). Although the SAR11 ALDH genes thought to be responsible for acetaldehyde degradation clustered with related genes

of *Escherichia coli*, *Vibrio cholera* and *Ralstonia eutropha*, the ubiquity of microbial acetaldehyde degradation remains uncertain. Furthermore, it has yet to be determined whether the same metabolic pathway is used by other acetaldehyde-degrading microorganisms or if an alternative pathway exists. By performing random mutation analysis, Yoshida (2019) identified a previously unknown oligotrophic pathway in *Rhodococcus erythropolis* strain N9T-4 that enables this microorganism to utilise acetaldehyde in nutrient-limited conditions. Results from the random mutation library indicated that acetaldehyde was converted to acetate via ALDH activity. Acetate was converted to acetyl-CoA, which entered the tricarboxylic acid (TCA) cycle for energy production. Interestingly, under the oligotrophic conditions, part of the TCA cycle was bypassed by the glyoxylate shunt, which converts isocitrate to succinate and malate. These findings suggested that acetaldehyde metabolism and the glyoxylate shunt were essential to the oligotrophic growth of *R. erythropolis* strain N9T-4. Given that the majority of prokaryotic genomes contain ALDH-encoding genes (Sophos & Vasiliou 2003), and therefore possess the necessary enzymatic tools for acetaldehyde metabolism, it is possible that a significant number of acetaldehyde-degrading microorganisms have yet to be discovered. As more acetaldehyde-degrading microorganisms are identified, considerable progress will be made in better understanding the metabolic pathway(s) of acetaldehyde degradation, which are currently limited to the studies performed by Halsey et al. (2017) and Yoshida (2019).

In this study, the genomes of two bacterial isolates exhibiting the ability to utilise acetaldehyde as a sole carbon source in Chapter 3 were sequenced and annotated to further characterise them and to identify the genetic potential for acetaldehyde degradation. Having examined the annotated genomes for genes reported to be involved in acetaldehyde metabolism, LC-MS/MS shotgun proteomic analysis was used to determine the pathway(s) of acetaldehyde metabolism used by *Rhodococcus* strain A14; the fastest acetaldehyde-degrading bacterial isolate.

The following hypotheses were tested.

1. The genes for acetaldehyde metabolism, specifically aldehyde dehydrogenase-encoding genes, will be present in both bacterial genomes.

2. Large-scale changes in the metabolism and stress response of *Rhodococcus* strain A14 will be detected in the proteome following growth on acetaldehyde compared to growth on the control substrate, sodium succinate.

3. Specifically, aldehyde dehydrogenases will be significantly up-regulated in the proteome of *Rhodococcus* strain A14 when acetaldehyde is the only available carbon source.

This research will advance our understanding of the mechanisms of microbial acetaldehyde degradation and will assist in characterising two previously unidentified acetaldehyde degraders.

4.2 Methodology

4.2.1 Bacterial cultures and DNA extraction

Pure cultures of *Rhodococcus* strain A14 and *Bacillus* strain A17, previously isolated from the Colne Estuary, Essex, were grown on Difco™ marine agar 2216 medium (Section 3.2.1) and were incubated at 20°C. Colonies of each culture were harvested after 72 hours and 48 hours of growth for *Rhodococcus* strain A14 and *Bacillus* strain A17, respectively. DNA was extracted from harvested colonies using a DNeasy PowerSoil Kit (Qiagen), separated by agarose gel electrophoresis (1.0% w/v), stained with SYBR™ Safe (Invitrogen), and was viewed on a Gel Doc™ EZ gel documentation system (Bio-Rad). DNA extracts were quantified via Quant-IT™ PicoGreen dsDNA Assay Kit (Thermo Fisher Scientific) using a

Nanodrop 3300 Fluorospectrometer (Thermo Fisher Scientific).

4.2.2 Genome sequencing

DNA extracts (1.91 - 3.78 ng/μL) were sent to MicrobesNG, Birmingham (UK) for genome

sequencing via the Illumina HiSeq sequencing platform and assembly. The methods

performed by MicrobesNG can be found at www.microbesng.com/microbesng-faq/ and are

summarised here. DNA extracts were quantified in triplicate using a Quant-IT™ dsDNA

High-Sensitivity Assay Kit (Thermo Fisher Scientific). A Nextera XT DNA Library Preparation

Kit (Illumina) was used to prepare genomic DNA libraries following the manufacturer's

protocol with two modifications: 1) 2 ng of DNA instead of 1 ng was used as the input

material, and 2) the PCR elongation step was increased to 1 minute from 30 seconds. DNA

quantification and genomic library preparation were performed on a Hamilton Microlab STAR

automated liquid handling system. Pooled libraries were quantified using the Kapa

Biosystems Library Quantification Kit on a LightCycler 96 (Roche Life Science) qPCR

machine. Genomic libraries were sequenced via the Illumina HiSeq sequencing platform

using a 250 bp paired-end protocol. Adapter sequences on the resulting reads were trimmed

using Trimmomatic 0.30 (Bolger et al. 2014) with a sliding window quality cut-off of Q15.

SPAdes version 3.7 (Bankevich et al. 2012) was used for de-novo assembly and Prokka

version 1.11 (Seemann 2014) was used to annotate contigs.

4.2.3 Genome annotation

FASTA files of genome assemblies were retrieved from MicrobesNG. Contigs were

visualised in the sequence alignment editor BioEdit version 7.0 (Hall 1999), with contigs

<250 bp in length removed from the assembly. Quality-controlled genome assemblies were

uploaded in FASTA format to the Rapid Annotation using Subsystem Technology (RAST)

prokaryotic genome annotation service (Aziz et al. 2008; Overbeek et al. 2014; Brettin et al.

2015) for annotation. Genes were grouped into subsystems based on their predicted

functions, which collectively perform a specific biological process or contribute to a structural complex (Overbeek et al. 2005). Proteins derived from these genes were grouped into protein families, termed FIGfams (Meyer et al. 2009), based on their function (Davis et al. 2016). Proteins within a single FIGfam are isofunctional homologues and therefore have identical functional roles (Meyer et al. 2009).

The quality-controlled genome assembly of *Rhodococcus* strain A14 was also submitted in FASTA format to the National Center for Biotechnology Information (NCBI) for annotation via the Prokaryotic Genome Annotation Pipeline (PGAP) (Tatusova et al. 2016). Biosample data, including the taxonomic identity and isolation source of *Rhodococcus* strain A14, were first submitted to the NCBI and were assigned a biosample submission number (SAMN14345171). After initial review of the genome, contigs found to contain adapter sequences were trimmed, and three short contigs identified as contaminants (386-387 bp in length) were removed. The revised genome sequence was resubmitted for annotation via the Prokaryotic Genome Annotation Pipeline and was assigned the accession number JAAOQS000000000.1. The whole genome shotgun (WGS) project was deposited at the DNA Data Bank of Japan (DDBJ), European Nucleotide Archive (ENA) and GenBank under the accession JAAOQS000000000.1.

4.2.4 Genome analysis – Taxonomic classification

The genome sequences of *Rhodococcus* strain A14 and *Bacillus* strain A17 were analysed using the Microbial Genomes Atlas (MiGA) tool (Rodriguez-R et al. 2018), using the NCBI Prok database as reference. This tool was used to assess the quality of individual genomes and to identify the closest relatives within the NCBI Prok database. Quality scores for each genome were calculated as completeness (%) minus five times the contamination score (%). Completeness (%) was calculated by establishing the presence or absence of 106 single-copy genes which are observed in almost every prokaryotic genome. Contamination (%) was

measured by counting the frequency that these genes were present in more than one copy.

The closest relatives to *Rhodococcus* strain A14 and *Bacillus* strain A17 in the NCBI Prok database were identified using the Average Nucleotide Identity (ANI) and Average Amino Acid Identity (AAI) calculators (Rodriguez-R & Konstantinidis 2016). Using these tools, the genome sequences of both isolates were compared to publicly available reference genomes to produce ANI and AAI scores. ANI and AAI scores were calculated using the best hits (one-way ANI/AAI) and reciprocal best hits (two-way ANI/AAI) methods (Goris et al. 2007) to ensure reliable taxonomic classification. These scores were compared to predetermined threshold values to establish taxonomic assignment.

4.2.5 Proteomics method optimisation

4.2.5.1 Culture preparation

Rhodococcus strain A14 was selected as the representative bacterial isolate for proteomic analysis, investigating the response of the proteome to the metabolism of acetaldehyde in comparison to sodium succinate as a non-acetaldehyde control. This isolate was selected due to its ability to grow quickly, to rapidly degrade acetaldehyde and the ease in which proteins could be extracted. Sodium succinate was used as an alternative carbon source to acetaldehyde due to it being a simple carbon compound and for its role as a key intermediate in the tricarboxylic acid (TCA) cycle.

To determine the time taken for cultures of *Rhodococcus* strain A14 growing on acetaldehyde (5 mM; ≥ 99.5% purity, Sigma-Aldrich) or sodium succinate (5 mM; Fisher Chemical) to reach mid-exponential growth phase, a time-course experiment involving regular measurements of optical density (OD_{600}) and acetaldehyde degradation was performed. Initially, a pre-culture of *Rhodococcus* strain A14 was set up by inoculating

360 mL of ONR7a seawater-nutrient medium (Dyksterhouse et al. 1995) (Section 2.2.2) with a colony of *Rhodococcus* strain A14 grown on Difco™ marine agar 2216 medium. The pre-culture was grown with 5 mM of sodium succinate by adding 40 mL of sodium succinate stock (50 mM) (Section 4.2.5.2) and was incubated on an orbital shaker (75 rpm) at 30°C for 72 hours. The pre-culture was centrifuged at 5000 × g for 20 minutes and the supernatant removed. The cell pellet was washed with 100 mL of modified ONR7a seawater-nutrient medium (without $FeCl_2•4H_2O$), vortexed and centrifuged at 5000 × g for 20 minutes. This wash step was repeated to ensure that residual sodium succinate was removed. The washed cell pellet was resuspended with 100 mL of ONR7a seawater-nutrient medium and was briefly vortexed to homogenise the cells. The resuspended cells were transferred to a conical flask (500 mL) and were incubated on an orbital shaker (75 rpm) for 1 hour at 30°C to starve the cells of nutrients.

4.2.5.2 Stock preparation

To prepare a 50 mM acetaldehyde stock solution, 99.72 mL of Milli-Q water was spiked with 280 μL of acetaldehyde (≥ 99.5% purity; Sigma-Aldrich) in a 125 mL serum bottle. After spiking, the serum bottle was immediately capped with a polytetrafluoroethene (PTFE) -lined butyl septum (Agilent) to ensure gas-tight conditions. The serum bottle was inverted several times to mix. To prepare a 50 mM sodium succinate stock solution, 10.81 g of sodium succinate was dissolved in 800 mL of Milli-Q water and autoclaved.

4.2.5.3 Acetaldehyde degradation and optical density

To prepare acetaldehyde-grown cultures of *Rhodococcus* strain A14, 8.8 mL of ONR7a seawater-nutrient medium was initially added to 125 mL serum bottles. Each serum bottle was inoculated with 200 μL of washed, starved *Rhodococcus* strain A14 cells and capped with PTFE-lined butyl septa. A total of 1 mL of acetaldehyde stock solution (50 mM) was added to each serum bottle using a 1 mL syringe (5 mM final concentration). To ensure that

acetaldehyde degradation measured within serum bottles inoculated with *Rhodococcus* strain A14 cells was a result of microbial activity, no-inoculum controls were also set up by replacing the 200 µL of culture with additional ONR7a seawater-nutrient medium. To establish sodium succinate cultures, 8.8 mL of ONR7a seawater-nutrient medium, 1 mL of sodium succinate stock solution (50 mM) and 200 µL of washed, starved *Rhodococcus* strain A14 cells were added to 125 mL serum bottles. Serum bottles were capped with PTFE-lined butyl septa. To confirm that *Rhodococcus* strain A14 cells did not grow in the absence of a carbon and energy source, no-substrate controls were set up, in which a 1 mL aliquot of Milli-Q water was added to each serum bottle in place of acetaldehyde or sodium succinate. All serum bottles were incubated in the dark and on an orbital shaker (75 rpm) at 30°C for the duration of the experiment.

At each time interval (0, 4, 8, 16, 22, 28 and 42 hours) serum bottles containing acetaldehyde-grown cultures of *Rhodococcus* strain A14, and the no-inoculum controls, were measured in triplicate for acetaldehyde degradation using GC-FID, as described in Section 2.2.2.

After GC-FID analysis, the lids of serum bottles containing acetaldehyde-grown cultures of *Rhodococcus* strain A14 were removed under a fume hood to allow the remaining acetaldehyde to volatilise. The optical density of acetaldehyde-grown cultures was measured at a wavelength of 600 nm using a Jenway 7300 spectrophotometer. The optical densities of sodium succinate-grown cultures and the no-substrate controls were measured for the same time point. These measurements were performed in triplicate and were repeated at each time interval (Figure 4.1).

Tx

Measure acetaldehyde
concentration

Acetaldehyde   VS   No-Inoculum Controls

Measure OD$_{600}$

Acetaldehyde   VS   Sodium Succinate   VS   No-Substrate Controls
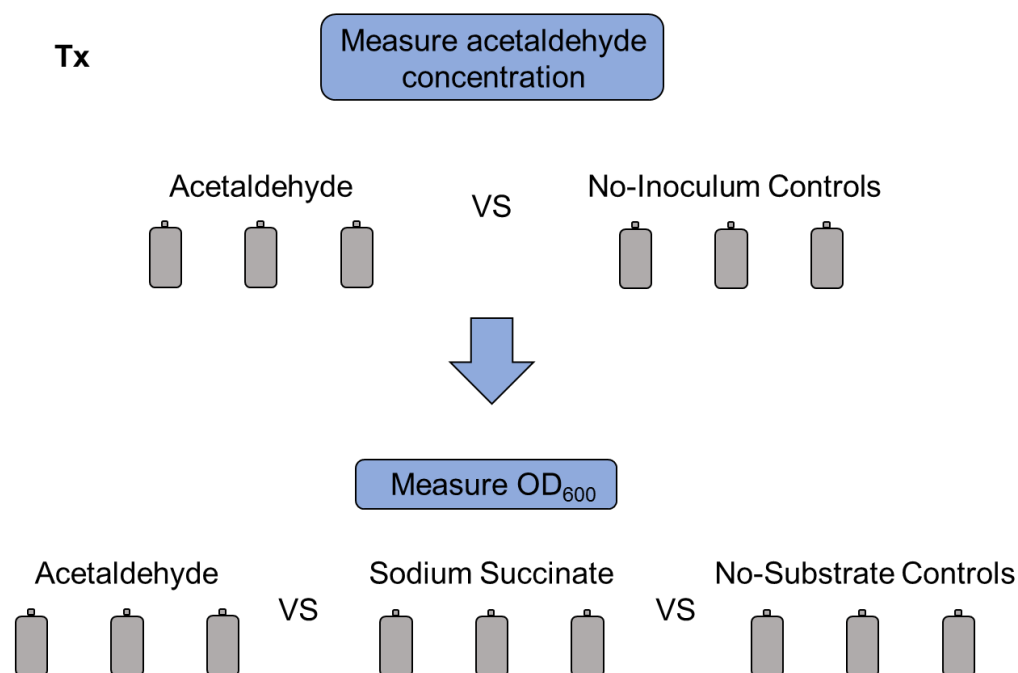
Figure 4.1 Workflow of the trial proteomic experiment after establishing a pre-culture of *Rhodococcus* strain A14. Acetaldehyde-grown cultures and the no-inoculum controls were measured for acetaldehyde degradation using GC-FID. Optical densities (OD$_{600}$) of the acetaldehyde-grown cultures, sodium succinate-grown cultures and the no-substrate controls were measured. Measurements were performed in triplicate and were repeated for each time point (Tx).

4.2.6 Proteomics

A fresh pre-culture of *Rhodococcus* strain A14 was prepared, washed, and starved following

the protocol described in Section 4.2.5.1. Acetaldehyde-grown cultures and sodium

succinate-grown cultures were set up as described in Section 4.2.5.3. A total of 20 replicates

were set up for each treatment. All serum bottles were incubated on an orbital shaker

(75 rpm) in the dark at 30°C for the duration of the experiment. Cultures were visually

inspected for growth every few hours.

The acetaldehyde-grown and sodium succinate-grown cultures of *Rhodococcus* strain A14

were harvested for cells after 56 hours and 32 hours of incubation, respectively. These

incubation times were selected based on the OD$_{600}$ and acetaldehyde concentrations

previously measured during the trial proteomic experiment (Figure 4.2). The OD$_{600}$ of

randomly selected cultures from both treatments was measured using a Jenway 7300 spectrophotometer to ensure that cultures had grown to an adequate density for harvesting and had reached the equivalent growth phase. An OD_{600} of 0.125 ± 0.009 (*n=4*) was measured for acetaldehyde-grown cultures, whilst an OD_{600} of 0.197 ± 0.005 (*n=4*) was measured for sodium succinate cultures. Within each treatment, groups of five individual replicates were pooled to produce a total of four replicates for cell harvesting. Pooled replicates (50 ml) were centrifuged at 11000 × *g* for 20 minutes (4°C) to produce a pellet. The supernatant was aspirated, and the pellet was transferred to a 1.5 mL microcentrifuge tube. Cell pellets were centrifuged at 7000 × *g* for 2 minutes to separate any residual liquid. The supernatant was removed, and the pellets were frozen at -80°C.

To prepare the samples for analysis using liquid chromatography-tandem mass spectrometry (LC-MS/MS) the cell pellets were thawed and washed with 2 mL of Dulbecco's phosphate-buffered saline. This solution was composed of 8 g of NaCl, 1.15 g of Na_2HPO_4, 0.2 g of KCl and 0.2 g of KH_2PO_4 in 1 L of Milli-Q water. Protein extraction and visualisation were performed as described by Gregson et al. (2020). Briefly, total protein was extracted by resuspending the cell pellets in 50 μL of protein extraction buffer (62.5 mM TRIS, 10% glycerol w/v, 12 mM dithiothreitol, 2% SDS v/v and 1 Pierce Protease Inhibitor Tablet per 50 ml) and heating the resuspended cell pellets in a water bath at 95°C for 12 minutes to lyse the cells. Resuspended cell pellets were centrifuged at 10500 × *g* for 5 minutes to remove cellular debris. Extracted proteins in the supernatant were visualised by SDS-PAGE. Briefly, 5 μL of loading buffer was added to 5 μL of protein extract and then incubated in a water bath at 90°C for 5 minutes. The loading-buffer stock solution was composed of 1.25 mL of TRIS-HCl (0.5 M), 2.5 mL of glycerol, 2 mL of SDS (10%), 0.2 mL of bromophenol blue (0.5%) and 3.55 mL of Milli-Q water. To prepare a working stock of loading buffer, 50 μL of 2-mercaptoethanol (Bio-Rad) was added to 950 μL of the loading-buffer stock solution. The denatured samples (5 μL) and 5 μL of PageRuler™ prestained protein ladder (Thermo

Fisher Scientific) were loaded onto a Mini-PROTEAN TGX precast 10% polyacrylamide gel (Bio-Rad). The loaded gel was run at 100 V for 1 hour using a 1× running buffer (15 g of TRIS, 72 g of glycine and 5 g of SDS in 1 L of Milli-Q water). The gel was stained overnight using Coomassie Brilliant Blue (0.1% Coomassie Brilliant Blue R-250, 50% methanol,10% glacial acetic acid) and was destained for 3 hours using a destaining solution (40% methanol, 10% glacial acetic acid). In collaboration with Dr Gergana Metodieva, an in-gel trypsin digest was used to cleave the extracted proteins into peptide fragments. Peptide fragments were extracted, dried and reconstituted in 20 μL of LC/MS-grade water containing 0.1% (v/v) formic acid, before being analysed on a hybrid linear trap quadrupole (LTQ)/Orbitrap Velos LC-MS/MS instrument (Thermo Fisher Scientific) following the method described by McKew et al. (2013). Briefly, fragmented peptide samples (2 μL) were injected from the microplate, desalted online, separated on a 15 cm-long pooled-tip nanocolumn, and were analysed by electrospray ionisation-tandem mass spectrometry using a hybrid LTQ/Orbitrap Velos LC-MS/MS instrument.

Initial data analysis was performed by Dr Metodi Metodiev in MaxQuant (Cox & Mann 2008), following the method of Gregson et al. (2019). Using the MaxQuant "Quant" module, raw data files from the LTQ/Orbitrap Velos instrument were converted to MSM files. Andromeda, an open-source search engine within MaxQuant (Cox et al. 2011), was used to identify peptides in sequence databases using the peptide fragmentation spectra. A false discovery rate (FDR) of 0.3% was used to filter peptides and proteins to obtain the final data set. Proteins were quantified by counting the number of MS/MS spectra that matched to the respective proteins. NCBI protein sequences from the *Rhodococcus* strain A14 genome were used for protein identification. Using the default settings in MaxQuant and Andromeda, proteins were validated with a minimum of one peptide. Proteins that were validated with only one peptide had to be clearly identified by peptides unique to the protein in question. Proteins identified as contaminants from the LC-MS/MS sample preparation, namely trypsin

and keratin, were removed from the final data set. To account for differences between runs, spectral counts were normalised to total spectral counts (where total spectral counts varied from 750 to 1647 per run). One acetaldehyde replicate was removed from the analysis due to an insufficient spectral count total (326). The final data set was filtered using two additional criteria: 1) Proteins with a mean spectral count of two or less in both treatments were removed; 2) Proteins with a mean spectral count of two or more in one treatment were removed if the protein was not detected in all of the replicates, and the mean spectral count in the alternative treatment was below two. Using these criteria, 363 proteins were removed from the final data set. The final data set included 252 proteins.

4.2.7 Statistical analysis and bioinformatics

Using the OMICS package of XLSTAT-Premium Version 2020.1.3 (Addinsoft), differential expression analysis was performed on the normalised spectral count data. To prevent proteins with missing values (zero) from being mistreated, the minimum expression value (*n=1*) was added to the mean spectral count of each protein within both treatments. This maintained the spectral count ratio between treatments. Differentially expressed proteins were identified by Students t-test with Tukey's Honestly Significant Difference (HSD) post-hoc test for pairwise comparisons, according to the factor "substrate" (two levels: acetaldehyde or sodium succinate). Post-hoc *p*-values were corrected using the Benjamini-Hochberg false discovery rate (Benjamini & Hochberg 1995). Proteins showing a significant increase ($p \leq 0.05$) in spectral counts, and therefore up-regulated during growth on acetaldehyde, were subjected to a BLASTp (Basic Local Alignment Search Tool) (Altschul et al. 1990) homology search using the NCBI nr (non-redundant sequences) database as reference. Protein family and domain analysis was performed in Pfam v32.0 (El-Gebali et al. 2019). The I-TASSER server (Zhang 2008) was used to predict secondary and tertiary protein structure and functional annotations on ligand-binding sites, and generated enzyme commission numbers and gene ontology terms. Fold-changes in protein spectral counts

between treatments were calculated by dividing acetaldehyde spectral counts ($n + 1$) by

sodium succinate spectral counts ($n + 1$).

4.3 Results and Discussion

4.3.1 Genome analysis

A total of 104 essential genes were detected within the *Rhodococcus* strain A14 genome

(Table 4.1), resulting in a completeness score of 98.10%. After applying a contamination

score of 7.50%, a final quality score of 60.59% (high) was calculated. The genome assembly

was composed of 359 contigs, with an N_{50} length of 66,413 bp. A total of 9,235 proteins were

predicted, with an average amino acid length of 308.65 and a coding density of 88.39%. For

Bacillus strain A17, a completeness score of 99.10% was calculated based on the detection

of 105 essential genes (Table 4.1). A quality score of 37.60% (intermediate) was determined

after applying a contamination score of 12.50%. The genome assembly of *Bacillus* strain

A17 was composed of 341 contigs and had an N_{50} length of 170,769 bp. The genome was

predicted to code for 6,128 proteins with an average amino acid length of 266.52 and a

coding density of 82.39%. A singular, complete 16S rRNA gene sequence was identified in

both genome assemblies.

Table 4.1 Genome assembly and annotation metrics of bacterial isolates *Rhodococcus* strain A14 and *Bacillus* strain A17. Assembly quality metrics are also shown. Genome analysis was performed in the Microbial Genomes Atlas (MiGA) tool (Rodriguez-R et al. 2018).

	Isolate	
	Rhodococcus strain A14	*Bacillus* strain A17
Total length (bp)	9,674,068	5,946,509
Contigs	359	341
N$_{50}$ (bp)	66,413	170,769
G+C content (mol %)	66.91	35.41
Predicted proteins	9,235	6,128
Average length (amino acids)	308.65	266.52
Coding density (%)	88.39	82.39
No. of complete 16S rRNA gene sequences	1	1
16S rRNA gene sequence length (bp)	1,516	1,550
Essential genes found (max. 106)	104	105
Completeness (%)	98.10	99.10
Contamination (%)	7.50	12.30
Quality score (%) *	60.59	37.60
Quality rating	High	Intermediate

* Quality score calculated as completeness (%) minus five times contamination (%).

The MiGA tool and ANI calculator were used to investigate the taxonomic relationships of the two acetaldehyde-degrading bacterial isolates (Table 4.2). An ANI value of >95% indicated that genomes belonged to the same species as the closest identified relative (Konstantinidis & Tiedje 2005; Goris et al. 2007; Richter & Rosselló-Móra 2009). Using the MiGA tool, *R. opacus* strain 1CP was identified as the closest relative within the NCBI Prok database to *Rhodococcus* strain A14, with an ANI score of 98.19%. *Rhodococcus* strain A14 was estimated to share 79.36% of its genome and 81.59% of its protein fraction with *R. opacus* strain 1CP. *Rhodococcus* strain A14 was confidently assigned to the species *Rhodococcus opacus* (p = 0.013), in agreement with the findings reported in Chapter 3. *B. mycoides* (ATCC 6462) was identified as the closest relative to *Bacillus* strain A17, with an ANI score of 94.29%, whilst *Bacillus* strain KBAB4 was confirmed as the next closest relative (94.14%). *Bacillus* strain A17 was estimated to share 82.26% of its genome and 78.89% of its protein fraction with *B. mycoides* (ATCC 6462). *Bacillus* strain A17 was confidently assigned to the species *Bacillus mycoides* (p = 0.028), in agreement with the findings reported in Chapter 3.

The aforementioned closest relatives of *Rhodococcus* strain A14 and *Bacillus* strain A17 were confirmed following independent genomic analysis using the ANI calculator (Table 4.2). Based on this analysis, *Rhodococcus* strain A14 was estimated to be most closely related to *R. opacus* strain 1CP (98.64%). *Rhodococcus* strain A14 was more distantly related to *Rhodococcus* strain WB9 (97.90%) and the type strains *R. wratislaviensis* (NBRC 100605) (94.42%), *R. opacus* (DSM 43205) (90.49%) and *R. erythropolis* (NBRC 15567) (79.35%). In agreement with the MiGA tool, *Bacillus* strain A17 was most closely related to *B. mycoides* (ATCC 6462) (94.42%) and *B. weihenstephanensis* (NBRC 101238) (94.42%). Following an ANI calculation between *B. mycoides* (ATCC 6462) and *B. weihenstephanensis* (NBRC 101238) (100%), and a review of the current nomenclature, it was concluded that these organisms were the same species; with *B. mycoides* formerly known as

B. weihenstephanensis. *Bacillus* strain A17 was more distantly related to *B. mycoides* strain KBAB4 (94.23%) and *B. thuringiensis* (DSM 2046) (88.52%).

Table 4.2 Closest relatives of bacterial isolates *Rhodococcus* strain A14 and *Bacillus* strain A17. Analysis was performed in the Microbial Genomes Atlas (MiGA) tool (Rodriguez-R et al. 2018) using the NCBI Prok database as reference. Average nucleotide identity (ANI) scores (%) were calculated using the ANI calculator (Rodriguez-R & Konstantinidis 2016) by comparing *Rhodococcus* strain A14 and *Bacillus* strain A17 with their closest relatives (based on entire genome sequence similarity). Results from the two-way ANI (reciprocal best hits) are shown. AAI: Average Amino Acid Identity.

	Isolate	
MiGA Analysis	*Rhodococcus* strain A14	*Bacillus* strain A17
Closest relative 1	*Rhodococcus opacus* strain 1CP	*Bacillus mycoides* (ATCC 6462)
ANI (%)	98.19	94.29
Genome fraction shared (%)	79.36	82.26
Species p-value	0.013	0.028
Sub-species p-value	0.364	0.378
AAI (%)	97.52	94.00
Protein fraction shared (%)	81.59	78.89
Closest relative 2	*Rhodococcus* strain WB9	*Bacillus mycoides* strain KBAB4
ANI (%)	97.58	94.14
Genome fraction shared (%)	84.66	76.69
AAI (%)	97.11	93.36
Protein fraction shared (%)	87.84	78.12
ANI Analysis (Two-way ANI) (%)		
R. opacus **strain 1CP**	98.64	
R. **strain WB9**	97.90	
R. wratislaviensis **(NBRC 100605)**	94.42	
R. opacus **(DSM 43205)**	90.49	
R. erythropolis **(NBRC 15567)**	79.35	
B. mycoides **(ATCC 6462)**		94.42
B. weihenstephanensis **(NBRC 101238)**		94.42
B mycoides **strain KBAB4**		94.23
B. thuringiensis **(DSM 2046)**		88.52

Rhodococcus opacus strain 1CP is a metabolically versatile member of the *Rhodococcus* genus (Gröning et al. 2014) originally isolated from contaminated soil using 4-chlorophenol and 2,4-dichlorophenol as sole carbon sources (Gorlatov et al. 1989). This versatility can be attributed to the genetic attributes commonly associated with rhodococci, including the possession of a large genome (4-10 Mbp), a considerable amount of gene redundancy (multiple enzyme homologs), the presence of large linear plasmids containing a diverse range of catabolic genes, and the ability to acquire a range of genes via linear plasmid-mediated horizontal gene transfer (Bell et al. 1998; Van Der Geize & Dijkhuizen 2004; Larkin et al. 2005; Tischler et al. 2009; Gröning et al. 2014; Cappelletti et al. 2019). These attributes enable members of this genus to degrade a wide range of organic compounds, including those with toxic and recalcitrant properties, such as chlorinated hydrocarbons and dibenzothiophene (Larkin et al. 2005; Cappelletti et al. 2019). Furthermore, these genetic properties allow rhodococci to resist stressful conditions, including desiccation, radiation and the presence of heavy metals (Cappelletti et al. 2019). It is unsurprising therefore, that *Rhodococcus* strain A14 demonstrated the ability to degrade acetaldehyde, particularly at the unnaturally high and generally toxic concentrations of 5 mM reported later in this chapter and 22.7 mM reported in Chapter 3. The genomic attributes of *Rhodococcus* strain A14, such as a genome length of 9.6 Mbp and a total of 9,235 predicted proteins, align with the features commonly observed in the *Rhodococcus* genus discussed above, which make this genus so genetically and physiologically diverse. A total of 55 aldehyde dehydrogenase-encoding genes and 6 acetaldehyde dehydrogenase-encoding genes were identified in the genome of *Rhodococcus* strain A14 following genome annotation in RAST. The presence of multiple aldehyde dehydrogenase and acetaldehyde dehydrogenase-encoding genes is also not surprising given the amount of gene redundancy often observed in the *Rhodococcus* genus. Furthermore, it has been shown that bacteria often possess 1-26 aldehyde dehydrogenase genes in their genome (Sophos & Vasiliou 2003), indicating that aldehyde dehydrogenases may exhibit functional diversity within and beyond the rhodococci. It is also

possible, given the ease in which members of the *Rhodococcus* genus exchange genetic

material through the conjugative transfer of plasmids (Larkin et al. 1998), that multiple

aldehyde dehydrogenase genes have been acquired via horizontal gene transfer. This may

account for the functional diversity of aldehyde dehydrogenase genes, as has been

observed for other catabolic genes encoding homologous enzymes involved in activities

such as chlorinated hydrocarbon transformation (Cappelletti et al. 2019). However, it is

important to note that ALDH genes may encode enzymes with different substrate

specificities and affinities (Cappelletti et al. 2019), and the presence of multiple ALDH genes

does not necessarily indicate redundancy. Given the genetic attributes of the *Rhodococcus*

genus and the functional diversity of genes, *Rhodococcus* strain A14 has significant

metabolic potential, which goes beyond the ability to degrade acetaldehyde. This metabolic

potential is dynamic based on the genomic flexibility of rhodococci.

Bacillus mycoides (ATCC 6462) is an aerobic, rod-shaped, spore-forming, non-motile

bacterium that forms rhizoidal colonies (Nakamura 1998). It is psychrotolerant, growing at

temperatures as low as 6°C, and is associated with food spoilage (Miller et al. 2018). *B.

mycoides* belongs to the *Bacillus cereus* group, which is composed of several *Bacillus*

species with closely related phylogeny, including *B. anthracis*, *B. cereus, B. thuringiensis*

and *B. pseudomycoides* (Ehling-Schulz et al. 2019). The genomes of these species are

highly conserved and typically range between 5.2-5.5 Mbp (Ehling-Schulz et al. 2019). A

marginally larger genome was measured for *Bacillus* strain A17, with a genome length of 5.9

Mbp. Although *Bacillus* strain A17 was confidently identified as *B. mycoides*, the phylogeny

of the *Bacillus cereus* group is highly uncertain. Ehling-Schulz et al. (2019), for example,

used multilocus sequence typing, amplified fragment-length polymorphism, and whole

genome sequencing to demonstrate the phylogenetic uncertainty of this group. Using these

techniques, 224 strains belonging to the *Bacillus cereus* group were separated into five

major clades but did not group exclusively by species. Consequently, species-level

identification of members of the *Bacillus cereus* group must be highly conservative to

minimise the misidentification of bacterial isolates. The delineation of species is complicated further by the conjugative transfer and transduction of plasmids, which has resulted in considerable diversity among strains of the *Bacillus cereus* group. Genetic exchange within the *Bacillus cereus* group is thought to be extensive, although less extensive than the *Rhodococcus* genus, and has been shown to include the exchange of virulence genes (Ehling-Schulz et al. 2019). This degree of exchange may explain the marginally larger genome of *Bacillus* strain A17 and may account for the protein coding density (82.39%) and the number of predicted proteins (6,128) in the genome; the latter being above the 5000 proteins encoded by a typical bacterial genome of 5 Mbp (Land et al. 2015). Following annotation in RAST, the genome of *Bacillus* strain A17 was shown to contain 6 aldehyde dehydrogenase-encoding genes and 3 acetaldehyde dehydrogenase-encoding genes. These genes may encode the enzymes needed for *Bacillus* strain A17 to degrade acetaldehyde.

4.3.2 Proteomics optimisation

During the preliminary growth experiment, *Rhodococcus* strain A14 demonstrated the ability to grow on both acetaldehyde (5 mM) and sodium succinate (5 mM) when these were the only available carbon sources (Figure 4.2). In both treatments, growth of *Rhodococcus* strain A14 was observed as suspended flocs. During growth on acetaldehyde, *Rhodococcus* strain A14 grew slowly, with an OD_{600} above 0.1 observed only after 42 hours of incubation. This may be attributed to the unnaturally high, and possibly toxic, concentrations of acetaldehyde used in this experiment, which may inhibit the regular metabolic activities of *Rhodococcus* strain A14. Despite this, acetaldehyde degradation was initially detected after 16 hours of incubation and complete acetaldehyde degradation was achieved following 42 hours of growth. The initial lag in acetaldehyde degradation likely represents the time required for the synthesis of proteins involved in acetaldehyde metabolism, such as aldehyde dehydrogenase enzymes, and possibly indicates a stress response by *Rhodococcus* strain

A14. After 42 hours of incubation, the proteome of *Rhodococcus* strain A14 may have fully shifted towards acetaldehyde metabolism, resulting in complete utilisation of the carbon source. This proteomic adjustment likely occurred after 22 to 28 hours of incubation when acetaldehyde degradation became considerably faster. Acetaldehyde concentration in the no-inoculum control bottles remained constant throughout the experiment, following an initial increase within the first 8 hours of incubation. This initial increase in concentration was attributed to the equilibration of acetaldehyde in the headspace of serum bottles. A similar increase in concentration during the first 8 hours of incubation was also measured in serum bottles containing acetaldehyde-grown cultures of *Rhodococcus* strain A14. Compared to the acetaldehyde treatment, sodium succinate-grown cultures of *Rhodococcus* strain A14 grew rapidly. Following 16 hours of incubation an OD_{600} of 0.117 was measured for sodium succinate-grown cultures. This can be attributed to sodium succinate being a simple, non-toxic carbon compound, which is readily utilised by microorganisms. Furthermore, enzymes necessary for sodium succinate metabolism and the utilisation of its derivatives, including enzymes that form part of the TCA cycle, are likely to be constitutively expressed given the importance of these enzymes to regular metabolic activity. Consequently, the proteome of *Rhodococcus* strain A14 required little adjustment when sodium succinate was the sole carbon source. The optical density of *Rhodococcus* strain A14 peaked after 28 hours of incubation (0.194) and was maintained for the remainder of the experiment (0.191) (Figure 4.2). Growth was not observed in the no-substrate controls throughout the experiment, with OD_{600} values consistently less than 0.035.
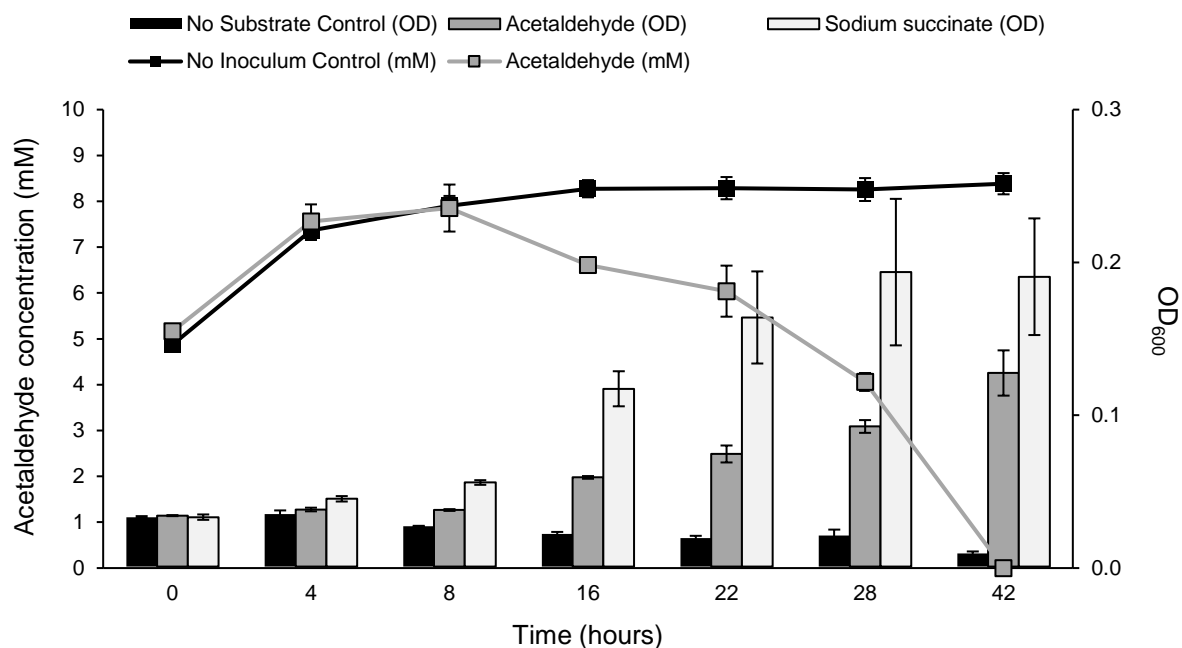
Figure 4.2 Growth of *Rhodococcus* strain A14 in the presence of acetaldehyde (5 mM) and sodium succinate (5 mM) represented as optical density (OD_{600}; bars), and the associated concentration of acetaldehyde in the headspace of serum bottles (lines). The mean of three replicates is plotted for each treatment (± S.E.). Serum bottles were incubated on an orbital shaker (75 rpm) in the dark at 30°C.

4.3.3 Proteomics

4.3.3.1 Acetaldehyde metabolism and the TCA cycle

A total of 9790 MS/MS spectra were assigned to 252 proteins (average of 1399 spectral counts per replicate and ranging from 1 to 86 spectral counts per protein) following the application of criteria used for data filtering (Section 4.2.6). Of the 252 proteins detected in the proteome of *Rhodococcus* strain A14 following growth on acetaldehyde and sodium succinate, 48 proteins were significantly differentially expressed across the two treatments (Figure 4.3). In the acetaldehyde treatment, 33 proteins were significantly up-regulated, whilst 15 proteins were significantly down-regulated, relative to the sodium succinate treatment.
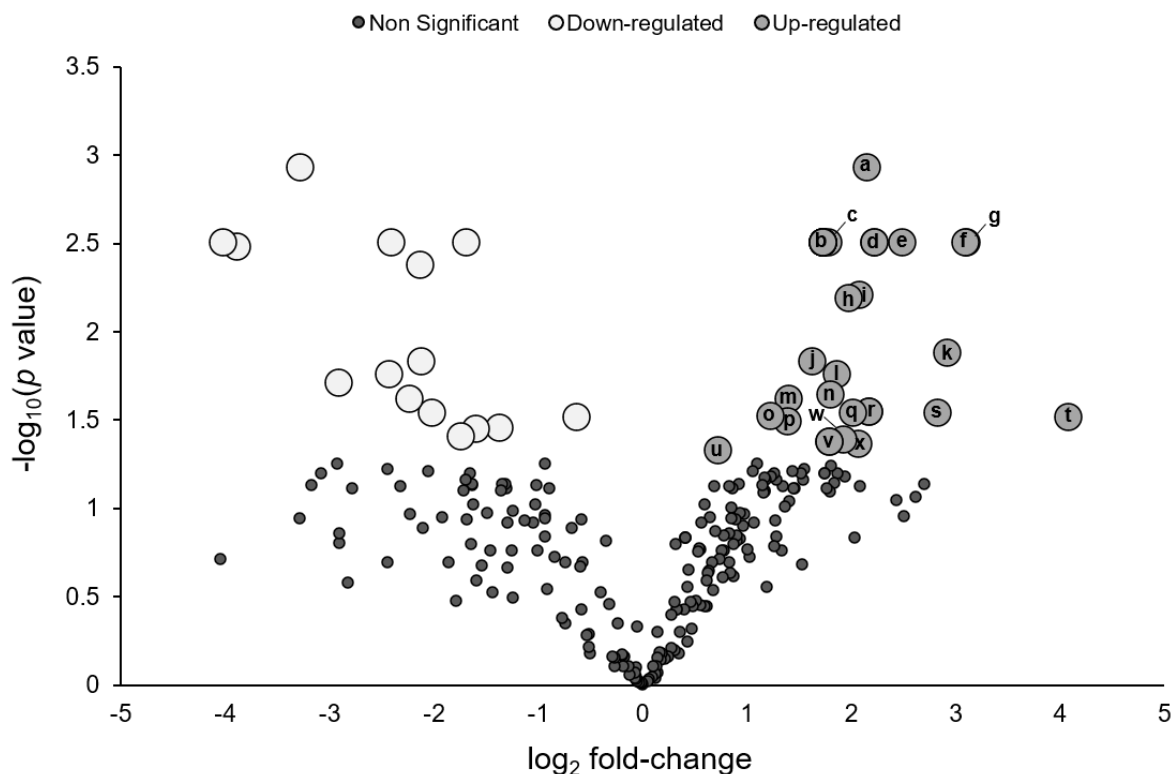
Figure 4.3 Volcano plot of normalised LC-MS/MS spectral counts comparing *Rhodococcus* strain A14 protein abundance during growth on sodium succinate (5 mM) and acetaldehyde (5 mM). Large circles (light and dark grey) represent differentially expressed proteins with *p*-values below 0.05. Large, dark grey circles containing letters represent proteins up-regulated during growth on acetaldehyde. a: dihydrolipoyl dehydrogenase (NHU42864.1); b: ethanolamine ammonia-lyase (NHU43876.1), rod-shape determining protein (NHU43240.1), 30S ribosomal protein S19 (NHU42293.1), RDD family protein (NHU42558.1), fatty acid-binding protein (NHU44612.1), GatB/YqeY domain-containing protein (NHU45627.1), tetratricopeptide repeat protein (NHU44386.1); c: aconitate hydratase (NHU47266.1); d: aldehyde dehydrogenase (NHU42048.1), FAD-dependent oxidoreductase (NHU42620.1); e: pyridoxal 5'-phosphate synthase (NHU46072.1); f: isocitrate lyase (NHU42882.1); g: aldehyde dehydrogenase (NHU43881.1); h: copper transporter (NHU47624.1); i: acetyl-CoA carboxylase subunit (biotin carboxylase) (NHU43406.1); j: 30S ribosomal protein S3 (NHU42295.1); k: penicillin-binding protein (NHU46759.1); l: phosphoenolpyruvate carboxykinase (NHU47300.1); m: Asp-tRNA/Glu-tRNA amidotransferase (NHU41287.1); n: transcription termination factor Rho (NHU47554.1); o: cold-shock protein (NHU45589.1); p: ribosome recycling factor (NHU41368.1); q: hypothetical protein (NHU44082.1); r: AMP-binding protein (NHU42462.1), adenosylhomocysteinase (NHU48026.1); s: sulfurtransferase (NHU49432.1); t: Rne/Rng family ribonuclease (NHU46057.1); u: phosphoglycerate dehydrogenase (NHU41296.1); v: inositol-3-phosphate synthase (NHU42723.1), RidA family protein (NHU49466.1); w: PDZ domain-containing protein (NHU44903.1); x: redox-regulated ATPase (YchF) (NHU41468.1).

Glycolysis / Gluconeogenesis
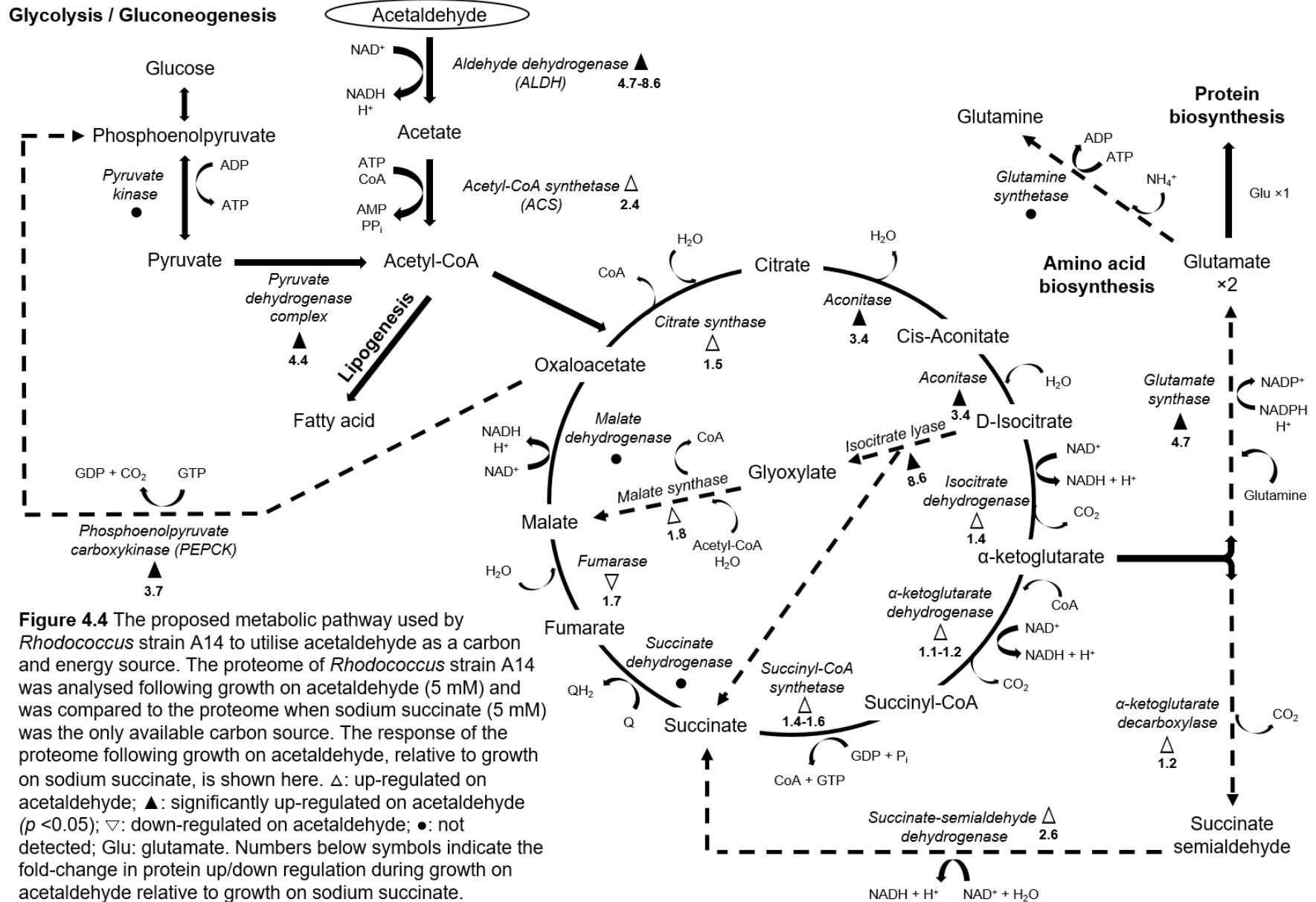
Figure 4.4 The proposed metabolic pathway used by *Rhodococcus* strain A14 to utilise acetaldehyde as a carbon and energy source. The proteome of *Rhodococcus* strain A14 was analysed following growth on acetaldehyde (5 mM) and was compared to the proteome when sodium succinate (5 mM) was the only available carbon source. The response of the proteome following growth on acetaldehyde, relative to growth on sodium succinate, is shown here. $\triangle$: up-regulated on acetaldehyde; $\blacktriangle$: significantly up-regulated on acetaldehyde (p <0.05); $\triangledown$: down-regulated on acetaldehyde; $\bullet$: not detected; Glu: glutamate. Numbers below symbols indicate the fold-change in protein up/down regulation during growth on acetaldehyde relative to growth on sodium succinate.

Of the 33 proteins with increased biosynthesis during growth on acetaldehyde, two were identified as having a role in the initial catabolism of acetaldehyde (Figure 4.5a). The two aldehyde dehydrogenases that had significantly higher spectral counts when *Rhodococcus* strain A14 was grown on acetaldehyde were NHU42048.1 and NHU43881.1. It is reasonable to propose that these proteins perform the initial step of acetaldehyde degradation, converting acetaldehyde to acetate via the reduction of the oxidised form of cofactor nicotinamide adenine dinucleotide (NAD^+) to NADH. Relative to the sodium succinate treatment, a fold-change of 4.7 and 8.6 was measured for aldehyde dehydrogenases NHU42048.1 and NHU43881.1 respectively, during growth on acetaldehyde (Figure 4.4). The initial catabolism of acetaldehyde by aldehyde dehydrogenase enzymes has previously been suggested. Halsey et al. (2017), for example, demonstrated that SAR11 strains HTCC1062 and HTCC7211 could oxidise acetaldehyde to CO_2 and incorporated ~30% of the utilised acetaldehyde into biomass (Halsey et al. 2017). By exploring their genomes, this group identified two putative aldehyde dehydrogenase genes, which clustered with *aldB* genes from *Escherichia coli*, *Vibrio cholera* and *Ralstonia eutropha*. The proteins encoded by these *aldB* genes have been shown to function as aldehyde dehydrogenase B enzymes, leading Halsey et al. (2017) to conclude that these aldehyde dehydrogenases were likely to be responsible for acetaldehyde oxidation. Furthermore, Halsey et al. (2017) identified a SAR11 gene with 44% sequence similarity to the *E. coli aldH* gene. The encoded protein has also been shown to function as an aldehyde dehydrogenase, but with low activity for acetaldehyde (Jo et al. 2008). These results are not conclusive in identifying the specific aldehyde dehydrogenase(s) responsible for the oxidation of acetaldehyde, primarily because SAR11 genomes, and bacterial genomes in general, contain multiple, paralogous aldehyde dehydrogenase genes (Sophos & Vasiliou 2003; Halsey et al. 2017). However, these results provide clear evidence that aldehyde dehydrogenases are involved in the initial step of acetaldehyde degradation, as suggested in this study.

Although not significantly up-regulated during growth on acetaldehyde, spectral counts of an

acetyl-CoA synthetase (NHU45608.1) were 2.4-fold higher when acetaldehyde was the only available carbon source (Figure 4.5a). This enzyme catalyses the conversion of acetate, the primary derivative of acetaldehyde, to acetyl-CoA, which enters the TCA cycle for energy production and is also utilised during lipogenesis (Brown et al. 1977) (Figure 4.4). This enzymatic reaction requires one adenosine triphosphate (ATP) and one coenzyme A (CoA) molecule. The putative pathway of acetaldehyde metabolism suggested by Halsey et al. (2017) for the SAR11 clade implies that acetyl-CoA synthetase (also known as acetate-CoA ligase) performs the second step of acetaldehyde metabolism, by converting acetate to acetyl-CoA. The up-regulation of acetyl-CoA synthetase NHU45608.1 in the proteome of the acetaldehyde-grown culture of *Rhodococcus* strain A14 provides further evidence for the initial steps of acetaldehyde metabolism proposed by Halsey et al. (2017). It is reasonable to suggest therefore that the primary and secondary reactions involved in acetaldehyde metabolism are likely to be conserved across multiple bacterial genera.

An ethanolamine ammonia-lyase (NHU43876.1), responsible for the conversion of ethanolamine to acetaldehyde and ammonia (NH_3) (Tsoy et al. 2009), was also significantly up-regulated when *Rhodococcus* strain A14 was grown on acetaldehyde (Figure 4.5a). The up-regulation of this enzyme was unexpected given that acetaldehyde was the only carbon source available to *Rhodococcus* strain A14. A potential source of ethanolamine may have been phosphatidylethanolamine, a phospholipid found in abundance in bacterial cell membranes (Garsin 2010). Using phosphodiesterase enzymes, phosphatidylethanolamine can be converted to glycerol and ethanolamine, with the latter cleaved into acetaldehyde and ammonia via ethanolamine ammonia-lyase activity (Garsin 2010). This process has been extensively studied in *Salmonella typhimurium*, where ethanolamine utilisation has been shown to occur within a multiprotein complex termed the carboxysome (Penrod & Roth 2006). The formation of this structure ensures acetaldehyde is compartmentalised to protect the cell from its toxic properties and to prevent the loss of an important carbon source

(Penrod & Roth 2006). It is not currently known whether carboxysome formation occurs in *Rhodococcus* strain A14, however, Yoshida et al. (2017) demonstrated that *Rhodococcus erythropolis* strain N9T-4 could form intracellular compartments termed oligobodies, although the physiological role of these structures was not determined. The up-regulation of ethanolamine ammonia-lyase (NHU43876.1) and the associated production of acetaldehyde may, in part, account for the up-regulation of aldehyde dehydrogenases NHU42048.1 and NHU43881.1 in the acetaldehyde-grown culture of *Rhodococcus* strain A14 (Figure 4.5a). However, it is difficult to determine the proportion of aldehyde dehydrogenase up-regulation that can be attributed to internal or external sources of acetaldehyde. The up-regulation of ethanolamine ammonia-lyase (NHU43876.1) may also indicate a stress response by *Rhodococcus* strain A14 to acetaldehyde. In the presence of aldehydes, cell membrane lipids, including phosphatidylethanolamine, can be modified, resulting in significant damage to the cell (Guo et al. 2012). To mitigate potential cellular damage, phosphodiesterase enzymes are used to catalyse the conversion of modified phosphatidylethanolamine to glycerol and ethanolamine, with ethanolamine converted to acetaldehyde and ammonia via ethanolamine ammonia-lyase. Accordingly, in the presence of acetaldehyde, phosphatidyl-ethanolamine in the cell membrane of *Rhodococcus* strain A14 may have been modified, resulting in the up-regulation of ethanolamine ammonia-lyase (NHU43876.1). However, other enzymes involved in membrane lipid metabolism were not significantly up-regulated in the proteome of *Rhodococcus* strain A14 during growth on acetaldehyde, making it difficult to confidently determine whether ethanolamine ammonia-lyase (NHU43876.1) was up-regulated as part of a stress response. Further investigation is necessary to determine the role of ethanolamine ammonia-lyase (NHU43876.1) and other enzymes in the stress response. This may include the growth of *Rhodococcus* strain A14 on a range of aldehydes compared to a control substrate, followed by proteomic analysis to establish whether ethanolamine ammonia-lyase (NHU43876.1) is exclusively up-regulated during growth on aldehydes.

Two proteins involved in the TCA cycle were significantly up-regulated during growth on acetaldehyde. Spectral counts of aconitate hydratase (NHU47266.1), an enzyme which catalyses the isomerisation of citrate to isocitrate via a *cis*-aconitate intermediate (Baothman et al. 2013), were 3.4-fold higher in the acetaldehyde treatment (Figure 4.5b). A dihydrolipoyl dehydrogenase (NHU42864.1) was also significantly up-regulated when acetaldehyde was the sole source of carbon (Figure 4.5b). This protein is the E3 subunit of two enzymatic complexes, namely the α-ketoglutarate dehydrogenase complex and the pyruvate dehydrogenase complex (De Kok et al. 1998). These complexes share the same subunit structure and consequently use the same coenzymes to catalyse enzymatic reactions (De Kok et al. 1998). In the TCA cycle, the α-ketoglutarate dehydrogenase complex catalyses the conversion of α-ketoglutarate to succinyl-CoA, with dihydrolipoyl dehydrogenase converting dihydrolipoate to lipoate. Dihydrolipoyl dehydrogenase performs the same reaction as part of the pyruvate dehydrogenase complex, however, this enzymatic complex catalyses the conversion of pyruvate to acetyl-CoA (De Kok et al. 1998). The E2 subunit of the α-ketoglutarate dehydrogenase complex, dihydrolipoamide succinyltransferase (NHU45763.1), was also detected, however, spectral counts were not significantly different between the acetaldehyde and sodium succinate treatments (Figure 4.5b). Additional enzymatic components of the TCA cycle, including citrate synthase (NHU48236.1), NADP-dependent isocitrate dehydrogenase (NHU42402.1), succinate-CoA ligase subunit alpha (NHU45992.1), ADP-forming succinate-CoA ligase subunit beta (NHU45991.1) and fumarate hydratase (class II) (NHU41484.1) were detected in the proteome of *Rhodococcus* strain A14 (Figure 4.5b). With the exception of fumarate hydratase (class II) (NHU41484.1), spectral counts of these proteins were higher in the acetaldehyde treatment, however, differences between treatments were not significant. This is likely due to the constitutive expression of proteins involved in the TCA cycle irrespective of carbon source, as this pathway is the main source of cellular energy under aerobic conditions (Ma et al. 2018). Two enzymes integral to the TCA cycle, succinate dehydrogenase and malate dehydrogenase, were not detected in the *Rhodococcus* strain A14 proteome (Figure 4.4).
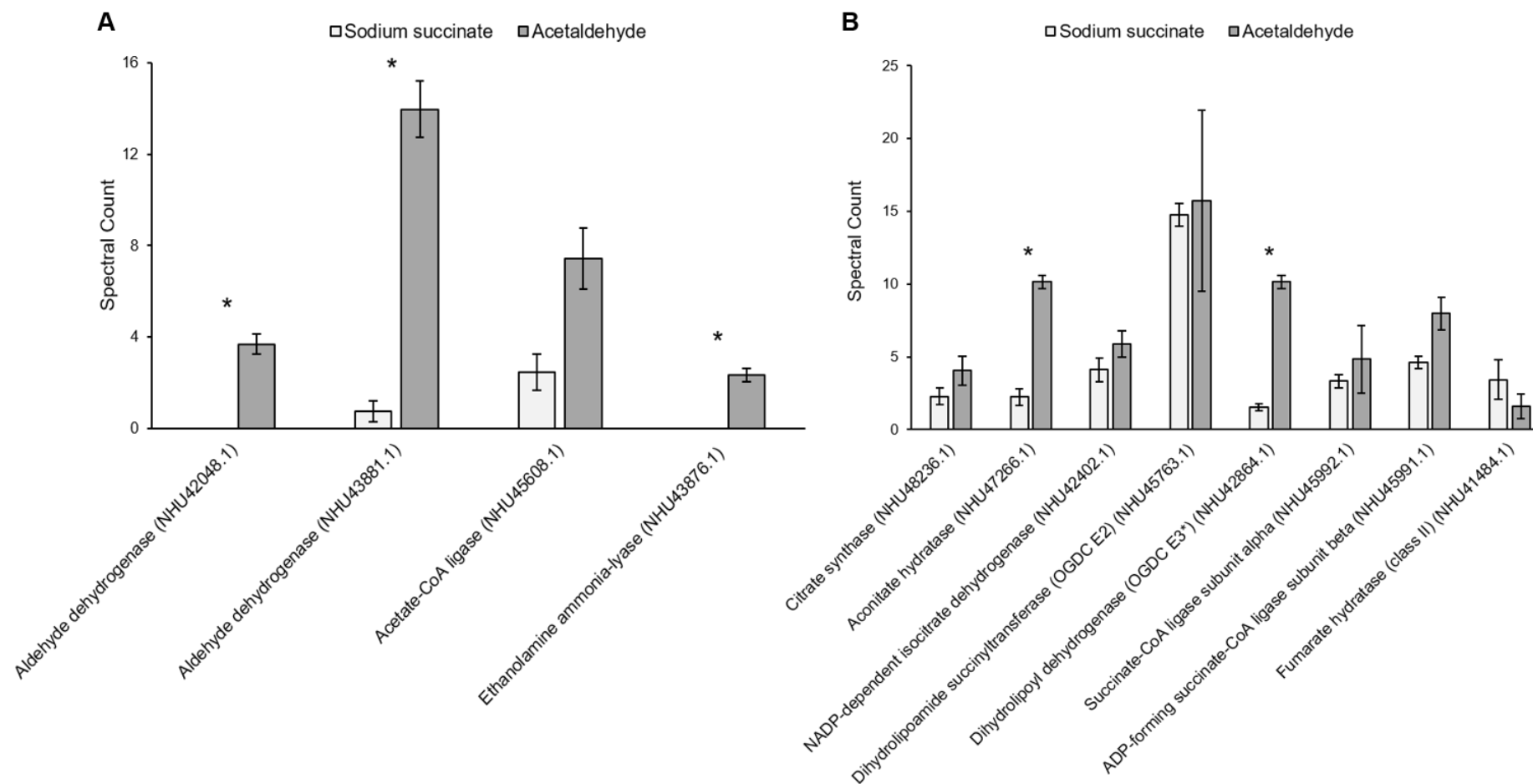
Figure 4.5 Normalised spectral counts of differentially expressed proteins in *Rhodococcus* strain A14 during growth on acetaldehyde (5 mM) (dark grey) and sodium succinate (5 mM) (light grey). A. Normalised spectral counts of proteins involved in the initial catabolism of acetaldehyde and its primary derivative, acetate. B. Normalised spectral counts of proteins belonging to the TCA cycle. The mean of three replicates is plotted for acetaldehyde spectral counts, whilst the mean of four replicates is plotted for sodium succinate spectral counts (± S.E.). * indicates significant difference between treatments (*p* <0.01); OGDC E3*: possible E3 subunit of α-ketoglutarate dehydrogenase complex.

4.3.3.2 The glyoxylate shunt and alternative metabolic pathways

Proteins constituting the glyoxylate shunt were detected in both the acetaldehyde and sodium succinate treatment (Figure 4.6). Isocitrate lyase (NHU42882.1), which catalyses the cleavage of isocitrate to glyoxylate and succinate (Dolan & Welch 2018), was significantly up-regulated when acetaldehyde was the sole carbon source. Relative to the sodium succinate treatment, spectral counts of isocitrate lyase NHU42882.1 increased 8.6-fold when *Rhodococcus* strain A14 was grown on acetaldehyde (Figure 4.4). Spectral counts of malate synthase (isoform G) (NHU49665.1), which uses acetyl-CoA and H_2O to convert glyoxylate to malate (Dolan & Welch 2018), were higher in the acetaldehyde treatment (1.8-fold), but this difference was not significant (Figure 4.6). The up-regulation of the glyoxylate shunt during growth on acetaldehyde indicates that *Rhodococcus* strain A14 shifted towards the conservation of acetaldehyde-derived carbon by bypassing the oxidative decarboxylation steps of the TCA cycle, which result in the loss of carbon as CO_2. The glyoxylate shunt is often up-regulated under conditions of oxidative and physiological stress (Ahn et al. 2016; Dolan & Welch 2018), and when acetyl-CoA is a direct product of a metabolic pathway (Ahn et al. 2016). As acetyl-CoA is a derivative of acetaldehyde, it is likely that *Rhodococcus* strain A14 responded to the carbon source, although it is also likely that growth on acetaldehyde induced physiological stress in *Rhodococcus* strain A14 due to its toxic properties, particularly at concentrations of 5 mM. In all circumstances, the up-regulation of the glyoxylate shunt indicates the preservation of carbon for biomass generation and growth, which is achieved by producing the gluconeogenic precursor, malate (Dolan & Welch 2018). It is important to note, however, that the up-regulation of the glyoxylate shunt is not an all-or-nothing switch between this and the complete TCA cycle (Dolan & Welch 2018). This is demonstrated by the continued expression of the bypassed components of the TCA cycle by *Rhodococcus* strain A14 when acetaldehyde was the sole carbon source (Figure 4.4), including NADP-dependent isocitrate dehydrogenase (NHU42402.1), succinate-CoA ligase subunit alpha (NHU45992.1), ADP-forming succinate-CoA ligase subunit beta

(NHU45991.1) and two subunits of the α-ketoglutarate dehydrogenase complex (NHU45763.1 & NHU42864.1) (Figure 4.5b). This partitioning of substrate-derived carbon helps to maintain a balance between energy and gluconeogenic precursor production (Dolan & Welch 2018). Interestingly, the glyoxylate shunt and gluconeogenesis have previously been identified as essential pathways in the oligotrophic growth of *Rhodococcus erythropolis* strain N9T-4 (Yano et al. 2015), a more distant relative of *Rhodococcus* strain A14 (Table 4.2). In this study, Yano et al. (2015) used deletion mutants to identify the genes essential for oligotrophic growth and obtained mutants with *aceA*, *aceB*, and *pckG* deletions, encoding isocitrate lyase, malate synthase and phosphoenolpyruvate carboxykinase, respectively. It was concluded that these proteins, and their associated metabolic pathways, were fundamental to the oligotrophy of *R. erythropolis* strain N9T-4. Although nutrients were in abundance in the current study, the findings of Yano et al. (2015) suggest that *Rhodococcus* strain A14 may also possess the ability to grow under oligotrophic conditions. These pathways may provide *Rhodococcus* strain A14 with the advantage of being able to tolerate temporary nutrient limitation whilst continuing to grow, and consequently may increase its range of environmental niches. This will require further investigation in future studies.

Although not significantly differentially expressed, proteins involved in an alternative pathway for α-ketoglutarate utilisation were detected following the growth of *Rhodococcus* strain A14 on acetaldehyde and sodium succinate. α-ketoglutarate decarboxylase (NHU44417.1), responsible for the interconversion of α-ketoglutarate to succinate semialdehyde and CO_2, was detected (Figure 4.6), however, only a 1.2-fold increase in spectral counts was measured in the acetaldehyde treatment (Figure 4.4). Similarly, an NAD-dependent succinate-semialdehyde dehydrogenase (NHU44514.1), which catalyses the interconversion of succinate semialdehyde to succinate, was detected (Figure 4.6). A 2.6-fold increase in protein abundance was measured following the growth of *Rhodococcus* strain A14 on acetaldehyde (Figure 4.4). Together these proteins facilitate the utilisation of α-ketoglutarate, whilst circumventing part of the TCA cycle that employs α-ketoglutarate dehydrogenase and

succinyl-CoA synthetase to convert α-ketoglutarate to succinate via a succinyl-CoA intermediate (Figure 4.4). The same alternative pathway for succinate production has been observed in oligotrophic *R. erythropolis* strain N9T-4 (Yano et al. 2015). Using enzymatic assays, the activity of all TCA cycle enzymes was detected in cell-free extracts of *R. erythropolis* strain N9T-4, with exception to α-ketoglutarate dehydrogenase. Instead, considerable α-ketoglutarate decarboxylase activity was detected, whilst moderate activity was measured for succinate semialdehyde dehydrogenase. It was concluded that *R. erythropolis* strain N9T-4 possesses a variant of the TCA cycle that uses succinate semialdehyde instead of succinyl-CoA as an intermediate in succinate production (Yano et al. 2015). This bypass is thought to conserve CoA, which can then contribute to acetyl-CoA synthesis that is necessary for the glyoxylate shunt. Combined with the significant increased biosynthesis of isocitrate lyase (NHU42882.1) and the higher spectral counts of malate synthase (isoform G) (NHU49665.1) (Figure 4.6), the expression of α-ketoglutarate decarboxylase (NHU44417.1) and NAD-dependent succinate-semialdehyde dehydrogenase (NHU44514.1), suggest that a similar metabolic pathway is used by *Rhodococcus* strain A14 when grown on acetaldehyde. This metabolic pathway utilises the same variant of the TCA cycle employed by *R. erythropolis* strain N9T-4.

Phosphoenolpyruvate carboxykinase (PEPCK) (NHU47300.1) was significantly up-regulated during the growth of *Rhodococcus* strain A14 on acetaldehyde (Figure 4.6). In the presence of guanosine-5'-triphosphate (GTP), PEPCK decarboxylates and phosphorylates oxaloacetate, derived from the TCA cycle, to phosphoenolpyruvate (PEP) (Figure 4.4). This is the first committed step of gluconeogenesis. Spectral counts of PEPCK were 3.7-fold higher in the acetaldehyde treatment (Figure 4.4). Additional proteins involved in gluconeogenesis were also detected within the proteome of *Rhodococcus* strain A14, including fructose bisphosphatase (class II) (NHU41483.1) and pyruvate carboxylase (NHU41322.1) (Figure 4.6). Although these proteins were more abundant in the acetaldehyde treatment, spectral counts were not significantly different. The significant up-

regulation of PEPCK (NHU47300.1) in the acetaldehyde treatment further implies that *Rhodococcus* strain A14 utilises the same metabolic pathway as *R. erythropolis* strain N9T-4 described by Yano et al. (2015). The increase in PEPCK (NHU47300.1) expression implies the presence of the gluconeogenic precursors malate and oxaloacetate. As both components of the glyoxylate shunt were up-regulated during growth on acetaldehyde, a supply of malate was readily available to PEPCK (NHU47300.1). This is strong evidence that, in the presence of acetaldehyde, *Rhodococcus* strain A14 commits to gluconeogenesis, ensuring that carbon is conserved for growth. Although not significantly up-regulated, the higher spectral counts of fructose bisphosphatase (class II) (NHU41483.1) and pyruvate carboxylase (NHU41322.1) are consistent with a commitment to gluconeogenesis.

Proteins with a dual role in gluconeogenesis and glycolysis, namely fructose-bisphosphate aldolase (class II) (NHU45472.1), glyceraldehyde-3-phosphate dehydrogenase (NHU48286.1) and phosphopyruvate hydratase (NHU41572.1) were detected in both treatments (Figure 4.6). With the exception of fructose-bisphosphate aldolase (class II) (NHU45472.1), these proteins were more abundant in the sodium succinate treatment, however spectral counts were not significantly different between treatments (Figure 4.6). The detection of these proteins in the acetaldehyde treatment, together with the significant up-regulation of PEPCK (NHU47300.1), further implies the commitment of *Rhodococcus* strain A14 to gluconeogenesis when acetaldehyde was the sole carbon source. Their detection in the sodium succinate treatment may be a result of constitutive expression, given the importance of both glycolysis and gluconeogenesis to regular metabolic activity. However, as PEPCK (NHU47300.1) was not up-regulated in the presence of sodium succinate, it is unlikely that these proteins were expressed for gluconeogenesis and may therefore have been involved in glycolysis.
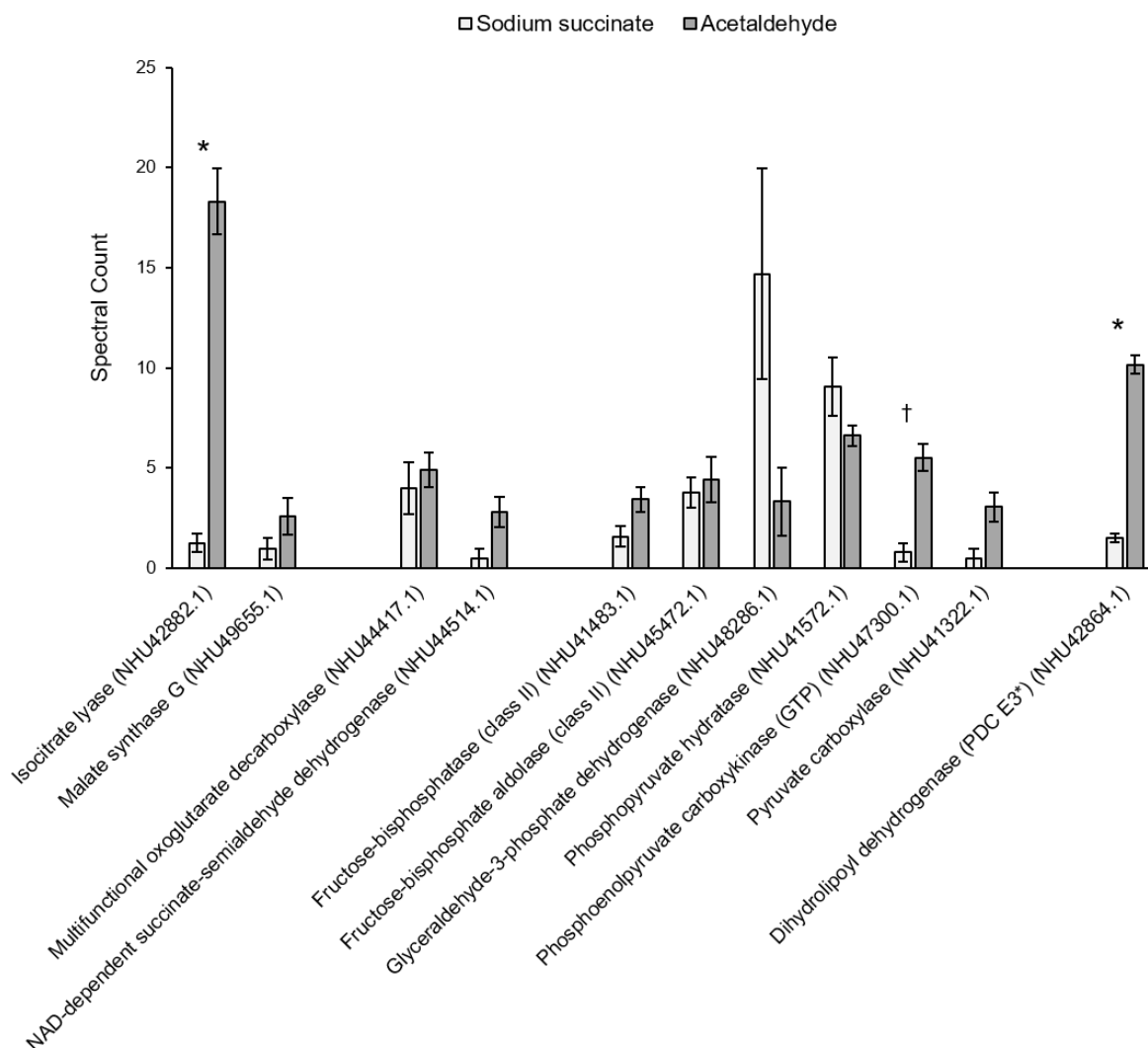
Figure 4.6 Normalised spectral counts of metabolic proteins detected in the proteome of *Rhodococcus* strain A14 during growth on acetaldehyde (5 mM) (dark grey) and sodium succinate (5 mM) (light grey). These proteins are active components of metabolic pathways including the glyoxylate shunt, glycolysis, and gluconeogenesis. The mean of three replicates is plotted for acetaldehyde spectral counts, whilst the mean of four replicates is plotted for sodium succinate spectral counts (± S.E.). * indicates *p*-value <0.01; † indicates *p*-value <0.05; PDC E3*: possible E3 subunit of pyruvate dehydrogenase complex.

4.3.3.3 Amino acid biosynthesis and structural proteins

Four of the 33 proteins with significantly increased biosynthesis during growth on acetaldehyde were identified as amino acid biosynthesis proteins (Figure 4.7a). Following a BLASTp sequence homology search, an FAD-dependent oxidoreductase (NHU42620.1) was identified as a putative glutamate synthase, responsible for catalysing the conversion of

α-ketoglutarate and glutamine to glutamate (Yan 2007). Under acetaldehyde conditions, spectral counts of the FAD-dependent oxidoreductase (NHU42620.1) increased 4.7-fold relative to the sodium succinate treatment (Figure 4.4). Glutamate resulting from the activity of glutamate synthase can represent up to 88% of all cellular nitrogen and provides the majority of nitrogen during the synthesis of nitrogen-containing compounds (Yan 2007). Glutamate is also necessary for the production of glutamine, a sensor of external nitrogen availability that can influence growth rate (Yan 2007). It is also used to regulate internal osmolarity by accumulating in the cell and partially counterbalances the internal K^+ pool (Yan 2007). The up-regulation of FAD-dependent oxidoreductase (NHU42620.1) suggests that nitrogen demand in *Rhodococcus* strain A14 increased during growth on acetaldehyde. This up-regulation may therefore indicate the increased biosynthesis of nitrogen-containing compounds, which necessitated increased expression of glutamate synthase to meet demand. Similar to the up-regulation of ethanolamine ammonia-lyase (NHU43876.1) (Section 4.3.3.1) and the two enzymatic components of the glyoxylate shunt (Section 4.3.3.2), the up-regulation of FAD-dependent oxidoreductase (NHU42620.1) indicates a possible stress response by *Rhodococcus* strain A14 to acetaldehyde. Acetaldehyde can impair cellular function and gene expression by forming adducts with proteins and DNA (Setshedi et al. 2010). To minimise the detrimental effect of these adducts, *Rhodococcus* strain A14 may increase protein biosynthesis, with the required nitrogen provided in the form of glutamate via the up-regulation of FAD-dependent oxidoreductase (NHU42620.1). Alternatively, the additional nitrogen may be provided in the form of ammonia (NH_3) resulting from the breakdown of ethanolamine via the activity of ethanolamine ammonia-lyase (NHU43876.1). The significant up-regulation of ribosome recycling factor NHU41368.1 (Figure 4.3) in the proteome of *Rhodococcus* strain A14 during growth on acetaldehyde provides strong evidence that protein turnover increased in response to the substrate, as this protein recycles ribosomes following the completion of protein synthesis. This increase in protein turnover would require additional nitrogen, which may be provided by the activity of FAD-dependent oxidoreductase (NHU42620.1). Collectively, the up-regulation of

ethanolamine ammonia-lyase (NHU43876.1), isocitrate lyase (NHU42882.1), malate synthase (isoform G) (NHU49665.1), FAD-dependent oxidoreductase (NHU42620.1), and ribosome recycling factor (NHU41368.1), suggests that these proteins contribute to a stress response by *Rhodococcus* strain A14 during growth on acetaldehyde.

Similarly, spectral counts of a pyridoxal 5'-phosphate synthase (NHU46072.1), which catalyses the interconversion of glutamine to glutamate, were 5.6-fold higher in the acetaldehyde treatment (Figure 4.7a). Adenosylhomocysteinase (NHU48026.1) and phosphoglycerate dehydrogenase (NHU41296.1) were also significantly up-regulated when acetaldehyde was the only available carbon source (Figure 4.7a), with 4.5 and 1.7-fold increases in spectral count, respectively. Adenosylhomocysteinase catalyses the conversion of *S*-adenosylhomocysteine to homocysteine and adenosine. Homocysteine resulting from this reaction can be used to produce the amino acids cysteine and methionine following further enzymatic reactions. Phosphoglycerate dehydrogenase catalyses the oxidation of 3-phosphoglycerate, a glycolysis intermediate, to 3-phosphohydroxypyruvate. This is the first committed step of serine biosynthesis and is also essential to cysteine and glycine biosynthesis. The up-regulation of these proteins suggests an additional requirement for amino acids by *Rhodococcus* strain A14, aligning with the previous suggestion that protein turnover increased during growth on acetaldehyde as part of a stress response. It is possible that the up-regulation of these proteins is co-ordinated with the up-regulation of ribosome recycling factor (NHU41368.1), FAD-dependent oxidoreductase (NHU42620.1), and ethanolamine ammonia-lyase (NHU43876.1) to provide the building blocks necessary for protein biosynthesis.

A penicillin-binding protein (NHU46759.1) was significantly up-regulated when *Rhodococcus* strain A14 was grown on acetaldehyde (Figure 4.7b). Members of this protein group bind to penicillin and other β-lactam class antibiotics (Hartman & Tomasz 1984), and catalyse reactions involved in the synthesis of cross-linked peptidoglycan, thus contributing to cell-

wall biosynthesis (Popham & Young 2003). Penicillin-binding proteins also regulate the timing, localisation and architecture of peptidoglycan polymerisation and, alongside cytoskeletal proteins, are fundamental in determining cell shape (Popham & Young 2003). Spectral counts of penicillin-binding protein (NHU46759.1) were 7.6-fold higher under acetaldehyde conditions, relative to the sodium succinate treatment. The up-regulation of penicillin-binding protein (NHU46759.1) suggests that *Rhodococcus* strain A14 became stressed in the presence of acetaldehyde, and in response increased the structural integrity of the peptidoglycan cell wall. The increased synthesis and cross-linking of peptidoglycan resulting from the increased expression of penicillin-binding protein (NHU46759.1) may help to ensure the survival of *Rhodococcus* strain A14 in the presence of acetaldehyde, which is known to be toxic, particularly at the unnaturally high concentration of 5 mM used here.

Based on a BLASTp sequence homology search, a hypothetical protein (NHU43240.1) was identified as a putative rod-shape determining protein. These proteins help to maintain the morphology of rod-shape bacterial cells and have been suggested to regulate the formation of penicillin-binding proteins (Figge et al. 2004). Rod-shape determining protein (NHU43240.1) was significantly more abundant in the acetaldehyde treatment (Figure 4.7b), with spectral counts 3.3-fold higher than the sodium succinate treatment. The up-regulation of this protein, together with penicillin-binding protein (NHU46759.1), further suggests that *Rhodococcus* strain A14 became physiologically stressed due to the high concentration of acetaldehyde. In response to this stress, rod-shape determining protein (NHU43240.1) was significantly up-regulated to maintain the structural integrity of the cells. The maintenance of a rod-shape morphology has also been suggested to maintain the surface area-to-volume ratio of a cell, which influences the ability of bacteria to communicate with their environment and acquire nutrients (Chang & Huang 2014). This suggests that, in the presence of acetaldehyde, the ability of *Rhodococcus* strain A14 cells to communicate with their environment and each other may have been reduced and necessitated the up-regulation of rod-shape determining protein (NHU43240.1) to receive information from their surroundings.

Furthermore, this morphology helps to maintain cellular polarity, with specific molecules being concentrated towards the poles of a cell, including proteins involved in cellular functions such as chromosome replication and segregation (Chang & Huang 2014). It has also been suggested that a rod-shape morphology may be optimal for cellular division by specifying a well-defined mid-plane axis for segregating organelles (Chang & Huang 2014). Rod-shape determining proteins also ensure that the two stages of cell wall morphogenesis, namely cell elongation and septation, co-ordinate with DNA replication and chromosome partitioning (Figge et al. 2004). The up-regulation of this protein also confirms that *Rhodococcus* strain A14 could grow on acetaldehyde and replicate, despite the high concentration.
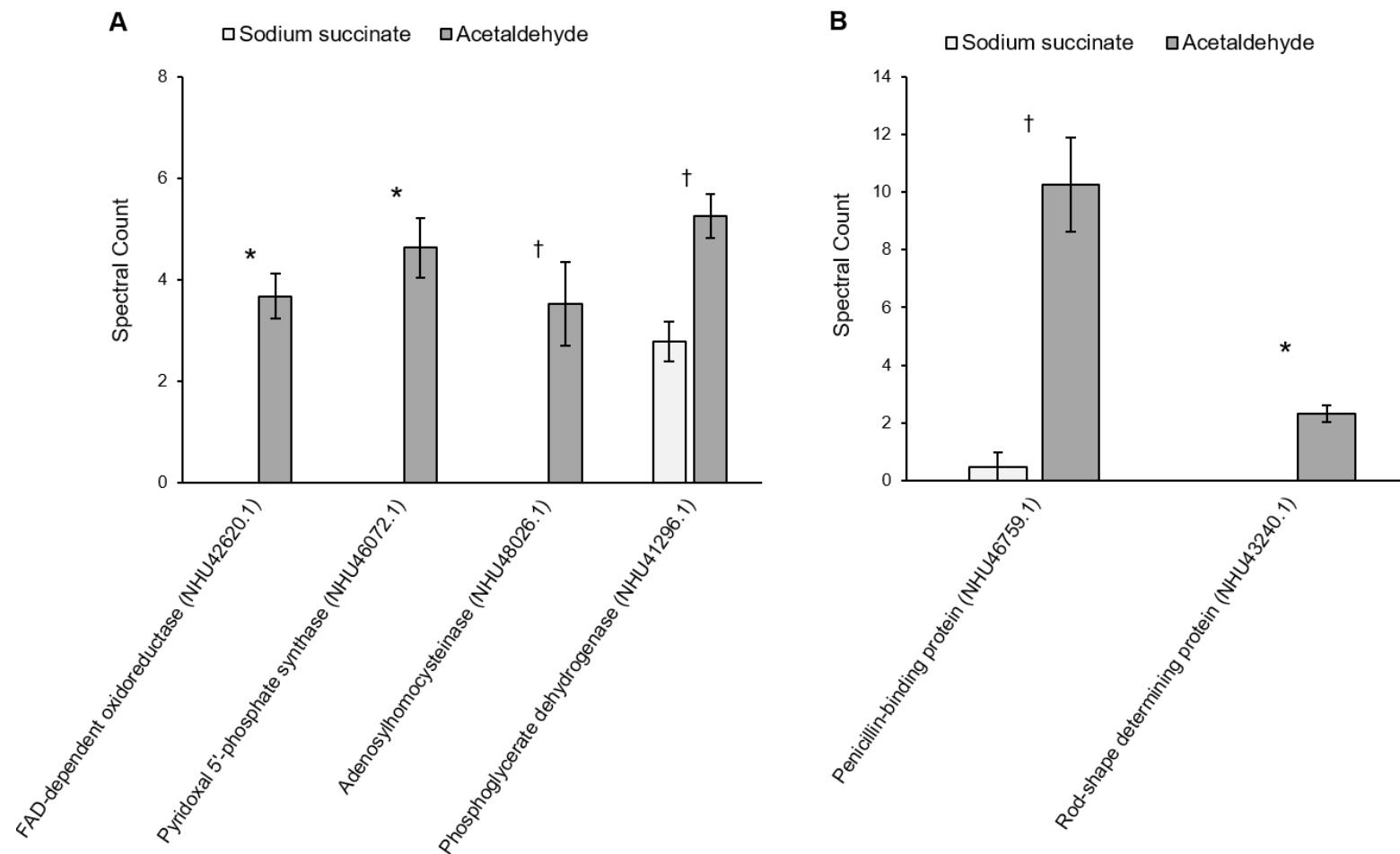
Figure 4.7 Normalised spectral counts of differentially expressed proteins in *Rhodococcus* strain A14 during growth on acetaldehyde (5 mM) (dark grey) and sodium succinate (5 mM) (light grey). A. Normalised spectral counts of amino acid biosynthesis proteins. B. Normalised spectral counts of proteins involved in cell wall structure and morphology. The mean of three replicates is plotted for acetaldehyde spectral counts, whilst the mean of four replicates is plotted for sodium succinate spectral counts (± S.E.). * indicates *p*-value <0.01; † indicates *p*-value <0.05.

4.4 Conclusion

Information regarding the bacterial pathways of acetaldehyde metabolism is sparse, with the work performed on *Rhodococcus erythropolis* strain N9T-4 and SAR11 strains HTCC1062 and HTCC7211 providing the most significant insight to date. To the best of my knowledge, this is the first study to investigate the bacterial pathway of acetaldehyde metabolism through the combined use of genome annotation and proteomics. These techniques have enabled the identification of the metabolic pathway used by *Rhodococcus* strain A14 to utilise acetaldehyde as a carbon source. In the process of discovering the pathway of acetaldehyde metabolism used by *Rhodococcus* strain A14, the identity of two acetaldehyde-degrading bacterial isolates was elucidated. *Rhodococcus* strain A14 and *Bacillus* strain A17 were identified as strains of *Rhodococcus opacus* and *Bacillus mycoides*, respectively. The genomes of both strains contained the genetic tools needed for the initial degradation of acetaldehyde, namely aldehyde dehydrogenase-encoding genes.

The proposed pathway of acetaldehyde metabolism used by *Rhodococcus* strain A14 (Figure 4.4) is analogous to that of *Rhodococcus erythropolis* strain N9T-4 and shares similarities with the initial metabolism of acetaldehyde suggested for the SAR11 clade. Upon entering the cell, acetaldehyde is oxidised to acetate via aldehyde dehydrogenases NHU42048.1 and NHU43881.1. Acetate is converted to acetyl-CoA via acetyl-CoA synthetase NHU45608.1, which enters the TCA cycle or is used during lipogenesis. At high concentrations of acetaldehyde, the glyoxylate shunt is up-regulated to bypass the oxidative decarboxylation steps of the TCA cycle, thus conserving acetaldehyde-derived carbon. An additional bypass, first converting α-ketoglutarate to succinate semialdehyde, followed by the conversion of succinate semialdehyde to succinate, conserves coenzyme A for the synthesis of acetyl-CoA used in the glyoxylate shunt. Phosphoenolpyruvate carboxykinase NHU47300.1 converts the gluconeogenic precursors malate and oxaloacetate to phosphoenolpyruvate, committing *Rhodococcus* strain A14 to gluconeogenesis and ensuring

continued biomass production and growth. During growth on acetaldehyde, proteins involved in the biosynthesis of amino acids are up-regulated to maintain the regular cellular activities of *Rhodococcus* strain A14, such as protein biosynthesis. During unfavourable environmental conditions, including high concentrations of toxic compounds such as acetaldehyde, *Rhodococcus* strain A14 up-regulates proteins involved in maintaining cell shape and structure. The up-regulation of penicillin-binding protein NHU46759.1 ensures peptidoglycan cell wall integrity is maintained and protects cellular components from the toxic external environment. Similarly, the up-regulation of rod-shape determining protein NHU43240.1 helps to maintain the morphology of *Rhodococcus* strain A14 cells, whilst also co-ordinates the stages of cell wall morphogenesis with cell replication. Collectively, this research has furthered our understanding of the mechanisms of bacterial acetaldehyde metabolism and has assisted in characterising two previously unidentified acetaldehyde degraders.

4.5 References

Ahn S, Jung J, Jang I, Madsen EL, Park W (2016) Role of glyoxylate shunt in oxidative stress response. J Biol Chem 291:11928–11938

Altschul SF (2014) BLAST algorithm. In: Encyclopedia of Life Sciences. pp 1–5. John Wiley & Sons, Ltd: Chichester

Altschul SF, Gish W, Miller W, Myers EW, Lipman DJ (1990) Basic local alignment search tool. J Mol Biol 215:403–410

Amann RI, Ludwig W, Schleifer KH (1995) Phylogenetic identification and in situ detection of individual microbial cells without cultivation. Microbiol Rev 59:143–169

Ansong C, Purvine SO, Adkins JN, Lipton MS, Smith RD (2008) Proteogenomics: Needs and roles to be filled by proteomics in genome annotation. Briefings Funct Genomics Proteomics 7:50–62

Aziz RK, Bartels D, Best A, DeJongh M, Disz T, Edwards RA, Formsma K, Gerdes S, Glass EM, Kubal M, Meyer F, Olsen GJ, Olson R, Osterman AL, Overbeek RA, McNeil LK, Paarmann D, Paczian T, Parrello B, Pusch GD, Reich C, Stevens R, Vassieva O, Vonstein V, Wilke A, Zagnitko O (2008) The RAST Server: Rapid annotations using subsystems technology. BMC Genomics 9

Bankevich A, Nurk S, Antipov D, Gurevich AA, Dvorkin M, Kulikov AS, Lesin VM, Nikolenko SI, Pham S, Prjibelski AD, Pyshkin AV, Sirotkin AV, Vyahhi N, Tesler G, Alekseyev MA, Pevzner PA (2012) SPAdes: A new genome assembly algorithm and its applications to single-cell sequencing. J Comput Biol 19:455–477

Baothman OAS, Rolfe MD, Green J (2013) Characterization of *Salmonella enterica* serovar Typhimurium aconitase A. Microbiology 159:1209–1216

Barco RA, Garrity GM, Scott JJ, Amend JP, Nealson KH, Emerson D (2020) A genus definition for Bacteria and Archaea based on a standard genome relatedness index. MBio 11:1–20

Baumgartner Jr WA, Cohen KB, Fox LM, Acquaah-Mensah G, Hunter L (2007) Manual curation is not sufficient for annotation of genomic databases. Bioinformatics 23:i41–i48

Bell KS, Philp JC, Aw DWJ, Christofi N (1998) The genus *Rhodococcus*. J Appl Microbiol 85:195–210

Benjamini Y, Hochberg Y (1995) Controlling the false discovery rate: A practical and powerful approach to multiple testing. J R Statstical Soc Ser B 57:289–300

Bolger AM, Lohse M, Usadel B (2014) Trimmomatic: A flexible trimmer for Illumina sequence data. Bioinformatics 30:2114–2120

Brettin T, Davis JJ, Disz T, Edwards RA, Gerdes S, Olsen GJ, Olson R, Overbeek R, Parrello B, Pusch GD, Shukla M, Thomason JA, Stevens R, Vonstein V, Wattam AR, Xia F (2015) RASTtk: A modular and extensible implementation of the RAST algorithm for building custom annotation pipelines and annotating batches of genomes. Sci Rep 5:

Brown TDK, Jones-Mortimer MC, Kornberg HL (1977) The enzymic interconversion of acetate and acetyl-coenzyme A in *Escherichia coli*. J Gen Microbiol 102:327–336

Cappelletti M, Zampolli J, Di Gennaro P, Zannoni D (2019) Genomics of *Rhodococcus*. Biology of *Rhodococcus*. pp 23–60. H. M. Alvarez (Ed.). Microbiology Monographs 16. Springer Nature Switzerland AG

Chang F, Huang KC (2014) How and why cells grow as rods. BMC Biol 12:54

Ciufo S, Kannan S, Sharma S, Badretdin A, Clark K, Turner S, Brover S, Schoch CL, Kimchi A, DiCuccio M (2018) Using average nucleotide identity to improve taxonomic assignments in prokaryotic genomes at the NCBI. Int J Syst Evol Microbiol 68:2386–2392

Cox J, Mann M (2008) MaxQuant enables high peptide identification rates, individualized p.p.b.-range mass accuracies and proteome-wide protein quantification. Nat Biotechnol 26:1367–1372

Cox J, Neuhauser N, Michalski A, Scheltema RA, Olsen JV, Mann M (2011) Andromeda: A peptide search engine integrated into the MaxQuant environment. J Proteome Res 10:1794–1805

Davis JJ, Gerdes S, Olsen GJ, Olson R, Pusch GD, Shukla M, Vonstein V, Wattam AR, Yoo H (2016) PATtyFams: Protein families for the microbial genomes in the PATRIC database. Front Microbiol 7:1–12

Delcher A, Harmon D, Kasif S, White O, Salzberg SL (1999) Improved microbial gene identification with GLIMMER. Nucleic Acids Res 27:4636–4641

Deloger M, El Karoui M, Petit M (2009) A genomic distance based on MUM indicates discontinuity between most bacterial species and genera. J Bacteriol 191:91–99

Dolan SK, Welch M (2018) The glyoxylate shunt, 60 years on. Annu Rev Microbiol 72:309–330

Dyksterhouse SE, Gray JP, Herwig RP, Lara JC, Staley JT (1995) *Cycloclasticus pugetii* gen. nov., sp. nov., an aromatic hydrocarbon-degrading bacterium from marine sediments. Int J Syst Bacteriol 45:116–123

Ehling-Schulz M, Lereclus D, Koehler TM (2019) The *Bacillus cereus* group: *Bacillus* species with pathogenic potential. Microbiol Spectr 7:

El-Gebali S, Mistry J, Bateman A, Eddy SR, Luciani A, Potter SC, Qureshi M, Richardson LJ, Salazar GA, Smart A, Sonnhammer ELL, Hirsh L, Paladin L, Piovesan D, Tosatto SCE, Finn RD (2019) The Pfam protein families database in 2019. Nucleic Acids Res 47:D427–D432

Figge RM, Divakaruni AV, Gober JW (2004) *MreB*, the cell shape-determining bacterial actin homologue, co-ordinates cell wall morphogenesis in *Caulobacter crescentus*. Mol Microbiol 51:1321–1332

Garsin DA (2010) Ethanolamine utilization in bacterial pathogens: Roles and regulation. Nat Rev Microbiol 8:290–295

Gevers D, Cohan FM, Lawrence JG, Spratt BG, Coenye T, Feil EJ, Stackebrandt E, van de Peer Y, Vandamme P, Thompson FL, Swings J (2005) Reevaluating prokaryotic species. Nat Rev Microbiol 3:733–739

Goris J, Konstantinidis KT, Klappenbach JA, Coenye T, Vandamme P, Tiedje JM (2007) DNA-DNA hybridization values and their relationship to whole-genome sequence similarities. Int J Syst Evol Microbiol 57:81–91

Gorlatov SN, Maltseva OV, Shevchenko VI, Golovleva LA (1989) Degradation of chlorophenols by a culture of *Rhodococcus erythropolis*. Microbiology 58:647–651

Graves PR, Haystead TAJ (2002) Molecular biologist's guide to proteomics. Microbiol Mol Biol Rev 66:39–63

Gregson BH, Metodieva G, Metodiev MV, Golyshin PN, McKew BA (2020) Protein expression in the obligate hydrocarbon-degrading psychrophile *Oleispira antarctica* RB-8 during alkane degradation and cold tolerance. Environ Microbiol 22: 1870–1883

Gregson BH, Metodieva G, Metodiev MV, McKew BA (2019) Differential protein expression during growth on linear versus branched alkanes in the obligate marine hydrocarbon-degrading bacterium *Alcanivorax borkumensis* SK2T. Environ Microbiol 21:2347–2359

Gröning JAD, Eulberg D, Tischler D, Kaschabek SR, Schlömann M (2014) Gene redundancy of two-component (chloro)phenol hydroxylases in *Rhodococcus opacus* 1CP. FEMS Microbiol Lett 361:68–75

Guo L, Chen Z, Amarnath V, Davies SS (2012) Identification of novel bioactive aldehyde-modified phosphatidylethanolamines formed by lipid peroxidation. Free Radic Biol Med 53:1226–1238

Hall TA (1999) BioEdit: a user-friendly biological sequence alignment editor and analysis program for Windows 95/98/NT. Nucleic Acid Symp Ser 41:95–98

Halsey KH, Giovannoni SJ, Graus M, Zhao Y, Landry Z, Thrash JC, Vergin KL, de Gouw J (2017) Biological cycling of volatile organic carbon by phytoplankton and bacterioplankton. Limnol Oceanogr 62:2650–2661

Hartman BJ, Tomasz A (1984) Low-affinity penicillin-binding protein associated with β-lactam resistance in *Staphylococcus aureus*. J Bacteriol 158:513–516

Henz SR, Huson DH, Auch AF, Nieselt-Struwe K, Schuster SC (2005) Whole-genome prokaryotic phylogeny. Bioinformatics 21:2329–2335

Jo JE, Mohan Raj S, Rathnasingh C, Selvakumar E, Jung WC, Park S (2008) Cloning, expression, and characterization of an aldehyde dehydrogenase from *Escherichia coli* K-12 that utilizes 3-hydroxypropionaldehyde as a substrate. Appl Microbiol Biotechnol 81:51–60

Karlsson R, Gonzales-Siles L, Boulund F, Svensson-Stadler L, Skovbjerg S, Karlsson A, Davidson M, Hulth S, Kristiansson E, Moore ERB (2015) Proteotyping: Proteomic characterization, classification and identification of microorganisms - A prospectus. Syst Appl Microbiol 38:246–257

Kim M, Oh HS, Park SC, Chun J (2014) Towards a taxonomic coherence between average nucleotide identity and 16S rRNA gene sequence similarity for species demarcation of prokaryotes. Int J Syst Evol Microbiol 64:346–351

De Kok A, Hengeveld AF, Martin A, Westphal AH (1998) The pyruvate dehydrogenase multi-enzyme complex from Gram-negative bacteria. Biochim Biophys Acta - Protein Struct Mol Enzymol 1385:353–366

Konstantinidis KT, Ramette A, Tiedje JM (2006) The bacterial species definition in the genomic era. Philos Trans R Soc B Biol Sci 361:1929–1940

Konstantinidis KT, Tiedje JM (2005) Genomic insights that advance the species definition for prokaryotes. Proc Natl Acad Sci USA 102:2567–2572

Land M, Hauser L, Jun S, Nookaew I, Leuze MR, Ahn T, Karpinets T, Lund O, Kora G, Wassenaar T, Poudel S, Ussery DW (2015) Insights from 20 years of bacterial genome sequencing. Funct Integr Genomics 15:141–161

Larkin MJ, Kulakov LA, Allen CCR (2005) Biodegradation and *Rhodococcus* - Masters of catabolic versatility. Curr Opin Biotechnol 16:282–290

Larkin MJ, De Mot R, Kulakov LA, Nagy I (1998) Applied aspects of *Rhodococcus* genetics. Antonie Van Leeuwenhoek 74:133–153

Lee I, Kim YO, Park SC, Chun J (2016) OrthoANI: An improved algorithm and software for calculating average nucleotide identity. Int J Syst Evol Microbiol 66:1100–1103

Loman NJ, Constantinidou C, Chan JZM, Halachev M, Sergeant M, Penn CW, Robinson ER, Pallen MJ (2012) High-throughput bacterial genome sequencing: An embarrassment of choice, a world of opportunity. Nat Rev Microbiol 10:599–606

Ma Y, Cui Y, Du L, Liu X, Xie X, Chen N (2018) Identification and application of a growth-regulated promoter for improving l-valine production in *Corynebacterium glutamicum*. Microb Cell Fact 17:1–10

Markowitz VM, Mavromatis K, Ivanova NN, Chen IMA, Chu K, Kyrpides NC (2009) IMG ER: A system for microbial genome annotation expert review and curation. Bioinformatics 25:2271–2278

McKew BA, Lefebvre SC, Achterberg EP, Metodieva G, Raines CA, Metodiev MV, Geider RJ (2013) Plasticity in the proteome of *Emiliania huxleyi* CCMP 1516 to extremes of light is highly targeted. New Phytol 200:61–73

Meyer F, Overbeek R, Rodriguez A (2009) FIGfams: Yet another set of protein families. Nucleic Acids Res 37:6643–6654

Miller RA, Jian J, Beno SM, Wiedmann M, Kovac J (2018) Intraclade variability in toxin production and cytotoxicity of *Bacillus cereus* group type strains and dairy-associated isolates. Appl Environ Microbiol 84:e02779-17

Nakamura LK (1998) *Bacillus pseudomycoides* sp. nov. Int J Syst Bacteriol 48:1031–1035

Overbeek R, Begley T, Butler RM, Choudhuri JV, Chuang HY, Cohoon M, de Crécy-Lagard V, Diaz N, Disz T, Edwards R, Fonstein M, Frank ED, Gerdes S, Glass EM, Goesmann A, Hanson A, Iwata-Reuyl D, Jensen R, Jamshidi N, Krause L, Kubal M, Larsen N, Linke B, McHardy AC, Meyer F, Neuweger H, Olsen G, Olson R, Osterman A, Portnoy V, Pusch GD, Rodionov DA, Rückert C, Steiner J, Stevens R, Thiele I, Vassieva O, Ye Y, Zagnitko O, Vonstein V (2005) The subsystems approach to genome annotation and its use in the project to annotate 1000 genomes. Nucleic Acids Res 33:5691–5702

Overbeek R, Olson R, Pusch GD, Olsen GJ, Davis JJ, Disz T, Edwards RA, Gerdes S, Parrello B, Shukla M, Vonstein V, Wattam AR, Xia F, Stevens R (2014) The SEED and the Rapid Annotation of microbial genomes using Subsystems Technology (RAST). Nucleic Acids Res 42:206–214

Pandey A, Mann M (2000) Proteomics to study genes and genomes. Nature 405:837–846

Penrod JT, Roth JR (2006) Conserving a volatile metabolite: a role for carboxysome-like organelles in *Salmonella enterica*. J Bacteriol 188:2865–2874

Popham DL, Young KD (2003) Role of penicillin-binding proteins in bacterial cell morphogenesis. Curr Opin Microbiol 6:594–599

Richardson EJ, Watson M (2013) The automatic annotation of bacterial genomes. Brief Bioinform 14:1–12

Richter M, Rosselló-Móra R (2009) Shifting the genomic gold standard for the prokaryotic species definition. Proc Natl Acad Sci USA 106:19126–19131

Rodriguez-R L, Konstantinidis KT (2016) The enveomics collection: a toolbox for specialized analyses of microbial genomes and metagenomes. PeerJ Prepr 4:e1900v1

Rodriguez-R LM, Gunturu S, Harvey WT, Rosselló-Mora R, Tiedje JM, Cole JR, Konstantinidis KT (2018) The Microbial Genomes Atlas (MiGA) webserver: Taxonomic and gene diversity analysis of Archaea and Bacteria at the whole genome level. Nucleic Acids Res 46:W282–W288

Rosselló-Mora R (2006) DNA-DNA reassociation methods applied to microbial taxonomy and their critical evaluation. In: Stackebrandt E (Ed.) Molecular Identification, Systematics, and Population Structure of Prokaryotes. pp 23–50. Springer, Berlin, Heidelberg

Saitou N, Nei M (1987) The neighbor-joining method: a new method for reconstructing phylogenetic trees. Mol Biol Evol 4:406–425

Schnoes AM, Brown SD, Dodevski I, Babbitt PC (2009) Annotation error in public databases: Misannotation of molecular function in enzyme superfamilies. PLoS Comput Biol 5:e1000605

Seemann T (2014) Prokka: Rapid prokaryotic genome annotation. Bioinformatics 30:2068–2069

Setshedi M, Wands JR, de la Monte SM (2010) Acetaldehyde adducts in alcoholic liver disease. Oxid Med Cell Longev 3:178–185

Sophos NA, Vasiliou V (2003) Aldehyde dehydrogenase gene superfamily: The 2002 update. Chem Biol Interact 143–144:5–22

Stackebrandt E (2003) The richness of prokaryotic diversity: There must be a species somewhere. Food Technol Biotechnol 41:17–22

Stackebrandt E, Goebel BM (1994) Taxonomic note: A place for DNA-DNA reassociation and 16S rRNA sequence analysis in the present species definition in bacteriology. Int J Syst Bacteriol 44:846–849

Tatusova T, Dicuccio M, Badretdin A, Chetvernin V, Nawrocki EP, Zaslavsky L, Lomsadze A, Pruitt KD, Borodovsky M, Ostell J (2016) NCBI prokaryotic genome annotation pipeline. Nucleic Acids Res 44:6614–6624

TheUniProtConsortium (2019) UniProt: A worldwide hub of protein knowledge. Nucleic Acids Res 47:D506–D515

Tischler D, Eulberg D, Lakner S, Kaschabek SR, van Berkel WJH, Schlömann M (2009) Identification of a novel self-sufficient styrene monooxygenase from *Rhodococcus opacus* 1CP. J Bacteriol 191:4996–5009

Tripp HJ (2013) The unique metabolism of SAR11 aquatic bacteria. J Microbiol 51:147–153

Tsoy O, Ravcheev D, Mushegian A (2009) Comparative genomics of ethanolamine utilization. J Bacteriol 191:7157–7164

van der Geize R, Dijkhuizen L (2004) Harnessing the catabolic diversity of rhodococci for environmental and biotechnological applications. Curr Opin Microbiol 7:255–261

Wayne LG, Brenner DJ, Colwell RR, Grimont PAD, Kandler O, Krichevsky MI, Moore LH, Moore WEC, Murray RGE, Stackebrant E, Starr MP, Truper HG (1987) Report of the ad hoc committee on reconciliation of approaches to bacterial systematics. Int J Syst Bacteriol 37:463–464

Yan D (2007) Protection of the glutamate pool concentration in enteric bacteria. Proc Natl Acad Sci USA 104:9475–9480

Yano T, Yoshida N, Yu F, Wakamatsu M, Takagi H (2015) The glyoxylate shunt is essential for CO2-requiring oligotrophic growth of *Rhodococcus erythropolis* N9T-4. Appl Microbiol Biotechnol 99:5627–5637

Yoon SH, Ha S, Lim J, Kwon S, Chun J (2017) A large-scale evaluation of algorithms to calculate average nucleotide identity. Antonie Van Leeuwenhoek 110:1281–1286

Yoshida N (2019) Oligotrophic growth of *Rhodococcus*. pp 87–101. In: Alvarez HM (Ed.). Biology of *Rhodococcus*. Microbiology Monographs 16. Springer Nature Switzerland AG

Yoshida N, Yano T, Kedo K, Fujiyoshi T, Nagai R, Iwano M, Taguchi E, Nishida T, Takagi H (2017) A unique intracellular compartment formed during the oligotrophic growth of *Rhodococcus erythropolis* N9T-4. Appl Microbiol Biotechnol 101:331–340

Zhang Y (2008) I-TASSER server for protein 3D structure prediction. BMC Bioinformatics 9

Chapter 5:

Microbial Assimilation and Dissimilation of ^{14}C-labelled Acetaldehyde in Riverine, Estuarine and Coastal Waters of South-West England

5.1 Introduction

The bidirectional exchange of biogenic volatile organic compounds (BVOCs), such as isoprene and methanol, between the atmosphere and terrestrial ecosystems has a significant effect on global atmospheric chemistry (Section 1.1), which in turn influences the global radiative balance, climate and air quality (Rinnan & Albers 2020; Trowbridge et al. 2020). It is estimated that ~1,000 Tg of carbon is released to the atmosphere in the form of BVOCs every year (Guenther et al. 2012) and that a considerable variety of BVOCs contribute to this flux. Isoprene comprises nearly half of global BVOC emissions, whilst methanol, ethanol, acetaldehyde, acetone, α-pinene, β-pinene, t-β-ocimene, limonene, ethene and propene collectively constitute 30% of global emissions (Guenther et al. 2012). In soils it is thought that, alongside adsorption and dissolution, microbial communities play a key role in BVOC uptake, yet the extent of microbial degradation is poorly understood (Rinnan & Albers 2020). This is despite suggestions that this biological sink is highly important to carbon cycling and the atmospheric concentration of BVOCs (Albers et al. 2018). Furthermore, the microorganisms responsible for BVOC degradation in soils are largely unknown, primarily due to difficulties in their cultivation (Rinnan & Albers 2020). Combined with limited information regarding specific rates of microbial BVOC degradation, this knowledge gap introduces doubt over the reliability of current estimates of gross BVOC emissions from soils, as these estimations do not consider their full microbial uptake capacity.

The knowledge gaps identified for BVOC uptake in soils can be applied to aquatic ecosystems, such as rivers, estuaries, and coastal regions, where even less is understood due to limited research effort. This is well demonstrated by examining ethanol cycling in surface waters. Ethanol emissions from the oceans have only been quantified in one study, with Beale et al. (2010) suggesting an ocean source of 4 Tg a^{-1} by extrapolating in-situ ethanol measurements from the Atlantic Ocean. Importantly, these estimates were based on a small data set and therefore the magnitude of ocean ethanol emissions are still uncertain. Furthermore, this study did not measure the microbial uptake of ethanol, which may significantly influence the amount of ethanol that reaches the atmosphere. To date, only one study has investigated the microbial degradation of ethanol in seawater at naturally occurring concentrations, and reported that biological degradation was primarily responsible for ethanol losses in Pacific Ocean seawater samples (de Bruyn et al. 2020). Although important, these findings do not provide enough information to determine the impact of microorganisms on the flux of ethanol from the marine environment. Moreover, the microorganisms responsible for ethanol degradation were not identified, meaning that our knowledge of microbial ethanol uptake remains limited. The role of rivers and estuaries in the global ethanol budget is also poorly understood, however, reports suggest that these ecosystems are likely a significant sink for atmospheric ethanol due to microbial activity, with ethanol converted to acetaldehyde (Avery et al. 2016). Despite this knowledge, microbial uptake rates of ethanol have only been measured in one river (Apoteker & Thévenot 1983) and to date, no measurements have been reported for estuaries. The microorganisms responsible for ethanol degradation in these ecosystems have also yet to be elucidated. The paucity of information regarding microbial uptake rates and the identity of BVOC-degrading microorganisms in aquatic ecosystems is not restricted to ethanol. With exception to methanol, few microbial BVOC uptake rates have been measured and the microorganisms responsible remain largely unidentified, despite the potential significance of microbial uptake in regulating atmospheric BVOC flux from surface waters.

With exception to highly recalcitrant compounds, all organic molecules contain carbon that can be harvested by heterotrophic microorganisms for growth (Rinnan & Albers 2020). Accordingly, it is likely that all BVOCs can be degraded by microorganisms. Oxygenated volatile organic compounds (OVOCs), such as methanol, acetone and acetaldehyde, are an important source of labile carbon and an energy source to microbial communities (Dixon et al. 2011a, 2013a, 2013b, 2014; Beale et al. 2015). As previously mentioned, these compounds can change the oxidative capacity of the atmosphere (de Bruyn et al. 2017) and can indirectly influence cloud formation (Section 1.1). Consequently, the microbial cycling of OVOCs is thought to exert considerable control over atmospheric chemical processes and, as a result, indirectly influences local and global climate. Dixon et al. (2013a), for example, demonstrated that microbial oxidation largely controls acetaldehyde concentrations in surface waters of the Atlantic Ocean, with 49 - 100% of acetaldehyde dissimilated to CO_2, strongly suggesting that the flux of acetaldehyde to the atmosphere is under significant microbial control and that microorganisms indirectly influence atmospheric chemistry.

In recent years significant progress has been made in understanding the sources of methanol, acetone and acetaldehyde in the marine environment. For acetone and acetaldehyde, the primary route of production is thought to be the photodegradation of chromophoric dissolved organic matter (CDOM) (Kieber et al. 1990; de Bruyn et al. 2011; Dixon et al. 2013a; Beale et al. 2015), whilst the majority of methanol is produced by phytoplankton and the breakdown of algal cells (Dixon et al. 2013a; Beale et al. 2015; Mincer & Aicher 2016; Halsey et al. 2017). Comparatively, our knowledge of marine OVOC sinks is limited to a handful of studies that suggest that microbial uptake is an important sink term, particularly for acetaldehyde (Dixon et al. 2013a). Dixon et al. (2014), for example, reported monthly microbial oxidation rates of 0.03 - 1 nmol L^{-1} day^{-1} for acetone in the western English Channel. Oxidation rates were highest in the winter (0.87 ± 0.21 nmol L^{-1} day^{-1}) and were lowest in the summer (0.06 ± 0.04 nmol L^{-1} day^{-1}), with surface temperatures measured at 8.5 - 8.9°C and 13.8 - 16.4°C, respectively. Intermediate oxidation rates were

measured in spring (0.18 ± 0.09 nmol L^{-1} day^{-1}) and autumn (0.11 ± 0.01 nmol L^{-1} day^{-1}). For

methanol, microbial oxidation rates of 2 - 146 nmol L^{-1} day^{-1} have been measured in surface

waters of the north-east Atlantic Ocean (Dixon et al. 2011). Similar to acetone, the highest

rates of methanol oxidation were measured in winter, whilst the lowest rates were measured

in summer, when surface temperatures ranged between 22.5 - 27.4°C and 13.5 - 17.8°C,

respectively. Sargeant et al. (2016) reported methanol oxidation rates of 16.8 - 268.8 nmol

L^{-1} day^{-1} in the western English Channel, with the highest rates of oxidation also measured

in winter. For acetaldehyde, microbial oxidation rates of 36 - 65 nmol L^{-1} day^{-1} have been

measured in the Atlantic Ocean during winter (Dixon et al. 2013a), accounting for 49 - 100%

of total acetaldehyde loss. The remaining losses may be attributed to chemical and

photochemical processes, and microbial assimilation, although this was not measured in this

study. Acetaldehyde oxidation rates were highest in the South Atlantic Gyre (65 nmol L^{-1}

day^{-1}), coinciding with temperatures of 20 - 25°C. Comparatively, the lowest microbial

oxidation rates were measured in the Equatorial Upwelling (36 nmol L^{-1} day^{-1}) and the North

Atlantic Gyre (41 nmol L^{-1} day^{-1}), with surface temperatures ranging between 25 and 30°C.

The microbial oxidation of acetone and methanol were also measured in this study, with

rates of 0.2 - 0.5 and 10 - 18 nmol L^{-1} day^{-1} measured, respectively. These findings are

important, however, due to the limited number of direct measurements of microbial OVOC

uptake rates in the marine environment, the extent to which marine microorganisms

influence global OVOC biogeochemical cycles remains uncertain. This has led to further

uncertainty regarding the magnitude and direction of OVOC air-sea fluxes (Beale et al. 2013;

Dixon et al. 2013a; Yang et al. 2013). This also applies to freshwater and estuarine

environments, where microbial uptake rates for methanol, acetone and acetaldehyde have

yet to be reported. Consequently, the influence of microbial communities on the flux of these

OVOCs to the atmosphere is poorly understood in riverine and estuarine environments.

Moreover, it is unclear whether microorganisms preferentially use OVOC-derived carbon for

assimilation into biomass (i.e. growth) or as a source of energy via dissimilation (oxidation)

to CO_2. Collectively, these uncertainties limit our ability to produce accurate global models of OVOC budgets.

Previous models of the global atmospheric acetaldehyde budget, such as those based on GEOS-Chem (Bey et al. 2001), generally agree on the primary and secondary sources of acetaldehyde (Singh et al. 2004; Millet et al. 2010). In the atmosphere, the photodegradation of alkenes, alkanes and isoprene represent the major source of acetaldehyde, whilst the photodegradation of CDOM and terrestrial plant growth and decay are considered primary sources in marine and terrestrial environments, respectively (Singh et al. 2004; Millet et al. 2010). Despite this consensus, the magnitude of these sources is a subject of debate. Singh et al. (2004) estimated a net acetaldehyde flux of 125 Tg a^{-1} from the marine environment, suggesting that oceans are the primary global source of acetaldehyde. Furthermore, atmospheric production was estimated to be equal to terrestrial plant growth and decay, with values of 35 Tg a^{-1}. Conversely, Millet et al. (2010) suggested that atmospheric production was the primary global source of acetaldehyde with estimates of 128 Tg a^{-1}, and that net acetaldehyde emissions from the marine environment were less than half of that predicted by Singh et al. (2004), with estimates of 57 Tg a^{-1}. The reason for this discrepancy is primarily due to the limited number of acetaldehyde measurements in the marine environment, combined with an insufficient understanding of the processes that control marine acetaldehyde concentrations (de Bruyn et al. 2017). This is made particularly apparent when we consider that estimates of net ocean emissions in these models do not acknowledge the activity of marine microorganisms and calculate the global air-sea flux of acetaldehyde based on the global distribution of CDOM light absorption at 300 nm derived from satellite ocean colour observations. The in-situ acetaldehyde photoproduction rate is calculated as a function of depth in the ocean mixed layer for each grid square of the Geos-Chem chemical transport model (CTM), using local values of CDOM light adsorption (300 nm), the incident near-UV solar radiation, and spectral light attenuation (Millet et al. 2010). Without considering the rates of microbial acetaldehyde uptake these modelled calculations

may overestimate acetaldehyde emissions from the marine environment. This situation also applies to riverine and estuarine environments, which are not considered in any current models of global acetaldehyde emissions. More generally, to improve the accuracy of the global acetaldehyde budget, future models should include microbial sink terms for both marine and terrestrial environments and include microbially-regulated acetaldehyde emissions from rivers and estuaries. However, increasingly accurate models are only possible with more measurements of in-situ acetaldehyde concentrations, production rates and microbial uptake rates.

In this study, the microbial assimilation and dissimilation of ^{14}C-labelled acetaldehyde was measured in riverine, estuarine, and coastal waters of south-west England during winter and summer. By establishing rates of microbial acetaldehyde uptake, this research will improve our understanding of the microbial contribution to the global biogeochemical cycle of acetaldehyde and, by comparing winter rates with measurements taken in summer by Webb (2016), will allow the influence of seasonality to be determined. These rates will also help to improve our understanding of the role that rivers, estuaries and coastal regions play as sources or sinks of acetaldehyde. The use of ^{14}C-labelled acetaldehyde will enable measurement of microbial uptake and the relative contribution of acetaldehyde as a source of energy (i.e. dissimilation to CO_2) versus use as a carbon source for growth (i.e. assimilation into biomass). Importantly, this will be performed at environmentally relevant concentrations, which have been shown to range between 1 - 38 nM in the marine environment (Section 1.6) and between 6 - 28 nM and 2 - 16 nM in the rivers and estuaries of south-west England during summer and winter, respectively (J. Dixon, pers. comm.) This will provide an accurate representation of microbial activities in the rivers, estuaries, and coastal regions of south-west England. Collectively, these findings will further demonstrate the connectivity between microorganisms, their environment, and the atmosphere.

The following hypotheses were tested:

H1. Microbial acetaldehyde uptake rates will be higher in riverine environments compared with estuaries and coastal sea.

This hypothesis is premised on the fact that rivers receive regular inputs of CDOM through the decay of terrestrially-sourced organic material, which is converted to acetaldehyde and thus maintains an active population of acetaldehyde-degrading microorganisms. The work of Roebuck et al. (2016) suggests that sediment porewaters in freshwater rivers may produce considerable amounts of ethanol and acetaldehyde. This may also be an important source of acetaldehyde-derived carbon for microorganisms in riverine environments. The continuous or regular availability of acetaldehyde in rivers may help to prime microbial communities for acetaldehyde degradation, by selecting for acetaldehyde degraders and/or activating the necessary enzymes.

H2. Microbial acetaldehyde uptake rates, the sum of microbial assimilation and dissimilation, will be significantly higher in summer than in winter in response to warmer surface waters.

Warmer environmental conditions should increase microbial and enzymatic activity, resulting in an increased uptake of acetaldehyde to meet energy and growth demands.

H3. Rates of microbial acetaldehyde dissimilation will be higher than microbial assimilation rates, suggesting that acetaldehyde is primarily used as an energy source rather than being assimilated for growth.

This hypothesis is premised on a similar finding by Halsey et al. (2017) using two strains of *Pelagibacter* SAR11, a clade of highly abundant and globally-distributed α-proteobacteria. Following the addition of acetaldehyde, both strains incorporated ~30% of the utilised acetaldehyde into biomass, whilst the remaining ~70% was dissimilated to CO_2.

5.2 Methodology

5.2.1 Sampling

Surface water samples (~5 L) were collected from riverine, estuarine and coastal waters of Devon and Cornwall between the 20th and 27th February 2020 (Figure 5.1). Riverine samples were collected from the East Dart (Postbridge), West Dart (Two Bridges), Walkham (Horrabridge), Meavy (Shaugh Bridge) and Plym (Shaugh Bridge) in Dartmoor, the River Inny in Cornwall, and four sites located on the River Tamar (Dutson, Polson Bridge, Horsebridge and Gunnislake). Estuarine water was sampled from Halton Quay, Cargreen and Saltash located on the Tamar Estuary, whilst coastal water was collected from long-term monitoring station, L4, in the western English Channel (50°15.00 N; 4°13.02 W); located approximately 10 km from the coast of Plymouth, UK. In-situ measurements of temperature, salinity, pH, dissolved oxygen (%), turbidity (NTU), ammonium (mg/L) and nitrate (mg/L) were recorded at the time of sampling using a YSI ProDSS handheld multiparameter water quality meter (Table 5.1). Within 6 hours of collection, surface water samples from each site were pumped directly into 305 mL acid-washed, quartz Duran bottles using a peristaltic pump, and were incubated in the dark at the in-situ surface temperature.

Labelled ^{14}C-acetaldehyde was purchased from American Radiolabeled Chemicals Inc. (Saint Louis, MO, USA) with a specific activity of 50 mCi mmol^{-1}. Primary stocks of ^{14}C-labelled acetaldehyde were diluted 1:10 with Milli-Q water (0.1 mCi ml^{-1}) and were stored in gas-tight vials in the dark at 4°C. Final concentrations of ^{14}C-acetaldehyde in samples ranged between 9.32 and 10.03 nM.
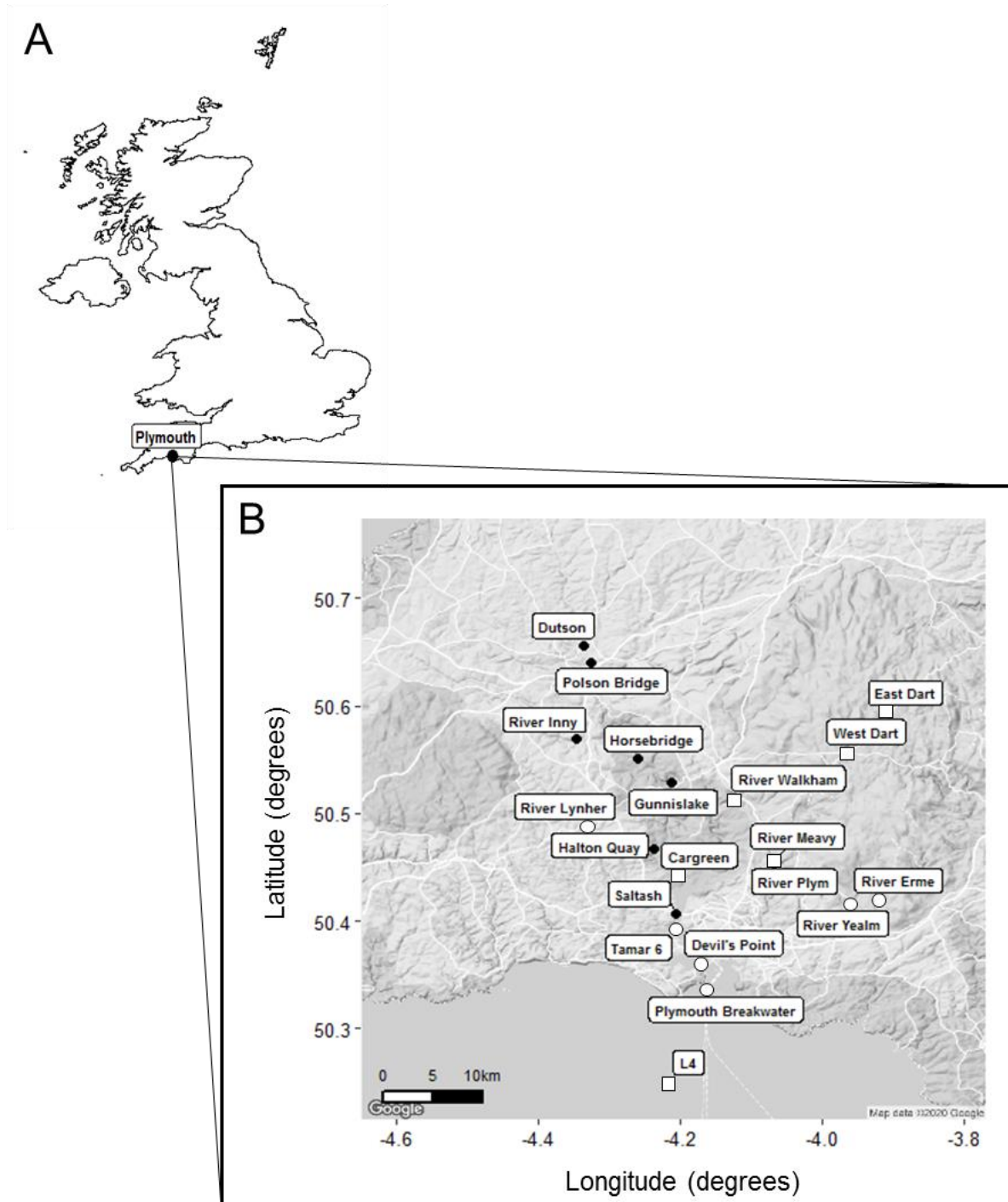
Figure 5.1 Location of sampling sites in the south-west of England. A) Map of UK showing the location of Plymouth. B) Map of Plymouth and the Tamar Valley showing the location of sampling sites. ●: site sampled in winter; ○: site sampled in summer by Christopher Webb (Webb 2016); □ site sampled in winter and summer.

5.2.2 Linear incorporation experiment

A time-course experiment was set up to determine the linear incorporation period of the ^{14}C label. A 50 μL aliquot of ^{14}C-labelled acetaldehyde stock was added to 305 mL of Gunnislake surface water (*n=12*), resulting in a final concentration of 6.9 - 7.8 nM (3.1 - 3.5 disintegrations per minute (DPM) μL^{-1}). Samples were incubated in the dark for 4 hours at the in-situ surface temperature. After 1 hour of incubation, triplicate sub-samples of surface water (1 ml) were taken to determine the microbial oxidation of ^{14}C-acetaldehyde to ^{14}CO$_2$, following the methods of Dixon et al. (2011a) (adapted from Connell et al. (1997) and Goodwin et al. (1998)). Aliquots of 1 mL were transferred to 2 mL microcentrifuge tubes with O-ring seals (Micrewtube, Simport Scientific™) to prevent the loss of ^{14}C-acetaldehyde and ^{14}CO$_2$ through volatilisation. To precipitate ^{14}CO$_2$ as Sr^{14}CO$_3$, 0.5 mL of SrCl$_2$•6H$_2$O (1 M) was added to each microcentrifuge tube. To neutralise the resulting hydrochloric acid, 20 μL of NaOH (1 M) was added to each tube, followed by 100 μL of Na$_2$CO$_3$ (1 M) to ensure adequate pellet formation. Microcentrifuge tubes were vortexed to homogenise the samples and were stored in the dark for 24 hours. Samples were vortexed and centrifuged at 16,000 × *g* for 10 minutes. The supernatant was aspirated, and the pellet washed twice with ethanol (80% v/v). The washed pellet was resuspended in 0.5 mL of NaOH (1 M; pH 11.7) to create a slurry, before the addition of 1 mL of liquid scintillation cocktail (OptiPhase HiSafe III; PerkinElmer, Inc.). Samples were vortexed and stored in the dark for 24 hours to minimise chemiluminescence resulting from the interaction between NaOH and the liquid scintillation cocktail. Samples were vortexed, placed in 20-mL liquid scintillation counting vials (PerkinElmer, Inc.) and analysed using a liquid scintillation counter (Tri-Carb 2910TR, PerkinElmer, Inc.).

The remaining volume of surface water (304 ml) was filtered through 0.2 μm Supor-200 (PALL Corporation) 47 mm diameter filter membranes using a vacuum pump (<10 cm Hg) to determine the assimilation of ^{14}C-labelled acetaldehyde into biomass. Filters were rinsed

with 2 mL of Milli-Q water and fixed with 2 mL of ethanol (80% v/v). Fixed filters were placed in 4-mL scintillation vials and were left to air-dry in a laminar flow cabinet for 24 hours. Filters were suspended in 4 mL of liquid scintillation cocktail (OptiPhase HiSafe III; PerkinElmer, Inc.) and analysed on a liquid scintillation counter (Tri-Carb 2910TR, PerkinElmer, Inc.). These protocols, assessing the microbial assimilation and dissimilation of ^{14}C-labelled acetaldehyde, were repeated every hour for the duration of the 4-hour incubation.

Uptake of the ^{14}C label during the microbial assimilation linear incorporation experiment was linear for the duration of the incubation period (R^2 = 0.994) (Figure 5.2), suggesting that incubations between 1 and 4 hours were suitable for assessing microbial acetaldehyde assimilation. Comparatively, an increase of 5 DPM was measured during the microbial dissimilation (oxidation) linear incorporation experiment between 1 and 4 hours (R^2 = 0.550) (Figure 5.3), indicating that the incubation went beyond the period of linear incorporation. Rates of microbial oxidation were therefore determined from the first hour of incubation during subsequent experiments. It is important to determine the duration of the linear incorporation period, as this provides an indication of the stability of the rate of microbial metabolism. Linear incorporation of the ^{14}C label demonstrates a consistent rate of microbial metabolism during the incubation period, whilst non-linear incorporation indicates a variable rate of metabolism. Data derived from the non-linear incorporation of the ^{14}C label do not provide reliable measures of microbial activity, therefore rates of microbial metabolism or uptake should only be determined during incubation periods of linear incorporation.
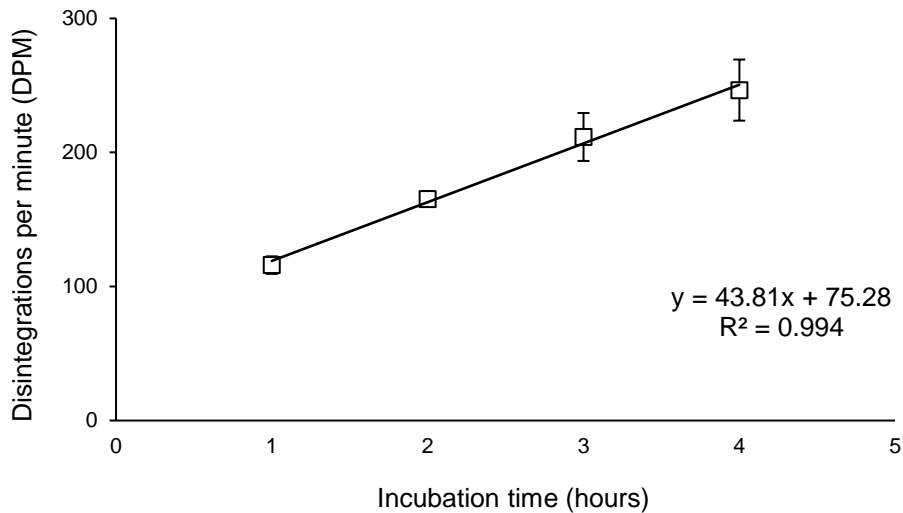
Figure 5.2 Time-course experiment showing the incorporation of the ^{14}C label into microbial biomass (assimilation) during a 4 hour incubation. The mean of three replicates is plotted for each time point (± S.E.). Incubations were performed with surface water samples from Gunnislake (River Tamar).
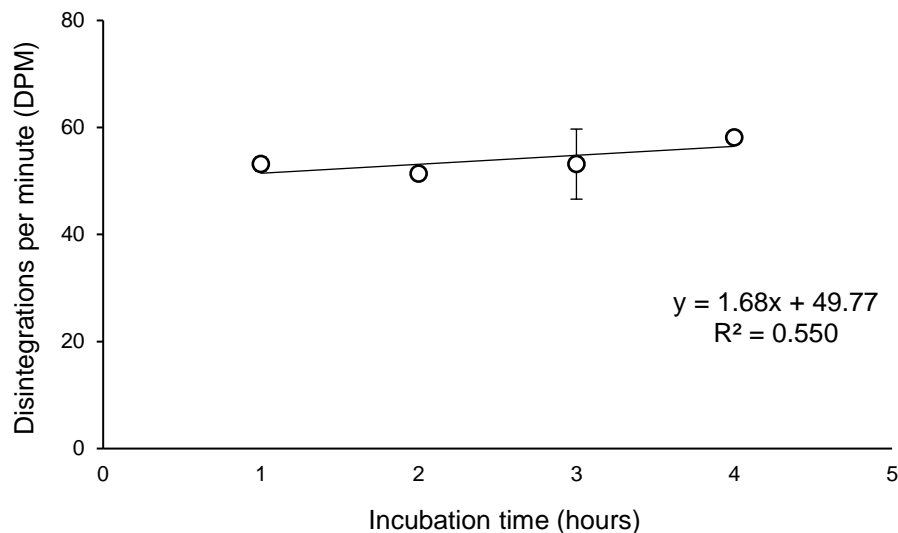
Figure 5.3 Time-course experiment showing the linearity of the microbial dissimilation of ^{14}C-acetaldehyde during a 4 hour incubation. The mean of three replicates is plotted for each time point (± S.E.). Incubations were performed with surface water samples from Gunnislake (River Tamar).

5.2.3 Method optimisation – Killed controls

Killed controls were used throughout this experiment to account for the effect of abiotic

processes, including chemiluminescence, the interaction of the ^{14}C label with microcentrifuge

tube walls, and scintillation counting error, in addition to the possibility of non-specific binding

of the ^{14}C label to microbial biomass. To determine the most-effective means of establishing

killed controls, three methods were considered, namely: filtration, filtration plus mercuric

chloride ($HgCl_2$), and filtration plus trichloroacetic acid (TCA). For all three methods, 305 mL

of surface water was filtered through 0.22 μm Sterivex™ filter units (Millipore) into acid-

washed, quartz Duran bottles in triplicate. To prepare $HgCl_2$-treated controls, 1 mL of filtered

surface water was removed from each bottle and replaced with 1 mL of $HgCl_2$ solution (3.5%

v/v final concentration). To prepare TCA-treated controls, 15.25 mL of filtered surface water

was removed from each bottle and replaced with 15.25 mL of TCA (≥99% purity; Acros

Organics) (5% final concentration). Bottles were inverted several times and incubated at the

in-situ surface temperature for 1 hour to allow the $HgCl_2$ and TCA to take effect. Bottles were

then spiked with 100 μL of ^{14}C-acetaldehyde stock, mixed and incubated at the in-situ

surface temperature for 3 hours. Sub-samples of treated surface water (1 ml) were taken

every hour to assess the microbial oxidation of ^{14}C-acetaldehyde into $^{14}CO_2$, following the

method outlined for the linear incorporation experiment (Section 5.2.2). After 3 hours of

incubation, water samples from each killed-control group were filtered onto 0.2 μM Supor-

200 (PALL Corporation) 47 mm diameter filter membranes using a vacuum pump (<10 cm

Hg) to determine the assimilation of ^{14}C-acetaldehyde into microbial biomass, following the

protocol of the linear incorporation experiment (Section 5.2.2).

Killed controls treated with TCA exhibited the lowest change in DPM during the 3 hour

incubation period following an assessment of microbial oxidation (Figure 5.4a-e) and

assimilation (Figure 5.4f). The largest increase in DPM counts was detected in the filtered-

only killed controls (Figure 5.4b, d & f), suggesting that live microorganisms were present

and actively taking up the ^{14}C label, despite filtration. DPM counts in the HgCl$_2$-treated killed controls were lower than the filtered-only killed controls but exhibited variability during hourly measurements of microbial oxidation (Figure 5.4a). This variability was attributed to the interaction of HgCl$_2$ with the ^{14}C label, resulting in increased photosensitivity. Accordingly, TCA treatment of surface water was identified as the optimal method to establish killed controls during the microbial acetaldehyde uptake experiments.

5.2.4 Microbial acetaldehyde uptake

Surface water samples from each site were pumped into 305 mL acid-washed, quartz Duran bottles (*n=3*) using a peristaltic pump and were incubated in the dark at the in-situ surface temperature. Killed controls were prepared as outlined in Section 5.2.3 using surface water from each site (*n=1*). The killed controls and surface water samples were spiked with 20 - 100 μL of ^{14}C-acetaldehyde stock (10 nM final concentration) and incubated for 3 hours at the in-situ surface temperature. Rates of microbial assimilation and dissimilation were measured using the methods described in Section 5.2.2.

5.2.5 Summer microbial acetaldehyde uptake

To investigate the effect of season on the rate of microbial acetaldehyde uptake, rates of acetaldehyde dissimilation and assimilation, measured between 7th and 26th July 2016 (Webb 2016), were compared with winter uptake rates measured here. Summer acetaldehyde dissimilation rates were measured in the East Dart, West Dart, Walkham, Meavy, Plym, Lynher, Erme and Yealm rivers, in addition to Cargreen, Tamar 6, Devil's Point, Plymouth Breakwater and station L4 (Figure 5.1). Summer assimilation rates were measured at the same sites, except for the rivers Meavy, Plym, Erme and Yealm.

5.2.6 Data analysis

The counting efficiency (E) of a ^{14}C internal standard (92.97%) was used to correct the DPM

counts for each sample (Equation 1). The counting efficiency was calculated by measuring

the ^{14}C internal standard on a Tri-Carb 2910TR liquid scintillation counter (PerkinElmer, Inc.)

and calculating the count rate (CPM) to DPM ratio. To calculate rates of microbial

acetaldehyde assimilation and dissimilation (nmol L^{-1} day^{-1}), corrected DPM counts of the

killed controls (d_C) were subtracted from sample DPM counts (d) to account for abiotic

processes (Equation 2). Control-corrected counts (DPM h^{-1}) were converted to Curies

(Ci mL^{-1} h^{-1}) (Equation 2) and were subsequently multiplied by the specific activity of the ^{14}C-

acetaldehyde stock (0.02 mol Ci^{-1}) (Equation 3). A decay rate was applied to the specific

activity of the ^{14}C-acetaldehyde stock to account for radioactive decay. These calculations,

adapted from Sargeant (2013), are shown below:

Equation 1.

$$E = 100 - 92.97 = 7.03$$

$$\frac{7.03}{100} = 0.0703$$

$$1 + 0.0703 = 1.0703$$

The counting efficiency (E) of the ^{14}C internal standard (92.97%) was subtracted from the

maximum efficiency value (100%). The resulting value was converted to a decimal and was

added to 1 to account for counting efficiency loss.

Equation 2.

$$dpm \times E = d$$

$$\left(\frac{d - d_c}{vt}\right) 4.5 \times 10^{-13} \times 10^9 = a \; (nCi \; mL^{-1} \; h^{-1})$$

DPM counts (*dpm*) were multiplied by *E* to correct for the counting efficiency. Corrected killed control counts (d_c) were subtracted from corrected sample counts (*d*) and were corrected for sample volume (*v*) and incubation time (*t*). Corrected sample counts were converted to Curies (Ci) by multiplying by 4.5×10^{-13}, with 1 DPM equivalent to 4.5×10^{-13} Ci. Curies were converted to nCi by multiplying by 10^9, resulting in *a* (nCi mL^{-1} h^{-1}). This equation was adapted from Sargeant (2013).

Equation 3.

$$a \times SA \times 1000 = m \ (nmol \ L^{-1} \ h^{-1})$$

$$m \times 24 = X \ (nmol \ L^{-1} \ day^{-1})$$

Sample counts (*a*) (nCi mL^{-1} h^{-1}) were multiplied by the specific activity (*SA*) of the ^{14}C-acetaldehyde stock (0.0199 mol Ci^{-1}) to convert to nmol mL^{-1} h^{-1}. This was multiplied by 1000 to convert to nmol L^{-1} h^{-1} (*m*). To convert to nmol L^{-1} day^{-1}, *m* was multiplied by 24. This equation was adapted from Sargeant (2013).

Winter and summer total acetaldehyde uptake rates were calculated for each site by combining microbial assimilation and dissimilation rates. Using XLSTAT-Premium Version 2020.1.3 (Addinsoft), a Pearson's correlation test (r) was performed to identify potential correlation between winter uptake rates and the corresponding environmental parameters for each site (Table 5.1). This analysis was not performed for summer uptake rates, as environmental parameters were not reported by Webb (2016) for these sampling sites.

Table 5.1 Environmental parameters recorded at sampling sites located in Devon and Cornwall, UK. Ammonium (NH_4^+) and nitrate (NO_3^-) were not measured at Tamar Estuary sites due to saltwater interference with sensors (NA). Measurements were recorded between 20th and 26th February 2020.

Date	River/Estuary	Site	Temperature (°C)	Salinity (ppt)	pH	Dissolved oxygen (%)	Turbidity (NTU)	NH_4^+ (mg/L)	NO_3^- (mg/L)	Run-off influence
20/02/20	River Tamar	Dutson	8.7	0.44	7.83	95.60	12.30	0.24	4.07	Arable
20/02/20	River Tamar	Polson Bridge	8.6	0.41	7.74	94.10	12.40	0.25	3.83	Arable
20/02/20	River Tamar	Horsebridge	8.8	0.40	7.72	96.80	9.00	0.35	4.65	Arable
20/02/20	River Tamar	Gunnislake	9.0	0.35	7.59	98.60	14.60	0.40	5.51	Arable
20/02/20	River Inny	River Inny	9.4	0.70	7.75	98.10	10.10	0.29	4.50	Arable
25/02/20	Tamar Estuary	Halton Quay	9.4	3.78	8.72	94.80	32.80	NA	NA	Arable
25/02/20	Tamar Estuary	Cargreen	9.4	3.46	7.39	94.20	35.90	NA	NA	Arable
25/02/20	Tamar Estuary	Saltash	9.3	5.66	7.44	95.40	19.80	NA	NA	Arable
26/02/20	East Dart River	Postbridge	4.8	0.67	7.91	95.90	2.10	0.37	0.40	Moor
26/02/20	West Dart River	Two Bridges	5.2	0.49	8.62	96.90	0.30	0.11	0.15	Moor
26/02/20	River Walkham	Horrabridge	7.1	0.99	8.04	99.70	0.80	0.12	0.60	Moor
26/02/20	River Meavy	Shaugh Bridge	7.6	1.01	9.20	99.80	1.10	0.09	0.55	Moor
26/02/20	River Plym	Shaugh Bridge	5.4	0.60	9.32	99.90	1.00	0.09	0.14	Moor
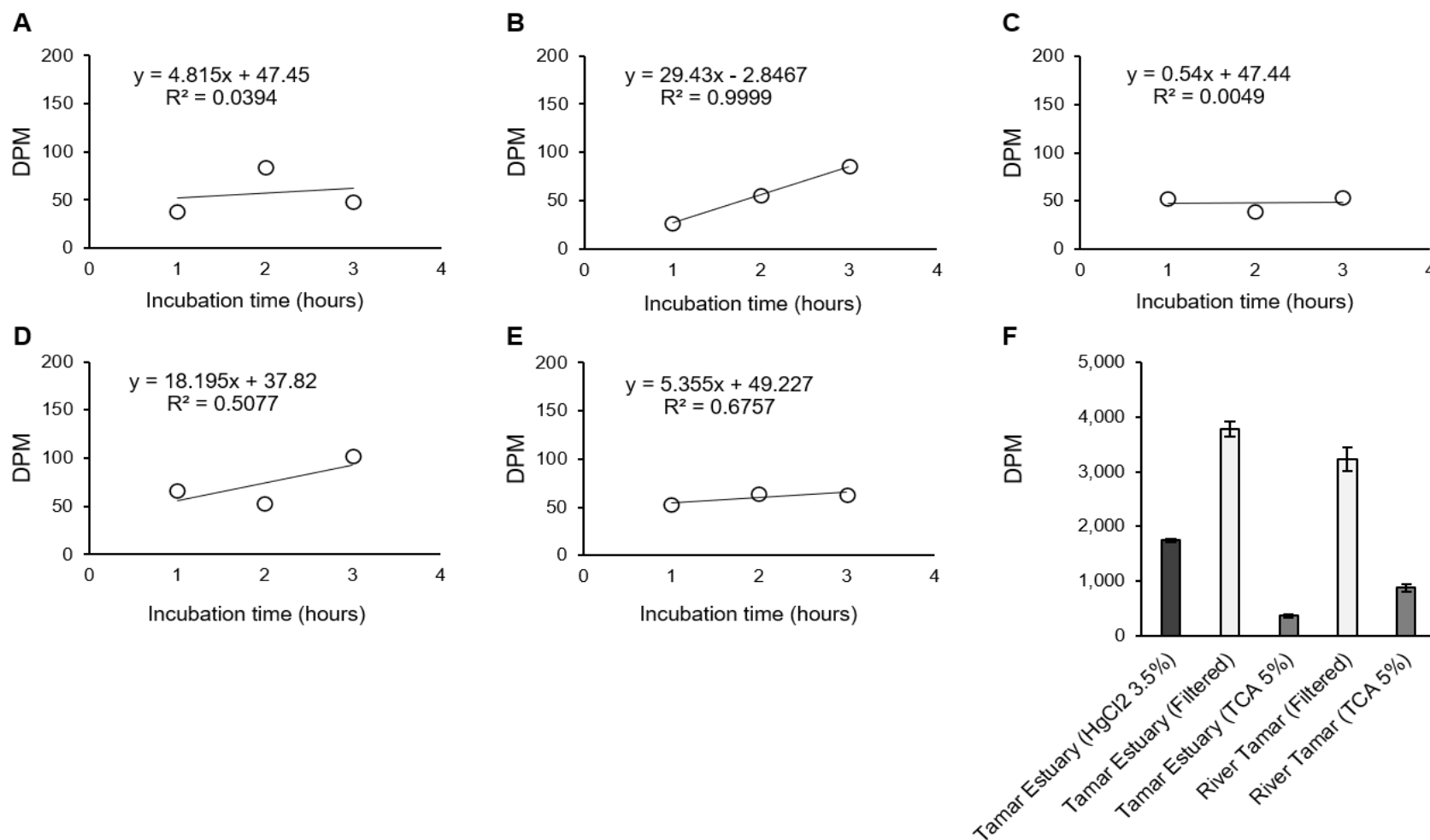
Figure 5.4 DPM counts of killed controls assessed for microbial oxidation (A-E) and assimilation (F) during a 3 hour incubation. A) $HgCl_2$-treated (3.5% v/v) Tamar Estuary surface water. B) Filtered-only Tamar Estuary surface water. C) TCA-treated (5%) Tamar Estuary surface water. D) Filtered-only River Tamar surface water. E) TCA-treated (5%) River Tamar surface water. F) DPM counts of $HgCl_2$-treated (3.5% v/v), filtered-only, and TCA-treated (5%) Tamar Estuary and River Tamar surface water used to assess the microbial assimilation of the ^{14}C label. Tamar Estuary and River Tamar surface water samples used here were from Saltash and Gunnislake, respectively.

5.3 Results

5.3.1 Microbial assimilation of acetaldehyde

Winter rates of microbial acetaldehyde assimilation ranged between 0.001 and 0.49 nmol L^{-1} day^{-1} (Table 5.2). In moorland-influenced rivers, acetaldehyde assimilation rates of 0.02 - 0.38 nmol L^{-1} day^{-1} were measured, with the Plym and Meavy exhibiting the highest rates of assimilation. In the arable-influenced River Inny, a winter assimilation rate of 0.09 ± 0.04 nmol L^{-1} day^{-1} was measured. The highest rate of acetaldehyde assimilation was measured at Gunnislake (0.49 ± 0.08 nmol L^{-1} day^{-1}), situated on the River Tamar. At the three other River Tamar sites assimilation rates ranged between 0.001 and 0.13 nmol L^{-1} day^{-1}. In the Tamar Estuary, assimilation rates of 0.06 - 0.09 nmol L^{-1} day^{-1} were measured, whilst surface water from station L4 exhibited an assimilation rate of 0.02 ± 0.02 nmol L^{-1} day^{-1}.

Summer rates of microbial acetaldehyde assimilation measured by Webb (2016) were significantly higher than winter assimilation rates, ranging between 3.84 and 14.16 nmol L^{-1} day^{-1} (Table 5.2). The highest rate of assimilation was measured in the moorland-influenced West Dart, whilst the lowest rate was measured at station L4. In the Lynher, the only river sampled in summer that was influenced by arable land use, an assimilation rate of 6.72 ± 0.17 nmol L^{-1} day^{-1} was measured. In the Tamar Estuary, rates of acetaldehyde assimilation ranged between 6.48 ± 1.02 nmol L^{-1} day^{-1} at Plymouth Breakwater and 13.92 ± 1.70 nmol L^{-1} day^{-1} at Devil's Point.

5.3.2 Microbial dissimilation of acetaldehyde

Rates of microbial acetaldehyde dissimilation were generally higher than rates of assimilation during both winter and summer (Table 5.2). Winter rates of acetaldehyde dissimilation ranged between 0.08 and 7.40 nmol L^{-1} day^{-1}. The highest rate of dissimilation was measured at the arable-influenced Polson Bridge, which is also located <100 m

downstream of a sewage treatment works, whilst the lowest dissimilation rate was measured in seawater at station L4 in the western English Channel. Dissimilation rates of 1.23 ± 0.54 and 1.00 ± 0.89 nmol L^{-1} day^{-1} were measured in the West Dart and Plym, respectively, whilst dissimilation rates for the East Dart, Walkham, and Meavy were below the limit of detection. In the River Inny, which is influenced by upstream discharges from a local cheese factory, a winter dissimilation rate of 1.93 ± 1.42 nmol L^{-1} day^{-1} was measured. Microbial dissimilation rates ranged between 2.54 and 4.16 nmol L^{-1} day^{-1} in the Tamar Estuary.

In summer, microbial acetaldehyde dissimilation rates ranged between 59.76 and 164.16 nmol L^{-1} day^{-1} and were considerably higher than winter rates (Table 5.2). The highest rate of dissimilation was measured in the Yealm, whilst the lowest rate was measured in the Walkham. In the arable-influenced River Lynher, a dissimilation rate of 85.44 ± 8.87 nmol L^{-1} day^{-1} was measured. Rates of acetaldehyde dissimilation in the Tamar Estuary ranged between 109.68 and 113.28 nmol L^{-1} day^{-1}, with the highest rates measured at Devil's Point and Tamar 6. At the coastal marine station L4, a summer dissimilation rate of 143.28 ± 6.24 nmol L^{-1} day^{-1} was measured.

5.3.3 Total uptake, turnover time, and bacterial growth efficiency

Total acetaldehyde uptake rates were calculated for each site by combining microbial assimilation and dissimilation rates (Table 5.2). Total uptake rates were consistently higher in the summer period, ranging between 71.52 and 147.12 nmol L^{-1} day^{-1}, compared to 0.10 - 7.44 nmol L^{-1} day^{-1} in the winter. In summer, microbial uptake rates were highest at station L4, whilst sites along the Tamar Estuary also exhibited high uptake rates of 117.84 - 126.96 nmol L^{-1} day^{-1}. Comparatively, uptake rates during winter were lowest at station L4, and ranged between 2.62 and 4.22 nmol L^{-1} day^{-1} in the Tamar Estuary. The lowest summer uptake rates were measured in the rivers Walkham, West Dart and East Dart, ranging between 71.52 and 89.52 nmol L^{-1} day^{-1}. In winter, uptake rates of 1.21 and 1.25 nmol L^{-1}

day^{-1} were measured for the Plym and the West Dart, respectively. Uptake rates could not be determined for the Meavy, Plym, Erme, and Yealm rivers in summer, as assimilation rates were not measured. Similarly, winter uptake rates for the East Dart, Walkham, and Meavy were not calculated, as dissimilation rates were below the limit of detection. In the River Tamar, winter uptake rates ranged between 1.03 and 7.44 nmol L^{-1} day^{-1}, with the highest rate measured at Polson Bridge, which is situated <100 m downstream of a sewage processing station.

A Pearson's correlation test was performed to assess the relationship between winter acetaldehyde uptake rates and the environmental parameters recorded in Table 5.1. Winter uptake rates correlated positively with temperature ($r = 0.411$), however this correlation was not significant ($p = 0.238$). Weaker positive correlations were also identified for nitrate ($r = 0.330$; $p = 0.47$), turbidity ($r = 0.319$; $p = 0.369$) and ammonium ($r = 0.200$; $p = 0.667$), however these relationships were also insignificant. No correlation was identified between winter uptake rates and salinity ($r = 0.035$; $p = 0.923$). A strong and significant negative correlation was identified between dissolved oxygen and winter uptake rates ($r = -0.758$; $p = 0.011$). To identify the drivers of this correlation, a Pearson's correlation test was performed on winter assimilation and dissimilation rates versus the same environmental parameters. No correlation was identified between assimilation rates and dissolved oxygen however, a strong negative correlation was identified between dissolved oxygen and dissimilation rates ($r = -0.768$; $p = 0.009$). To ensure that this correlation was not driven by the dissolved oxygen measurements at Polson Bridge, which may result from increased nitrification due to the close proximity of a sewage treatment works, a Pearson's correlation test was performed on winter dissimilation rates versus dissolved oxygen measurements, excluding Polson Bridge. A strong and significant negative correlation was similarly identified between dissolved oxygen and dissimilation rates ($r = -0.764$; $p = 0.016$). A weak negative correlation was also identified for pH ($r = -0.375$), although this relationship was not significant ($p = 0.286$).

Microbial turnover times, defined as the time taken for microorganisms to completely utilise an added carbon source or nutrient, were calculated for acetaldehyde by dividing the concentration of added acetaldehyde by the total uptake rate. Turnover times were fastest during the summer, ranging from 0.8 - 2.7 hours, compared to 4.2 - 40.1 hours in winter (Table 5.2). In summer, turnover times were fastest at station L4 and were slowest in the River Lynher. In the Tamar Estuary, summer turnover times ranged between 1.5 and 2.4 hours, with the faster turnover times measured in surface water sampled closest to station L4 (Devil's Point and Plymouth Breakwater). Turnover times of 1.7 - 2.4 hours were measured in moorland-influenced rivers. In winter, turnover times were fastest in the Plym and, in contrast to summer, were slowest at station L4. In the Tamar Estuary, turnover times ranged between 5.9 and 7.1 hours and were generally faster than riverine environments, with the rivers Inny and Tamar exhibiting turnover times of 16.7 hours and 6.2 - 11.1 hours, respectively.

Bacterial growth efficiency, the proportion of carbon converted into biomass rather than respired as CO_2 (from a scale of 0 to 1), was highly variable during the winter period, ranging from <0.01 - 0.48 (Table 5.2). In riverine environments, the highest bacterial growth efficiencies were calculated for the Plym (0.17) and Gunnislake (0.48), whilst the lowest bacterial growth efficiencies were calculated for Horsebridge (<0.01), Polson Bridge (0.01) and the West Dart (0.01). In the Tamar Estuary, winter bacterial growth efficiencies ranged between 0.01 and 0.03, whilst a bacterial growth efficiency of 0.22 was measured for L4. In summer, bacterial growth efficiencies were less variable and ranged between 0.03 and 0.17. In the East Dart, West Dart, Walkham and Lynher, bacterial growth efficiencies of 0.11, 0.17, 0.16, and 0.07 were calculated, respectively. In the Tamar Estuary, bacterial growth efficiencies ranged between 0.05 and 0.11, with the highest bacterial growth efficiency measured in surface waters from Devil's Point. At L4, summer bacterial growth efficiency was considerably lower than in winter, with a bacterial growth efficiency of 0.03 measured.

Table 5.2 Microbial assimilation, dissimilation, total uptake, turnover time, and bacterial growth efficiency of ^{14}C-acetaldehyde in riverine, estuarine, and coastal water samples from south-west England during winter (20-27th February 2020) and summer (7-26th July 2016). Summer data (highlighted in grey) were collected by Christopher Webb, as reported in Webb (2016). The mean of three replicates is plotted for winter assimilation rates (± S.E.), except for Horsebridge (*n=1*), whilst the mean of two replicates is plotted for summer assimilation rates (± S.E.), except for Cargreen (*n=1*). The mean of three replicates is plotted for winter and summer dissimilation rates (± S.E.). NA: not available; <LOD: below limit of detection; -: data not collected.

Site	Assimilation (nmol L^{-1} d^{-1}) Winter	Summer	Dissimilation (nmol L^{-1} d^{-1}) Winter	Summer	Total uptake (nmol L^{-1} d^{-1}) Winter	Summer	Turnover time (hours) Winter	Summer	Bacterial growth efficiency Winter	Summer
Dutson	0.13 ± 0.11	-	3.39 ± 2.87	-	3.52	-	10.3	-	0.04	-
Polson Bridge	0.04 ± 0.03	-	7.40 ± 2.84	-	7.44	-	6.2	-	0.01	-
Horsebridge	0.001	-	4.32 ± 2.27	-	4.32	-	11.1	-	<0.01	-
Gunnislake	0.49 ± 0.08	-	0.54 ± 0.20	-	1.03	-	8.7	-	0.48	-
River Inny	0.09 ± 0.04	-	1.93 ± 1.42	-	2.02	-	16.7	-	0.05	-
Halton Quay	0.09 ± 0.01	-	3.32 ± 0.56	-	3.41	-	5.9	-	0.03	-
Cargreen	0.06 ± 0.01	9.60	4.16 ± 2.66	109.68 ± 1.25	4.22	119.28	6.8	2.4	0.01	0.08
Saltash	0.08 ± 0.01	-	2.54 ± 0.83	-	2.62	-	7.1	-	0.03	-
Tamar 6	-	9.12 ± 0.85	-	113.28 ± 4.85	-	122.40	-	1.7	-	0.07
Devil's Point	-	13.92 ± 1.70	-	113.04 ± 0.55	-	126.96	-	1.5	-	0.11
Plymouth Breakwater	-	6.48 ± 1.02	-	111.36 ± 3.19	-	117.84	-	1.5	-	0.05
L4	0.02 ± 0.02	3.84 ± 1.36	0.08 ± 0.06	143.28 ± 6.24	0.10	147.12	40.1	0.8	0.22	0.03
East Dart	0.03 ± 0.01	9.60 ± 0.51	<LOD	79.92 ± 10.39	NA	89.52	NA	1.8	NA	0.11
West Dart	0.02 ± 0.01	14.16 ± 2.55	1.23 ± 0.54	70.08 ± 11.36	1.25	84.24	23.8	1.7	0.01	0.17
Walkham	0.04 ± 0.02	11.76 ± 1.53	<LOD	59.76 ± 6.51	NA	71.52	NA	2.4	NA	0.16
Meavy	0.38 ± 0.02	-	<LOD	148.80 ± 2.91	NA	NA	NA	NA	NA	NA
Plym	0.21 ± 0.01	-	1.00 ± 0.89	145.92 ± 11.36	1.21	NA	4.2	NA	0.17	NA
Lynher	-	6.72 ± 0.17	-	85.44 ± 8.87	-	92.16	-	2.7	-	0.07
Erme	-	-	-	159.36 ± 4.71	-	NA	-	NA	-	NA
Yealm	-	-	-	164.16 ± 20.92	-	NA	-	NA	-	NA

5.4 Discussion

Oxygenated volatile organic compounds, such as methanol, acetone, and acetaldehyde can significantly influence the oxidative capacity of the atmosphere, leading to indirect effects on the global radiative balance and climate. Compared to OVOC sources, our knowledge of OVOC sinks is poor. This is despite suggestions that microbial uptake in terrestrial soils and aquatic ecosystems may significantly contribute to OVOC biogeochemical cycles by mediating the flux of OVOCs to the atmosphere. The results of this study demonstrate that acetaldehyde flux is under considerable microbial control in aquatic ecosystems and that acetaldehyde-degrading microorganisms are present and active in freshwater rivers, estuaries, and nearshore coastal zones (L4, western English Channel). To the best of my knowledge, this study reports the first microbial uptake rates of acetaldehyde from riverine and estuarine environments during winter and in combination with summer measurements from Webb (2016) demonstrates for the first time the large effect of seasonality on these rates. These findings contribute to our current understanding of acetaldehyde cycling in aquatic ecosystems and suggest that riverine, estuarine, and marine environments present an important biological sink that is currently not recognised in global models of the acetaldehyde budget.

Microbial acetaldehyde uptake rates in summer were highest in surface waters from marine station L4 and were lowest in moorland and arable-influenced rivers. This is surprising given that rivers are thought to receive regular inputs of CDOM from the breakdown of terrestrially derived organic material, which is converted to acetaldehyde and other low molecular weight organic compounds, and acts as a carbon and energy source for microorganisms (de Bruyn et al. 2011). It was hypothesised that the regular availability of acetaldehyde in rivers would help to prime microbial communities for acetaldehyde degradation, either by selecting for specific acetaldehyde-degrading microorganisms or by activating the enzymes necessary for acetaldehyde degradation, such as aldehyde dehydrogenases (see Chapter 4). Similar

changes in microbial community composition and enzyme activation have been observed in soils in response to a variety of carbon sources such as trichloroacetic acid (Albers et al. 2010; Rinnan & Albers 2020). The summer uptake rates reported here for the rivers Lynher, Walkham, East Dart, and West Dart suggest that the regular availability of acetaldehyde in these environments does not pre-condition microbial communities to acetaldehyde any more than microbial communities in the Tamar Estuary and at station L4. One explanation for this may be that estuaries and coastal seas also receive inputs of CDOM. This may be terrestrially sourced in estuaries given the connectivity between estuaries and terrestrial environments (Nedwell et al. 2016), whilst in coastal seas and the open ocean, the grazing and viral lysis of phytoplankton has also been identified as a source of CDOM (de Bruyn et al. 2011). In both environments, the photodegradation of CDOM would likely result in the production of acetaldehyde and other organic compounds, which could be utilised as a carbon and energy source by microbial communities and may pre-condition these communities to acetaldehyde. It has also been suggested that terrestrially-derived CDOM in rivers can be transported to estuarine and marine environments before it is degraded (Callahan et al. 2004). In this scenario, the degradation of terrestrially sourced CDOM in estuaries, coastal regions and the open ocean would act as an additional source of acetaldehyde in these environments that may help to pre-condition these microbial communities to acetaldehyde more than microbial communities in rivers, as might be expected with limited CDOM transportation. This may help to explain the higher rates of microbial acetaldehyde uptake measured in surface waters from L4 and the Tamar Estuary during summer compared to uptake rates in rivers. Alternatively, the high uptake rates measured at station L4 may result from coastal microbial communities being primed for acetaldehyde degradation by acetaldehyde derived from the demethylation of dimethylsulfoniopropionate (DMSP). It has previously been demonstrated that marine DMSP concentrations correlate closely with phytoplankton abundance, with DMSP concentrations and phytoplankton biomass in the Yellow Sea and Bohai Sea, for example, peaking in summer (Yang et al. 2014). As mentioned in Section 1.6, the final reaction of the DMSP

demethylation pathway results in the conversion of methylthioacryloyl-CoA to acetaldehyde and CO_2 via the methylthioacryloyl-CoA hydratase, DmdD (Curson et al. 2011). The acetaldehyde resulting from this pathway may help to prime coastal microbial communities for degradation, either by selecting for specific acetaldehyde-degrading microorganisms or by activating the enzymes necessary for acetaldehyde degradation. This hypothesis could be tested in future studies by measuring both DMSP concentrations and acetaldehyde uptake rates in coastal and marine environments during summer to determine if uptake rates correlate with the production of DMSP. Furthermore, seawater incubation experiments with and without DMSP could be performed to assess whether the capacity for microbial acetaldehyde uptake is enhanced when microbial communities are first primed with acetaldehyde derived from DMSP demethylation. Consequently, based on the summer uptake rates measured in the rivers of south-west England, hypothesis one (H1) was rejected.

An alternative explanation for the lower summer uptake rates in rivers compared with estuaries may be the influence of seasonality on CDOM sources. In summer, it is likely that less terrestrially-sourced organic material, such as leaf litter, will enter river systems compared to autumn and winter months, resulting in lower riverine concentrations of CDOM. Following photodegradation, this would also result in limited amounts of acetaldehyde and other low molecular weight organic compounds for microbial communities to use as a carbon and energy source. Accordingly, microbial communities in rivers would be less pre-conditioned to acetaldehyde than microbial communities in estuaries and coastal seas, where alternative sources of CDOM, and therefore acetaldehyde, are available. This hypothesis may also help to explain the microbial acetaldehyde uptake rates measured in winter, which were lowest at L4 and were highest at sites located along the Tamar Estuary and river. The increased loading of organic material, such as leaf litter and detritus, into rivers during winter could result in increased concentrations of CDOM. The breakdown of CDOM could result in elevated concentrations of acetaldehyde, facilitating the growth of

acetaldehyde-degrading microorganisms that may be present in riverine environments, or increasing the up-expression of enzymes involved in acetaldehyde degradation within the microbial community, although UV levels are generally lower during winter months, resulting in less CDOM photodegradation. The microbial community would therefore be pre-conditioned to acetaldehyde, which may explain the higher uptake rates measured in the River Tamar sites, although pre-conditioning may not occur in fast-flowing rivers and estuaries, or when sources of acetaldehyde are infrequent. However, this hypothesis is not supported by the findings of Beale et al. (2015), which reported acetaldehyde concentrations of 4 - 37 nM at station L4 during an annual study, with the highest concentrations recorded during autumn and winter. This suggests that coastal zones also experience higher acetaldehyde concentrations during winter months and that the low uptake rates measured at L4 were not due to limited substrate availability. This suggests that other factors are likely to be responsible for the lower summer acetaldehyde uptake rates measured in rivers, and winter uptake rates measured at station L4.

An alternative hypothesis for the low uptake rates measured in rivers during summer may be the effect of enhanced UV radiation on microbial communities. UV radiation is considerably higher during summer and has been shown to cause damage to the DNA and cellular machinery of heterotrophic bacteria (Ruiz-González et al. 2013). This may be direct damage by the absorption of photons from UV-B (280 - 320 nm) or indirect oxidative damage resulting from the formation and accumulation of reactive oxygen species (ROS) due to UV-A (320 - 400 nm). UV-A can penetrate further into the water column than UV-B and cumulatively causes more damage to bacterial cells (Ruiz-González et al. 2013). Water levels in rivers are also generally lower in summer than in winter, suggesting that UV-A may penetrate significantly further into the water column during summer and could damage a significant proportion of the microbial community, resulting in lower acetaldehyde uptake rates. It is important to note that CDOM photodegradation is initiated by UV-B absorption (Section 1.2), so although CDOM photodegradation, and therefore acetaldehyde production,

would be higher due to increased UV-B radiation in summer, the microbes responsible for acetaldehyde degradation may simultaneously be damaged by the enhanced UV radiation. Accordingly, the low summer uptake rates measured in rivers may be a result of elevated UV levels, however, this requires further investigation, as the damage caused to bacteria by UV exposure can also be repaired by mechanisms including photoenzymatic repair, nucleotide excision repair, and post-replication repair (Ruiz-González et al. 2013). The effect of UV radiation on riverine microbial communities could be investigated by monitoring the overall metabolic activity of microorganisms. This could include measuring the degradation and incorporation of other tracer molecules, such as glucose, amino acids, thymine, and leucine, as the utilisation of these molecules provides a clear indication of the regular cellular activities of microorganisms. Limited uptake and incorporation of these tracer molecules would suggest that UV radiation damages the cellular machinery and may be responsible for the low summer acetaldehyde uptake rates measured in rivers.

Another hypothesis for the low uptake rates measured at station L4 during winter may be the effect of lower temperatures on microbial activity or compositional changes in microbial communities that coincide with seasonal change. Winter uptake rates correlated positively with temperature (r = 0.411), suggesting that lower temperatures may decrease the activity of acetaldehyde-degrading microorganisms. The relationship between uptake rate and temperature was not significant (p = 0.238), however, this was based on a small sample size ($n=10$) and a limited temperature range. Future investigations are therefore necessary to determine if microbial acetaldehyde uptake rates are controlled by temperature and if compositional changes of the microbial community contribute to significant differences in acetaldehyde uptake.

Microbial acetaldehyde uptake rates were considerably higher in summer compared to winter, in agreement with hypothesis two (H2). These results demonstrate for the first time that microbial acetaldehyde uptake rates in rivers, estuaries, and coastal seas respond to

seasonal changes. It was proposed that the increase in microbial uptake rates in summer would be in response to elevated surface temperatures, with warmer surface waters resulting in increased microbial enzymatic activity. Unfortunately, environmental parameters including temperature were not recorded during the summer sampling season, so it is difficult to conclusively identify the environmental factor(s) most responsible for the increase in microbial uptake rates. To provide an indication of the environmental factor most responsible for influencing microbial acetaldehyde uptake rates, the relationship between winter microbial uptake rates and the environmental parameters recorded in Table 5.1 was investigated. A positive but non-significant correlation was identified between winter uptake rates and temperature; however, it is important to note that this was based on a limited number of sampling sites (*n=10*) and a small temperature range. This finding is surprising given that previous studies have shown that microbial OVOC oxidation rates regularly exhibit an inverse relationship with temperature. Dixon et al. (2014), for example, measured the highest rates of microbial acetone oxidation during winter in the western English Channel, with temperatures ranging between 8.5 and 8.9°C. The lowest rates of acetone oxidation were measured in summer, with a temperature range of 13.8 - 16.4°C. Similarly, Sargeant et al. (2016) showed that rates of methanol oxidation in coastal waters of the western English Channel were highest in autumn and winter months and were lowest in spring and summer. Beale et al. (2015) also measured the highest rates of acetone oxidation in winter at coastal station L4 in the western English Channel and reported that acetaldehyde oxidation rates were highest in late autumn (October - November) and were lowest in spring. With the exception of dissolved oxygen, no significant correlation was identified between winter uptake rates reported here and any other environmental parameter recorded at the time of sampling. This suggests that microbial community composition may be an important factor driving acetaldehyde uptake rates. A strong and significant negative correlation was identified between winter uptake rates and dissolved oxygen. Further investigation revealed that this correlation was driven by microbial dissimilation and not assimilation. One possible

explanation for this is that reduced levels of dissolved oxygen induce stress in aerobic microorganisms, resulting in increased cellular activity and therefore higher energy demands. These energy demands are met by increasing the rate of dissimilation, ensuring that the cell can survive the change in environmental conditions. Future studies should investigate the effect of dissolved oxygen concentrations on the rate of microbial dissimilation and assimilation to establish the validity of this correlation. Understanding the reason(s) for this relationship and the cellular mechanisms behind it may help to identify a previously overlooked environmental factor that significantly influences microbial acetaldehyde uptake.

Rates of microbial acetaldehyde dissimilation were significantly higher than microbial assimilation rates in both winter and summer, in agreement with hypothesis three (H3). This suggests that microorganisms predominantly use acetaldehyde as an energy source, but still assimilate a small proportion of acetaldehyde-derived carbon into biomass. The predominant utilisation of acetaldehyde as an energy source has been observed previously. Halsey et al. (2017), for example, demonstrated that two strains of *Pelagibacter* SAR11, namely HTCC1062 and HTCC7211, could dissimilate and assimilate ^{14}C-labelled acetaldehyde. It was shown that microbial dissimilation accounted for ~70% of acetaldehyde uptake, whilst the remaining ~30% of utilised acetaldehyde was incorporated into cell biomass. By extrapolating the rates of acetaldehyde dissimilation it was estimated that the global SAR11 community could oxidise more acetaldehyde than is currently estimated to be globally produced. It was therefore suggested that the majority of acetaldehyde in the marine environment may be recycled instead of entering the atmosphere, although CO_2 resulting from acetaldehyde oxidation could still exchange with the atmosphere, particularly in surface waters. Similarly, Dixon et al. (2013a) reported that microbial oxidation in surface waters of the Atlantic Ocean accounted for 49 - 100% of acetaldehyde losses. These findings further demonstrate that microorganisms primarily dissimilate acetaldehyde for energy production and that microbial assimilation accounts for a small proportion of acetaldehyde uptake. For

other OVOCs, such as methanol and acetone, the preference of microorganisms to dissimilate or assimilate these carbon sources is less clear. In the same study, Dixon et al. (2013a) attributed 10 - 50% of methanol losses in surface waters of the Atlantic Ocean to microbial oxidation, suggesting that methanol concentrations are controlled by microbial dissimilation rather than assimilation, although assimilation rates were not measured. Conversely, Dixon et al. (2013b) reported that microorganisms in the nutrient-rich Mauritanian coastal upwelling assimilated 57% of methanol into biomass, demonstrating that the preference of microorganisms to dissimilate or assimilate methanol is uncertain and likely depends on a number of environmental factors. Dixon et al. (2013a) also showed that microbial oxidation accounted for 0.5 - 13% of acetone losses in surface waters of the Atlantic Ocean, implying that acetone concentrations are under less microbial control than methanol and acetaldehyde. This was also concluded by Dixon et al. (2014), which reported relatively low marine microbial oxidation rates of 0.03 - 1 nmol L^{-1} day^{-1} for acetone in the western English Channel. However, in both studies the rate of microbial acetone assimilation was not measured, making it difficult to determine whether microorganisms preferentially dissimilate acetone for energy or assimilate acetone-derived carbon into biomass. Based on the findings of Halsey et al. (2017) and the results of this study, it seems likely that microbial dissimilation accounts for the majority of microbial OVOC uptake, although it is important to note that not all OVOCs are utilised by microorganisms in the same way. This is demonstrated by the differences in acetaldehyde, methanol and acetone losses in seawater attributed to microbial dissimilation, as reported by Dixon et al. (2013a).

The bacterial growth efficiencies reported in Table 5.2 clearly demonstrate the low proportion of acetaldehyde-derived carbon converted into biomass rather than respired as CO_2. With exception to the River Tamar (at Gunnislake), marine station L4 and the River Plym, bacterial growth efficiencies in winter were low, ranging between <0.01 and 0.05. This suggests that as much as 95 - 99% of utilised acetaldehyde is respired as CO_2. Similar bacterial growth efficiencies have been reported for methanol, with Dixon et al. (2011b)

reporting bacterial growth efficiencies of 0.02 - 0.04 in surface waters of the oligotrophic, tropical north-east Atlantic Ocean. The low bacterial growth efficiencies were suggested to reflect the low availability of nutrients and dissolved organic carbon, in addition to the high energetic costs of growing in an ocean gyre (Dixon et al. 2011b). It may be concluded therefore that microorganisms in the rivers, estuaries, and coastal seas of south-west England have increased energy demands because of the environmental conditions in these aquatic systems, and do not allocate much acetaldehyde-derived carbon to growth. This does not seem to be the case for the River Tamar (at Gunnislake), marine station L4 and the River Plym, where only 52%, 78% and 83% of acetaldehyde-derived carbon was respired as CO_2, respectively. This suggests that environmental conditions at these sites are less energy demanding and that microorganisms can allocate more acetaldehyde-derived carbon to growth. With exception to the rivers Walkham and the West Dart, summer bacterial growth efficiencies were also low, ranging between 0.03 and 0.11. These growth efficiencies also suggest a high energy cost for microorganisms living in rivers, estuaries, and coastal seas, possibly due to the environmental conditions in these systems, which prevents these microorganisms from allocating carbon to biomass. In the rivers Walkham and the West Dart, 83% and 84% of acetaldehyde-derived carbon was respired as CO_2, respectively. The bacterial growth efficiencies reported for these sites suggest that environmental conditions are more conducive to growth, thus more carbon is diverted to biomass. It is unclear which environmental parameter is responsible for the high energy demands in these systems, and it is likely that more than one parameter results in a reduction of microbial growth in favour of meeting the necessary energy demands. Future studies should investigate the relationship between environmental parameters and bacterial growth efficiencies to establish which parameters are primarily responsible for inducing a shift towards high energy production and away from microbial growth.

The results of this study demonstrate that the microorganisms found in freshwater rivers, estuaries, and coastal seas represent an important acetaldehyde sink that is not currently

recognised in global models of acetaldehyde emissions. Previous models have calculated acetaldehyde flux from the marine environment based on CDOM photodegradation (Singh et al. 2004; Millet et al. 2010), which does not consider the activity of marine acetaldehyde degraders. In this study, microbial uptake rates from coastal station L4 were the highest reported during summer, suggesting that microbial communities in coastal seas can significantly influence the atmospheric flux of acetaldehyde. Previous global models of acetaldehyde have also not included emissions from freshwater rivers and estuaries, as acetaldehyde emissions have yet to be reported from these environments. Future investigations are needed to establish acetaldehyde emissions from these environments and to improve the accuracy of global models. The results of this study, however, suggest that acetaldehyde emissions from freshwater rivers and estuaries will also be under considerable microbial control, particularly during summer. The microbial uptake rates reported here for freshwater rivers, estuaries, and coastal seas suggest that previous global models of acetaldehyde have overestimated acetaldehyde emissions by excluding microbial sink terms. By including microbial sink terms and acetaldehyde emissions from freshwater rivers and estuaries, future models will become increasingly accurate. To improve these models further, it is essential that future research focusses on measuring in-situ acetaldehyde concentrations, production rates and microbial uptake rates, particularly in freshwater rivers, estuaries, coastal seas, and open oceans.

To improve our understanding of the biogeochemical cycle of acetaldehyde, future work should further investigate the relationship between microbial acetaldehyde uptake rates and environmental parameters, including temperature and dissolved oxygen concentration. The effect of temperature should be a key focus given the strong relationship between microbial oxidation rates and cooler surface temperatures reported in previous studies. The effect of dissolved oxygen concentration should also be investigated given the strong negative correlation with microbial dissimilation rates identified in this study. The relationship between CDOM concentration and microbial acetaldehyde uptake rates should also be examined to

determine if the regular or continuous availability of acetaldehyde, resulting from CDOM photodegradation, pre-conditions microbial communities to acetaldehyde, resulting in higher microbial uptake rates. Similarly, the relationship between microbial acetaldehyde uptake rates and DMSP concentration, particularly in coastal and marine environments, should be explored in more detail. This study investigated the effect of seasonality on microbial acetaldehyde uptake rates in freshwater rivers, estuaries, and coastal seas, and demonstrated for the first time that microbial uptake rates are significantly influenced by season. To further improve our understanding of the effects of seasonality on microbial acetaldehyde uptake rates, future studies should measure microbial uptake rates during autumn and spring. This would provide an indication of the annual cycle of microbial acetaldehyde uptake in aquatic ecosystems. The bacterial growth efficiencies measured in this study suggest that microorganisms in freshwater rivers, estuaries, and coastal seas have a high energy demand and allocate a relatively small amount of acetaldehyde-derived carbon to biomass. Future research should investigate the environmental parameters that drive this energy demand, which may help to identify the environmental parameters that drive the microbial dissimilation and assimilation of acetaldehyde.

5.5 Conclusion

This study has demonstrated that microorganisms represent a fundamental acetaldehyde sink in the freshwater rivers, estuaries, and coastal seas of south-west England. To the best of my knowledge, this is the first study to report winter microbial acetaldehyde uptake rates in freshwater rivers and estuaries. This study is also the first to investigate the effect of seasonality on microbial acetaldehyde uptake rates and has demonstrated that uptake rates are significantly higher in summer compared to winter. Although previous studies have identified an inverse relationship between microbial OVOC oxidation rates and temperature, no such correlation was identified for the winter uptake rates reported here. Winter uptake rates did exhibit a strong negative correlation with dissolved oxygen concentration, with

further investigation revealing that this was driven by dissimilation and not assimilation. In winter and summer, dissimilation rates were consistently higher than assimilation rates, suggesting that acetaldehyde is predominantly used by microorganisms as an energy source, although a small proportion of acetaldehyde-derived carbon is assimilated into biomass. This was reflected by bacterial growth efficiencies, which indicated that 52 - 99% of acetaldehyde-derived carbon is respired as CO_2 via dissimilation. This metabolic rebalancing was thought to reflect the environmental conditions found in the freshwater rivers, estuaries, and coastal seas of south-west England, although further investigations are needed to identify the environmental parameters driving this demand. The highest summer uptake rates were measured in coastal and estuarine environments, despite suggestions that the regular or continuous availability of acetaldehyde in freshwater rivers, via CDOM photodegradation, may pre-condition these microbial communities to acetaldehyde uptake. Seasonal variation in CDOM availability, DMSP concentration, UV radiation, and temperature were considered as key factors driving these uptake rates. These findings will improve our current understanding of acetaldehyde cycling in aquatic ecosystems, and in turn contribute to our knowledge of the global biogeochemical cycle of acetaldehyde. Given the considerable microbial control of acetaldehyde measured in freshwater rivers, estuaries, and coastal seas, future models of the global acetaldehyde budget must include a microbial sink term for aquatic ecosystems.

5.6 References

Albers CN, Hansen PE, Jacobsen OS (2010) Trichloromethyl compounds - Natural background concentrations and fates within and below coniferous forests. Sci Total Environ 408:6223–6234

Albers CN, Kramshøj M, Rinnan R (2018) Rapid mineralization of biogenic volatile organic compounds in temperate and Arctic soils. Biogeosciences 15:3591–3601

Apoteker A, Thévenot DR (1983) Experimental simulation of biodegradation in rivers: oxygen, organic mater and biomass concentration changes. Water Res 17:1267–1274

Avery GB, Foley L, Carroll AL, Roebuck JA, Guy A, Mead RN, Kieber RJ, Willey JD, Skrabal SA, Felix JD, Mullaugh KM, Helms JR (2016) Surface waters as a sink and source of atmospheric gas phase ethanol. Chemosphere 144:360–365

Beale R, Dixon JL, Arnold SR, Liss PS, Nightingale PD (2013) Methanol, acetaldehyde, and acetone in the surface waters of the Atlantic Ocean. J Geophys Res Ocean 118:5412–5425

Beale R, Dixon JL, Smyth TJ, Nightingale PD (2015) Annual study of oxygenated volatile organic compounds in UK shelf waters. Mar Chem 171:96–106

Beale R, Liss PS, Nightingale PD (2010) First oceanic measurements of ethanol and propanol. Geophys Res Lett 37:1–5

Bey I, Jacob DJ, Yantosca RM, Logan JA, Field BD, Fiore AM, Li Q, Liu HY, Mickley LJ, Schultz MG (2001) Global modeling of tropospheric chemistry with assimilated meteorology: Model description and evaluation. J Geophys Res 106:23073–23095

de Bruyn WJ, Clark CD, Pagel L, Takehara C (2011) Photochemical production of formaldehyde, acetaldehyde and acetone from chromophoric dissolved organic matter in coastal waters. J Photochem Photobiol A Chem 226:16–22

de Bruyn WJ, Clark CD, Senstad M, Barashy O, Hok S (2017) The biological degradation of acetaldehyde in coastal seawater. Mar Chem 192:13–21

de Bruyn WJ, Clark CD, Senstad M, Toms N, Harrison AW (2020) Biological degradation of ethanol in Southern California coastal seawater. Mar Chem 218:

Callahan J, Dai M, Chen RF, Li X, Lu Z, Huang W (2004) Distribution of dissolved organic matter in the Pearl River Estuary, China. Mar Chem 89:211–224

Connell TL, Joye SB, Miller LG, Oremland RS (1997) Bacterial oxidation of methyl bromide in Mono Lake, California. Environ Sci Technol 31:1489–1495

Curson ARJ, Todd JD, Sullivan MJ, Johnston AWB (2011) Catabolism of dimethylsulphoniopropionate: Microorganisms, enzymes and genes. Nat Rev Microbiol 9: 849-859

Dixon JL, Beale R, Nightingale PD (2011a) Microbial methanol uptake in northeast Atlantic waters. ISME J 5:704–716

Dixon JL, Beale R, Nightingale PD (2011b) Rapid biological oxidation of methanol in the tropical Atlantic: Significance as a microbial carbon source. Biogeosciences 8:2707–2716

Dixon JL, Beale R, Nightingale PD (2013a) Production of methanol, acetaldehyde, and acetone in the Atlantic Ocean. Geophys Res Lett 40:4700–4705

Dixon JL, Beale R, Sargeant SL, Tarran GA, Nightingale PD (2014) Microbial acetone oxidation in coastal seawater. Front Microbiol 5:1–9

Dixon JL, Sargeant S, Nightingale PD, Murrell JC (2013b) Gradients in microbial methanol uptake: Productive coastal upwelling waters to oligotrophic gyres in the Atlantic Ocean. ISME J 7:568–580

Goodwin KD, Schaefer JK, Oremland RS (1998) Bacterial oxidation of dibromomethane and methyl bromide in natural waters and enrichment cultures. Appl Environ Microbiol 64:4629–4636

Guenther AB, Jiang X, Heald CL, Sakulyanontvittaya T, Duhl T, Emmons LK, Wang X (2012) The model of emissions of gases and aerosols from nature version 2.1 (MEGAN2.1): An extended and updated framework for modeling biogenic emissions. Geosci Model Dev 5:1471–1492

Halsey KH, Giovannoni SJ, Graus M, Zhao Y, Landry Z, Thrash JC, Vergin KL, de Gouw J (2017) Biological cycling of volatile organic carbon by phytoplankton and bacterioplankton. Limnol Oceanogr 62:2650–2661

Kieber RJ, Zhou X, Mopper K (1990) Formation of carbonyl compounds from UV-induced photodegradation of humic substances in natural waters: Fate of riverine carbon in the sea. Limnol Oceanogr 35:1503–1515

Millet DB, Guenther A, Siegel DA, Nelson NB, Singh HB, de Gouw JA, Warneke C, Williams J, Eerdekens G, Sinha V, Karl T, Flocke F, Apel E, Riemer DD, Palmer PI, Barkley M (2010) Global atmospheric budget of acetaldehyde: 3-D model analysis and constraints from in-situ and satellite observations. Atmos Chem Phys 10:3405–3425

Mincer TJ, Aicher AC (2016) Methanol production by a broad phylogenetic array of marine phytoplankton. PLoS One 11:1–17

Nedwell DB, Underwood GJC, McGenity TJ, Whitby C, Dumbrell AJ (2016) The Colne Estuary: A long-term microbial ecology observatory. Adv Ecol Res 55:227–281

Rinnan R, Albers C (2020) Soil uptake of volatile organic compounds: Ubiquitous and underestimated? J Geophys Res Biogeosciences 1–5

Roebuck JA, Avery GB, Felix JD, Kieber RJ, Mead RN, Skrabal SA (2016) Biogeochemistry of ethanol and acetaldehyde in freshwater sediments. Aquat Geochemistry 22:177–195

Ruiz-González C, Simó R, Sommaruga R, Gasol JM (2013) Away from darkness: A review on the effects of solar radiation on heterotrophic bacterioplankton activity. Front Microbiol 4:1–24

Sargeant SL (2013) Microbial utilisation of methanol in seawater. PhD thesis, University of Warwick

Sargeant SL, Murrell JC, Nightingale PD, Dixon JL (2016) Seasonal variability in microbial methanol utilisation in coastal waters of the western English Channel. Mar Ecol Prog Ser 550:53–64

Singh HB, Salas LJ, Chatfield RB, Czech E, Fried A, Walega J, Evans MJ, Field BD, Jacob DJ, Blake D, Heikes B, Talbot R, Sachse G, Crawford JH, Avery MA, Sandholm S, Fuelberg H (2004) Analysis of the atmospheric distribution, sources, and sinks of oxygenated volatile organic chemicals based on measurements over the Pacific during TRACE-P. J Geophys Res 109:1–20

Trowbridge AM, Stoy PC, Phillips RP (2020) Soil biogenic volatile organic compound flux in a mixed hardwood forest: Net uptake at warmer temperatures and the importance of mycorrhizal associations. J Geophys Res Biogeosciences 125:1–14

Webb C (2016) Turnover of acetaldehyde in natural waters. MSc thesis, Plymouth University

Yang M, Nightingale PD, Beale R, Liss PS, Blomquist B, Fairall C (2013) Atmospheric deposition of methanol over the Atlantic Ocean. Proc Natl Acad Sci USA 110:20034–20039

Yang GP, Song YZ, Zhang HH, Li CX, Wu GW (2014) Seasonal variation and biogeochemical cycling of dimethylsulfide (DMS) and dimethylsulfoniopropionate (DMSP) in the Yellow Sea and Bohai Sea. J Geophys Res-Oceans 119:8897–8915

Chapter 6:

General Discussion

6.1 Microbial acetaldehyde degradation in aquatic environments

The preceding chapters of this thesis have demonstrated that microbial acetaldehyde degradation occurs in freshwater, estuarine, and marine environments. In Chapter 2, microbial acetaldehyde degradation was detected in acetaldehyde enrichments from the Colne Estuary, River Colne, and River Gipping, whilst the findings of Chapter 5 demonstrated that microbial acetaldehyde degradation also occurs in-situ in the freshwater rivers, estuaries, and coastal seas of south-west England. To the best of my knowledge, this thesis, combined with the unpublished work of Webb (2016), is the first to report rates of microbial acetaldehyde degradation in freshwater and estuarine environments and the first to identify the microorganisms responsible in these systems. Our current knowledge of microbial acetaldehyde degradation has been restricted to marine environments, with suggestions that marine microorganisms can significantly limit the flux of acetaldehyde to the atmosphere. Dixon et al. (2013), for example, demonstrated that the microbial dissimilation of acetaldehyde to CO_2 accounted for 49 - 100% of acetaldehyde loss in the Atlantic Ocean, suggesting that microorganisms can exert considerable control over marine acetaldehyde emissions. Halsey et al. (2017) also showed that two strains of *Pelagibacter* SAR11, namely HTCC1062 and HTCC7211, could dissimilate acetaldehyde to CO_2 and assimilate acetaldehyde-derived carbon into biomass. Based on the estimated abundance (2.4×10^{28} cells) and global distribution of SAR11 in marine environments, it was suggested that the global SAR11 community could utilise more acetaldehyde than is currently estimated to be produced. The findings reported in this thesis also suggest that modelled estimates of acetaldehyde emissions from the marine environment are considerably overestimated, as these estimates do not consider the microbial consumption of acetaldehyde. Previous models of the global acetaldehyde budget, which are based on the global distribution of

CDOM light absorption at 300 nm or seawater acetaldehyde concentrations from the Atlantic Ocean, have suggested that marine emissions range from 38 - 125 Tg a^{-1} (Singh et al. 2004; Millet et al. 2010; Read et al. 2012). However, by accounting for microbial consumption and extrapolating acetaldehyde flux from the Atlantic Ocean, Beale et al. (2013) estimated global marine acetaldehyde emissions of 17 Tg a^{-1}, demonstrating that global models of the acetaldehyde budget are likely overestimated by excluding the activity of microorganisms. Microbial acetaldehyde degradation was shown to occur at environmentally relevant concentrations at coastal station L4 in the western English Channel (Chapter 5), with acetaldehyde primarily dissimilated to CO_2 for energy production, reiterating that the effect of microorganisms on marine acetaldehyde emissions must be included in global emission models to accurately estimate acetaldehyde flux to the atmosphere, as highlighted by the estimations of Beale et al. (2013).

The findings of Chapters 2 and 5 also suggest that microorganisms can control acetaldehyde emissions in freshwater rivers and estuaries and thus limit its flux to the atmosphere. However, acetaldehyde emissions from these environments have not been quantified, despite suggestions that acetaldehyde can be produced from multiple sources. Roebuck et al. (2016), for example, identified the microbial breakdown of organic matter as an important source of acetaldehyde in freshwater sediments, with slower production rates in autumn and winter months allowing acetaldehyde to diffuse into the overlying water column. The photodegradation of chromophoric dissolved organic matter (CDOM) has also been identified as a major source of acetaldehyde in rivers and estuaries (Kieber et al. 1990), with the absorption of UV-B (280 - 320 nm) resulting in the production of acetaldehyde and other low molecular weight carbonyl compounds from CDOM photobleaching (Kieber et al. 1990; de Bruyn et al. 2011). Although acetaldehyde emissions from riverine and estuarine environments have yet to be measured and included in global models of the acetaldehyde budget, the findings reported in this thesis show that these emissions are under microbial control. Future work is needed to firstly measure the water-to-air flux of acetaldehyde from

riverine and estuarine environments, followed by additional measurements of microbial acetaldehyde uptake to determine the amount of control that microorganisms have on acetaldehyde emissions from these environments. This will help to gauge the importance of microorganisms in riverine and estuarine acetaldehyde cycling, as well as facilitating the identification of these environments as sources or sinks of acetaldehyde and how this may change with season. This will contribute to our current understanding of the global acetaldehyde cycle and subsequently will help to improve the accuracy of future models of the global acetaldehyde budget, although it should be noted that freshwater habitats, such as lakes and rivers, only represent 0.26% of all freshwater on Earth (Carpenter et al. 2011), thus the contribution of freshwater acetaldehyde sources and sinks to the global budget is likely to be negligible. Similarly, continued research effort is required to gain a better understanding of the microbial acetaldehyde sink in the marine environment. Previous studies have provided evidence that marine acetaldehyde emissions are significantly controlled by microbial activity (Beale et al. 2013; Dixon et al. 2013; Halsey et al. 2017), however, the magnitude of these emissions is still unclear; although estimations by Beale et al. (2013) suggest that global marine acetaldehyde emissions are considerably smaller than previously thought due to microbial activity. Increasing the number of measurements of marine acetaldehyde uptake rates will therefore contribute to accurate estimates of acetaldehyde emissions and elucidate the role of microorganisms as a global acetaldehyde sink. Collectively, these measurements will improve our understanding of the global acetaldehyde cycle.

6.2 Diversity of microbial acetaldehyde degraders

Current understanding of the diversity of acetaldehyde-degrading microorganisms is based on only a handful of studies that have predominantly isolated acetaldehyde degraders from marine or marine-influenced environments. Gao et al. (2018), for example, isolated 12 acetaldehyde-degrading bacteria from 2000 m deep seawater of the West Pacific Ocean,

belonging to the genera *Bacillus*, *Halomonas*, *Pseudoalteromonas*, *Pseudomonas*, and *Vibrio*. As discussed in Section 6.1, Halsey et al. (2017) identified *Pelagibacter* SAR11 strains HTCC1062 and HTCC7211 as acetaldehyde degraders and demonstrated that these strains dissimilated ~70% of acetaldehyde to CO_2 and assimilated the remaining ~30% into biomass. Liu et al. (2015) isolated *Shewanella mangrovi* from mangrove sediments collected from Zhangzhou, China, and reported acetaldehyde degradation at a concentration of 22.7 mM (1000 mg L^{-1}). Recently, Yoshida (2019) used gene-deletion mutation to propose a pathway of acetaldehyde metabolism in *Rhodococcus erythropolis* strain N9T-4, an extremely oligotrophic bacterium isolated from crude oil. Based on the activity of an aldehyde dehydrogenase towards acetaldehyde, it was suggested that *R. erythropolis* strain N9T-4 uses trace amounts of acetaldehyde from the atmosphere as a carbon and energy source, with acetaldehyde converted to acetyl-CoA that enters the tricarboxylic acid (TCA) cycle. The findings of Chapters 2 and 3 show that other bacterial taxa also contribute to acetaldehyde degradation and that the acetaldehyde-degrading community is diverse. The genus *Pseudomonas* was shown to dominate the bacterial communities of the Colne Estuary, River Colne, and River Gipping acetaldehyde enrichments following an addition of 2.27 mM of acetaldehyde (Chapter 2), suggesting that this genus is an important member of the acetaldehyde-degrading community. OTU6, a close relative of *P. benzenivorans*, represented the majority of all bacterial sequences in the Colne Estuary, River Colne, and River Gipping enrichments, indicating that this taxon is a key acetaldehyde degrader in both estuarine and freshwater environments. OTUs closely related to *P. stutzeri*, *P. koreensis*, and *P. putida* were also highly abundant in the acetaldehyde enrichments, suggesting that a considerable number of pseudomonads are capable of utilising acetaldehyde as a carbon and energy source. OTUs assigned to the genus *Arcobacter* were also identified as key acetaldehyde-degraders in the Colne Estuary, River Colne, and River Gipping enrichments (Chapter 2). OTU142, a close relative of *A. nitrofigilis*, was highly abundant in the Colne Estuary enrichments, whilst OTU299, a close relative of *A. suis*, *A. defluvii*, and *A. ellisii* was the most abundant *Arcobacter* species in the River Colne and River Gipping enrichments. To

the best of my knowledge, this is the first study to identify *Arcobacter* species as acetaldehyde degraders.

It is important to note that *Pseudomonas* and *Arcobacter* were the most abundant genera following enrichment with 2.27 mM of acetaldehyde but were not detected in the bacterial community at the higher acetaldehyde concentration (Chapter 2). This suggests that acetaldehyde concentrations of 22.7 mM were toxic to most acetaldehyde degraders and did not support their growth, especially after repeated enrichments. This also indicates that different acetaldehyde concentrations may favour different bacterial taxa, as has been observed for other volatile organic compounds. The dominant genera of isoprene-degrading communities, for example, depend on isoprene concentration, with *Rhodococcus* regularly dominating environments with higher isoprene concentrations (150 - 5000 ppm) and genera such as *Gordonia*, *Ramlibacter*, and *Pelomonas* dominating under low isoprene concentrations (25 ppm) (Carrión et al. 2020). Similarly, methanotrophs have been shown to respond differently to a range of methane concentrations. Methanotrophs with a high affinity for methane, recently termed the atmospheric methane-oxidising bacteria (atmMOB) (Cai et al. 2020), can initiate uptake at low methane concentrations (0.8 - 280 nmol L^{-1}) and consume atmospheric methane (1.7 ppb), whilst methanotrophs with a low affinity for methane only initiate uptake at concentrations of 0.8 - 66 μmol L^{-1} (Huber-Humer et al. 2008; Jiang et al. 2010). These findings suggest that under environmentally relevant concentrations of acetaldehyde, other bacterial genera may dominate and significantly contribute to acetaldehyde degradation, whilst *Pseudomonas* and *Arcobacter* may play more of a secondary role in acetaldehyde degradation at these concentrations or may not be involved at all. The ability of *Rhodococcus erythropolis* strain N9T-4 to utilise atmospheric acetaldehyde (Yoshida 2019) provides a strong indication that different bacterial taxa will dominate microbial communities in response to a range of acetaldehyde concentrations. Based on the findings of Yoshida (2019), oligotrophic acetaldehyde degraders, such as *R. erythropolis* strain N9T-4, may dominate under atmospheric acetaldehyde concentrations

and naturally occurring concentrations measured in aquatic environments, whilst taxa such as *Pseudomonas* and *Arcobacter* may only dominate at higher concentrations. Future investigations employing a range of acetaldehyde concentrations may therefore reveal a greater diversity of acetaldehyde-degrading microorganisms in freshwater, estuarine and marine environments.

The screening of bacterial strains for the ability to utilise acetaldehyde as a sole carbon and energy source provided further evidence that the diversity of acetaldehyde degraders is significantly underestimated (Chapter 3). All 17 isolates cultivated from the Colne Estuary exhibited the ability to degrade acetaldehyde, with *Halobacillus* strains A4 and A5, *Rhodococcus* strain A14, and *Bacillus* strain A17 identified as key acetaldehyde degraders (Chapter 3). Furthermore, 14 previously identified bacterial strains belonging to the Actinobacteria, Bacteroidetes, Proteobacteria, and Verrucomicrobia degraded acetaldehyde. To the best of my knowledge this is the first study to identify acetaldehyde degraders within the Bacteroidetes and Verrucomicrobia, suggesting that a considerable number of acetaldehyde degraders have yet to be identified in other bacterial phyla, and that the capacity to consume acetaldehyde is a normal part of the metabolism of most microbes. Importantly, acetaldehyde degradation was not exhibited by all of the screened bacterial strains. The hydrocarbon degraders *Thalassolituus oleivorans* (MIL-1), *Cycloclasticus zancles* (78-ME), *Marinobacter hydrocarbonoclasticus* (SP17), and *Oleispira antarctica* (RB-8) did not utilise acetaldehyde as a sole carbon and energy source (Chapter 3). It was hypothesised that obligate hydrocarbonoclastic bacteria would be able to utilise acetaldehyde as a carbon and energy source, as this compound is a key intermediate of hydrocarbon degradation pathways that is oxidised to acetate via the activity of aldehyde dehydrogenase enzymes. The meta-cleavage pathway for the degradation of aromatic hydrocarbons was considered as a key feature that may enable *Pseudomonas* species and other metabolically versatile taxa to utilise acetaldehyde (Chapter 2), however, the findings of Chapter 3 suggest that obligate hydrocarbon-degrading microorganisms do not utilise

acetaldehyde as a carbon and energy source, although this may have resulted from the lack of a suitable growth substrate, such as aromatic hydrocarbons, which may induce the aldehyde dehydrogenase enzymes necessary for the co-metabolism of acetaldehyde. To provide an explanation for this, future studies should employ techniques such as proteomics to investigate the expression of proteins in the proteome of other hydrocarbon-degrading bacteria during acetaldehyde enrichment, to establish whether aldehyde dehydrogenase enzymes necessary for acetaldehyde degradation are up-regulated in response to the carbon source. This will help to confirm that hydrocarbon-degrading bacteria cannot use acetaldehyde as a carbon and energy source and simultaneously improve our understanding of the diversity of acetaldehyde degraders. Future studies could also perform gene-deletion mutation experiments on a genetically tractable hydrocarbon degrader, such as *Pseudomonas putida*, to establish the genes, and therefore proteins, necessary for acetaldehyde degradation and to determine if these genes are part of the meta-cleavage pathway for the degradation of aromatic hydrocarbons.

Acetaldehyde degradation has also been shown to occur under anaerobic conditions (Schmidt et al. 2014; Trifunović et al. 2020). The acetogenic bacterium, *Acetobacterium woodii*, isolated from marine estuary sediments (Balch et al. 1977), grew anaerobically on 5 mM of acetaldehyde (Trifunović et al. 2020), whilst the strictly anaerobic *Pelobacter carbinolicus* and *P. acetylenicus* have also been shown to degrade acetaldehyde (Schmidt et al. 2014). The activity of anaerobic acetaldehyde degraders was not considered in this thesis, however, the findings of Schmidt et al. (2014) and Trifunović et al. (2020) suggest that anaerobic acetaldehyde degraders are an important, yet poorly studied, component of the microbial acetaldehyde sink. Further investigations of anaerobic acetaldehyde degradation in freshwater, estuarine, and marine environments may reveal a diverse group of acetaldehyde degraders that may significantly contribute to microbial acetaldehyde degradation. These investigations should also focus on wetland environments, such as moors, given their anaerobic conditions and high concentrations of CDOM.

The role of Fungi and Archaea in microbial acetaldehyde degradation is not clear and, to date, no study has identified or isolated a fungal or archaeal acetaldehyde degrader from the environment. The findings of the Colne Estuary acetaldehyde enrichment experiments (Chapter 2) suggest that the Sordariomycetes may be able to utilise acetaldehyde as a carbon and energy source. The relative abundance of the Sordariomycetes significantly increased in Brightlingsea replicate Bottle B1 following enrichment with the higher acetaldehyde concentration (22.7 mM). This also coincided with significant increases in fungal ITS2 copies, observations of fungal-like biomass and acetaldehyde degradation. However, the relative abundance of *Lutimonas* and *Loktanella* also significantly increased in Bottle B1, making it difficult to identify the microorganism responsible for acetaldehyde degradation. Members of the phylum Ascomycota, which includes the Sordariomycetes, have been shown to degrade aromatic hydrocarbons such as toluene (Prenafeta-Boldú et al. 2006), which involves the conversion of catechol to acetyl-CoA via an acetaldehyde intermediate. The Sordariomycetes may therefore possess the enzymes necessary for acetaldehyde degradation and may represent a previously unknown class of acetaldehyde-degrading fungi, although further research is necessary to confidently identify the Sordariomycetes as acetaldehyde degraders. This may require their isolation and identification, and the screening of fungal isolates for the ability to degrade acetaldehyde. Genome sequencing and proteomics could also be used to determine if the Sordariomycetes possess the aldehyde dehydrogenase-encoding genes needed for acetaldehyde degradation, and to establish whether these proteins are up-regulated during growth on acetaldehyde. To complement these culture-dependent techniques, methods such as DNA stable-isotope probing (DNA-SIP) could also be used to identify the microorganisms that assimilate ^{13}C-labelled acetaldehyde into cellular biomass and therefore identify with more confidence the microorganisms responsible for acetaldehyde degradation. This technique could also be used to determine the role of archaea in acetaldehyde degradation, although the findings of this thesis suggest that the Archaea are not competitive in using acetaldehyde as a carbon and energy source under the conditions of the enrichments.

6.3 Mechanisms of microbial acetaldehyde degradation

The oxidation of acetaldehyde to acetate by aldehyde dehydrogenase enzymes represents the key reaction in the acetaldehyde metabolic pathway (Chapter 4). Halsey et al. (2017) proposed a potential pathway of acetaldehyde metabolism for SAR11, which is initiated by the oxidation of acetaldehyde to acetate and results in acetaldehyde-derived carbon being dissimilated to CO_2 or being assimilated into biomass for growth. A similar pathway was identified for *Rhodococcus* strain A14 following growth on 5 mM of acetaldehyde (Chapter 4). Two aldehyde dehydrogenase enzymes were significantly up-regulated in the proteome of *Rhodococcus* strain A14, demonstrating that multiple aldehyde dehydrogenases can simultaneously oxidise acetaldehyde to acetate. In agreement with the metabolic pathway proposed for SAR11, acetyl-CoA synthetase was also up-regulated in the proteome of *Rhodococcus* strain A14, indicating that acetate is converted to acetyl-CoA that can either enter the TCA cycle for energy production or is used to synthesise fatty acids via lipogenesis. These findings show that the primary and secondary reactions in the acetaldehyde metabolic pathway are conserved amongst acetaldehyde-degrading bacteria.

With the exception of succinate dehydrogenase, fumarase, and malate dehydrogenase, all enzymatic components of the TCA cycle were up-regulated or significantly up-regulated in the proteome of *Rhodococcus* strain A14 during growth on acetaldehyde (Chapter 4), demonstrating that some acetaldehyde is dissimilated to CO_2 for energy production. However, to bypass the oxidative decarboxylation steps of the TCA cycle and to conserve a proportion of acetaldehyde-derived carbon for growth, *Rhodococcus* strain A14 also up-regulates the glyoxylate shunt, which converts isocitrate to succinate and the gluconeogenic precursor, malate. The up-regulation of the glyoxylate shunt has been associated with oxidative and physiological stress (Ahn et al. 2016; Dolan and Welch 2018) and when acetyl-CoA is the direct product of a metabolic pathway (Ahn et al. 2016). As acetyl-CoA is a derivative of acetaldehyde, this suggests that *Rhodococcus* strain A14 responded to the

carbon source, rather than oxidative or physiological stress. Accordingly, the findings of Chapter 4 demonstrate that *Rhodococcus* strain A14, and possibly other acetaldehyde-degrading bacteria, partition acetaldehyde-derived carbon to maintain a balance between the production of energy and gluconeogenic precursors. This has also been observed in *Rhodococcus erythropolis* strain N9T-4 (Yano et al. 2015), a more distant relative of *Rhodococcus* strain A14, during growth under oligotrophic conditions, suggesting that the glyoxylate shunt and gluconeogenesis are essential to survival during unfavourable conditions.

The microbial assimilation and dissimilation of ^{14}C-acetaldehyde in the Colne Estuary (Chapter 2) and the freshwater rivers, estuaries, and coastal seas of south-west England (Chapter 5) also shows clear partitioning of acetaldehyde-derived carbon. Rates of microbial dissimilation were higher than microbial assimilation rates during summer and winter, suggesting that the majority of acetaldehyde-derived carbon is used for energy production under favourable growth conditions, in agreement with the findings of Halsey et al. (2017) for *Pelagibacter* SAR11 strains HTCC1062 and HTCC7211 (Section 6.2). Based on the findings of Chapter 4, the assimilation of acetaldehyde-derived carbon into biomass may only be preferred over acetaldehyde dissimilation during unfavourable growth conditions, such as the limited availability of nutrients, as was observed for *R. erythropolis* strain N9T-4 (Yano et al. 2015). This suggests that rates of microbial assimilation may occasionally be higher than microbial dissimilation rates, although the exact environmental conditions that cause this shift require further investigation. Based on the findings reported for *Rhodococcus* strain A14 and *R. erythropolis* strain N9T-4, this scenario would result in the up-regulation of the enzymatic components of the glyoxylate shunt and gluconeogenesis pathway to conserve carbon for assimilation into biomass. The up-regulation of the glyoxylate shunt is facilitated by an alternative pathway for succinate production from α-ketoglutarate in *Rhodococcus* strain A14, which conserves coenzyme A for the synthesis of acetyl-CoA used in the glyoxylate shunt (Chapter 4). This bypass of the TCA cycle has also been observed in

R. erythropolis strain N9T-4 during growth under oligotrophic conditions (Yano et al. 2015), suggesting that it may be essential for the assimilation of acetaldehyde-derived carbon by acetaldehyde-degrading bacteria. The up-regulation of phosphoenolpyruvate carboxykinase also commits *Rhodococcus* strain A14 to gluconeogenesis by decarboxylating and phosphorylating oxaloacetate from the TCA cycle to phosphoenolpyruvate. This ensures that carbon is assimilated into biomass during growth on acetaldehyde. Accordingly, these findings suggest that acetaldehyde is predominantly used as an energy source under favourable growth conditions via the oxidative decarboxylation steps of the TCA cycle. However, during unfavourable growth conditions, acetaldehyde is primarily assimilated into biomass via the glyoxylate shunt and gluconeogenesis pathway to ensure survival. Further research is necessary to determine if the same metabolic pathway used by *Rhodococcus* strain A14 and *R. erythropolis* strain N9T-4 is used by all acetaldehyde-degrading bacteria or if an alternative pathway for acetaldehyde degradation exists.

Aldehyde dehydrogenase enzymes are also involved in the final reaction of the meta-cleavage pathway for the degradation of aromatic hydrocarbons such as toluene, benzene, xylenes, and naphthalene, converting acetaldehyde to acetyl-CoA (Yen & Gunsalus 1985; Greated et al. 2002; Johnsen et al. 2005; Banu & Prasad 2017). The complete set of genes encoding this pathway are often found on catabolic plasmids in metabolically-diverse genera such as the *Pseudomonas* and *Rhodococcus* (Greated et al. 2002; Larkin et al. 2005), including the TOL plasmid pWW0 and NAH7 plasmid of *Pseudomonas putida* (Yen and Gunsalus 1985; Greated et al. 2002). Many of these catabolic plasmids are self-transmissible and have a broad host range, allowing degradative pathways to be acquired by different species (Stephanopoulos et al. 1998). Consequently, the metabolic pathway for acetaldehyde degradation could also be acquired by different bacterial taxa via the conjugative transfer of plasmids, transduction, or transformation.

6.4 Future work

The findings of this thesis have demonstrated that acetaldehyde-degraders represent an important, yet poorly studied, group of microorganisms that can significantly influence the atmospheric flux of acetaldehyde from freshwater, estuarine, and marine environments. Although the preceding chapters have shown that acetaldehyde degraders are present and active in these environments, constitute a diverse group of microorganisms, and use aldehyde dehydrogenase enzymes in conjunction with the glyoxylate shunt and gluconeogenesis pathway to metabolise acetaldehyde, further research is necessary to improve our understanding of their role in the global acetaldehyde cycle and the effect that this has on the global carbon cycle. As alluded to in Section 6.1, more research effort is needed to quantify in-situ rates of microbial acetaldehyde uptake in freshwater, estuarine, and marine environments to accurately estimate the magnitude of the microbial acetaldehyde sink. This should also include investigations into the diel cycles of acetaldehyde uptake and the effect of seasonal change. Furthermore, more measurements of acetaldehyde production in these environments are needed over temporal and spatial scales to enhance our understanding of acetaldehyde cycling. Together, these measurements will improve the accuracy of future models of the global acetaldehyde budget, which have so far omitted microbial acetaldehyde sink terms and have not included acetaldehyde emissions from rivers and estuaries.

To develop a better understanding of their diversity, future studies should attempt to isolate more acetaldehyde degraders from freshwater, estuarine, and marine environments. Although microorganisms have been shown to utilise acetaldehyde as a carbon and energy source through the use of ^{14}C-radiolabelling techniques (Beale et al. 2013; Dixon et al. 2013), only a handful of acetaldehyde degraders have been isolated and identified (Schmidt et al. 2014; Liu et al. 2015; Halsey et al. 2017; Gao et al. 2018; Trifunović et al. 2020), limiting our understanding of their diversity. It will be particularly important to isolate

acetaldehyde-degrading microorganisms using environmentally relevant concentrations of acetaldehyde, in contrast to the unnaturally high concentrations used in this thesis, to confidently identify the microorganisms that are responsible for acetaldehyde degradation under natural conditions. However, isolation using such low concentrations of acetaldehyde may be difficult and the use of cultivation-independent techniques may be necessary to identify acetaldehyde degraders in mixed cultures and to link phylogeny to function. As mentioned in Section 6.2, DNA-SIP can be used to confidently identify the microorganisms in environmental samples that use a particular substrate (Dumont & Murrell 2005). This technique involves the incubation of environmental samples with ^{13}C-labelled substrate to allow the incorporation of labelled carbon into the biomass of active microorganisms. DNA is extracted from the microbial community and is subjected to caesium chloride buoyant density-gradient centrifugation to separate the heavier ^{13}C-DNA from the lighter ^{12}C-DNA (Dumont & Murrell 2005). The ^{13}C-DNA is isolated and can be used as a template in PCR using primers that amplify the rRNA gene of Bacteria, Fungi or Archaea, or indeed any other gene of interest. The resulting PCR products can then be sequenced to identify the microorganisms responsible for substrate utilisation. This technique should be applied in future studies to identify the microorganisms responsible for acetaldehyde degradation in freshwater, estuarine, and marine environments and simultaneously improve our current understanding of their diversity. Importantly, this technique avoids the issue of being unable to cultivate the microorganisms suspected of being responsible for substrate utilisation, as was observed in this thesis. *Pseudomonas* was identified as the most abundant genus in the Colne Estuary, River Colne, and River Gipping enrichments (Chapter 2), however, pseudomonads were not isolated in Chapter 3, preventing further investigations that could confirm their ability to degrade acetaldehyde; although close relatives that have previously been cultivated could also be tested. DNA-SIP provides a clear link between phylogeny and function that removes the need for cultivation, although the isolation of microorganisms can provide an opportunity for characterisation (Chapter 3) and valuable insights into the mechanisms of substrate utilisation (e.g. proteomics; Chapter 4).

Future studies should also investigate microbial acetaldehyde degradation at the single-cell level using techniques such as NanoSIMS (nanoscale secondary ion mass spectrometry). In recent years, this technique has been used in combination with stable-isotope probing (NanoSIP) to trace the metabolic activities of single microbial cells and to map their distribution within microbial assemblages (e.g. biofilms and microbial mats) at high spatial resolution (50 nm) (Musat et al. 2012; Pett-Ridge and Weber 2012; Nuñez et al. 2018; Mayali 2020). NanoSIMS has also been used to visualise cell-to-cell interactions and how microorganisms interact with their surrounding environments (Pett-Ridge & Weber 2012; Nuñez et al. 2018). Combined with fluorescence in-situ hybridisation (FISH), NanoSIP can be used to identify microorganisms with specific metabolic activities (Mayali 2020). The cells of interest are identified via fluorescence microscopy following the hybridisation of a fluorescent probe with a target sequence (e.g. 16S rRNA gene). These cells are then subjected to NanoSIMS analysis to quantify the stable isotopes of interest (Mayali 2020). Another advantage of this technique is that it operates at ultra-low minimum detection limits (ppb) (Rollog et al. 2019), allowing precise quantification of stable-isotope-labelled substrates incorporated by individual microbial cells. This technique could be applied in future studies to visualise the uptake of acetaldehyde into microbial cells and to show where acetaldehyde-derived carbon is assimilated and distributed in the cell. Furthermore, in combination with FISH, NanoSIP could be used to reliably identify the microorganisms involved in acetaldehyde degradation using ^{13}C-labelled acetaldehyde as a substrate.

The pathway of acetaldehyde degradation proposed for *Rhodococcus* strain A14 (Chapter 4) has also been identified in *R. erythropolis* strain N9T-4 (Yano et al. 2015) and has been suggested for the SAR11 clade (Halsey et al. 2017). This suggests that this pathway may be conserved amongst acetaldehyde-degrading bacteria, however, further investigations are needed to determine if an alternative pathway exists. This may be particularly important if acetaldehyde-degrading fungi and/or archaea are identified and isolated, as it is possible that these microorganisms may possess a different pathway for acetaldehyde metabolism

than bacteria. Combined with genome sequencing, proteomics may facilitate the identification of an alternative microbial acetaldehyde degradation pathway and may also assist in identifying specialist acetaldehyde degraders, which have yet to be discovered.

Collectively, this research will improve our understanding of the diversity of acetaldehyde-degrading microorganisms, the mechanisms of microbial acetaldehyde degradation, and the environments in which acetaldehyde degraders are found. This will improve current estimates of the magnitude of the microbial acetaldehyde sink and will demonstrate the control that microorganisms have on acetaldehyde flux to the atmosphere. This will increase the accuracy of future models of the global acetaldehyde budget and enhance our understanding of the global acetaldehyde cycle.

6.5 References

Ahn S, Jung J, Jang I, Madsen EL, Park W (2016) Role of glyoxylate shunt in oxidative stress response. J Biol Chem 291:11928–11938

Balch WE, Schoberth S, Tanner RS, Wolfe RS (1977) *Acetobacterium*, a new genus of hydrogen-oxidizing, carbon dioxide-reducing, anaerobic bacteria. Int J Syst Bacteriol 27:355–361

Banu H, Prasad KP (2017) Role of plasmids in microbiology. J Aquac Res Dev 8:466

Beale R, Dixon JL, Arnold SR, Liss PS, Nightingale PD (2013) Methanol, acetaldehyde, and acetone in the surface waters of the Atlantic Ocean. J Geophys Res Ocean 118:5412–5425

de Bruyn WJ, Clark CD, Pagel L, Takehara C (2011) Photochemical production of formaldehyde, acetaldehyde and acetone from chromophoric dissolved organic matter in coastal waters. J Photochem Photobiol A Chem 226:16–22

Cai Y, Zhou X, Shi L, Jia Z (2020) Atmospheric methane oxidizers are dominated by upland soil cluster alpha in 20 forest soils of China. Microb Ecol 80:859–871

Carpenter SR, Stanley EH, Vander Zanden MJ (2011) State of the world's freshwater ecosystems: Physical, chemical, and biological changes. Annu Rev Env Resour 36:75–99

Carrión O, McGenity TJ, Murrell JC (2020) Molecular ecology of isoprene-degrading bacteria. Microorganisms 8:1–15

Dixon JL, Beale R, Nightingale PD (2013) Production of methanol, acetaldehyde, and acetone in the Atlantic Ocean. Geophys Res Lett 40:4700–4705

Dolan SK, Welch M (2018) The glyoxylate shunt, 60 years on. Annu Rev Microbiol 72:309–330

Dumont MG, Murrell JC (2005) Stable isotope probing - Linking microbial identify to function. Nat Rev Microbiol 3:499–504

Gao B, Shang X, Li L, Di W, Zeng R (2018) Phylogenetically diverse, acetaldehyde-degrading bacterial community in the deep sea water of the West Pacific Ocean. Acta Oceanol Sin 37:54–64

Greated A, Lambertsen L, Williams PA, Thomas CM (2002) Complete sequence of the IncP-9 TOL plasmid pWW0 from *Pseudomonas putida*. Environ Microbiol 4:856–871

Halsey KH, Giovannoni SJ, Graus M, Zhao Y, Landry Z, Thrash JC, Vergin KL, de Gouw J (2017) Biological cycling of volatile organic carbon by phytoplankton and bacterioplankton. Limnol Oceanogr 62:2650–2661

Huber-Humer M, Gebert J, Hilger H (2008) Biotic systems to mitigate landfill methane emissions. Waste Manag Res 26:33–46

Jiang H, Chen Y, Jiang P, Zhang C, Smith TJ, Murrell JC, Xing XH (2010) Methanotrophs: Multifunctional bacteria with promising applications in environmental bioengineering. Biochem Eng J 49:277–288

Johnsen AR, Wick LY, Harms H (2005) Principles of microbial PAH-degradation in soil. Environ Pollut 133:71–84

Kieber RJ, Zhou X, Mopper K (1990) Formation of carbonyl compounds from UV-induced photodegradation of humic substances in natural waters: Fate of riverine carbon in the sea. Limnol Oceanogr 35:1503–1515

Larkin MJ, Kulakov LA, Allen CCR (2005) Biodegradation and *Rhodococcus* - Masters of catabolic versatility. Curr Opin Biotechnol 16:282–290

Liu Y, Shang X, Yi Z, Gu L, Zeng R (2015) *Shewanella mangrovi* sp. nov., an acetaldehyde-degrading bacterium isolated from mangrove sediment. Int J Syst Evol Microbiol 65:2630–2634

Mayali X (2020) NanoSIMS: Microscale quantification of biogeochemical activity with large-scale impacts. Ann Rev Mar Sci 12:449–467

Millet DB, Guenther A, Siegel DA, Nelson NB, Singh HB, de Gouw JA, Warneke C, Williams J, Eerdekens G, Sinha V, Karl T, Flocke F, Apel E, Riemer DD, Palmer PI, Barkley M (2010) Global atmospheric budget of acetaldehyde: 3-D model analysis and constraints from in-situ and satellite observations. Atmos Chem Phys 10:3405–3425

Musat N, Foster R, Vagner T, Adam B, Kuypers MMM (2012) Detecting metabolic activities in single cells, with emphasis on nanoSIMS. FEMS Microbiol Rev 36:486–511

Nuñez J, Renslow R, Cliff JB, Anderton CR (2018) NanoSIMS for biological applications: Current practices and analyses. Biointerphases 13:03B301

Pett-Ridge J, Weber PK (2012) NanoSIP: NanoSIMS applications for microbial biology. pp 375–408. In: Navid A (Ed.). Microbial Systems Biology. Methods in Molecular Biology (Methods and Protocols). Humana Press, Totowa, NJ

Prenafeta-Boldú FX, Summerbell R, Sybren de Hoog G (2006) Fungi growing on aromatic hydrocarbons: Biotechnology's unexpected encounter with biohazard? FEMS Microbiol Rev 30:109–130

Read KA, Carpenter LJ, Arnold SR, Beale R, Nightingale PD, Hopkins JR, Lewis AC, Lee JD, Mendes L, Pickering SJ (2012) Multiannual observations of acetone, methanol, and acetaldehyde in remote tropical Atlantic air: Implications for atmospheric OVOC budgets and oxidative capacity. Environ Sci Technol 46:11028–11039

Roebuck JA, Avery GB, Felix JD, Kieber RJ, Mead RN, Skrabal SA (2016) Biogeochemistry of ethanol and acetaldehyde in freshwater sediments. Aquat Geochemistry 22:177–195

Rollog M, Cook NJ, Guagliardo P, Ehrig K, Ciobanu CL, Kilburn M (2019) Detection of trace elements/isotopes in olympic dam copper concentrates by nanoSIMS. Minerals 9:1–25

Schmidt A, Frensch M, Schleheck D, Schink B, Müller N (2014) Degradation of acetaldehyde and its precursors by *Pelobacter carbinolicus* and *P. acetylenicus*. PLoS One 9:1–23

Singh HB, Salas LJ, Chatfield RB, Czech E, Fried A, Walega J, Evans MJ, Field BD, Jacob DJ, Blake D, Heikes B, Talbot R, Sachse G, Crawford JH, Avery MA, Sandholm S, Fuelberg H (2004) Analysis of the atmospheric distribution, sources, and sinks of oxygenated volatile organic chemicals based on measurements over the Pacific during TRACE-P. J Geophys Res 109:1–20

Stephanopoulos GN, Aristidou AA, Nielsen J (1998) Examples of pathway manipulations: Metabolic engineering in practice. pp 203–283. In: Stephanopoulos GN, Aristidou AA, Nielsen J (Eds.). Metabolic Engineering. Academic Press

Trifunović D, Berghaus N, Müller V (2020) Growth of the acetogenic bacterium *Acetobacterium woodii* by dismutation of acetaldehyde to acetate and ethanol. Environ Microbiol Rep 12:58–62

Webb C (2016) Turnover of acetaldehyde in natural waters. MSc thesis, Plymouth University

Yano T, Yoshida N, Yu F, Wakamatsu M, Takagi H (2015) The glyoxylate shunt is essential for CO2-requiring oligotrophic growth of *Rhodococcus erythropolis* N9T-4. Appl Microbiol Biotechnol 99:5627–5637

Yen KM, Gunsalus IC (1985) Regulation of naphthalene catabolic genes of plasmid NAH7. J Bacteriol 162:1008–1013

Yoshida N (2019) Oligotrophic growth of *Rhodococcus*. pp 87–101. In: Alvarez HM (Ed.). Biology of *Rhodococcus*. Microbiology Monographs 16. Springer Nature Switzerland AG